AUGMENTATION OF MASS TRANSFER THROUGH ELECTRICAL MEANS AND NUTRIENT ENRICHMENT FOR SUSPENSION AND ENTRAPMENT CELL CULTURES

by

YU-HSIANG DAVID CHANG

M.S. Chemical Engineering
Massachusetts Institute of Technology
(1989)

Submitted to the Department of Chemical Engineering in Partial Fulfillment of the Requirements for the Degree of

DOCTOR OF PHILOSOPHY IN CHEMICAL ENGINEERING

at the

MASSACHUSETTS INSTITUTE OF TECHNOLOGY

May 1994

Signature of Author:_____
Department of Chemical Engineering
May 20,1994

Certified by:_____
Daniel I. C. Wang
Professor of Chemical Engineering
Thesis Supervisor

Certified by:_____
Alan J. Grodzinsky
Professor of Electrical Mechanical and Bioengineering
Thesis Supervisor

Accepted by:_____
Robert E. Cohen
Professor of Chemical Engineering
Chairman, Committee for Graduate Students

Augmentation of Mass Transfer through Electrical Means and Nutrient Enrichment for Suspension and Entrapment Cell Cultures

by

Yu-Hsiang David Chang

Submitted to the Department of Chemical Engineering
on May 20, 1994, in partial fulfillment of the
requirements for the degree of
Doctor of Philosophy in Chemical Engineering

Abstract

Improving cell culture performance is one of the major challenges for a biochemical engineer. Nutrient limitations (oxygen, glucose and amino acids) and cellular waste product accumulation (lactate and ammonia) are two factors limiting cell growth and protein production in suspension and entrapped cell cultures. In this research, the possibility of using enriched medium and electrokinetic transport phenomena (electroosmosis and electrophoresis) to overcome the above limitations is explored.

E. coli was entrapped in κ-carrageenan and agarose hydrogel slabs. The total cell densities increased by 140% and 80%, respectively, in κ-carrageenan and agarose under an electric current density of 180 A/m^2, as compared to the control cultivations in the absence of the electric field. A mathematical model considering the intra-hydrogel transport and cell growth kinetics was developed, and this model successfully simulated the time-dependent cell growth in the hydrogels under different electric current densities. The model showed that in κ-carrageenan, 80% of the increase in cell density was attributed to the removal of the toxic waste products and 20% of the increase was due to the augmented glucose transport. The majority of the entrapped *E. coli* cells (>70%), based on this model, proliferated anaerobically even though the medium outside the hydrogel slab was maintained oxygen-rich. Hybridoma cells were also entrapped in an alginate/agarose gel blend in the presence of 70 A/m^2, but no discernible difference in cell growth was observed compared to the control cultivation.

In suspension hybridoma cultures, an electric current density of 50 A/m^2 was applied to the cultures using commercial medium, DMEM. Cell-produced ammonia and lactate were effectively removed and hence both cell growth and antibody production were enhanced. However, the enhancement was limited (less than 50%) due to the nutrient depletion. Therefore, enriched medium in conjunction with a higher electric current density of 75 A/m^2 were used in the subsequent cultures. All of the amino acid and vitamin concentrations in the enriched medium were concentrated by 5 times above the levels in DMEM. The final cell density and antibody titer increased from 3.9×10^6 to 9.1×10^6 cells/ml and from 170 to 510 mg/L, respectively, compared to the control culture using the same enriched medium in the absence of the electric field. The enhanced cell growth and antibody production were mainly attributed to the complete removal of ammonia (maintained below 2 mM) and the higher nutrient concentrations. Cellular metabolism was analyzed, and the results suggested that the enriched medium caused the overflow metabolism of nutrients, especially glucose, and thus resulted in an excess production of lactate and a significant increase in osmolarity. This increased osmolarity is believed to be the major cause of cell death.

In order to decelerate cellular metabolism and increase specific antibody productivity in the suspension hybridoma cultures using the enriched medium in the presence of 75 A/m^2, 0.7 mM sodium butyrate was added during the mid-exponential growth phase of the culture. It was found that 0.7 mM sodium butyrate was able to decrease the glucose metabolism by 25% and increased the specific antibody productivity by 60% compared to the culture in the absence of sodium butyrate. Sodium butyrate, however, slightly retarded cell growth. As a result, a final antibody titer of 650 mg/L was achieved.

Thesis Supervisor: Daniel I. C. Wang
Alan J. Grodzinsky

Title: Professors

ACKNOWLEDGEMENTS

The stay at MIT was the most memorable experience in my life. Although it took me seven years of effort to get my Ph.D. degree (plus one "bonus" master degree in chemical engineering practice), I enjoyed every second I have spent. I can still recall the moment when I passed the qualification exam, presented my thesis proposal, and tried to "convince" my thesis committee I have done a good jobs during thesis progress reports. What I have learned from these are not only the specialty for my career, but also a good attitude for facing the challenges in real life. It is impossible to go through this long journey without help from others. I don't think a few words can truly express my appreciation to these people, but I will keep these in mind and hopefully I can return these favors in the future!

First of all, I would like to thank my family, especially my fiancé I-Ching. I thank her for giving me her love and support and bring me such joy and happiness. I wish to express my greatest gratitude to my father who past away five years ago. He encouraged me to pursue my interests and study overseas. His dedication to work and family is a role model for my future. I would like to also thank my mother and sister for their spiritual support from miles away. Their love and support gave me the courage and confidence to take on the challenges.

This thesis could not be accomplished without my thesis advisors Daniel Wang and Alan Grodzinsky. Daniel has provided me with great support and wise guidance on this project. His discipline, demand for perfection and dedication to work taught me valuable lessons. I will never forget the "largest" coin is always in the dark. Alan showed me the path in the electrical engineering fields. His brilliant knowledge and wisdom always guided me in the right direction. His patience and encouragement convinced me the impossible is possible as long as you persist. I am also very grateful to my thesis committee Charles Cooney and Greg Stephanopoulos for their valuable suggestions and moral support. This thesis could not progress successfully without their constructive criticism.

Some of the work presented in this thesis was completed with the assistance of several undergraduate students from MIT and other schools. I would like to thank Neeraj Gandhi, Diane Hern, Albert Lin, Chia-Chin Lin, Hsin-Chien Tai, Vivian Tung and Robert William. Thanks are also expressed to the BPEC staff, Audrey Child, Sonia Foster and Lynne Lenker for their tremendous efforts in running BPEC behind the scenes. Their timely signatures often save me from running out of stationery and laboratory stock.

The BPECers have provided their support and friendship in many ways. To my dear office mates, Brian Kelley, Dan Lasko, Per Lindell and Steve Meier, thanks for taking the phone messages and putting up with my Chinese conversation. Thanks also go to the Bldg.-20 BPECers: Enno Adema, Mark Applegate, Keqin Chen, Tzyy-Wen Chiou, Peter Freier, Gino Grampp, Sherry Guu, Chris Hwang, Gautum Nayar, Greg Nyber, Don Orton, Ed Osawa, Marc Shelikoff, Troy Simpson, Rahul Singhvi, Dave Stevenson, Nick Valkanis, Bruce Woodson, Liangzhi Xie, Yizu Zhu and Craig Zupke. The discussions about politics, arts, cultures, current events and even research really enriched my knowledge. Of course, my Bldg.-16 bodies deserve recognition for sharing their protein knowledge with me and showing their supports in Beam seminars. Thanks go to Anna Hagen, Beth Junker, Steve Lee, Kai-Chee Loh, Christine Moore, Greg O'Connor, Eric Scharin and Margaret Speed. Special thanks to Kai-Chee, Gautum and Steve for spending their time to help me put this thesis together, and to Liangzhi and Keqin for sharing their valuable knowledge with me.

At last, I would like to acknowledge the National Science Foundation of the United States of America for financially supporting this research from Biotechnology Process Engineering Center at MIT through the Engineering Research Center Initiative under cooperative agreement CDR-88-03014.

Table of Content

LIST OF FIGURES

LIST OF TABLES

I. INTRODUCTION

I.1 Fermentation-Based Bioprocesses

I.1.1 Historical Review

Fermentation technology has been used since antiquity to produce foods and beverages, such as yogurt, cheese, vinegar and alcohol. Its potential for making other useful products was not realized until early this century. Fermentation was first used to produce important industrial chemicals and fuels during World War I (Demain and Solomon, 1981). The biological synthesis of healthcare products was then pioneered in the early 1940s, when the process was developed for the production of penicillin (Aharonowitz and Cohen, 1981; Demain and Solomon, 1981). This development clearly demonstrated the potential of biological synthesis to produce therapeutic products, and the fermentation-based biotechnology process industry has grown rapidly since then. Currently, many pharmaceuticals and bulk industrial chemicals, in addition to foods and beverages, are being produced biologically. Fermentation-based bioprocesses are being used to produce organic acids, amino acids, and enzymes, in addition to many healthcare diagnostics and therapeutics, such as antibiotics and vaccines (Eveleigh, 1981). The importance of fermentation-based bioprocess is shown by the substantial growth in pharmaceutical industry. Microbially-produced pharmaceuticals, nearly 90% of which are antibiotics, now constitute a multibillion dollar per year market (Aharonowitz and Cohen, 1981; Demain and Solomon, 1981).

In the mid 1970s, the number of products that can be manufactured in large quantities biologically has markedly expanded since the advent of recombinant DNA technology (Cohen, 1975). Progress in genetic engineering in the last two decades has generated tremendous exciting opportunities for useful products made by both prokaryotes (bacteria) and

eukaryotes (yeast, mammalian, plant, and insect cells). Genetic engineering techniques enable foreign genes to be inserted and highly expressed in desired host organisms through the introduction of suitable expression vectors. This markedly increases both the variety and the quality of products that can be produced biologically (Hopwood, 1981). Moreover, genetic engineering techniques significantly improve the economic feasibility of manufacturing many biological products by increasing the rates of product formation and the final product concentration, which can not be achieved by using traditional non-recombinant methods.

The initial products of genetic engineering primarily are high value-added, often previously unavailable, therapeutic proteins, expressed in bacterial, yeast and mammalian systems (Fieschko, 1989; Drew, 1985). The manufacture of commodity chemicals, fuels, and enzymes has lagged because of lower economic margins and stringent regulatory requirements governing the large-scale fermentation of recombinant organisms leading to higher costs (Khosrovi and Gray, 1985). To date among the bacteria cells, *Escherichia coli* is the most popular host for expressing foreign proteins (Fieschko, 1989; Khosrovi and Gray, 1985) due to its high growth rate relative to other bacteria and its well-understood biology. But the lack of post-translational processing capabilities of bacterial cells force the choice of eukaryotic cells as host organisms to produce proteins which require post-translational processing.

I.1.2 Fermentation-Based Bioprocess Overview

The modern bioprocess engineering for recombinant cells containing systems to produce healthcare-related protein products should consist of the following (Spier, 1991):

• The formulation of a growth medium.

The medium should be designed in a way that all nutrient requirements for supporting cell growth and product formation are met, and all constituent nutrients are being most efficiently consumed in order to minimize waste product formation, especially toxic end-products.

• The cell inoculum to the growth medium in a bioreactor.

The bioreactor should contain all control accessories in order to maintain the constant, optimal culture environment. The bioreactor should be also designed to support high density cell growth without any nutrient limitation, especially oxygen, and to avoid the physical damage on cells.

• The incubation for cell growth and the replenishment of depleted nutrient with supplement medium.

The purpose of using supplement medium is to replenish the limiting nutrients, to regulate the growth pattern and to avoid overflow of nutrient metabolism.

• The removal of the spent growth medium.

This spent medium could contain crude products as long as those products are non-growth-related and constitutively secreted.

• The addition of the medium into which the product is to be secreted.

• The incubation for product formation.

• The discharge of the product-containing medium.

• The concentration, purification, and, if necessary, modification of the products.

• The bottling, labeling, packing, storage, and dispatch of the final product.

In order to arrive at the most cost-effective way of manufacturing a product, the bioprocess engineer should consider the following guiding principles :

• The medium should be as its lowest cost.

• The medium has to be as free from protein if possible in order to simplify the downstream purification process.

• The cells should be productive.

• The process should attain the product at the lowest cost.

• The downstream operation should contain as few stages as possible and each stage should be as effective as practicable.

I.1.3 Economic Aspects of Fermentation-Based Bioprocesses

The economics of fermentation-based bioprocesses depend on the scale of operation and the type of product being made. Generally speaking, the cost of manufacturing a product decreases as the production scale increases. However, at a fixed scale of operation, process costs vary widely depending on types of products. Fermentation-based bioprocesses usually are classified as being fermentation or recovery cost-intensive. Many of the traditional fermentation-related products are commodity chemicals, which are generally low-value and produced in large volumes. Recent progress in genetic engineering capabilities has led to the development of processes for producing fine chemicals, diagnostics and therapeutics, which are generally high-valued products but produced in relatively small volume.

The production of commodity chemicals is generally fermentation cost-intensive, i.e., the unit cost of a bulk product primarily depends on the yield on substrate and on the fermentation cycle time. Thus the strategies for improving the profitability of commodity chemical production focus on either using cheaper substrate, improving product yield, or improving bioreactor volumetric productivity (Wang, 1985). Recovery costs for commodity chemicals tend to vary inversely with the final product

concentrations in the broths (Atkinson and Mavituna, 1983). Therefore the objective of production phase for commodity chemicals is to maximize product concentration in order to minimize recovery costs.

The production of fine chemicals, especially pharmaceuticals, and biological therapeuticals is primarily recovery cost-intensive due to the stringent product purification requirements. These products require multiple stages of purification trains that are generally expensive in both capital and operating costs (Baily and Ollis, 1986). These costs tend to be proportional to the number of processing stages employed (Atkinson and Mavituna, 1983). Therefore the strategies for improving the economics of fine chemical and therapeuticals production are aimed at reducing recovery cost. Fermentation broths are usually dilute, and final cell densities and product concentrations are usually less than 1 to 10% by weight. As a result, product recovery contributes as much as 50% of bulk therapeutic drug costs, and as much as 90% of the manufacturing costs for lower volume biologicals such as recombinant protein products. Recovery costs for higher valued recombinant protein products also depend on the final form of the product (intracellular inclusion body, intracellular solubilized proteins, or extracellular proteins, etc), as well as on the final broth composition. It is extremely desirable to integrate production and downstream purification phases in order to simplify the downstream purification process (Baily and Ollis, 1986; Cooney, 1985). For example, to increase final product titer by using a complex medium will make subsequent product purification more costly. Therefore a defined medium when employed and the cell production yield might be sacrificed in considering recovery economics. Nevertheless, when the process integration is considered, a high yield in production phase is still necessary for economical reasons (Fieschko, 1989; Khosrovi and Gray,

1985). Therefore, in processes to produce recombinant proteins the goal must also consider the maximum product concentration attainable.

In many cases it is necessary to achieve high cell density to maximize final product concentration. For example, in processes in which the product remains intracellular and the expression level is fixed, final product titer is determined primarily by the final cell density. If the product is secreted either during the growth phase or near the end of growth phase, the final product titer is also increased by increasing the cell density. The final titer of recombinant protein product depends on both the specific expression rate and the cell density. Increasing either of these quantities is desirable since it improves the process yield (Fieschko, 1989). The improvement of specific expression efficiency is primarily achieved through genetic engineering approaches. The maximization of cell density is obtained through bioreactor design, medium optimization, and manipulation of fermentation control and operation.

I.2 Motivation

In order to achieve higher final product titer in fermentation-based bioprocess for therapeutics production, it is necessary to maximize cell density as well as specific protein production rate. After optimization of the specific expression level of therapeutic protein in a recombinant cell line, a biochemical engineer's role is to manipulate the fermentation process in order to offer the optimal environment for supporting cell growth. Unfortunately, many fermentation processes suffer from several limitations. Among them, nutrient limitation and waste product accumulation are two important factors limiting cell growth and productivity. Those adverse behaviors are further complicated in immobilized cell systems owing to the poor mass transfer in the cell-

entrapped matrix. Therefore cell's viability and growth are much lower in immobilized cell systems, even though the local cell density within the cell-entrapped matrix could be higher than that in the suspension cell systems.

Prokaryotic cells in general can tolerate a wide range of osmolarity variation and the culture medium is also much simpler than that for eukaryotic cells. Thus, the culture medium enrichment for prokaryotic cells can be achieved by increasing the necessary nutrient concentrations by several fold without encountering many adversities to the cell's behavior. On the other hand, eukaryotic cells can tolerate only small changes in the osmolarity from the optimal value as well as having complex nutrient requirements. For example, amino acids, vitamins, inorganic salts, sugar and growth factors are all essential for most animal cells. Therefore the nutrient enrichment for eukaryotic cells has to be considered thoroughly for all essential nutrients and the final osmolarity has to be maintained near the optimal value. When the nutrients are enriched, there is generally less problems for the freely suspended cells in their access to the nutrients in the culture medium. But it is not true for immobilized cells within supporting matrix owing to the low transport rate, i.e., diffusion only, and the extremely high cell density in cell-contained matrix. Therefore convective transport in addition to diffusion would be quite beneficial for immobilized cell systems in order to ensure the sufficient supply of nutrients to the cells.

Some cell metabolic products are known on their inhibitory effects on either cell growth or productivity. For instance, organic acids produced by prokaryotic cell cultivation are known to hinder the cell growth. Lactate and ammonia produced in animal cell culture not only change the pH but also directly affect cellular functionality. Nevertheless, the

existence and accumulation of these inhibitory cell products limit cell growth and product formation, and this inhibition is more severe in immobilized cell systems owing to the diffusional-limited transport in and out of the matrix. To effectively remove the accumulated inhibitory products in cell culture, a selective and efficient convective transport is imperative, especially for immobilized cell systems.

Recently dc electric field was found to be capable of inducing convective transport within hydrogels (Grimshaw and Grodzinsky, 1990). This electric-field-induced convection might provide a solution to overcome nutrient limitation and inhibitory product accumulation in immobilized cell systems (since hydrogels are the most common supporting matrices for whole viable cell immobilization). In addition, the electrophoretic movement of the inhibitory electrically-charged products induced by the dc electric field could provide an additional mean to remove the accumulated inhibitory products in suspension cell systems.

I.3 Specific Objectives

In this research, the possibility of using enriched culture medium in the presence of a dc electrical field (i.e. electrokinetics, which is composed of electroosmosis and electrophoresis) to enhance mass transfer is explored in order to overcome the nutrient limitation and inhibitory product accumulation in various cell culture systems. The specific objectives of this study are summarized as follow:

Hydrogel-Entrapment Cell Cultures :

(1) Screening and characterization of various hydrogels.

• Screening criteria are based on the highest intra-membrane electroosmosis and the optimal biocompatibility for cell entrapment. In

addition, the factors which affect the intra-membrane electroosmosis will be investigated.

(2) Examining the electrokinetic phenomena within cell-entrapped hydrogels.

- Use of microorganisms to demonstrate the effects of augmented nutrient and waste products transport on cell growth by dc electric fields will be exaimed.
- Determining the feasibility of application of dc electric fields on entrapped hybridomas.

(3) Developing a mathematical model to integrate intraphase mass transport with cell growth kinetics to provide insights in the overall biological and engineering phenomena within the cell-entrapped hydrogel in the presence of electric fields.

Suspension Hybridoma Cultures :

(1) To study the effects of applied dc electric fields on culture medium.

- To develop methodology to maintain the chemostat of a culture medium in the presence of dc electric fields.
- To test the effectiveness of ammonia and lactate removal by applied dc electric fields in cell-free conditions and to measure their electrical mobilities.
- To determine the required dc electric current strength, based on electrical mobility measurements, for complete removal of inhibitory products, especially ammonia.

(2) Studying the toxicity of ammonia and lactate on hybridomas, and the reversibility of this toxicity by applied dc electric fields.

(3) Studying the effects of electrokinetics on batch hybridoma culture using commercially available culture medium such as DMEM.

(4) Studying the effects of nutrient enrichment together with electrokinetics on glutamine/glucose fed-batch hybridoma cultures.

- To formulate enriched culture media based on MEM composition.
- To apply higher strengths of dc electric fields in order to completely remove the cell-produced wastes.

(5) To investigate the influence of sodium butyrate on hybridoma culture.

- Using sodium butyrate to decelerate cell growth as well as nutrient metabolism and concomitantly increase specific monoclonal antibody production.

(6) To develop a mathematical model to describe overall cell growth, nutrient consumption, waste production and MAb production in electrokinetics-applied, nutrient-enriched suspension hybridoma cultures.

I.4 Thesis Organization

This thesis is organized into six sections. A review of the relevant literature is presented in Section-II, with the emphasis on cell growth kinetics and transport phenomena in both suspension and hydrogel-entrapment cell cultures, and on the applications of electric fields on biological systems. The materials and methods are summarized in Section-III. The results and discussion are presented in Section-IV which is divided into four chapters. The first chapter presents the hydrogel characterization which includes the studies of electrically-induced intra-membrane transport and hydrogel biocompatibility. The second chapter describes the effects of electric fields on cultured cells entrapped in hydrogels. A mathematical model is also developed to explain the overall phenomena within the hydrogel. The third chapter presents the characterization studies of suspension hybridoma cultures and electrokinetics, including the studies of toxicity due to lactate and

ammonia, the effects of electric fields on culture medium chemostat and the optimization of sodium butyrate feeding strategy. The last chapter describes the effects of nutrient enrichment and electrokinetics on suspension hybridoma cultures. The final two sections summarize the conclusions reached in this research and recommendations for future work.

II. LITERATURE REVIEW

II.1 General Features of Cultured Cells

II.1.1 Simple Microorganisms

Industrial microorganisms show wide diversity in metabolic activities, especially in their capabilities to produce primary and secondary metabolites. Bacteria, yeasts, and molds possess the greatest application potential (Aharonowitz and Cohen, 1981; Demain and Solomon, 1981; Cooney, 1981) in the pharmaceuticals industry. Bacteria are unicellular, prokaryotic organisms with a dimension of a few micrometer. Bacteria generally replicate by the process of binary fission, therefore they do not have a wide age distribution. Bacteria can also exist as groups or chains, e.g. streptococci (chains) and staphylococci (clusters). Some gram-positive bacteria, such as *Actinomycetes, Streptomyces and Nocardia,* grow by the process of hyphae chain elongation and branching (e.g. elongation at the tip, also called apical growth). Yeasts are eukaryotic organisms which belong to the fungi, but do not form asexual spores. The most common form of yeast division is budding fission, but mycelial growth by chain elongation and branching is also observed in some yeasts under aerobic condition. While yeasts are typically single-celled, their progeny or daughter cells often do not separate, and have a characteristic dimension of 3 to 5 μm. Molds predominantly grow by hypha chain elongation and branching. The intertwining strands of hyphae are called mycelium. In fungi, the cells may be multinucleate and may contain a variety of organelles. In submerged culture, shear forces could cause hyphae fragmentation and result in shorter but more branched mycelia. They may also form pellets, which could cause transport limitation in the pellet cores.

Microorganisms have rapid growth rates and can reach considerably high density. They are generally resistant to adverse environments, and are easily accessible as hosts for producing recombinant protein products. On the other hand, they usually lack the capability of processing protein products post-translationally, or process the protein products incorrectly (folding). Hence simple microorganisms are mostly suitable for secondary metabolites and simpler therapeutic proteins, natural or recombinant, without needing post-translational modification. The typical products include antibiotics, insulin and α-interferon etc. In these instances, high density of cells could cause severe oxygen transfer limitation, and it becomes the major concern of aerobic microbial bioreactor design.

II.1.2 Recombinant Mammalian Cells

The lack of proper post-translational processing and accurate folding of protein products in simple microorganisms makes animal cells, especially mammalian cells indispensable for the production of many therapeutic and diagnostic protein products. For instance, non-glycosylated erythropoietin (EPO) and granulocyte/macrophage colony stimulating factor (GM-CSF) are cleared rapidly from circulation *in vivo*, and the activities of improperly folded tissue type plasminogen activator (tPA) is repressed compared to that of native protein (Cumming, 1991). Consequently, mammalian cells are usually chosen to produce the more complex proteins for the pharmaceutical industry. Mammalian cells, however, do not have protective cell wall, which makes them susceptible to damage by fluid shear forces. Mammalian cells grow slowly, and their final cell density and product titer are often orders of magnitude lower than comparable microbial fermentations. In addition, mammalian cells

require complex and expensive culture medium to grow. All the above limitations create serious challenges for the biochemical engineer.

II.2 Prospects of Cell Cultures and Bioreactors

A number of bioreactor has been developed for large-scale cultivation processes. These bioreactors are divided into two categories: those in which the cells grow separately from any support, i.e. suspension cell cultures, and those in which the cells are in porous matrices or on solid supports, i.e., immobilization cell cultures.

II.2.1 Suspension Cell Cultures

The most common industrial bioreactors for cell cultures are those in which cells grow freely in suspension. They include traditional stirred-tank reactors and bubble-column reactors. The major advantages of these bioreactors are that they offer a homogeneous environment with respect to pH, dissolved oxygen, and metabolite concentrations. They can be easily monitored and controlled in various respects. Owing to their simplicity of structure and operation, they generally offer the highest reliability and remain the most popular in industry.

However, cells are freely suspended and exposed to shear forces generated by agitation and gas sparging. The weaker or shear sensitive cells, such as mammalian cells, insect cells and mycelial cells, are more susceptible to these shear force damage (Kunas and Papoutsakis, 1990; Orton, 1993). Fortunately, the levels of agitation at which this damage occurs are well above those required for adequate mixing, although the same levels could severely damage anchorage-dependent, animal cells microcarrier cultures (Croughan and Wang, 1989).

The stirred tank bioreactors are the most common industry

standard for production of therapeutics and pharmaceuticals. The multi-billion-dollared industry of antibiotics production generally has the manufacturing capacity greater than 100,000 liters (Aharonowitz and Cohen, 1981), and the stirred tank fermentors are the most commonly production units for this large-scale operation. In modern animal cell culture industry, for example, multi-thousand-litered suspension cultures for the production of monoclonal antibodies by hybridoma cell lines are routinely used through stirred-tank operation (Backer *et al.*, 1988). Mammalian cells can grow to a final density of 2-5x10^6 cells/ml in batch operational mode.

Bubble columns are cylindrical reactors in which air is sparged into the medium through a gas distributor at its base. The rising action of the bubbles creates a recirculation in the column which keeps cells suspended and environment homogeneous. Airlift fermentors are one type of bubble-column in which a concentric draft tube is inserted (Katinger *et al.*, 1979). Bubbles rise through the inner tube to create a circulating flow pattern. Airlift fermentors have been used to produce monoclonal antibodies on an industrial basis (Birch *et al.*, 1985).

Suspension cell cultures can grow but attain low cell and product concentrations in the batch mode; hence other operation modes are employed for enhancing reactor productivity. Fed-batch mode is directly achieved by simply feeding supplement medium to replenish depleted nutrients and thus maximize cell productivity (Glacken *et al.*, 1989). It is routinely used on industrial basis. Other operational modes, such as semi-continuous and continuous cultures, are used mainly as tools to determine growth kinetics as well as for production. An order of magnitude increase in reactor productivity can be achieved in continuous cultures than in batch cultures, but more complicated equipments such as cell retention

devices are required.

One internal cell retention device is the spinner filter (Varecka and Scheirer, 1987). A spinner filter is a cylindrical wire cage attached to the rotating impeller shaft. Cell-free medium is withdrawn from the center of the cage, but the fouling of the cage screen can cause serious problems (Esclade *et al.*, 1991). External tangential flow filtration is another common method for cell retention (Velez *et al.*, 1989; Maiorella *et al.*, 1991). Culture broth is recycled through the filter and a cell-free filtrate is withdrawn. One drawback is that high shear generated in the filter causes damage on animal cells. Gravity sedimentation is another alternative for cell retention. The reactor comprises a long tube in which cells can settle, and the cell-free medium can be withdrawn from the outer space between tube and reactor (Takazawa *et al.*, 1988). Other cell separation techniques that have been used include external centrifugation (Schimazaki *et al.*, 1986) and an internal dialysis membrane (Comer *et al.*, 1990).

II.2.2 Immobilization Cell Cultures

Cell immobilization can protect cells from fluid shear forces, facilitate cell/medium (Kennedy and Cabral, 1983) or product/medium (King *et al.*, 1987) separation, and increase local cell concentrations to near tissue-like densities. Therefore it is possible to operate immobilized cells in a continuous culture and to obtain higher final product titers. Furthermore, some researchers have suggested that immobilization can improve the genetic stability of hybridoma cells (Lee and Palsson, 1990) and protect cells from damage by cryogenic preservation (Kojima *et al.*, 1990). Finally, many animal cell lines need to attach on a substratum to proliferate.

The supporting matrices, however, generates a heterogeneous culture environment. This not only increases the system complexity but also limits the scalability of immobilized cell cultures. The immobilized cells are concentrated on or in the supporting matrices and the local microenvironment in which cells reside and experience are markedly different from the macroenvironment of culture. Since sensors are generally not able to measure the microenvironment, it is difficult to monitor and control cell growth, viability, and metabolite concentrations in immobilized cell cultures. The diffusion-only transport mechanism within the supporting matrices results in poor mass transfer. This restricts the nutrient supply to immobilized cells and the removal of toxic products from immobilized cells. All of these disadvantages limit the use of immobilized cell systems in industry. Immobilization cell cultures are only widely used for production of beverage, food products, and industrial products by microbial cells. Nevertheless, they have the potential to produce high-valued therapeutics by immobilized animal cells. A recent review of immobilized cell cultures can be found in a paper by Scott (1987).

Cell immobilization can be achieved by either attachment (Mattiasson, 1983; Aunins and Wang, 1989) or entrapment (Mattiasson, 1983). Many cells have the ability to adhere to other organisms (aggregate) or to solid surface (requirement for animal cells). This attachment, which may be natural or induced, can offer an inexpensive and effective method for immobilization. Entrapment holds the cells either within the interstices of porous materials, such as sponge or fibrous substance, or by the physical restrains by membranes or encapsulation with gel matrices. Hence entrapment represents a means of immobilization that does not significantly depend on cellular properties, and is by far the most popular for cell immobilization. Various types of

immobilized-cell bioreactors are reviewed by Karel *et al.* (1985). The most common ones include hollow-fiber bioreactors (Hu and Peshwa, 1991), traditional bioreactors, such as stirred-tank and bubble column, used for microcarriers (Hu and Wang, 1987), microencapsules (Posillico, 1986) or hydrogel beads (Nilsson *et al.*, 1987), and fixed packed-bed bioreactor using glass beads (Looby and Griffiths, 1988), porous ceramic beads (Park and Stephanopoulos, 1993), ceramic matrices (Lydersen, 1987; Applegate, 1991), or glass fibers (Chiou, 1992).

II.2.3 Hydrogel Entrapment of Cells

A hydrogel is defined as a polymeric material which exhibits the ability to swell in water and retain a significant fraction of water within its structure without dissolution. Hydrogels are generally porous which allows small molecules to readily diffuse within the matrices. Most importantly, hydrogels are highly biocompatible and easy to process. Currently hydrogel entrapment is the most important and widely-used immobilization technique. It has great potential for organ transplantation and drug delivery systems (Salter and Kell, 1991). Mattiasson (1983) reviewed various hydrogels for viable cell immobilization, which include synthetic hydrogels, such as polyacrylamide, polyurethane and other acryl polymers, and natural hydrogels, such as alginate, κ-carrageenan, agar, agarose, collagen and cellulose. The chemical structures of various hydrogels are summarized in Figure-2.1.

Synthetic hydrogels are generally less biocompatible owing to their unreacted toxic monomer residues and the deleterious gelling procedures. However, they possess the flexibility of being tailored for different cell lines (Sefton *et al.*, 1986). Synthetic hydrogels, especially polyacrylamide, are widely used for microbial cell immobilization. Freeman and Aharonowitz

Figure-2.1: Chemical structures of various hydrogels

Natural Hydrogels

- κ-Carrageenan

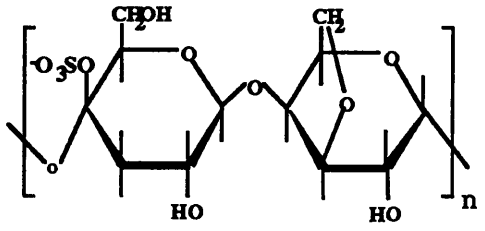

- Alginate

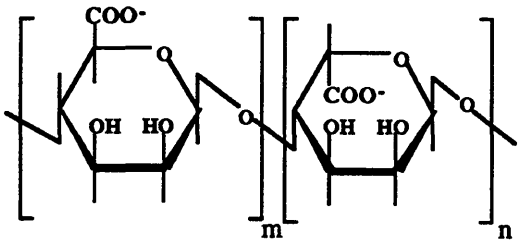

- Agarose

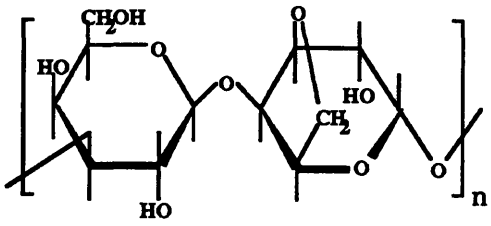

Synthetic Hydrogels

- Polymethacrylic Acid (PMAA)

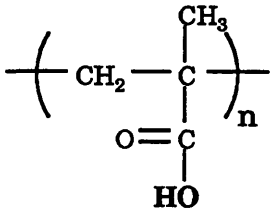

- Polydimethylaminoethyl Methacrylate (PDMAEMA)

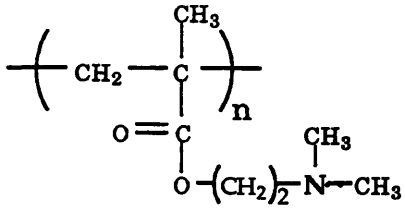

- Polymethyl Methacrylate (PMMA)

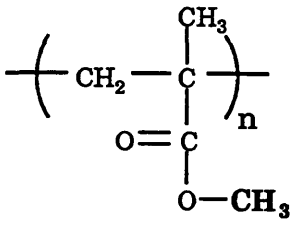

(1981) presented a mild method for immobilizing *Saccharomyces clavuligerus* cells. The cells were suspended in a solution of pre-formed, linear, water-insoluble polyacrylamide. The prepolymerized backbone polymers were then crosslinked, in the presence of viable cells, under low temperature and compatible physiological conditions, and thus avoid the contact of toxic acrylamide monomers with cells. Recently several water-insoluble acrylate-derived hydrogels were used to successfully immobilize animal cells. Sefton *et al.*, (1987) encapsulated anchorage dependent human diploid fibroblasts (HDF) and Chinese hamster ovary (CHO) cells in a polyacrylate gel blend. The encapsulated cells were viable but did not grow, presumably because of the lack of a compatible surface for adherence. Gharapetian *et al.*, (1986) developed a polyacrylate hydrogel blend for encapsulating hybridoma cells. The encapsulated cells remained viable, replicated and produced antibodies eight days after encapsulation. Although the above few immobilizations were successful, the general applicability of synthetic hydrogels to animal cell immobilization is still uncertain.

Natural hydrogels are generally obtained from cellular products and hence possess much higher biocompatibility than synthetic hydrogels. All natural hydrogels can successfully entrap microbial cells, and therefore the choice of hydrogels for microbial immobilization is based on economic concern. Alginate (Kierstan and Bucke, 1977), carrageenan (Chibata *et al.*, 1987) and agar (Toda and Skoda, 1975) are the most commonly used hydrogels for microbial immobilization. On the other hand, animal cells require more stringent environment and they have been only successfully entrapped in alginate (Bucke, 1987), agarose (Nilsson *et al.*, 1986) and collagen (Dean *et al.*, 1987). Liquid alginate gels solidify to form either microencapsules or solid gel matrices in the

presence of polycationic species such as calcium ions (Haggstrom and Molin, 1980), polylysine (King *et al.*, 1987), and chitosan is another type of natural hydrogels (Vorlop and Klein, 1987; Overgaard *et al.*, 1991). It was also shown that the permeability (molecular weight cut-off) of alginate microcapsule's membrane can be controlled by adjusting the gelation time and the molecular weight of polycationic polymer (King *et al.*, 1987). This enables the effective isolation of protein products, such as monoclonal antibody (MAb), within the microencapsules and prevents the contamination from serum proteins. With the addition of chelating agents such as EDTA, phosphate or citrate ions, alginate hydrogel can be disrupted and viable cells can be recovered (Domurado et al, 1988). It is noteworthy that phosphate ions should be absent from the culture medium if calcium-alginate hydrogels are present. Liquid κ-carrageenan gels interact with potassium ions to form solid hydrogel, and its structure strength and stability are superior to that of calcium-alginate (Arnaud *et al.*, 1989). However, κ-carrageenan is only suitable for microbial immobilization. Agarose and agar readily change from liquid to solid states by temperature reduction. Recent development in agaroses enables the gelling temperature to be reduced close to 37°C (Nilsson *et al.*, 1986). Collagen is allowed to gel when the pH is adjusted to basic value (>8.5) (Constantinides, 1980). In conclusion, all natural hydrogels are biocompatible and can be solidified through very mild procedures. Therefore animal cells are preferentially immobilized in natural hydrogels. Owing to the comparably larger pores and weaker mechanical strength of natural hydrogels, these matrices are prone to physical deterioration by hydrodynamic shear forces. Cells also tend to leak out of hydrogel matrices as they grow to high concentration (Salter and Kell, 1991).

Influences of hydrogel matrices on immobilized cells have been well studied in the past. Shirai *et al.* (1988, 1989) entrapped anchorage-dependent baby hamster kidney cells in alginate gel particles. Gelation by calcium ions results in the formation of clearly vacant spaces (referred as "channels"). The animal cells grow well three-dimensionally in the channels but proliferate little outside the channels. Therefore the alginate-gel-filled matrices actually inhibit the growth of anchorage-dependent cells. But the actual causes of inhibition are unknown. Nilsson *et al.* (1986) entrapped hybridoma cells in various concentrations, ranging from 1% to 3%, of agarose hydrogels. Cell growth was severely inhibited (reduced by 50%) at 3% of agarose hydrogel. Consequently, both alginate and agarose hydrogels have certain negative impacts on entrapped animal cells even though they are already considered the most biocompatible hydrogels.

The growth and behavior of hydrogel-entrapping cells differ from those of suspension cells. Wada *et al.* (1980) used scanning electron microscopy to investigate immobilized yeasts in alginate gel, and revealed that cell colonies assembled near the gel surface. A similar distribution of *E. coli* cells near the surface of κ-carrageenan gel was also observed by Barbotin *et al.* (1990). It was assumed that the limitation of nutrients, presumably oxygen or carbon source, and the accumulation of cellular wastes are the major causes of the uneven cell density distribution in gel. It was later theoretically calculated by Chang and Moo-Young (1988) that the oxygen penetration depths are 50-200 μm for microbes and 500-1000 μm for animal cells, respectively. Lee *et al.* (1993) observed significant increases (about 60% to 200%) in specific MAb production rate (q_{MAb}) when hybridomas were entrapped in alginate gel beads. This increase in q_{MAb} of entrapped hybridomas was reversible as hybridomas were

recovered from entrapment. Wohlpart *et al.* (1990) studied the growth and respiration of alginate-entrapped hybridomas and compared those with suspension culture. It was shown that there was no significant difference in specific oxygen consumption rate, but there was a marked reduction in growth rate. Similar results for κ-carrageenan-entrapped *E. coli* were also observed by Huang *et al.* (1990).

II.3 General Requirements of Cultured Cells

II.3.1 General Requirements of Simple Microorganisms

Common industrial microorganisms include yeasts, molds, bacteria and actinomycetes (filamentous bacteria). These microorganisms can be divided into three groups according to their oxygen requirement (Aharonowitz and Cohen, 1981; Phaff, 1981). The strict aerobes which always require oxygen to grow include prokaryotic streptomycetes and most filamentous fungi; the strict anaerobes which can grow only in the absence of oxygen are represented by bacteria *Genus clostridium*; the facultative organisms which can grow either with or without oxygen are represented by most industrial yeasts. Anaerobic metabolism is always less efficient than respiration because only part of the energy stored in the organic compounds is exploited. But anaerobic fermentation is essential for producing commodity chemicals such as organic acids and ethanol. Aerobic growth extract a maximum amount of energy from substrates for cell mass and secondary metabolite biosyntheses, and aerobic fermentation is the major way for current production of pharmaceuticals and therapeutics (McMillian, 1990).

The optimal temperatures for microorganisms are cell-strain specific, and sometimes the optimal temperature for cell growth is different from that for product synthesis (Aiba *et al.*, 1973). Most

microorganisms grow best at 25°C to 37°C, but thermophiles grow at higher temperatures: 40°C to 45°C. The optimal pH for the growth of most microorganisms is about 7.0, and most microorganisms can stand a wide range of pH variation, i.e., up to 3 pH units (Aiba *et al.*, 1973). Sometimes for the concern of highest product yield from substrate, pH might be changed from the growth optimum. For yeast and *lactobacillus* fermentations, it is desired to operate at pH 4.5. It is because that pH 4.5 completely inhibits most bacteria growth but only slightly affects yeast and *lactobacillus*, hence bacteria contamination can be largely decreased. In addition, the fast growth of microorganisms can quickly produce a large amount of metabolic intermediates which can significantly change the medium pH. Therefore an accurate and reliable pH control is crucial in microorganism fermentation.

Most unicellular microorganisms are resistant to shear forces and other hydrodynamic impacts because of their rigid cell wall structure and smaller cell sizes. But filamentous cells can be broken by vigorous agitation. This sometimes becomes beneficial to fermentation process because the pellet sizes can be reduced, and hence the transport limitation within the filamentous cell pellets is decreased (Righelato, 1975).

II.3.2 General Requirements of Mammalian Cells

Animal cells, especially mammalian cells, are industrially important because of their capability of producing active therapeutics (see "Introduction" section). The common species for deriving cell lines include amphibian, avian, fish, insect and mammal. Among them, mammalian cells are most often used for therapeutics production. Some of the mammalian cell lines frequently encountered include CHO cells (chinese hamster ovary), 3T3 cells (mouse), WI-3, MRC-5, IMR-90 cells (all human

diploid lung), and BHK-21 cells (baby hamster kidney) (McGarrity, 1979). Most primary mammalian cells are anchorage-dependent, and the transformed cell lines are anchorage-independent. Mammalian cells required serum or substituted growth factors to grow.

The optimal temperature for mammalian cell growth is 37°C, but 1 to 2°C difference from optimal growth is sometimes desirable for product formation (Sureshkumar and Mutharasan, 1990; Bloemkolk et al,, 1992). The growth and productivity of mammalian cells are not strongly affected by dissolved oxygen (DO) concentrations ranging from 15% to 100% of air-saturation (Meilhoc *et al.*, 1990), but toxicity can be encountered when DO is greater than 100% of air-saturation. The specific oxygen uptake rate (OUR) depends on the carbohydrate source. Mammalian cells can withstand only limited variation of pH, generally ±0.4 pH unit from the optimal. The optimal pH is cell-line specific and in general is between pH 6.8 to 7.5. The virus-transformed cells and human cancer cells prefer more acidic pH than fibroblast cells, and cells from monkey and rat have a broader pH range than human or mouse cells (Freshney, 1987). In certain instances the optimal pH for cell growth is different from that for product formation (Miller and Blanch, 1991). The pH of culture medium is controlled by the equilibrium relationship between $NaHCO_3$ buffer solution and CO_2 in the gas phase.

Mammalian cells do not have rigid cell wall and hence are able to stand only a narrow range of osmolarity change (± 40 mOsm/Kg from optimal value). The optimal osmolarity for mammalian cells range from 260 to 320 mOsm/Kg (Freshney, 1987). Mouse cells prefer higher osmolarity (310 mOsm/Kg) than human cells (290 mOsm/Kg). Elevated osmolarity tends to reduce cell growth but can increase the specific productivity of product formation (Ozturk and Palsson, 1991). Agitation-

related hydrodynamic forces can induce cell growth and removal of mammalian cells from microcarriers, but do not affect viable cell growth (Croughan and Wang, 1991). The relative size of an turbulent eddy in a microcarrier cell culture plays an important role, which is characterized by Kolmogorov length scale (Croughan, 1988). When the relative length scales approach one another, the greater damage occur for the microcarrier-immobilized mammalian cells. The influence of agitation on suspension cells is not as critical as that for anchorage-dependent cells. Cell damage mainly arises from the time-average flow-fields, hence the amount of damage on suspension cells increases with the increase of viscosity (Croughan and Wang, 1991). Direct bubbling is the easiest and most reliable way for oxygenation. But the bubble burst at the liquid surface causes severe cell death (Orton, 1993). The addition of pluronic acids F-68 effectively protect cells from bubble damage.

II.4 Nutrient Requirements of Cultured Cells

II.4.1 Nutrient Requirements of Simple Microorganisms

All microorganisms require adequate supply of carbon and nitrogen sources (Aiba *et al.*, 1973). Microbial cells can utilize a wide variety of carbon-sources, which includes various sugars (glucose and lactose), polysaccharides and organic compounds (methanol and glycerol). The carbon-source is mainly used for energy (ATP) production as well as for cell mass synthesis. Aerobic growth provides a more efficient incorporation of carbon-source substrate into cell mass, typically 50-55% conversion versus 10% in anaerobic fermentations (McMillian, 1990). The other major component of cell mass is nitrogen (10% of dry cell weight). Nitrogen sources include ammonia and ammonium salts, but some microorganisms have absolute requirement for organic nitrogen such as

amino acids, purines, pyrimidines, and vitamins (Aiba *et al.*, 1973). In industrial fermentations crude animal and plant extracts can provide an inexpensive supply of organic nitrogen compounds. The addition of crude extracts can accelerate the rate of microbial growth, but concomitantly complicate the downstream protein product isolation. Another important components for supporting microbial growth are the minerals. Phosphorus, potassium, sulphur and magnesium are required in a significant amount. Ion, copper, cobalt, manganese, zinc and molybdenum essentially required in trace amounts can be obtained from the impurities or other ingredients in medium (Aiba *et al.*, 1973).

II.4.2 Mammalian Cell Nutrient Requirements

A complete culture medium for mammalian cells is composed of amino acids, vitamins, inorganic salts (including buffer), sugar, organic supplements (e.g. TCA cycle intermediates, nucleotides), hormones and growth factors (supplied individually or through serum addition) (Freshney, 1987). The detailed metabolism of various nutrients is summarized below.

Glucose Metabolism

Glucose is one of the major energy and carbon sources for the biosynthesis of nucleotides, lipids, and carbohydrates (Lazo, 1981; Graff *et al.*, 1965; McKeehan, 1986; Reitzer *et al.*, 1980). Glucose is metabolized through glycolysis, pentose phosphate cycle and the TCA cycle. In the TCA cycle acetyl CoA is degraded to two CO_2 and twelve ATP molecules are produced. In addition to the major function for ATP production, TCA cycle also provides intermediates for amino acid biosynthesis. The pentose phosphate cycle is essential for nucleotide biosynthesis as well as for

NADPH production. In the glycolytic pathway, one glucose molecule produces two pyruvate molecules and two ATP molecules. Under anaerobic condition, pyruvate is oxidized to lactate for regenerating NADH for further glycolysis. Lactate is transported *in-vivo* to liver and reduced to pyruvate. In animal cell culture, however, both normal and transformed cells have high flux from glucose to lactate even if sufficient oxygen is present. Hence a large amount of lactate is accumulated in the culture medium. No conclusive explanation is available for this extraordinary high glycolytic flux. Lactate production rate can be greatly decreased by maintaining low glucose during cultivation (Glacken *et al.*, 1986; Hu *et al.*, 1987), which implies that high lactate production rate in culture might be due to the overflow of glucose metabolism (McKeehan, 1986). Another possible explanation for the lactate overproduction is to ensure optimal supply of biosynthetic intermediates (Eigenbrodt *et al.*, 1985).

Glutamine Metabolism

Glutamine is the precursor for protein biosynthesis, and the major donor of amino group in non-essential amino acid biosynthesis. Glutamine also provides the necessary nitrogen for nucleotide biosynthesis. Glutamine has been shown to be one of the major energy sources for cells in culture (Zielke *et al.*, 1984). Glutamine is metabolized through non-enzymatic degradation and glutaminolysis. Glutamine is very unstable in culture medium, and spontaneously and non-enzymatically decomposes into pyrrolidone-carboxylate and ammonia. The decomposition has been shown to be a first order reaction with respect to glutamine (Glacken *et al.*, 1986). Glutaminolysis is the pathway for oxidizing glutamine to pyruvate. The first irreversible step of glutaminolysis is the glutaminase-catalyzed

hydrolysis of glutamine to yield glutamate and ammonia. The second step of glutaminolysis is the removal of the amino group from glutamate to yield α-ketoglutarate and ammonia. This step is catalyzed by either glutamate dehydrogenase or aminotransferase. Ammonia produced by these reactions is the major source of accumulation in the culture medium.

Amino Acid Metabolism

The importance of amino acids in mammalian cell culture is well known (Eagle, 1959; Duval *et al.*, 1991; Lambert and Pirt, 1975; Lazo, 1981). Amino acids are the precursors for protein biosynthesis. Some amino acids, such as glutamine, aspartate and glycine are also used for nucleotide biosynthesis (Batt and Kompala, 1988; Kelley, 1972). Glutamine and some branched amino acids, such as leucine, isoleucine and valine can also be used as energy sources (Lazo, 1981; Miller *et al.*, 1989). There are nine essential amino acids required by cultured mammalian cells, although individual requirement of a specific cell line for amino acids vary significantly. Other non-essential amino acids are often added to compensate for a particular cell type's to meet the total biosynthetic demand. The concentrations of amino acids usually limit the maximum cell density attainable, cell survival and cell growth rate.

Vitamin Metabolism

Eight vitamins were shown to be essential for mammalian cell cultures and are supplemented in Minimal Eagle's Medium (MEM) (Eagle, 1959). Current concentrations of various vitamins are determined empirically because of shortage of available research results. Vitamins are unstable at culture condition, hence a significant amount of vitamins

is suspected to be spontaneously degraded. Vitamins are precursors for many enzymes and coenzymes. For instance, nicotinamide is the precursor for NAD(H) and NADP(H), and riboflavin is the precursor for FAD(H_2). Some vitamins, such as choline and inositol, are largely used to synthesize phospholipids for cell membranes. Vitamins limitation is usually expressed in terms of cell survival and growth rate rather than maximum cell density (Freshney, 1987).

Serum Components

Serum is often used in mammalian cell cultures ever since cell culture systems were established. Serum is expensive, inconsistent in quality between batches, and complicates downstream purification processes. Chemically defined serum-free media have been recently developed (Kitano, 1991). Serum substitutes include hormonal supplements (insulin *et al.*), growth factors (EGF, PDGF *et al.*), transport proteins (transferrin, albumin and lipoproteins), attachment factors (fibronectin and extracellular matrix *et al.*) and other miscellaneous supplements (polyamines *et al.*). The required serum substitute concentration in serum-free medium is cell-line specific and usually determined empirically.

Inorganic Salts

Inorganic salts in a basal medium includes calcium magnesium, potassium, sodium, chloride, phosphate, sulphate, and bicarbonate (Eagle, 1956; Kitano, 1991). Calcium is essential for cell attachment, and bicarbonate interacts with CO_2 in gas phase to buffer the medium pH. Most importantly, those salts contribute to the proper osmolarity of the culture medium.

II.4.3 Nutrient Enrichment for Mammalian Cell Cultures

As described in the previous section, current commercial culture media are designed empirically. Usually glucose and glutamine are the first ones to be depleted. However, accumulated cellular wastes also inhibit cell growth before depletion of nutrients. Glacken (1987) supplemented the standard DMEM with four times the standard concentrations of all amino acids, and through a fed-batch operation that maintained the glutamine limitation was able to show a significant reduction in ammonia production and a marked increase in MAb production. Jo *et al.* (1990; 1993a) fortified vitamin and amino acid concentrations by five times over the standard RPMI-1640 nutrient concentrations, and the hybridoma growth and MAb production were increased by four fold. Since the cells cultivated by Jo *et al.* possesses a extremely low specific ammonia production rate and a high ammonia tolerance (25 mM), which are very uncommon for most mammalian cell lines. This enhancements in both cell growth and productivity are suspected to be attainable in the cultures cultivating normal mammalian cells. Jo *et al.* (1993b) stepwisely increased the nutrient concentrations by five, ten and twenty times over the standard RPMI-1640 nutrient concentrations, and significant increases in cell growth and MAb production were observed in all case However, the increases were not proportional to the level of nutrient fortification. The final cell densities and MAb titers were similar in both the 10X and 20X cases, and were only 30% higher than that of 5X case. This was due to growth inhibition by accumulated cellular wastes such as ammonia.

II.4.4 Effects of Sodium Butyrate on Cultured Mammalian Cells

Sodium butyrate, a pharmacological agent, at millimolar concentrations can produce many morphological and biochemical modifications on cultured cells. These include arrest of cell proliferation, induction of protein synthesis, inhibition of cell differentiation, and reversion of transformed characteristics of cells to normal behaviors (Kruh, 1982). Generally speaking, a hyperacetylation of histone resulted from an inhibition of histone deacetylase by sodium butyrate weakens the electrostatic interactions with the DNA strands. This decrease in interaction between histone and DNA is believed to increase DNA accessibility and to potentiate its template functions (Boffa *et al.*, 1981; Kruh, 1982; Parker *et al.*, 1987). Sodium butyrate is best known for retarding cell growth with a concomitant increase in protein synthesis (Kooistra *et al.*, 1987; Nathan *et al.*, 1990; Palermo *et al.*, 1991; Oh *et.al.*, 1993). Therefore sodium butyrate could decelerate cell metabolism, i.e., decrease metabolite consumption/production rates, but stimulating protein synthesis. Sodium butyrate, therefore, has the potential to prolong cell longevity by decreasing waste accumulation during culture.

II.5 Cellular End Product/Waste Inhibition

II.5.1 End-Product Inhibition on Simple Microorganisms

Many microbial fermentations, especially anaerobic processes, face the problem of end-product inhibition. End-product inhibition is best known in alcohol and organic acid fermentations. The toxic effects of ethanol on yeasts have been extensively studied (Ghose and Tyagi, 1979). It was shown that the inhibition results in a low final product concentration of ethanol (3-4%) (Avgerinos, 1982). Herrero (1983) found that the fatty acid composition of *C. thermocellum* membranes is altered in the presence of ethanol. This alternation might play a role in growth inhibition by reducing the activity of glycolytic enzymes associated with

the membranes. Wang and Wang (1984) have elucidated the inhibitory effects of acetic acid on the growth of *C. thermoaceticum*. They have found that the undissociated form of acetic acid is much more toxic than the ionized acetate ion. Similar inhibitory effects were observed in lactate fermentation by *Lactobacillus delbrueckii* (Yabannavar, 1988). There have been several papers on the mechanisms of inhibition by organic acids (Cobley and Cox, 1983; Bender and Marquis, 1987). Organic acids are known to allow protons to enter the cell and thus they counteract the action of proton pumps. Consequently, organic acids interfere with the maintenance of the proper pH gradient across the cell membrane. Cells attempt to counteract this alternation in pH by consuming as much energy as needed in membrane energization. The increased consumption of energy by the cell at the membrane level in the presence of organic acids can result in less ATP available for biosynthesis and thus inhibit cell growth.

In anaerobic *E. coli* fermentation using glucose, the typical end-product composition is summarized in Table-2.1 (Morris, 1985; Ataai and Shuler, 1985; Karel and Robertson, 1989). The major products of anaerobic fermentation of *E. coli* are ethanol, lactate, acetate, formate, ethanol, CO_2, and H_2, and the minor product is succinate. All the above organic acids and ethanol can inhibit *E. coli* growth. In aerobic *E. coli* fermentation using glucose, the cells use oxygen as terminal electron acceptor and therefore glucose can completely assimilated to CO_2 (Payton and Haddock, 1985). When *E. coli* grows on a high glucose concentration and at a high growth rate, the glucose can repress cell growth and some metabolic intermediates are produced as an alternative electron acceptor. This is known as Crabtree effect. These metabolic intermediates often inhibit *E. coli* growth.

Table-2.1: Products from anaerobic *E. coli* fermentation*

1.0 mol glucose was metabolized:

- 0.84 mol used for producing primary metabolites and energy
- 0.16 mol used for cell mass synthesis

Compounds	Quantity (mol)
Proton	2.4
Acetate	0.8
Formate	1.4
Ethanol	0.8
Lactate	0.1
Succinate	0.05
ATP	2.5

* Condensed from Karel and Robertson (1989)

II.5.2 Waste Product Inhibition on Mammalian Cells

Ammonia and lactate are the major inhibitory waste products in mammalian cell cultures. Ammonia is produced by glutaminolysis and by non-enzymatic degradation of glutamine. Concentration of ammonia in cell culture is determined by the mode of reactor operation, type of cell line and glutamine concentration (Butler and Spier, 1984). Most of the studies in the past emphasized the inhibition of ammonia on cell growth. Although ammonia inhibited cell growth in many reported studies, the sensitivity of the growth rate to ammonia concentration varied among the cell lines (Glacken, 1987; Miller *et al.*, 1988a; Ozturk *et al.*, 1992). Ammonia concentration in the range of 2 to 10 mM was shown to inhibit cell growth by 50%. The effects of ammonia on metabolic rates and cell productivity have been also studied but the results varied significantly. Glacken (1987) reported a decrease in specific antibody production in response to increasing ammonia concentration. However, McQueen and Bailey (1991) did not observed any change in specific antibody production as a result of ammonia addition. The influences of metabolic rates of various nutrients by added ammonia were studied by Miller *et al.* (1988a) and by McQueen and Bailey (1991), but no conclusive results were obtained. The toxicity of ammonia is believed to arise from its lysomotrophic property, i.e., an increase of intracellular pH, especially the lysosomal pH, in response to the addition of ammonia (Adema ,1989; Doyle & Butler, 1990). By varying the pH in the culture medium it can be shown that the toxicity is proportional to the ammonia molecule (NH_3), rather than ammonium cation (NH_4+).

Lactate is mainly produced from glycolysis, but can also be produced in small amount from glutamine metabolism. The concentration of lactate in mammalian cell culture depends on the glucose concentration, types of

cell line, and mode of bioreactor operation. In the batch mode, lactate concentration can be as high as 35 mM (Ozturk *et al.*, 1992). Lactate inhibition to mammalian cells is attributed to medium acidification during glycolysis. The tolerance to lactate varies markedly among different cell lines (Glacken, 1987; Miller *et al.*, 1988a). Generally 20 to 40 mM lactate can reduce cell growth by 50%. The changes of metabolic rates are much less than the changes of cell growth in response to the addition of lactate. In addition, the large quantity of lactate accumulated in the medium can significantly change the medium osmolarity.

II.5.3 *In-Situ* Removal of Cellular End Products/Wastes

Organic acids and alcohol produced by fermentation can be continuously removed through various methods. Ethanol can be removed from cell broth by vacuum fermentation (Cysewski and Wilke, 1977) or flash fermentation (Ghose et al, 1984). But these methods are only limited to the products which are more volatile than water, and not applicable to organic acids. An alternative way to remove ethanol is by adsorption. Wang *et al.* (1981) used activated carbon to remove ethanol in a yeast fermentation. The toxicity of absorbent and non-specific adsorption of other materials have been shown to be potential problems. Organic acids can be removed *in-situ* by the use of anion exchange resins (Tangu and Ghose, 1981; Srivastava *et al.*, 1992). The release of toxic ions from resins, non-specific ion-exchange, and high cost of ion-exchange resins are the major disadvantages of this process. Dialysis has also been reported to separate organic acid products (Friedman and Gaden, 1970). Another method of product removal is by liquid-liquid extraction (Yabannavar, 1988). Solvent toxicity is the major problem, and the efficiency of acid extraction is rather poor. The uses of membranes (Matsumura and Markl,

1986) and hydrogel entrapment (Yabannavar, 1988) to separate the solvent from the cells help to overcome the problem of solvent toxicity.

Recently electrodialysis was applied for separating organic acids from cell broth *in-situ* (Nomura *et al.*, 1987, 1988; Ishizaki *et al.*, 1990). The separation of acids and control of pH can be achieved at the same time. A significant increase (more than 5 times) in lactic acid production was achieved through the use of electrodialysis (Hongo *et al.*, 1986). Fouling of anion-exchange membranes by cells was observed to be a problem, but was avoided by cell immobilization (Nomura *et al.*, 1987). Scalability is another potential problem for electrodialysis fermentation. The electrodialysis technique has been only applied to microbial fermentation.

Hecht *et al.* (1990) used a hollow fiber supported gas membrane to remove ammonium from a 10-litered antibiotic fermentation. Both the cell growth and antibiotic production were increased by several fold. Piskin and Chang (1981) flushed an air stream to successfully remove urea and ammonia from cell-free dialysate in an oxygenator. The ammonia removal rate increased with increasing either the dialysate flow rate or the air flow rate.

The removal of cellular wastes from mammalian cell culture is much more challenging because of the stringent requirement of the culture medium and the higher sensitivity of mammalian cells to changes in the environment. Although *in-situ* removal of lactate has been successfully achieved through various approaches in microbial processes, little success has been obtained in applying these techniques to mammalian cell cultures. Masayoshi *et al.* (1990) attempted to use inorganic absorbent to remove ammonium from hybridoma culture. Owing to the toxicity of the absorbent, little success was observed. The only technique successfully developed for *in-situ* removal of mammalian

cell wastes is dialysis (Kasehagen *et al.*, 1991; Linardos *et al.*, 1992). Dialysis tubing with a low molecular weight cut-off (MWCO) membrane was coiled inside a hybridoma cell bioreactor. Fresh medium containing no serum passed through the tubing. The low molecular weight inhibitors, such as lactate and ammonia were removed, while essential nutrients were replenished and high molecular weight protein products remained in the bioreactor. The final protein titer in dialysis culture was several fold greater than that in a typical batch culture. Recently, a biological approach for medium ammonia detoxification was reported by Bebbington *et al.* (1992). A glutamine synthetase (GS) -contained vector was transfected into myeloma cells. The GS catalyzes the formation of glutamine from ammonia and glutamate. The successful transfectants can proliferate in a glutamine-free medium. Although GS was used primarily as a amplifiable selectable marker for transfection in this study, it is capable of completely prevent the formation of ammonia through cellular metabolism.

II.6 Mass Transfer in Bioreactors

II.6.1 Mass Transfer in Solution

The mass transfer phenomena in submerged fermentation processes with freely suspended cells has been well studied (McMillan, 1990; Bailey and Ollis, 1986). In submerged aerobic fermentation, the dissolved oxygen concentration is rather low, usually less than 10 mg/L. Oxygen solubility can be increased by 10 to 20 fold by the addition of hexadecane (Ju and Ho, 1989; Ho *et al.*, 1990) or perfluorocarbon (Junker *et al.*, 1990; McMillan, 1990) to aqueous medium. In addition, the diffusivity of oxygen is also increased by about one fold in the presence of these organic solvents.

The oxygen transfer from the gas phase to the cells is controlled by

mass transfer resistance at the liquid-gas interface (Wang *et al.*, 1979). The volumetric mass transfer rate, N_A (mM/hr), can be described by eq (2.1),

$$N_A = k_L a\,(C^*-C_L) \quad \text{----------(2.1)}$$

The overall volumetric mass transfer coefficient in liquid phase, [$k_L a$ (1/hr)], can be enhanced by increasing impeller agitation speed (rpm), gas power input per unit volume (Watt/m^3), and the superficial gas velocity (m/hr).

II.6.2 Mass Transfer in Hydrogels

The mass transfer behaviors in cells-entrapped hydrogels include interphase and intraphase processes and have been reviewed by Radovich (1985). The interphase mass transfer includes all the transport resistances which bring substrates to, or remove products from, the surface of the hydrogel matrix. The intraphase mass transfer occurring in hydrogel matrix is usually quantified through the analysis of diffusion and reactionin porous media. This analysis results in an effectiveness factor, which is defined as a ratio of the actual reaction rate to the reaction rate which would occur if all the interior of the biocatalyst particle was exposed to the same reactant concentration as the exterior of the particle. Satterfield (1970), and Klein and Vorlop (1983) presented the quantitative estimation of the effectiveness factor in term of a Thiele modulus, which is a product of a length parameter (the ratio of the particle's volume to surface area for diffusion) and a diffusion-reaction parameter. A significant intraphase convection induced by interphase convection is only present in macroporous particles (pore size larger than 10 μm), such as mycelial pellets and ceramic beads (Stephanopoulos and Tsiveriotis, 1989; Park and Stephanopoulos, 1993). In hydrogel systems only the

mechanism of diffusion is considered and the intraphase mass transfer is independent of interphase mass transfer.

There have been a number of papers investigating the effective diffusion coefficients of various chemicals in hydrogel matrices. Margaritis *et al.* (1986) measured glucose diffusivity in calcium-alginate by a radioactive tracer technique and showed that the diffusivity is about 80% of that in water. Hannoun and Stephanopoulos (1986) investigated the diffusion coefficients of glucose and ethanol in cell-free and cell-occupied calcium-alginate membranes. Their results indicated that the diffusivities in 2% Ca-alginate are about 10% lower than that in water. Kurosawa *et al.* (1989) measured the oxygen diffusivity in the Ca-alginate gel beads which had entrapped yeast cells. They found that the oxygen diffusivity ranged from 2.1 to 2.5×10^{-5} cm^2/sec, which is about 80 to 99% of that in pure water. Nguyen and Luong (1986) measured the diffusivity of glucose in κ-carrageenan gels. They concluded that these diffusivities are smaller than in water and they decrease with increases in gel concentrations. They found that glucose diffusivity in water was 6.8×10^{-6} cm^2/sec, whereas the diffusivity in 4% κ-carrageenan gel was about 4.2×10^{-6} cm^2/sec. Bassi *et al.* (1987) measured effective diffusivities of lactose and lactic acid in 3% agarose gel membrane. They reported that the lactose diffusivity is about 4×10^{-6} cm^2/sec and the lactic acid diffusivity is about 2.7×10^{-6} cm^2/sec in the 3% agarose gel.

The intraphase mass transfer coupling with viable cell kinetics has been experimentally and theoretically quantified in the past. Chang and Moo-Young (1988) estimated the oxygen concentration profiles in cell-entrapped gels. They defined an oxygen penetration depth, i.e., a distance from gel surface at which oxygen concentration decreases to zero. They assumed a homogeneous cell distributions in the gel, constant specific

oxygen uptake rates and an effective intraparticle oxygen diffusivity. It was shown that the oxygen penetration depth is 50-200 μm for microbial cells and 500-1000 μm for animal cells. As discussed earlier, entrapped cells preferentially grow near the gel surface. Hence the assumption of homogeneous cell distribution is not realistic and errors shall be expected under this assumption. Hooijmans *et al.* (1990) used an oxygen microsensor to measure the oxygen concentration profile in *E. coli*-entrapped κ-carrageenan gel beads and slabs. They found that the oxygen penetration depth was 100 μm, and in the early phase *E. coli* growth was not significantly affected by the gel matrix. Wittler *et al.* (1986) used an oxygen microprobe to measure the oxygen penetration depth in *Penicillium* pellets and the oxygen concentration profiles near the pellet surface. They found that the oxygen penetration depth was 150 μm and the oxygen was completely depleted in the pellet core (typically the diameters of pellets range from 1.5 to 2.5 mm). The oxygen supply to the surrounding liquid-interphase near the pellet shows no severe limitation, i.e., no obvious oxygen gradient was observed near the interface. These experimental results agreed quite well with the estimated oxygen penetration depths even though homogeneous cell distributions were assumed.

II.7 Electrically-Augmented Transport

II.7.1 Electrically-Induced Convection in Solution

Electrically-induced convection of charged macromolecules, cells and ions in solution is associated with electrophoresis, which has been known for decades. Electrophoresis is the phenomena that involves charged particle migration in an electric field. The electrophoretic velocity, v, is equal to the force on the particle (charge, Q, times field

strength, E) divided by the friction constant, f. We can express the electrophoretic mobility, u, as:

$$u = v/E = Q/f \qquad \text{----------(2.2)}$$

This description, however, neglects the fact that the countercharge, -Q, near the particles can generate a substantial counterforce and thus reduce the electrophoretic mobility. Overbeek and Bijsterbosch (1979), and Grimshaw (1989) described some theoretical approaches to calculate electrophoretic mobility.

II.7.2 Electrically-Induced Permeability Change and Convection in Hydrogels

Hydrogel membranes whose permeability can be controlled electrically or chemically were studied by Weiss *et al.*(1986), Grodzinsky and Weiss (1985). They concluded that membrane permeability to neutral or charged solutes can be changed through the alteration of effective pore size of the membrane, and by electro-diffusion caused by an intra-membrane ionic gradient which can be electrically (by transmembrane electric field) or chemically (by cross-membrane pH difference) induced. The magnitudes of changes in permeability depend greatly on the relation between solute size and membrane equivalent "pore size" (membrane hydration) for solutes up to 6000 daltons in molecular weight. Pasechnik and Alimardanov (1979) modified the permeability of proteins in an ultrafiltration membrane by the application of a trans-membrane electric field. Radovich and Sparks (1980) studied an electrophoretic technique for the ultrafiltration of charged macrosolutes, such as proteins. In their study, the applied electric field controlled the build-up of retained macrosolutes at the membrane surface. Resultant fluxes were 75% to 500% higher than the normal ultrafiltration flux. Selectivity was also

improved by 2 to 6 fold for the separation of protein solutions. Burgmeyer and Marray (1982) studied an "ion gate membrane." In this membrane the voltage-controlled electrochemical reaction within a poly(pyrrole) redox membrane cast on a gold grid changed the permeability of the membrane to certain ions.

Eisenberg and Grodzinsky (1984) reported that an applied transmembrane electric field is able to alter intramembrane ionic profiles in collagen membranes via an electrodiffusion mechanism. This change results in part from a change in the restricted diffusion of solutes within the membrane. Bhaskar *et al.* (1985) applied a transmembrane electric field to a thin liquid crystalline membrane, and found that the permeability of the membrane for small organic permeants was increased by 50 to 60%.

All the above studies on electrically-controlled transport in hydrogel membranes focused on specific transport mechanisms. These studies were generalized by Grimshaw (1989) and Grimshaw *et al.* (1989), who studied the transport of fluorescently-labelled proteins through uncharged polyacrylamide (PA) and the charged polymethacrylic acid (PMAA) membranes. It was found that dynamic control of protein transport can be achieved through the modulation of electrical forces which directly alter solute flux and membrane microstructure. They also identified four distinct mechanisms for controlling solute flux: (1) Electromechanical deformation of the hydrogel membrane: because of a change in the ionization state of the polyelectrolyte hydrogel; (2) Electrophoretic migration of "charged" solutes within the hydrogel membrane: effective only for charged solutes and independent of hydrogels; (3) Electroosmotic solvent flux within the "charged" hydrogel membrane: effective only for charged hydrogels and independent of solutes; (4) Electrostatic

partitioning of charged solutes into charged membranes which could vary the solute concentration gradient within hydrogel membrane. The detailed theoretical considerations and explanations of electrically-induced intraphase mass transfer will be discussed in Section-III.

According to the above results, convective solute transport through hydrogels can be induced through the modulation of trans-membrane electric field. For neutral solutes such as dissolved oxygen and glucose, the augmentation of transport across a "charged" hydrogel is achieved mainly by the electroosmotic solvent flux. For charged solutes, such as ammonium, lactate and organic acid ions, the augmentation of transport across the "charged" membrane is due to the integrated effects of the above four electrically-induced transport mechanisms. Electroosmotic flow has the potential of providing the most significant transport augmentation in "charged" hydrogels, either cationic or anionic. By selecting and optimizing hydrogels (i.e., type, composition, and matrix density of hydrogel), and by choosing the operating conditions (such as applied current density), the maximum attainable intraphase convective flow can be obtained. This electrically-induced intraphase convection in hydrogels, which can not be obtained by any other approach, may offer a potential solution to overcome the mass transfer limitation in cell-entrapped hydrogels.

II.8 Effects of Applied Electric Fields on Cells

Studies of the influences of applied electric fields on cells were initially motivated by the naturally existing electric fields *in-vivo*. Cells within mammalian connective and skeletal tissues are regularly exposed to time-varying electric currents. These currents may well regulate growth and remodelling of tissues and alter cellular functions.

It is well known that electrical stimulation (around 20 μAmp of dc electric fields) can accelerate the healing of defects in bone and tendon (Friedenberg et. al., 1971; Lavine et. al., 1972; Miller et. al., 1984; Robinson, 1985). Luther and Peng (1983) applied a dc electric field (5 to 15 V/cm) to study the galvanotropic response of cultured Xenopus epithelial cells. They detected the changes in the cell axis as well as redistribution of a band of actin. Onuma and Hui (1986) studied electric field-induced (10 V/cm, 2.5 to 5 mAmp) cell shape changes and preferential orientation of mouse embryo fibroblast. They found that this response required a calcium influx across the plasma membrane. Cooper and Schliwa (1985) examined the motility of fish epidermal cells in the presence and absence of a dc electric field. With 0.5-15 V/cm of dc electric fields, single epidermal cell, cell clusters, and cell sheets migrate toward the cathode. But cell clusters and sheets break apart into single migratory cells in the upper range of these electric field strengths.

Finaz *et al.* (1984) used successive electric pulses of about 1.5 KV/cm (50 μsec duration) to induce cell fusion known as electrofusion. Tonequzo *et al.* (1986) described the technique of "electroporation." The cell suspension exposed to a brief electric impulse results in the transfer of DNA into cells. This DNA entry is believed to occur via local areas of reversible membrane breakdown (pores) created by the external electric field of about 3.8 KV/cm. Wollheim *et al.* (1987) investigated the regulation of exocytosis in electrically-permeabilized insulin-secreting cells. The cells were exposed to high voltage discharge (3 KV/m) for membrane permeabilization, and the overall structure of cells was preserved after permeabilization. In this preparation insulin secretion was stimulated by calcium ions. This membrane permeabilization is highly reproducible and does not perturb the membranes of intracellular organelles.

MacGinitie *et al.* (1987) studied the possible roles of endogenous and applied electric currents (less than 1.2 mA/cm^2) on the biosynthetic behavior of connective tissues. Electric currents were applied over a wide range of amplitudes and frequencies. MacLeod *et al.* (1987) examined the effects of electric currents (0.1 to 1 mA/cm^2) on protein biosynthesis in mammalian fibroblast. The modulation of proline incorporation into extracellular and intracellular proteins by electric fields with frequency ranging from 0.1 to 1000 Hz was measured. These studies demonstrated that electric currents at physiological strengths can stimulate alternations in biosynthesis and therefore may influence tissue growth, remodelling and repair. Suzuki *et al.* (1986) used electric fields (rectangular pulse with strength of 40 V/cm and frequency of 5 KHz) to activate the metabolic activities of hybridoma cells and increase MAb production. It was found that after 48 hours of incubation, the concentrations of lactic acid and MAb were approximately 30% and 10% higher than the control respectively, with a concomitant 16% increase in cell concentration. Longer periods of electric pulse application, however, caused an inhibitory effect on the cell growth. It was assumed that reactive oxygen species such as superoxide and hydrogen peroxide generated by electrophoresis cause this inhibition. Kojima *et al.* (1992) cultured human carcinomas on the surface of a platinum-coated electrode for four days. A low dc voltage of constant potential, ranging from 0.2 to 0.4 V, was applied to modulate carcinoembryonic antigen (CEA) production. The secreted CEA was over twice the amount produced in normal culture. Lyte *et al.* (1991) cultured mouse lymphomas on a platinum-coated plate in the presence of low-level constant direct currents. Enhancement of growth was observed over the range of 0.1 to 10μAmp, and suppression was observed when higher than 10 μAmp.

As a conclusion, applied electric fields can influence cultured cells in different ways. They can change the shape and motility of the cells, generate local areas of membrane breakdown for electrofusion and electroporation, affect the cell biosynthetic processes, and even cause lysis of cells. These effects depend on the frequency and amplitude of the electric fields as well as the cell lines.

II.9 Mathematical Modeling of Cell Growth and Metabolism

Immobilized microbial fermentation has been thoroughly investigated in the past. Melick *et al.* (1987) developed a mathematical model for ethanol production in a packed bed fermenter containing *Zymomonas mobilis* entrapped in spheres of calcium alginate. Luong *et al.* (1985) modeled ethanol fermentation with *Zymomonas mobilis* entrapped in potassium-κ-carrageenan. Their model, based on extended Monod kinetics, also considered product inhibition. Brink and Tramper (1986) modeled the effects of mass transfer and product inhibition on the kinetics of propene epoxidation by immobilized *Mycobacterium* cells. They concluded that substrate diffusion in gel matrix was the limiting factor. Yabannavar (1988) studied the extractive fermentation of lactic acid by immobilized *Lactobacillus delbrueckii* in κ-carrageenan gel beads. The production of lactic acid by the bacteria was accompanied by its dissociation to form lactate and proton. The intraphase effective diffusivities were used to account the mass transfer limitation. Product inhibition was accounted for by an experimentally-obtained inhibitory function. This inhibition was incorporated into Monod growth kinetics. This simulated results agreed well with the experimental findings.

Kinetic modelling of hybridoma cell growth and immunoglobulin (Ig) production was conducted by various investigators. Bree *et al.* (1988),

Glacken (1987), and Miller *et al.* (1988a, 1989) developed unstructured models based on Monod kinetics. The specific growth and death rates, and the specific MAb production rate were found to be functions of glutamine, glucose, ammonia and lactate concentrations. The kinetic parameters can only be obtained experimentally. The results also suggested that Ig production is non-growth associated. The structured models require an understanding of detailed cell metabolism and regulation. Several simple structured models have been developed. Suzuki *et al.* (1988) proposed that hybridoma cells arrested in the G1 phase of cell cycle produce considerably higher Ig, while the times the cells traversed the S, G2 and M phases Ig production is approximately constant. Based on this model, methods to arrest cells in the G1 phase might be able to yield higher Ig production rates. Such methods could include exposure of cells to drug (e.g. thymidine) and stresses (e.g. oxygen depletion and osmolarity elevation). This hypothesis, however, needs further testing. Savinell *et al.* (1989) examined the maximum Ig rate of synthesis, based on the rates of mRNA synthesis, the velocity of RNA polymerase II and the spacing of the nucleotides. Bibila and Flickinger (1991) developed a structured unsegregated model to describe Ig synthesis based on the intracellular balances of heavy and light chain coding mRNAs, the intracellular balances of heavy and light chains, and the description of the kinetics of heavy and light chain assembly. More complex structured models were also introduced in order to understand the detailed cell behavior. Of particular interest is the regulation of carbon flow from the glycolytic and glutaminolytic pathways through the TCA cycle and to the formation of various amino acids (Kell and Westerhoff, 1986; Zupke, 1993). These studies intended to identify the rate-controlling pathways and steps in a complex metabolic network. The development of a complete kinetic

description of all enzymes in the metabolic pathway is likely to be a formidable task. Although this has been attempted for simple microorganism such as *E. coli*, the large number of constants involved and the coupling of the resulting mass balances present difficulties and questionable reliability of the predicted results.

III. MATERIALS AND METHODS

III.1 Cell Strain (Line) and Stock Culture Maintenance

III.1.1 *Escherichia coli*

E. coli was obtained from American Type Cell Collection (ATCC, Rockville, MD) and is designated ATCC-15224. Stock cultures are maintained on agar slants at 4°C, and are transferred monthly. Luria-Bertani (LB) agar medium (Maniatis *et al.*, 1982) was used for strain propagation.

E. coli ATCC-15224 is a prototrophic, gram-negative, facultative anaerobic capable of rapid growth on defined minimal medium. This strain produces constitutively β-galactosidase. Cell mass is the major product during aerobic cultivation, although small amounts of mixed acids, primarily acetate, are secreted during aerobic growth. Cell mass, mixed organic acids and alcohols are the major products during anaerobic cultivation.

III.1.2 Hybridoma Cells

Suspension and entrapment of hybridoma cells were performed using ATCC-CRL-1606, a BALB/c mouse hybridoma, a cell line producing anti-human-fibronectin IgG monoclonal antibody (Schoen *et al.*, 1982). The kinetics of growth and antibody production have been studied by Glacken *et al.* (1989). A 1 ml aliquot of hybridoma cells was obtained frozen at an unknown passage number. The culture was thawed rapidly and diluted 20-fold in Dulbecco's Modification of Eagle's Medium (DMEM, Sigma Chemical Co., St. Louis, MO, Cat#9161) supplemented with 10% (v/v) fetal bovine serum (FBS, Sigma Cat#F4884, Lot#48F-0026) and 6 mM of glutamine (Sigma). Cells were propagated at 37°C for 7 days in a 10%

CO_2 incubator, and diluted as necessary to maintain the cell concentration below $1x10^6$ cells/ml. For long term cell stock maintenance, cell density less than $1x10^6$ cells/ml were centrifuged at 200 g for 10 minutes and resuspended in DMEM supplemented with 20% (v/v) FBS and 10% (v/v) dimethyl sulfoxide. One-ml aliquots of the suspension were slowly frozen to -70°C. The frozen aliquots were then transferred to liquid nitrogen for long term storage.

For each culture, a new aliquot was thawed rapidly and propagated in DMEM supplemented with 5% FBS, 6 mM glutamine, 25 units/ml penicillin, 25 μg/ml streptomycin, and 50 μg/ml neomycin (Sigma, Cat#9032). Cells were maintained at 37°C in a 10% CO_2 incubator. Cells were diluted during their exponential growth phase by seven- to ten-fold every 2-3 days. Cell viability was maintained at greater than 95%, and only cells that had been maintained in propagation for less than one month were used in subsequent experiments.

III.2 Preparation of Culture Media

III.2.1 Culture Media for *Escherichia coli*

An enriched culture medium, designated SLB, was used for cultivating *E. coli* ATCC-15224. The composition of SLB broth is shown in Table-3.1. All nutrient concentrations in SLB broth were increased one- to two-fold above those of the normal LB broth. SLB/KCl broth, which was SLB broth supplemented with 0.32% (w/v) KCl, was used only in κ-carrageenan entrapment experiments.

Table - 3.1 : The compositions of LB, SLB and SLB/KCl broths

Reagents	LB (g)	SLB (g)	SLB/KCl (g)
Glucose	1	20	20
Tryptone	10	20	20
Yeast Extract	5	15	15
NaCl	10	5	2.5
KCl	N/A	N/A	3.2
Deionized Water	1000 (ml)	1000 (ml)	1000 (ml)

III.2.2 Culture Media for Hybridoma Cells

Basic Culture Media

Two types of basic media, DMEM and XMEM, were used for the propagation of hybridoma cell stock: the early studies of suspension hybridoma cultures with applied dc electric fields, and the entrapment hybridoma cultures. Unless otherwise specified, the medium was purchased from Sigma Chemical Co. in liquid form. The composition and supplemented components in DMEM have been described earlier in section 1.2. XMEM was formulated using DMEM powder (Sigma Cat#D5030), which is deficient in sodium bicarbonate, glucose, glutamine and phenol red. This DMEM powder was reconstituted with an adequate amount of deionized water supplemented to 4 mM $NaHCO_3$, 10 mM HEPES, 25 mM of glucose, 6 mM glutamine, 5% FBS, 15 mg/L phenol red, 25 units/ml penicillin, 25 μg/ml streptomycin and 50 μg/ml neomycin. The liquid medium was sterilized by filtration through 0.22 μm filter paper. The XMEM is designed to be pH-buffered by normal air without CO_2, as constrast to normal DMEM which is buffered by CO_2-rich air.

Enriched Culture Media

The enriched media for certain fed-batch hybridoma cultures were formulated after fortifications of all essential and non-essential amino acids and vitamins in DMEM. The increase in these nutrient concentrations will result in an increase in the osmolarity if the other components in DMEM remain unchanged. In order to maintain the desired osmolarity, the concentration of sodium chloride was decreased to compensate for the elevation in osmolarity. Other inorganic salts were the same as those in DMEM. To formulate the enriched media, four stock solutions were first prepared. These stock solutions were prepared as concentrated solutions based on the formulae for Minimum Essential Medium (MEM). The first one was a 50 times concentrated, essential amino acid stock solution (Sigma Cat#M7020). The second was a 100 times concentrated, non-essential amino acid stock solution (Sigma Cat#M7145), and the third was a 100 times concentrated, vitamin stock solution (Sigma Cat#M6895). The fourth was a 10 times concentrated, inorganic salt stock solution, which included $CaCl_2$, KCl and $MgSO_4$. To avoid precipitation, NaH_2PO_4 and $NaHCO_3$ solutions were prepared separately from the other salts. All chemicals were purchased from Sigma Chemical Co.. The NaCl concentration in the medium was calculated such that the total concentration of all of the solutes (approximately equal to the osmolarity) was maintained at 300 mM. In addition, 2.5 M glucose and 200 mM glutamine stock solutions were also used to prepare the enriched media. The formulae for these stock solutions are shown in Table-3.2.

There were two types of enriched media, and these were designated as f5MEM and f10MEM. All amino acid and vitamin concentrations were five and ten times concentrated than those in MEM for f5MEM and f10MEM, respectively. Since the nutrient concentrations in DMEM were

Table-3.2: Formulas of various stock solutions for enriched media

Essential Amino Acid Stock Solution (50 X)*

Components	(mM)
Arginine	30.0
Cystine	6.2
Histidine	10.0
Isoleucine	20.0
Leucine	20.0
Lysine	20.0
Methionine	5.1
Phenylalanine	10.0
Threonine	20.0
Tryptophan	2.5
Tyrosine	10.0
Valine	20.0

Non-Essential Amino Acid Stock Solution (100 X)

Components	(mM)
Alanine	10.0
Asparagine	11.4
Aspartic Acid	10.0
Glutamic Acid	10.0
Glycine†	10.0
Proline	10.0
Serine†	10.0

Vitamin Stock Soln (100 X)

Components	(mM)
Choline	0.72
Folic Acid	0.23
Inositol	1.1
Nicotinamide	0.82
Pantothenate	0.42
Pyridoxal	0.49
Riboflavin	0.03
Thiamine	0.30
NaCl	145.5

Salt Stock Solution§ (10 X)

Components	(mM)
CaCl2.2H2O	18.00
KCl	53.70
MgSO4.7H2O	7.70

Misc. Stock Solution

Components	(mM)
NaCl	445.0
NaHCO3	440.0
NaH2PO4	9.1
Phenol Red	11.2
Glutamine	200.0
Glucose	2500.0

* Glutamine is prepared separately at 200 mM
† Additional glycine was added in both f2DMEM and f5DMEM
§ NaCl, NaHCO3 and NaH2PO4 were prepared separately

twice as that in MEM, the nutrient concentrations in f5MEM and in f10MEM were approximately 2.5 times and 5 times those in DMEM, respectively. The initial glucose and glutamine concentrations were 25 and 6 mM, respectively. All enriched media were also supplemented with 5% (v/v) FBS, 25 units/ml penicillin, 25 μg/ml streptomycin and 50 μg/ml neomycin.

A supplemental medium was prepared and used for nutrient replenishment in hybridoma fed-batch cultures. This supplemental medium contained all amino acids (20 times in concentration), vitamins (40 times in concentration), phenol red, NaCl, $NaHCO_3$ and FBS, but excluded all other inorganic salts in DMEM. The NaCl was added in order to maintain the total concentration for all the solutes at 350 mM. One molar glucose and 200 mM glutamine solutions were used in fed-batch culture for replenishment. All media were sterilized by filtration through 0.22 μm filter paper. The amounts of the stock solutions required for preparing various media, and their final formulae are shown in Table-3.3 and -3.4.

III.3 Preparation of Hydrogels

III.3.1 Hydrogel for Intra-membrane Transport Studies

Preparation of Hydrogel Membrane

The hydrogels used in the experiments include commercially available natural prosucts such as agarose and agar, and synthetic polymers, such as PMAA (polymethacrylic acid) and PDMAEMA (polydimethylaminoethyl methacrylate) and their related copolymers. For fabricating a hydrogel membrane, two clean, dry, flat glass plates and a teflon, ring spacer with a desired thickness were used. The spacer was placed on the bottom glass plate, and the melted natural hydrogels or a

Table-3.3: Requirements of various stock solutions for enriched media

Stock Solution	f2DMEM (ml)	f5DMEM (ml)	Supplement (ml)
Essential Amino Acid	100	200	40
Non-Essential Amino Acid	100	100	20
Vitamin	100	200	40
Inorganic Salts	100	100	-
NaCl	100	11.5	-
NaHCO3	100	100	0.126 (g)
NaH2PO4	100	100	-
Phenol Red	4	4	0.4
Glutamine	30	30	-
Glucose	10	10	-
Water	286	162	-

All media were adjusted to pH 7.2 before use

† Additional glycine and serine were added in both f2DMEM and f5DMEM

Table-3.4: Formulas of various enriched media

	MEM	DMEM	f5MEM	f10MEM	Supplement
Ess. Amino Acid	(mM)	(mM)	(mM)	(mM)	(mM)
Arginine	0.60	0.40	3.00	6.00	12.00
Cysteine	0.12	0.32	0.62	1.24	2.47
Glutamine	2.00	4.00	6.00	6.00	0.00
Histidine	0.20	0.20	1.00	2.00	4.01
Isoleucine	0.40	0.80	2.00	4.00	8.00
Leucine	0.40	0.80	2.00	4.00	8.00
Lysine	0.40	0.80	2.00	4.00	8.00
Methionine	0.10	0.20	0.51	1.00	2.02
Phenylalanine	0.20	0.40	1.00	2.00	4.00
Threonine	0.40	0.80	2.00	4.00	8.00
Tryptophan	0.05	0.08	0.25	0.50	1.00
Tyrosine	0.20	0.57	1.00	2.00	4.00
Valine	0.40	0.80	2.00	4.00	8.00
Non-Ess. Amino Acid	(mM)	(mM)	(mM)	(mM)	(mM)
Alanine	0.0	0.0	0.10	1.00	2.00
Asparagine	0.0	0.0	0.11	1.14	2.27
Aspartic Acid	0.0	0.0	0.10	1.00	2.00
Glutamic Acid	0.0	0.0	0.10	1.00	2.00
Glycine	0.0	0.4	1.00	2.00	18.00
Proline	0.0	0.0	0.10	1.00	2.00
Serine	0.0	0.4	1.00	2.00	18.00
Vitamins	(μM)	(μM)	(μM)	(μM)	(μM)
Choline	7.16	28.70	71.60	143.30	286.50
Folic Acid	2.27	9.10	22.70	45.30	90.60
Inositol	11.1	40.00	111.00	222.00	444.00
Nicotinamide	8.19	32.80	81.90	163.80	327.60
Pantothenate	4.20	16.80	42.00	83.90	167.90
Pyridoxal	4.91	19.70	49.10	98.20	196.50
Riboflavin	0.27	1.06	2.66	5.30	10.60
Thiamine	2.96	11.90	29.60	59.30	118.60
Inorganic Salts	(mM)	(mM)	(mM)	(mM)	(mM)
CaCl2.2H2O	1.80	1.80	1.80	1.80	0.00
KCl	5.37	5.37	5.37	5.37	0.00
Fe(NO3)3-9H2O	0.00	0.0003	0.0003	0.0003	0.0003
MgSO4.7H2O	0.40	0.40	0.40	0.40	0.00
NaCl	116.3	109.5	59.1	34.2	58.2
NaHCO3	26.2	44.0	44.0	44.0	15.0
NaH2PO4	1.02	0.91	0.91	0.91	0.00
Glucose	10	25	25	25	0

mixture of monomers and crosslinker for the synthetic hydrogels were pipetted onto the glass surface inside the spacer. The top glass plate was slowly lowered onto the lower plate to ensure that no air bubbles were trapped between the two plates. The two plates were held together with metal clamps, and placed vertically either at room temperature for the natural hydrogels or in a 60°C water bath for 4 hours in the case of the synthetic hydrogels. The casting procedure for hydrogel membrane is schematically illustrated in Figure-3.1. After the membranes were cast, they were carefully removed from the glasses, rinsed in deionized water for several hours and then stored in electrolyte solutions for later transport experiments. Alginate and κ-carrageenan were solidified in the presence of Ca^+ and K^+, respectively. For fabricating these two hydrogel membranes, the above procedure was used with the exception that two filter papers (8 μm pore size, Millipore Inc.) replaced the glass plates used for casting the hydrogels. The liquid hydrogels sealed in between these two filter papers were incubated in either $CaCl_2$ or KCl solutions respectively for 25 minutes until the membranes set.

Agarose is a highly purified natural polysaccharide isolated from crude agar gel. Its chemical structure indicates no charged groups at all conditions. Agarose powder (SeaKem HEEO®) was purchased from FMC Co. (Rockland, ME) which is designed for electrophoretic uses and has the highest fixed charge density. Two percent (w/v) agarose membranes were prepared with thicknesses ranging from 500 to 1000 μm. However, agar often contains charged impurities such as sulfuric acid, glucuronic acid and pyruvic acid, and it possesses net negative charge. Five percent (w/v) agar (Difco Co., Bacto-Agar) membranes were prepared with thicknesses ranging from 500 to 1000 μm. Alginate hydrogel has fixed carbonate groups on its gel matrix, and hence is negatively charged. Sodium

alginate used at 1.25% (w/v) (CellPrep®) was purchased from FMC Co.. The gelation of the alginate solution was achieved by incubating in a 1.5% (w/v) $CaCl_2$ solution. κ-carrageenan hydrogel has fixed sulphate groups on its structure, and hence is negatively charged. The 3.5% and 5% (w/v) potassium-κ-carrageenans were prepared by dissolving the sodium-κ-carrageenan powder (FMC Co.) in deionized water and then incubation in a 2% (w/v) KCl solution.

The PMAA membranes were prepared according to the procedure described by Grimshaw (1989). The MAA monomers (10 ml, PolyScience) were crosslinked in the presence of the following chemicals; the crosslinker, which was 0.4 or 0.05 ml triethylene glycol dimethacrylate (TEGDMA, PolyScience); the initiators, which included 0.3 ml of 40% (w/v) ammonium persulfate and 0.3 ml 15% (w/v) sodium metabisulfite solution; 3 ml ethylene glycol (PolyScience) and 2 ml deionized water. The carbonate groups on PMAA backbones give PMAA net negative charges. PDMAEMA membranes were crosslinked using TEGDMA (1.1% molar ratio versus DMAEMA) as a crosslinker.

Three different factors affecting electroosmotic properties of κ-carrageenan were investigated. These include the cell load, the fixed charge density, and the gel strength reinforcing agents. In order to study the effects of cell loads, hybridoma cells, CRL-1606, were centrifuged and resuspended in 3.5% (w/v) sodium-κ-carrageenan liquid at concentrations of $1x10^7$ and $7x10^7$ cells/ml-gel respectively. The cell/gel mixture was cast in a 2% KCl solution using the same procedure as described earlier. To identify the effects of fixed charge densities on gel matrices, three different κ-carrageenan-agarose blends were prepared. These gel blends were kept warm (>45°C) before being cast. Finally, the effects of hydrogel additives were studied. The κ-carrageenan hydrogel additives for

reinforcing gel structure strength and enhancing immobilization include polyethyleneimine (PEI) (Takata *et al.*, 1982), glutaraldehyde (GA) and hexamethylene diamine (HMDA) (Nishida et al., 1979). Since these additives could interact with the fixed charge groups on gel matrices, a reduction in inducible electroosmosis was expected. A 1.9% (w/v) PEI solution was prepared in deionized water, which was then mixed with 3.5% (w/v) sodium-κ-carrageenan at a 1 to 7 volume ratio. This mixture was cast into membranes using the standard procedure for casting. To identify the GA-HMDA effects, a potassium-κ-carrageenan gel membrane was first prepared. These hydrogel membranes were incubated in a 12.5% (w/v) GA solution for 15 minutes and in a 2% (w/v) KCl-0.08 M HMDA solution for another hour. The cast membranes were rinsed thoroughly with deionized water and then stored in electrolyte solutions.

Measurement of Intra-membrane Solvent Flux (Electroosmosis)

A transport chamber for measuring the transmembrane solvent flux was constructed based on a modification of the one described by Grimshaw (1989). As shown in Figure-3.1, the chamber was constructed from two half cells which were made of acrylic plastic. Each half cell held 100 ml of a well-stirred electrolyte solution. The membrane was laid between the two half cells, which were mounted together and sealed with gaskets. The synthetic hydrogel membrane was directly mounted, as opposed to the natural hydrogel membrane which was first laid down between the two filter papers (Millipore Co., cellulose acetate, 8 μm pore size) to reinforce structural strength before being mounted. The area of membrane exposed to the solution was 4.8 cm^2. A dc current power supply delivered a transmembrane electric field via a pair of salt bridge electrodes placed in the solution. Each electrode was made of a platinum strip

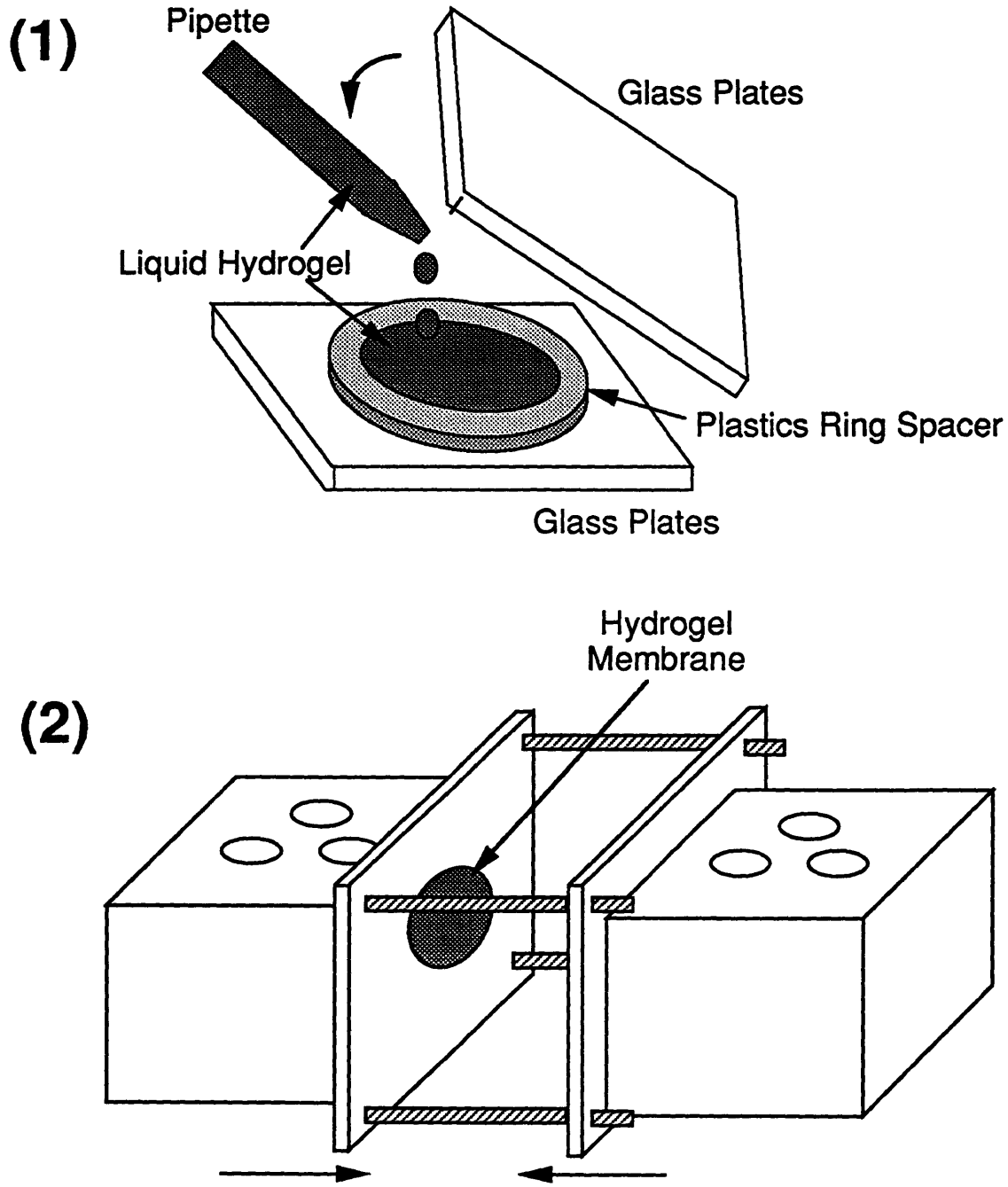

Figure-3.1: (1) The apparatus for casting hydrogel membranes used for the measurements of intra-membrane transport. (2) The transport chamber with the hydrogel membrane mounted in between two half cells.

separated from the electrolyte solution by a polyacrylamide gel salt bridge filled with 1.5 M KCl solution.

The overall experimental set-up is schematically shown in Figure-3.2. The two half cells of the transport chamber were designated upstream and downstream baths with respect to the direction of solvent flux. The upstream bath was open to the air, and the downstream bath was connected via a thin tube to a beaker filled with an electrolyte solution (KCl or DMEM), which was placed on an electronic balance. Transmembrane solvent flux was determined by the rate of change of the measured weight on the balance. The balance was kept covered to avoid evaporation from the beaker. The KCl solution was used for synthetic hydrogel experiments, and DMEM was used for natural hydrogel experiments.

III.3.2 Hydrogels for Cell Entrapment

E. coli: Hydrogel Slab Casting and Dissolution

κ-carrageenan and agarose hydrogels were used to entrap viable *E. coli* cells. Only gel slabs were prepared since no gel beads were used in the *E. coli* entrapment study. Sodium κ-carrageenan gel powder (Sigma Chemical) was dissolved in 20 mM HEPES solution at 60°C to achieve a 3.5% (w/v) concentration, and the pH was adjusted to 7.2. The melted κ-carrageenan hydrogel was kept at 45°C before mixing with the cells. A KCl solution at 2% (w/v), with the pH adjusted to 7.0, was used for gel casting. Seakem LE® agarose powder (FMC Co.) was dissolved in 20 mM HEPES solution at 100°C to obtain a 2% (w/v) concentration. The melted agarose hydrogel will not set if kept in a 45°C water bath but readily solidified at room temperature. Both the liquid hydrogels and KCl solution were sterilized in a steam autoclave at 121°C for 25 minutes.

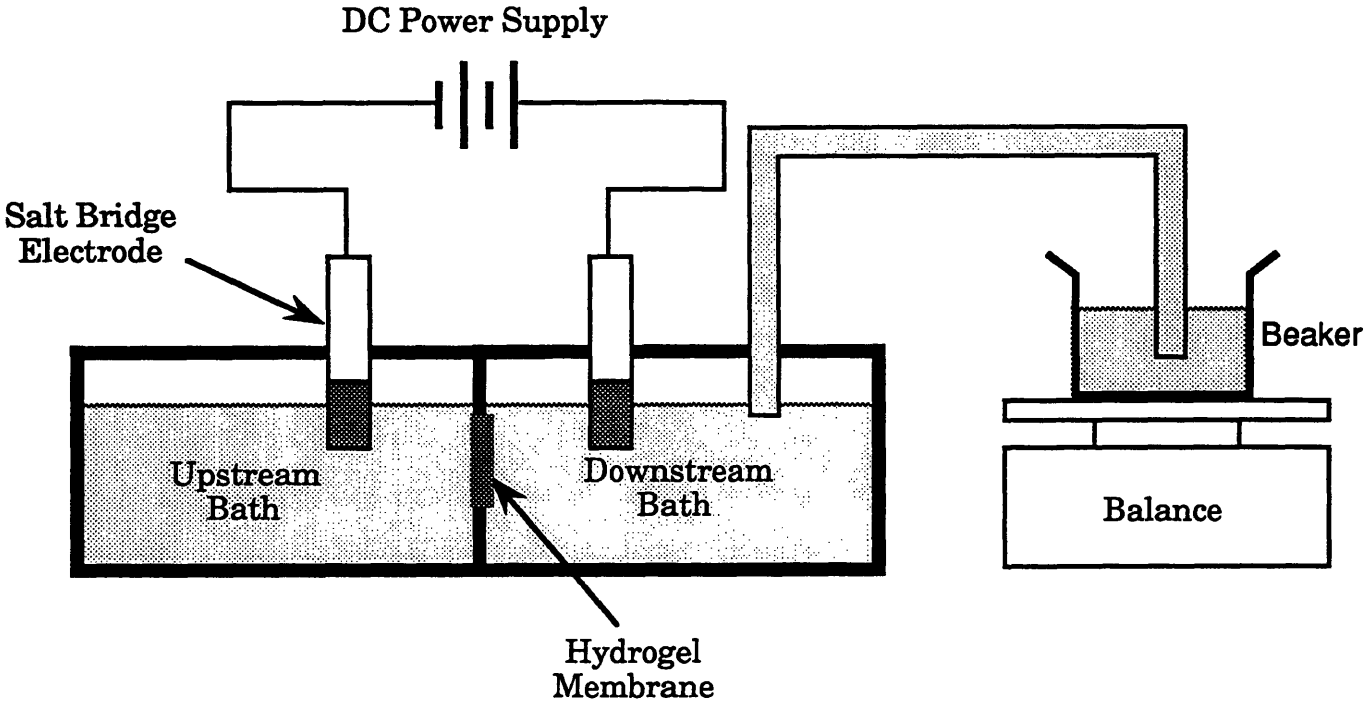

Figure-3.2: The transport chamber for measuring the intra-membrane electroosmotic solvent flux. The downstream half cell of the chamber is sealed, which forces the intra-membrane flow to be transferred through a tubing to a beaker laid on a balance. The solvent flux is therefore measured by reading the variation of the liquid weight from the balance.

For casting a hydrogel slab, a rectangular polysulfone frame, as shown in Figure-3.3, was used. The opening in the frame has dimensions of 1.4 H x 2.9 W x 0.65 D (cm). This opening was sealed to generate a slab-shaped cavity by attaching two filter papers (Millipore Co., cellulose acetate, 8μm pore size) on both sides of the frame with silicon glue. Two holes were drilled vertically through the top of the frame for liquid gel injection. A 21-gauge sterile syringe was used to inject the hydrogel/cell-mixture. The melted liquid hydrogels were quickly mixed with an adequate amount of cells and then injected into the cavity before the hydrogels started gelling. For κ-carrageenan, the hydrogel slab was later incubated in a 2% (w/v) KCl solution for 30 minutes. For agarose, the hydrogel slab was kept in the culture chamber until it has completely solidified. The above gel-casting procedure was conducted in a laminar flow hood to ensure sterility.

At the end of the hydrogel-entrapped *E. coli* culture, the two filter papers were removed from the frame. The hydrogel-slab together with its restraining frame was removed from the culture chamber and placed horizontally on a glass plate. A rectangular teflon plate, having exactly the same dimensions as the frame opening and a thickness of 500 μm, was inserted between the hydrogel slab and the glass plate. Each teflon plate will raise the hydrogel slab by 500 μm above the top of the frame, and a sharp blade was used to slice horizontally through the exposed part of the hydrogel slab. A second teflon plate was added beneath the hydrogel slab, and the slicing procedure was repeated. The hydrogel slab was finally divided into eleven thin slices. Each hydrogel slice was collected in a centrifuge tube and its weight was accurately measured by an electronic balance. This measured weight was used as an indication of the actual thickness of the hydrogel slice. The entire procedure is schematically

shown in Figure-3.3.

The hydrogel slices were then dissolved to release *E. coli* cells for cell enumeration. One ml of 0.9% (w/v) NaCl solution was added to each centrifuge tube containing a hydrogel slice. This aliquot was then incubated for about 10-15 minutes at 100°C in a water bath until the hydrogel has completely dissolved. The preliminary study showed that this dissolution procedure did not affect the total *E. coli* cell concentration. However, cell viability can not be obtained using this gel dissolution procedure and only total cell number can be obtained.

Hybridoma Cell Entrapment

For entrapment of hybridoma cells, hydrogels of higher quality are required. The cell-culture-tested alginate and κ-carrageenan gel solutions from FMC Co. were chosen for the hybridoma entrapment studies. A sterile sodium alginate solution (CellPrep®, 1.25%(w/v)) was cast into solid hydrogel by incubating in a 1.5% (w/v) $CaCl_2$ solution for 25 minutes. A sterile sodium κ-carrageenan solution (CellPrep®, 3.5% (w/v)) was cast into solid hydrogel by incubating in a 2% (w/v) KCl solution for 25 minutes. The SeaKem HEEO® and SeaPlaque® agarose powders (FMC Co.) were dissolved at 100°C in phosphate buffered saline (PBS) at either 1% or 4% (w/v) concentration. The melted agarose solution was maintained at 45°C before blending with other hydrogel and mixing with hybridoma cells.

Hydrogel beads were used for hydrogel biocompatibility studies. The hybridoma cell suspension was gently mixed with liquid hydrogel at a ratio of one to four to obtain a total volume of 15 ml. Two hundred and fifty ml gel-casting solution, which was either KCl or $CaCl_2$, was placed in a crystallization dish and gently stirred by a magnetic stir-bar. A sterile syringe mounted with a 21-gauge needle was loaded with the cell/hydrogel

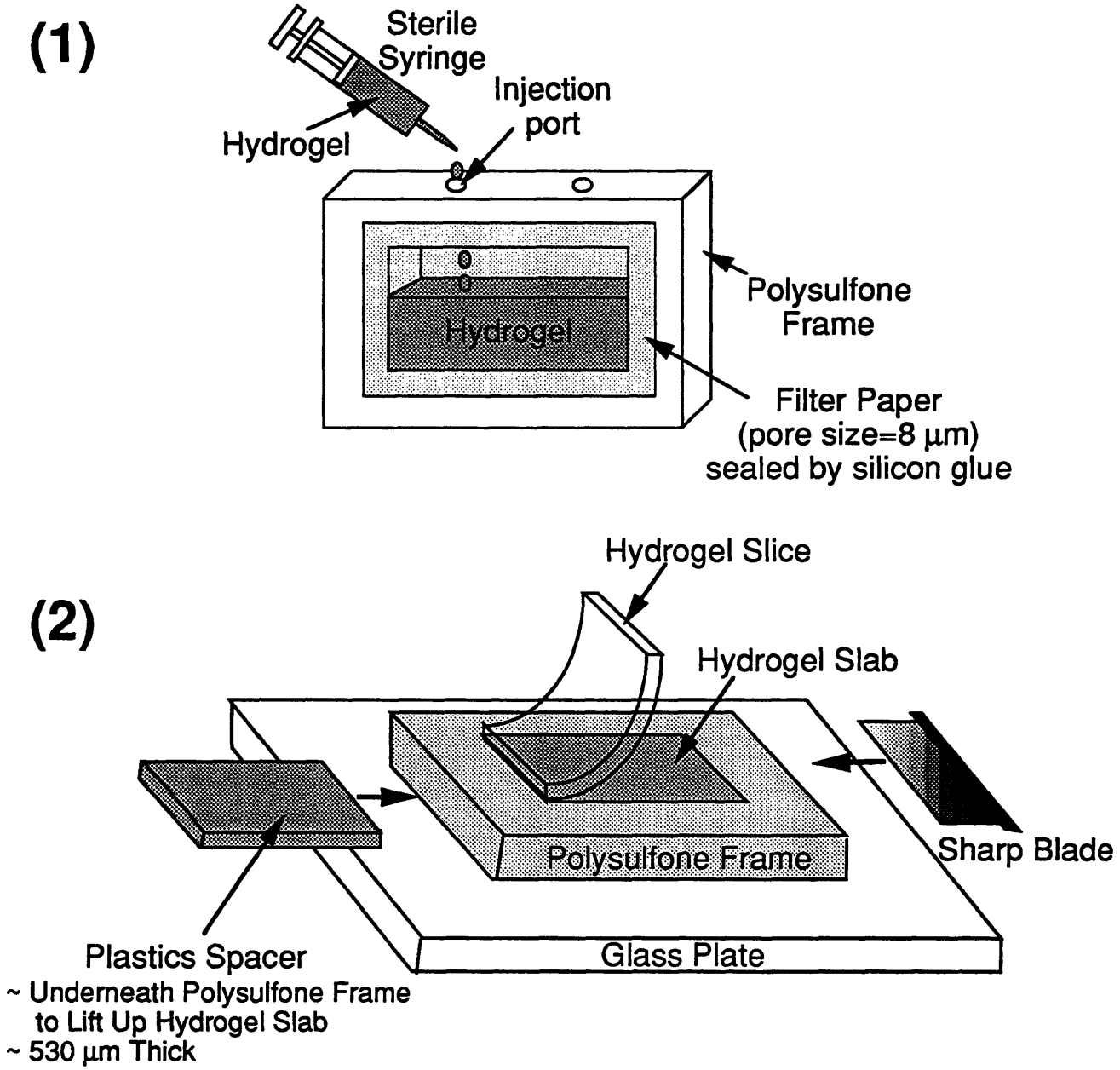

Figure-3.3: (1) A polysulfone rectangular frame used for casting cell-entrapped hydrogel slab for hydrogel-entrapment cultures. A slab-like cavity in the frame is formed by sealing two filter papers on both sides of the frame. (2) The procedure for slicing the cell-contained hydrogel slab. Each hydrogel slice is 530 μm thick. The procedure is repeated until the hydrogel slab is completely sliced into 11 pieces.

mixture, and was then injected dropwise into the gel-casting solution. The resulting hydrogel beads, typically 1 to 3 mm in diameter, were incubated in the respective gel-casting solution for 25 minutes. These hydrogel beads were recovered from the gel-casting solution using a filter funnel, and washed thoroughly with 300 ml PBS solution. These beads were then transferred into a T-175 flask containing 50 ml DMEM. The entire procedure mentioned above was conducted aseptically in a laminar flow hood. For monitoring entrapped cell proliferation, five gel beads were taken from the T-flask and dissolved to release the hybridoma cells for cell enumeration. The weight of the gel beads was carefully measured and later used to calculate the volume. Five ml disodium EDTA (1% (w/v) EDTA in 0.085 M NaCl, pH=7.4) and 5 ml 1% (w/v) sodium citrate solutions were used to dissolved approximately 0.2 g of alginate and 0.2 g of κ-carrageenan hydrogel beads, respectively. Dissolution was completed in 5 to 10 minutes at 37°C. The dissolved gel/cell mixture was directly used for cell enumeration.

To study hybridoma-entrapped cell cultures in the presence of an applied dc electric field, slab form of alginate-agarose hydrogel blend was used. Since calcium ions will be removed from the calcium-alginate solid hydrogels in the presence of the applied dc electric fields, it is necessary to add neutral hydrogel to maintain the integrity of the alginate hydrogel structure. The electrically neutral agarose was selected to blend with the alginate. The 1.25% (w/v) CellPrep® alginate solution and the melted 4% (w/v) SeaPlaque® agarose gel were mixed at a ratio of 9 to 1, with final concentrations of the blended hydrogels at 1.125% (w/v) alginate and 0.4% (w/v) agarose. This liquid hydrogel blend was kept at 45°C in a water bath. The hydrogel slab was cast and dissolved by the same procedures as described earlier for pure alginate gel with the exception that the

temperature required for gel dissolution was 65°C instead of 37°C.

III.4 Application of dc Electric Fields on Cultured Cells

III.4.1 Construction of Culture Apparatus

A culture chamber used to apply the dc electric field to the cultures is schematically shown in Figure-3.4. There are two different sizes of the rectangular chambers. The small chamber (90 ml working volume) was used for all *E.coli* cultures and entrapment of hybridoma cultures, and the large chamber (240 ml working volume) was used for all suspension hybridoma cultures. The culture chambers were made of polysulfone plastics. It had an opening on the top, which was covered and sealed by a rectangular polysulfone plate. This cover plate had multiple holes which allowed the insertion of probes and sampling tubes. These probes and sampling tubes were pierced through the silicon rubber stoppers, and the stoppers were squeezed half way through the holes to insure a tight seal.

For suspension cultures, the chamber was divided into three compartments by two polysulfone frames with glued filter papers (teflon filter paper, 0.22 μm pore size, Millipore Co.). Cells were confined within the central compartment by these filter papers and maintained in suspension by a magnetic stir-bar.

For hydrogel entrapment cultures, a rectangular frame, as shown in Figure-3.4, was mounted vertically inside the small chamber. The bottom, the left and the right sides of the frame were glued to the interior wall of the chamber in order to completely seal these junctions. Culture medium was used to fill up the chambrer to the exact height of the vertically-mounted frame. Therefore the culture medium and dc electric current could only travel through the hydrogel slab, and would not bypass the hydrogel slab through the top of the frame. In addition, the electroosmotic

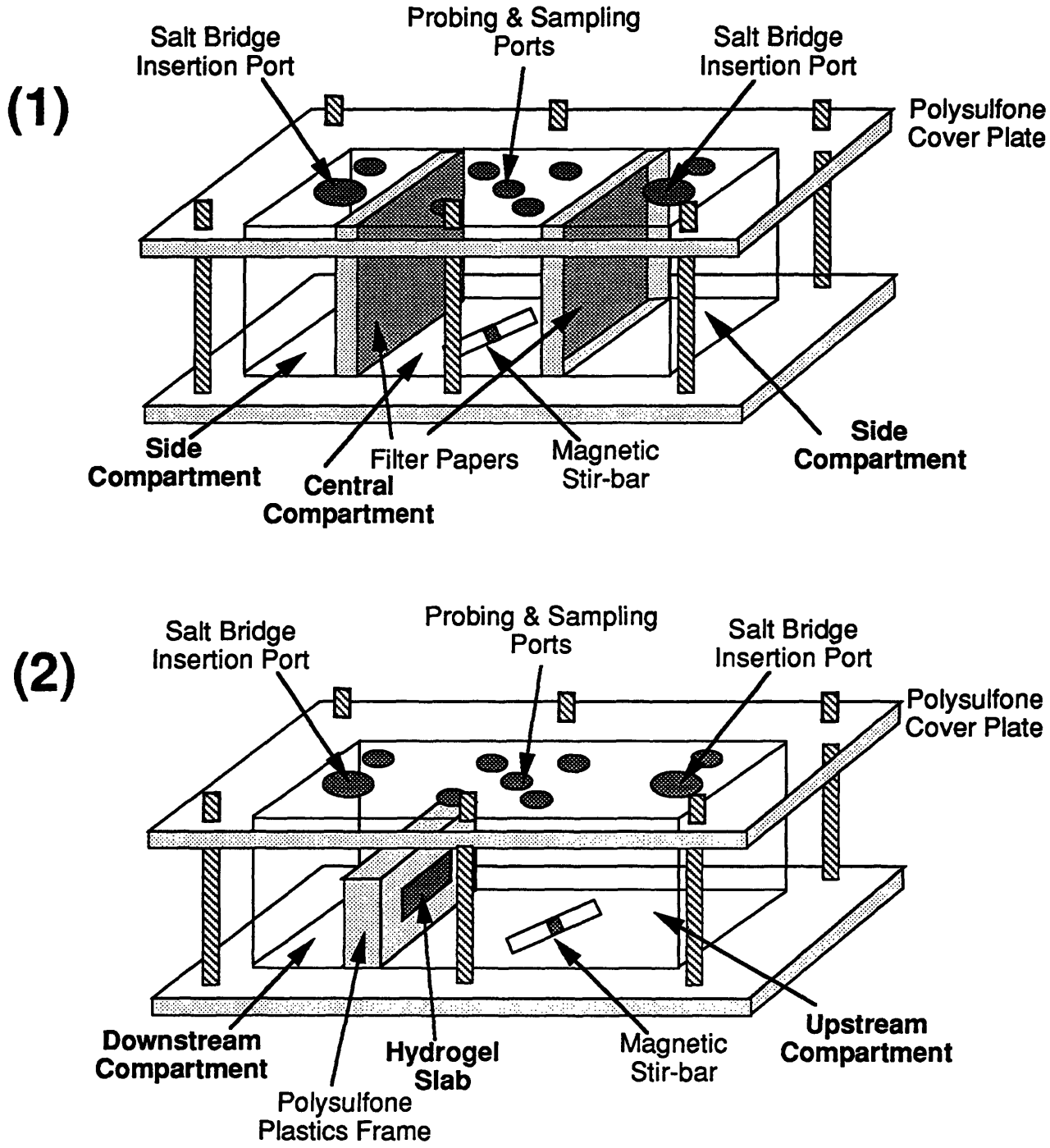

Figure-3.4: (1) The culture chamber for suspension cell cultures. The chamber is divided into three compartments by two filter papers. Cells are suspended in the central compartment by a magnetic stir-bar. (2) The culture chamber for hydrogel-entrapment cultures. The medium bath is vigorously agitated by a magnetic stir-bar in the upstream compartment. Both chambers are oxygenated through surface aeration.

solvent flux traveled from the upstream side of the medium bath to the downstream side through the hydrogel slab and accumulated in the downstream side, which subsequently returned to the upstream bath through the top of the frame.

Finally the effects of *in-situ* removal of the externally-added ammonium on cultured hybridomas were investigated by using a glass cylindrical reactor, which is shown in Figure-3.5. This reactor was modified from a crystallization dish with a dimension of 6.5 cm (dia.) x 5.0 cm (height) and a working volume of 90 ml. This glass dish was covered by a polysulfone plate, which had multiple holes to allow salt bridges, probes and sampling tubes to be inserted into the reactor. The cells were freely suspended in the reactor by a magnetic stir-bar without confinement.

The salt bridges used during cultivation, shown in Figure-3.5, were made of U-shape pyrex glass tubes with a diameter of 1.5 cm. There were two pairs of salt bridges, which were designated the inner and the outer pairs. The inner pair of salt bridges had one end inserted into the culture chamber and immersed in culture medium. This end of the salt bridge was sealed with dialysis membrane (Spectrum Inc., Spectra/Por®, MWCO=12,000) and teflon tape and wrapped with aluminum foil. These salt bridges were sterilized by autoclaving, and then filled with 2.5% (w/v) SeaKem LE® agarose gel (prepared in either DMEM or LB broth). The outer pair of salt bridges did not require sterilization and was filled with 2.5% (w/v) agar (prepared in 0.5 M NaCl). There were two pairs of electrode baths. The inner pair of electrode bath contained either DMEM w/o serum or LB broth, and the outer pair contained a 0.5 M NaCl/20 mM $NaHCO_3$ solution. The pH of these electrode baths were pre-adjusted to 7.2 before use. The platinum plates were immersed in the outer electrode baths for delivering the dc electric field. The DMEM-based solution and

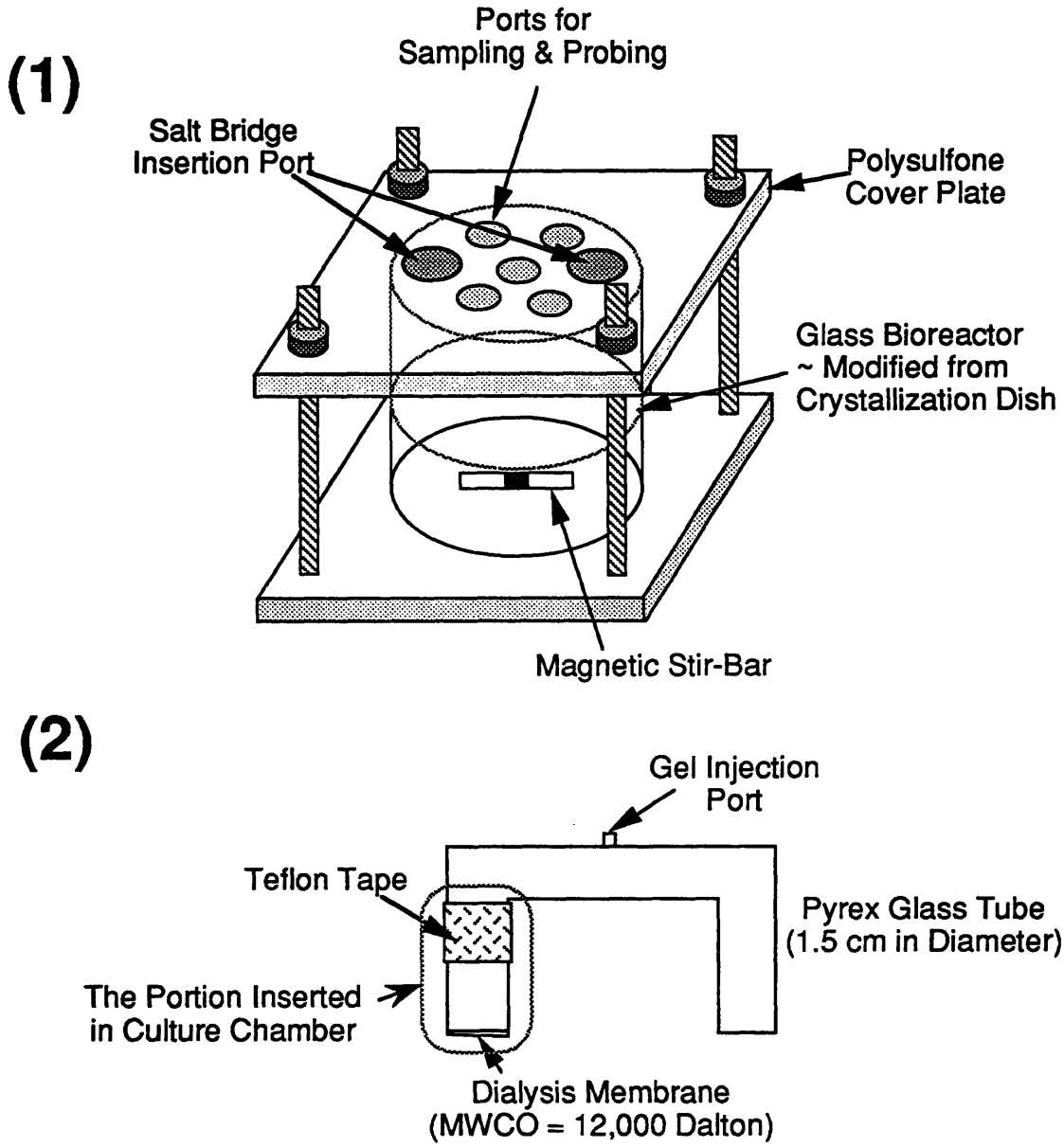

Figure-3.5: (1) The culture chamber used for studying the effects of electrokinetics on suspended hybridoma cells. This chamber is modified from a crystallization dish. Cells directly contact the inserted salt bridges. Chamber is oxygenated through surface aeration. (2) The inner set of salt bridges. The portion of salt bridge inserted in culture chamber is wrapped up by tin foil and sterilized by autoclave. The melted gel (either agarose or agar) is injected into the salt bridge through the injection port on the salt bridge. The teflon tape could provide the tight sealing between the salt bridge and the port on cover plate. The dialysis membrane could prevent the removal of MAb by electrophoresis and offer the sterility.

gel were used exclusively for all hybridoma cultures, and the LB broth-based solutions were used for all *E. coli* cultures.

The pH of the culture medium was monitored and controlled through an autoclaveable pH electrode (Cole Palmer, Model#G-05662-10) and a pH controller (Cole Palmer, Chemcadet®). The pH was adjusted through the addition of 1 N NaOH or 1 N HCl, and through the modulation of CO_2 concentration (between 0 to 10%) in the gas phase. Since the pH controller cannot be isolated from the ground, the applied direct current interfered with the inserted pH probes. To reduce the interference, a cylindrical metal shield was mounted onto the probe. This metal shield was completely covered by silicon glue to avoid contact with culture medium and thus eliminated the electrolysis on the metal surface in the presence of dc electric fields. The dissolved oxygen (DO) was measured off-line by a DO microelectrode (Microelectrode Inc., Cat#MI-730). The DO level was adjusted through adjusting the oxygen content (between 20% to 50% of total air content) in the gas phase. The inlet air was sterilized through an air-filter (Gelman Co.). The temperature was measured by an immersed thermocouple, and controlled through a heating mat (Cole Palmer, Kapton®) and a PID temperature controller (Cole Palmer Co., Digi-Sense®). The constant temperature was maintained through the balance between the heating from the heating mat underneath the chamber and the cooling through the ambient air.

III.4.2 Application of dc Electric Fields

A schematic diagram of the experimental set-up for applying DC electric fields on cultured cells in suspension is shown in Figure-3.6. The construction of the rectangular culture chamber, salt bridges and electrode baths has already been discussed in the previous section. For the suspension

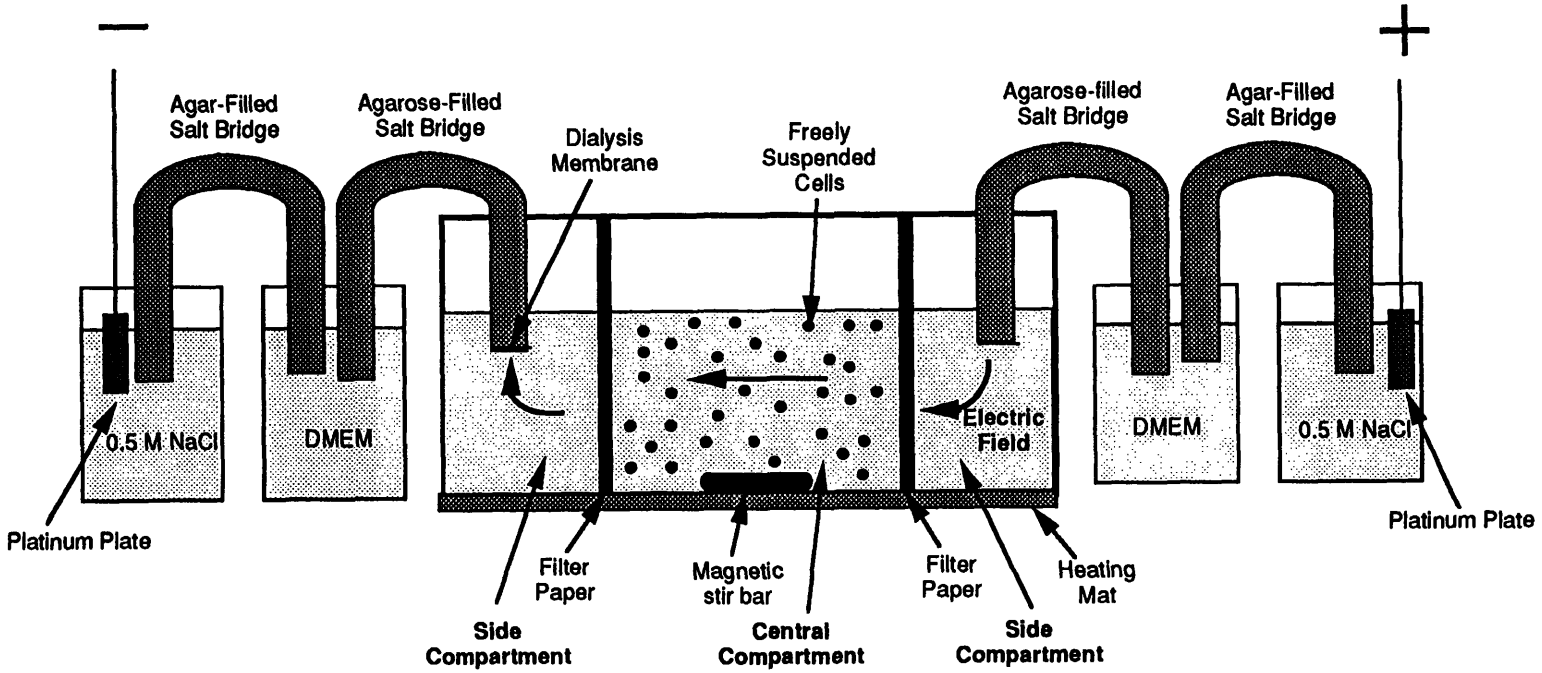

Figure-3.6: The experimental set-up for studying the effects of electrokinetics on suspension cell cultures. The rectangular chamber is divided into three compartments by two vertically-mounted filter papers. Cells are confined within the central compartment and suspended by a magnetic stir-bar. Cells are oxygenated with either atmospheric air or 50% oxygen-contained air through surface aeration. Both the electrode baths and salt bridges are replaced periodically in order to maintain the chemostatic condition of culture medium and to prevent the toxic electrolytic products from entering the culture chamber.

cell cultures, cells were confined within the central compartment of the rectangular culture chamber. This arrangement prevents direct contact between the cells and the irregular electric fields emanating from the salt bridges. In contrast, in the case of the cylindrical reactor used for studying the effects of *in-situ* removal of externally-added ammonium on hybridomas, cells were freely suspended and therefore were in direct contact with the electric fields emanating from the inserted salt bridges.

Two pairs of electrode baths and two pair of salt bridges placed in series were used to achieve the long-term application of DC electric fields on cultured cells. The outer pair of salt bridges was used to isolate the toxic electrolytic products from entering the culture chamber while the inner pair was used to maintain chemostatic condition of the culture medium. The electrode baths and culture chamber were connected through these salt bridges to maintain a continuity of the electric current. Both electrode baths and salt bridges were replaced periodically, every 24 to 48 hours, to further ensure the exclusion of toxic electrolytic products from the culture chamber. The replacement of salt bridges was conducted in the laminar flow hood. The gels in the used salt bridges were melted and discarded while the glass salt bridges were recycled for further uses.

The same strategy, as shown in Figure-3.7, was adopted for applying electric fields on entrapment cell cultures.

III.5 Operation of Batch and Fed-Batch Cultures

III.5.1 *E. coli* Cultures

Both suspension and hydrogel-entrapment *E. coli* cultures were performed in the small rectangular culture chamber and only in batch mode, i.e., using SLB medium without nutrient replenishment. All *E. coli* cultures were performed at 37°C and at an initial pH of 7. The cultures were

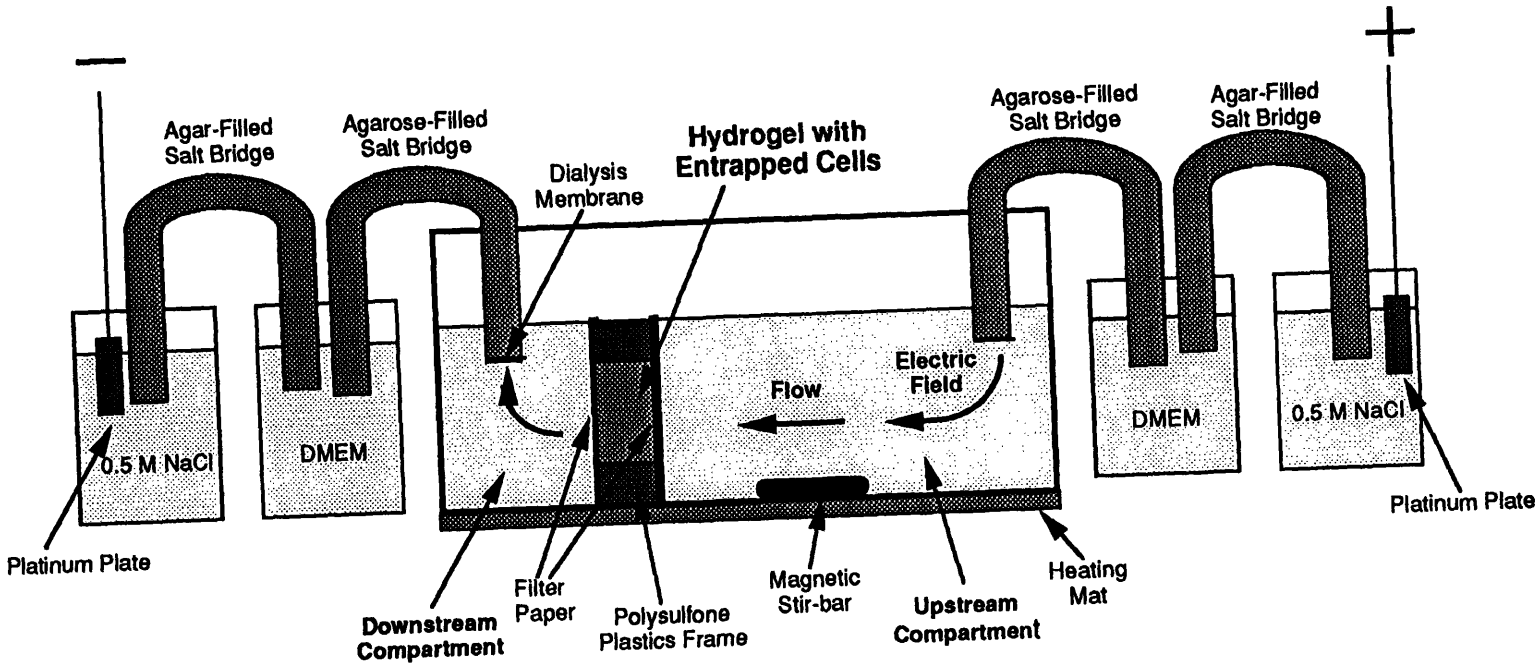

Figure-3.7: The experimental set-up for studying the effects of electrokinetics on hydrogel-entrapped cell cultures. Cells are entrapped in a vertically-mounted hydrogel slab. Culture medium is only vigorously stirred in the upstream compartment and oxygenated through surface aeration. The level of liquid medium is the same as the height of the polysulfone plastics frame. Both the electrode baths and salt bridges are replaced periodically. At the end, the hydrogel slab is removed from the polysulfone plastics frame, then sliced and dissolved to released the cells for enumeration.

oxygenated through surface aeration by atmospheric air, and the dissolved oxygen (DO) level was monitored off-line. The DO decreased to zero after two hours of cultivation for the suspension *E. coli* cultures whereas the DO was still remained above 30% of air saturation in the medium bath after 9 hours of cultivation in hydrogel-entrapment *E. coli* cultures. The cell broth was sampled hourly for the suspension *E. coli* cultures. In hydrogel-entrapment *E. coli* cultures, the hydrogel slab was not removed for analysis until the end of the culture, which was either 8 or 10 hours of cultivation.

III.5.2 Hybridoma Cultures

The hydrogel-entrapment hybridoma cultures were performed either in the small culture chamber (65 ml working volume, for electric-field-applied cultures) or in T-175 flasks (for hydrogel biocompatibility studies), and were operated in a semi-continuous mode. The entrapment cultures with applied electric fields lasted for 11 days in XMEM, and the culture medium was completely replaced every 4 to 5 days. The hydrogel slab was not removed until the end of the cultivation, and only the cell density in the hydrogel slab was analyzed. The hydrogel biocompatibility studies were performed in DMEM for 15 to 25 days. The culture medium was sampled daily, and five hydrogel beads were taken every 6 days for the entrapped cell density analysis.

The suspension hybridoma cultures were performed in the large culture chamber (150 to 220 working volume), and were operated in batch or fed-batch mode. XMEM was used in the batch and the glutamine fed-batch suspension cultures. The initial glutamine concentration was 4 mM, and an additional 4 mM was fed in the glutamine fed-batch cultures. The enriched culture media were used in the later fed-batch cultures. In the fed-batch culture using f5MEM, only glutamine and glucose were periodically

replenished. In the fed-batch culture using f10MEM, the supplement medium as well as the glucose and glutamine were periodically fed to replenish all possible depleted nutrients. The feeding rates were determined based on the previously-measured nutrient consumption rates. The sample of cell broth was taken from all three compartments of the culture chamber every 12 hours. The amount of feeding and amount of sampling for each compartment was determined by the volume ratio between the compartments so that the medium levels remained the same in each compartment. Cell density and metabolite concentrations were analyzed for each sample. All suspension hybridoma cultures were performed at 37°C, pH 7 and at 20% or greater of air saturation in DO.

III.6 Effects of Various Chemicals on Cultured Hybridomas

III.6.1 Sodium Lactate

The studies of lactate toxicity on hybridomas, CRL-1606, were conducted in T-75 flasks. The lactate toxicity was believed to be the resultant osmolarity change from the production of lactate (Ozturk *et al.*, 1992). A NaCl solution was added to a separate flask in order to raise the osmolarity as much as the sodium lactate solution. This NaCl-added culture could be used to isolate other effects on the cells in addition to the osmolarity change by sodium lactate A 400 mM sodium lactate (Sigma Chemical) and a 400 mM sodium chloride (Sigma Chemical) stock solutions were prepared. Hybridoma cells resuspended in fresh DMEM were mixed with the same amount of either sodium lactate or sodium chloride stock solution in different flasks. In addition, the same amount of PBS was added to a separate flask as the control experiment. This could eliminate the dilution effect produced by the addition of the above stock solutions. The concentration of hybridoma inoculum was $2x10^5$ cells/ml, and the concentrations of sodium

lactate investigated were 40 and 80 mM.

III.6.2 Ammonium Chloride

The studies of ammonia toxicity and ammonia adaptation of hybridomas, CRL-1606, were first conducted in T-75 flasks. A 200 mM ammonium chloride (Sigma Chemical) stock solution was prepared. Hybridoma cells resuspended in fresh DMEM were mixed with an adequate amount of ammonium chloride stock solution to obtain an initial ammonium concentrations of 12.5 mM. Hybridoma cells in DMEM without any stock solution added was used as the control.

For studying the effects of *in-situ* removal of the externally-added ammonium by an applied electric field, various amounts of the ammonium chloride stock solution were added to the cylindrical reactor at the beginning of each culture. The initial ammonium concentrations were 7.5, 9.5 and 12.5 mM. The electric fields were applied either at the beginning of the culture or after a time lag of twelve hours. The control experiment was conducted with applied electric field but without the addition of ammonium chloride. All experiments were performed in DMEM (90 ml working volume) and at the total electric currents ranging from 60 to 75 mAmp.

III.6.3 Sodium Butyrate

The optimization of sodium butyrate feeding was initially conducted. In order to achieve maximum increase in immunoglobulin production, both the timing and the amount of sodium butyrate fed are critical and must be determined. This screening and optimization studies were performed in T-175 flask. Hybridoma cells were resuspended in fresh DMEM at $2x10^5$ cells/ml as inoculum for all experiments. Two hundred mM of sodium butyrate (Sigma Chemical) stock solution was prepared. An adequate

amount of sodium butyrate stock solution was added to the broth to attain concentrations of sodium butyrate ranging from 0.5 to 5 mM at different phases of cell growth. The cell growth and immunoglobulin production were analyzed.

In one of the electrokinetic, fed-batch hybridoma culture, sodium butyrate was fed once during the culture in order to decelerate cellular metabolism. The optimal feeding strategy of sodium butyrate was determined based on the previous screening study. as soon as the sodium butyrate was added, the inner pair of salt bridges and electrode baths were changed. These inner pairs of salt bridges and electrode baths were made up of DMEM supplemented with 0.75 mM sodium butyrate. This ensured that sodium butyrate was permanently present and invariant after the feeding in the presence of DC electric fields.

III.7 Analytical Methods

III.7.1 Cell Enumeration and Cell Viability

For measuring the *E. coli* cell density, a Hewlett Packard spectrophotometer (Model 8452) was used to measure the absorbance at 660 nm. In the case of entrapped cells, the gel matrix was first dissolved using a NaCl solution, and the absorbance of the resultant solution was measured. All of the samples were diluted when necessary to obtain the optical density (O.D.) below 0.6 to stay within the linear range of the instrument. Preliminary studies showed that the existence of hydrogel matrix and the elevated temperature (~50°C) did not interfere with the absorbance measurements at 660 nm. It was found experimentally that 1 O.D. unit is equivalent to 0.47 g/L of dry cell weight

For measuring the cell density and viability of the freely suspended hybridoma cells, a hemacytometer at 100X magnification in combination

with a phase contrast objective microscope were used to visualize and enumerate the trypan-blue (2 g/L in PBS) stained hybridoma cells. For measuring the total cell densities of entrapped hybridoma cells, the hydrogel matrix was first dissolved in EDTA or sodium citrate solution. The resultant solution was further diluted with isotonic saline solution. A Coulter Z_F electronic particle counter (Coulter Electronics, Hialeah, FL) was used to measure the total cell numbers in 0.5 ml of this diluted solution. The preliminary study showed that the presence of EDTA, sodium citrate and the dissolved gel did not affect the counting accuracy.

Viability of entrapped hybridoma cells was qualitatively determined by MTT (3-(4,5-dimethylthiazol-2-yl)-2,5 diphenyl) assay (Al-Rubeai and Spier, 1989). The assay is based on the capacity of mitochondrial enzymes of viable cells to transform the MTT tetrazolium salt (yellow) into the MTT formazan (blue). The hybridomas-entrapped hydrogel slab kept in the 6-well petri dish was incubated with a 0.5% (w/v) MTT solution (Sigma, Cat#M2128, prepared in PBS at pH 7.4) for one hour. Only the top of hydrogel slab contacted the MTT assay solution. The resultant penetration depths and intensities of the blue stains were used as the qualitative indictions of entrapped hybridoma viabilities.

III.7.2 Glucose, Lactate and Ammonia

Glucose, lactate and ammonia concentrations were all measured enzymatically (Sigma Chemical). The glucose concentration was determined through the reaction catalyzed by hexokinase and glucose-6-phosphate dehydrogenase to convert glucose to 6-phosphogluconate (Cat#16-UV). The lactate concentration was determined through the reaction catalyzed by lactate dehydrogenase to convert lactate to pyruvate (Cat#826-UV). The ammonia concentration was determined through the

reaction catalyzed by glutamate dehydrogenase to incorporate ammonia into glutamate (Cat#170-UV). These reactions result in concomitantly proportional changes of NAD(P)H, which could be measured at 340 nm absorbance by a spectrophotometer.

III.7.3 Amino Acids

All amino acid concentrations, except for cysteine, proline and histidine (undetectable by current protocol), were determined by a Hewlett Packard 1090 chem station HPLC using a hypersil C18 column and diode array detector. A precolumn OPA derivatization was performed automatically using a modification of a published method (Schuster, 1984).

III.7.4 Monoclonal Anti-Fibronectin Immunoglobulin G

Murine immunoglobulin G (IgG) concentrations were measured using an indirect ELISA. A solution containing an anti-murine-IgG, goat polyclonal antibody (Sigma, Cat#M8770), designated antigen, was first added to the 96-well microtiter plate at a concentration of 1 μg/ml for coating. The coating of antigen was completed after one hour of incubation at room temperature. Bovine serum albumin (Pierce, Cat#37525X) was then added to each well and incubated for half an hour for post-coating the unbound interior area of the well in order to prevent further binding with antigens or antibodies. The standard solutions of murine IgG-κ (Sigma, Cat#M9269) and the samples were added to the wells. The antibodies in the solutions, designated primary antibodies, would bind to the coated antigens. A second solution containing anti-mouse-IgG, goat polyclonal antibodies conjugated with horseradish peroxidases (Pierce, Cat#31436H; 5000X dilution), designated secondary antibodies, were then added to the wells, and these enzyme-conjugated secondary antibodies would bind to

the primary antibodies. Finally, the enzyme substrate solution (Pierce, Cat#37615) was added to the wells, and a reaction is accompanied by a color change at a wave length of 405 nm. The absorbance in each well of the microtiter plate was read by a 96-well microplate reader (Molecular device Co.) at 405 nm.

It is necessary to dilute the primary antibody titers below 0.1μg/ml to stay within the sensitive, linear response range of this assay. Note that each well in the microtiter plate was thoroughly washed to remove unbound compounds before the addition of next assay solution.

III.8 Mathematical Modeling

III.8.1 Hydrogel-Entrapment *E. coli* Cultures

This mathematical modeling includes the investigations of electrically-induced intra-membrane transport, cell growth kinetics and metabolism, and the coupling of intra-membrane transport with various biological phenomena. In addition, the temperature rise resulting from the applied electric fields in hydrogel slab was also theoretically analyzed.

Mathematical modeling of cell growth kinetics generates a system of nonlinear, parabolic partial differential equations which must be solved numerically. A numerical package DO3PBF, provided by the Numerical Algorithms Group (NAG FORTRAN) on a VAX machine was used. DO3PBF integrates a system of nonlinear (or linear) parabolic partial differential equations with one space variable, using the method of lines and Gear's method. The parabolic equations are approximated by a system of ordinary differential equations in time for the variables at the meshpoints, which is obtained by replacing the space derivatives by finite differences. Forty-one meshpoints equally spaced from upstream side to downstream side of hydrogel slab were used in the numerical solution. A

time accuracy of 0.5×10^{-4} hr was used in all the simulations. The FORTRAN source code for the simulation is provided in Appendix-I.

The theoretical analysis of temperature variation based on a steady-state energy balance generate a linear ordinary differential equation which can be solved analytically.

III.8.1.1 Electrically-Induced Intra-membrane Transport

An understanding of the transport rates induced by electrical forces is essential to explain experimental results and to delineate the underlying mechanisms. With this motivation, a one-dimensional continuum model (Nussbaum, 1986; Nussbaum and Grodzinsky, 1987; Grimshaw et. al., 1989) has been formulated to describe changes of solute and solvent flux in membranes in response to transmembrane electric fields. This model ignores the effect of membrane hydration induced by electric fields (see Grimshaw *et al.*, 1990).

The flux for the i-th salt species within a membrane, which considers phenomena including diffusion, electrical migration and forced convection, can be represented by,

$$\Gamma_i = \Phi\left(-\overline{D}_i \frac{\partial \overline{C}_i}{\partial x} + \overline{\mu}_i \frac{Z_i}{|Z_i|} \overline{C}_i E\right) + W_i \overline{C}_i U \qquad \text{----------(3.1)}$$

where Γ_i = i-th salt species flux (mole/m^2-hr)
Φ = membrane porosity
$\overline{D}_i$ = effective intra-membrane diffusivity (m^2/hr)
$\overline{C}_i$ = intra-membrane concentration of ion i (mole/m^3)
$\overline{\mu}_i$ = effective intra-membrane electrical mobility (m^2/Volt-hr)
Z_i = electric charge of species i
E = local electric field gradient (Volt/m)
U = area-average fluid velocity relative to the solid matrix (m/hr)
W_i = hindrance factor for convective transport (nearly unity for ions and small solutes)

Φ can be related to membrane crosslinking density (Reinhart and Peppas,1984). Wi depends on the solute size and hydrodynamic interaction. Both of these can be determined experimentally.

The flux must satisfy the continuity condition of:

$$\frac{\partial C_i}{\partial x} = \frac{\partial \Gamma_i}{\partial x} \qquad \text{----------(3.2)}$$

Darcy's law can be used to describe the fluid flow driven by both fluid pressure gradient and electroosmosis,

$$U = -k'\left(\frac{\partial P}{\partial x} + Z_m \bar{C}_m F E\right) \qquad \text{----------(3.3)}$$

where k' = hydraulic (Darcy) permeability (m^4/Nt-hr)
$\partial P/\partial x$ = a gradient in fluid pressure across the membrane (Nt/m^3)
$\bar{C}_m$ = concentration of ionized charge group in membrane (mole/m^3)
Z_m = electric valence of ionized charge group in membrane
F = Faraday constant (96490 Coul/mole)

Note that osmosis due to steric hindrance of macrosolutes has been neglected.

The transmembrane current density, J, is equal to the total applied current,

$$J = F \Sigma (Z_i \Gamma_i) \qquad \text{----------(3.4)}$$

Electroneutrality requires the sum of the concentrations of the fixed charges on gel matrix and the mobile ionic charges be zero at each position,

$$Z_m \bar{C}_m + \Sigma Z_i \bar{C}_i = 0 \qquad \text{----------(3.5)}$$

The above equations were used to formulate the following equations for the electrically-induced intra-membrane transport.

If no hydraulic pressure gradient and only electroosmotic solvent

flux exists, then eq.(3.3) can be written as,

$$U = -k' Z_m \bar{C}_m F E \quad \text{----------(3.6)}$$
$$= k_i J$$

where k_i = electroosmotic coupling coefficient (m^3/Amp-sec)

J = applied current density (A/m^2)

Combining eqs. (3.1), (3.4), and (3.5), one obtains:

$$k_i = \frac{-k' Z_m \bar{C}_m}{\Phi \Sigma \bar{\mu}_i |Z_i| \bar{C}_i + k' (Z_m \bar{C}_m)^2 F} \quad \text{----------(3.7)}$$

Although k_i can be calculated through the above known parameters which can be determined independently, in this case k_i was directly measured experimentally as described in Section-III.3.1. As for $\bar{\mu}_i$ and $\bar{D}_i$, they are assumed to differ from their free solution values by a similar hindrance factor, the Nernst-Einstein relation,

$$\frac{\bar{D}_i}{\bar{\mu}_i} = \frac{RT}{Z_i F} \quad \text{----------(3.8)}$$

Therefore, as long as $\bar{D}_i$ is known (generally it can be obtained experimentally), $\bar{\mu}_i$ can be calculated from eq. (3.8). For analyzing the hydrogel-entrapment cell cultures, the effective diffusivity of solutes in hydrogels were obtained form published experimental data (Yabannavar, 1988).

The flux eq. (3.1) used for solute transport can be rewritten as:

$$\Gamma_s = -\Phi \bar{D}_s \left(\frac{\partial \bar{C}_s}{\partial x} + \frac{Pe \bar{C}_s}{\delta_0} \right) \quad \text{----------(3.9)}$$

where δ_0 = membrane thickness

The effective Peclet number, including electrophoresis and electroosmosis, is,

$$Pe = \delta_0 \left(\frac{\Phi \bar{\mu}_s E + W_s U}{\Phi \bar{D}_s} \right) \quad \text{----------(3.10)}$$

$\bar{\mu}_s$ is zero for neutral solute, otherwise it can be determined from eq. (3.8). The effect of membrane porosity, Φ, was lumped into the effective diffusivity, $\bar{D}_s$, which can be obtained from published experimental data. The convective restriction, W_s, was assumed unity for all solutes.

Inserting this solute flux eq. (3.9) into the continuity eq. (3.2) results in,

$$\frac{\partial \bar{C}_s}{\partial t} = \bar{D}_s\left(\frac{\partial^2 \bar{C}_s}{\partial x^2} + \frac{Pe}{\delta_0}\frac{\partial \bar{C}_s}{\partial x}\right) \qquad \text{----------(3.11)}$$

The above one-dimensional continuum model can be used to explain the magnitude and kinetics of the electrically-induced changes in the solute flux perpendicular across the membrane, and therefore can be used to quantify the concentrations of substrate and metabolites in the cell-entrapped hydrogel slab.

III.8.1.2 Kinetics of *E. coli* Cell Growth

The cell growth kinetics was analyzed based on the following assumptions:

- The inoculum is homogeneous.
- There is only one rate-limiting nutrient.
- The inhibitory function of end products can be generalized into one single equation.
- A Monod type of kinetics is applicable.

$$\frac{\partial N}{\partial t} = \mu N \qquad \text{----------(3.12)}$$

$$\mu = \frac{\mu_{max} C_s}{K_m + C_s} f_i(C_w) \qquad \text{----------(3.13)}$$

$$f_i(C_w) = \left(1 - \frac{C_w}{C_{w1}}\right)\exp\left(-\frac{C_w}{C_{w2}}\right) \qquad \text{----------(3.14)}$$

Where N = cell density in gel matrix (g-cell/m^3-gel)

C_s = concentration of rate-limiting nutrient (mole/m^3)
μ_{max} = maximum specific growth rate (hr^{-1})
K_m = equivalent Michaelis-Menton constant (mole/m^3)
C_w = concentration of waste product (mole/m^3)
$f_i(C_w)$ = generalized inhibitory function of end products

The unknown inhibitory function $f_i(C_w)$, considered a generalized inhibition of all different inhibitory end products such as various organic acids and ethanol, can only be obtained experimentally. It has been found by Yabannavar (1988) that lactate and lactic acids produced by *lactobacillus* inhibited cell growth and productivity differently. Experimentally, it was determined that there is a linear inhibitory function (i.e., $1-C_w/C_{w1}$) for the dissociated lactate and an exponential function (i.e., $\exp(-C_w/C_{w2})$) for the undissociated lactic acid. Therefore, the undissociated form ,i.e., lactic acid, has a much stronger inhibitory effect on cell growth than the lactate ion, which is the dissociated form. At pH of 5, there is only about 6% of the total acid present in the undissociated form; but even this small amount could cause serious inhibition than that from the dissociated acid.

The movement of undissociated, neutrally charged acid could only be affected by electroosmosis, not by electrophoresis. Therefore, it is important that the mass balance consider both forms of the acid separately. In addition, these two forms of the acid are coupled through instantaneous equilibrium between dissociation and association of the acid, and this further complicated the overall mass balance of the acid. Consequently, the generalized inhibitory function for entrapped *E. coli* is extremely complicated and must be obtained experimentally. It is therefore decided to use an empirical approach to assess this inhibitory function, and to neglect the individual dissociation and association

reactions of various acids and to lump these influences into the empirically-obtained inhibitory function. The details will be explained later in the "Results and Discussion" section.

III.8.1.3 Coupling of Mass Transfer with *E. coli* Cell Metabolism

The kinetics of nutrient consumption was analyzed based on the following assumptions:

- All transport-related parameters are constant.
- Luedeking and Piret (1950) model, $Q_s = A*\mu+B$, is applicable, namely that the specific uptake rate is linearly correlated to specific growth rate.
- Only one rate-limiting nutrient, i.e., either glucose for anaerobic situation or oxygen for the aerobic system, exists.
- The variation of medium bath composition is negligible, i.e., the concentration of nutrient remains constant, and the concentrations of end products are zero in the medium bath. This is a reasonable assumption since the volume of the hydrogel slab is much smaller than the total volume of the culture medium, and the time of cultivation was comparatively short (less than 10 hours).

The nutrient mass balance is shown as follows,

$$\frac{\partial C_s}{\partial t} = \overline{D}_s \frac{\partial^2 C_s}{\partial x^2} - V_x \frac{\partial C_s}{\partial x} - Q_s N \qquad \text{----------(3.15)}$$

$$Q_s = \frac{Q_{s,max} C_s}{K_m + C_s} + m_s \qquad \text{----------(3.16)}$$

$$V_x = k_i J \qquad \text{----------(3.17)}$$

subject to boundary conditions of:

$X = -L,\ C_s = C_{s,b}$

$X = L,\ C_s = C_{s,b}$

and initial condition of:

$t = 0,\ C_s = C_{s,b}$

where C_s = concentration of nutrient in hydrogel (mole/m^3)
$\overline{D_s}$ = effective diffusivity of nutrient in hydrogel (m^2/hr)
V_x = electroosmotic flow rate (m/hr)
k_i = electroosmotic coupling coefficient (m^3/hr-Amp)
J = applied electric current density (A/m^2)
L = half thickness of hydrogel slab (m)
m_s = specific non-growth-associated (maintenance) nutrient uptake rate (mole/g-cell-hr)
Q_s = specific nutrient uptake rate (mole/g-cell-hr)
$Q_{s,max}$ = max. specific nutrient uptake rate (mole/g-cell-hr)

Since neither glucose nor oxygen is electrically charged, only electroosmosis contributes to convection.

The following assumptions were made for analyzing the kinetics of end product production:

- All transport-related parameters are constant.
- One generalized rate-inhibiting end product exists.
- The end product is diluted to zero when it enters the medium bath, i.e., the concentration of end product at the interface is zero.

The mass balance of end product is:

$$\frac{\partial C_w}{\partial t} = \overline{D}_w \frac{\partial^2 C_w}{\partial x^2} - V_x' \frac{\partial C_w}{\partial x} + Q_w N \quad \text{----------(3.18)}$$

$$V_x' = k_i * J \pm \frac{\overline{\mu_w}\, J}{\sigma} \quad \text{----------(3.19)}$$

$$Q_w = Y_{w/s}\, Q_s \quad \text{----------(3.20)}$$

subject to boundary conditions of:

$X = -L,\ C_w = 0$

$X = L,\ C_w = 0$

and initial condition of:

$t = 0,\ C_w = 0$

Where $\overline{D_w}$ = effective diffusivity of waste product (m^2/hr)
Q_w = specific waste production rate (mole/g-cell-hr)

$Y_{w/s}$ = yield of waste versus nutrient

V_x' = convective flow rate (m/hr), which comprises electroosmosis (K_iJ) & electrophoresis ($\pm \frac{\overline{\mu_w}J}{\sigma}$)

$\overline{\mu_w}$ = electrical mobility (m^2/Volt-hr), which can be estimated from Nernst-Einstein's relationship, as described in eq. (3.8).

III.8.2 Steady-State Analysis of Hydrogel-Entrapment Hybridoma Cultures

In order to estimate the oxygen penetration depth in the hybridoma cells-contained hydrogel slab, a steady-state condition and a homogeneous distribution of cell density are assumed. In the presence of a dc electric field and a κ-carrageenan hydrogel slab, we develop a steady-state equation to describe the oxygen concentration in the hydrogel slab:

$$k_iJ\left(\frac{\partial C_o}{\partial X}\right) = \overline{D_o}\left(\frac{\partial^2 C_o}{\partial X^2}\right) - q_oN \quad \text{----------(3.21)}$$

Subject to boundary conditions of:

$X = 0$ & L, $C_o = C_{o,b}$

where C_o = oxygen conc. in hydrogel slab (mM)

$\overline{D_o}$ = effective diffusivity of oxygen in hydrogel (cm^2/sec)

q_o = specific oxygen uptake rate of hybridoma cell (mmol/cell-sec)

N = entrapped hybridoma cell density (cells/ml)

$C_{o,b}$ = saturated oxygen conc. in medium bath (mM)

This equation can be solved analytically:

$$C_o = \left(C_{o,b} - \frac{q_bN}{k_iJ}\frac{L}{\exp\left(\frac{k_iJL}{\overline{D_o}}\right)-1}\right) + \frac{q_oN}{k_iJ}\frac{L}{\exp\left(\frac{k_iJL}{\overline{D_o}}\right)-1}\exp\left(\frac{k_iJ}{\overline{D_o}}X\right) - \frac{q_bN}{k_iJ}X \quad \text{-------(3.22)}$$

By assuming the 10% of air-saturation as the critical oxygen concentration, i.e., $C_o = 0.1 \times C_{o,b}$, we can calculate the distance, designated the oxygen penetration depth, at which oxygen concentration decreases to the critical value.

III.8.3 Temperature Variation in Hydrogel Slab

A steady state condition was assumed for energy balance within a hydrogel slab with a thickness of L in the presence of dc electric fields:

$$\rho \bar{C}_v V_x \frac{\partial T}{\partial X} = k_T \frac{\partial^2 T}{\partial X^2} + \frac{J^2}{\sigma} \quad \text{----------(3.23)}$$

where ρ = hydrogel density (1000 Kg/m^3)
$\bar{C}_v$ = specific heat capacity of hydrogel (4.1*10^{-3} joule/Kg-°C)
k_T = thermal conductivity (0.628 joule/m-s-°C)
σ = electrical conductivity (1.5 mho/m)
J = applied current density (A/m^2)
J^2/σ = volumetric heat production rate (watt/m^3)
$V_x = k_i * J$ = convective flow rate (m/s)

The boundary conditions are,

$X = 0, T = T_b$ (medium bath temperature)
$X = L, T = T_b$

The above parameters, considered constants, were calculated based on the properties of the culture medium. The k_i value was experimentally obtained. The temperature of the medium bath, T_b, was maintained constant at the gel/medium interface. The term on the left-hand side of eq.(3.23) represents the convective energy flow provided by electroosmosis, and the terms on the right include the conductive energy flow and the volumetric heat production generated by the electric fields. Eq.(3.23) can be solved analytically as shown in eq.(3.24),

$$T = \frac{BL}{A(1-e^{AL})}(e^{AX} - 1) + \frac{BX}{A} + T_b \quad \text{----------(3.24)}$$

$$A = \frac{\rho \bar{C}_v k_i J}{k_T} \qquad B = \frac{J^2}{k_T \sigma}$$

The temperature profile is apparently asymmetric and shifts towards the downstream side with respect to the direction of convection.

IV. RESULTS AND DISCUSSION

IV.1 SCREENING AND CHARACTERIZATION OF HYDROGELS

In order to illustrate the effects of electrokinetic phenomena on hydrogel-entrapped cells, various hydrogels were screened in order to select a hydrogel possessing the highest intra-membrane electroosmosis and the optimal biocompatibility for cell entrapment. In addition, the factors affecting the intra-membrane electroosmosis need to be characterized.

IV.1.1 Intra-membrane Transport Through Hydrogel

All intra-membrane transport experiments were conducted using the apparatus shown in Figure-3.2. The measurement of intra-membrane flux for each hydrogel was repeated at least twice, with the electric current density and electric polarity varied for each experiment. The representative time profiles of accumulated volumetric flow for κ-carrageenan and agarose are shown in Figures-4.1, and a plot of flow rate versus electric current density for various hydrogels is shown in Figure-4.2. The electroosmotic coupling coefficient, k_i, is calculated using the following relation:

$$k_i = V_x / J \quad \text{----------(4.1)}$$

where V_x = intra-membrane solvent flux, which is obtained from the slope of the curve in the volumetric flow rate profile
J = electric current density, which is obtained by dividing the total electric current with the exposed area of hydrogel membrane

The k_i value of a hydrogel is strongly related to the fixed charge density and permeability of the hydrogel matrix. Since natural hydrogels are

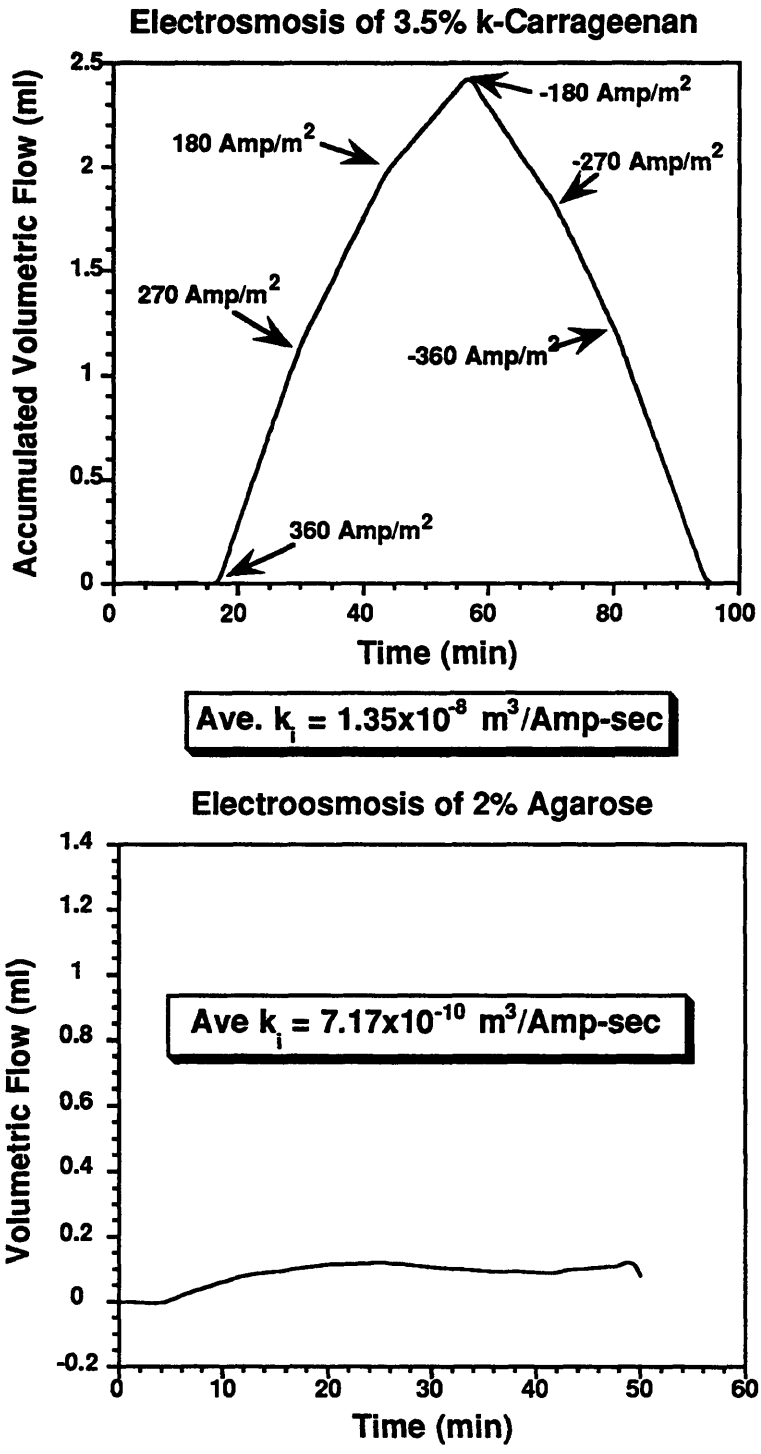

Figure-4.1: The representative profiles of accumulated volumetric flow for k-carrageenan and agarose. The average ki was calculated by dividing the volumetric flow rate by electric current density.

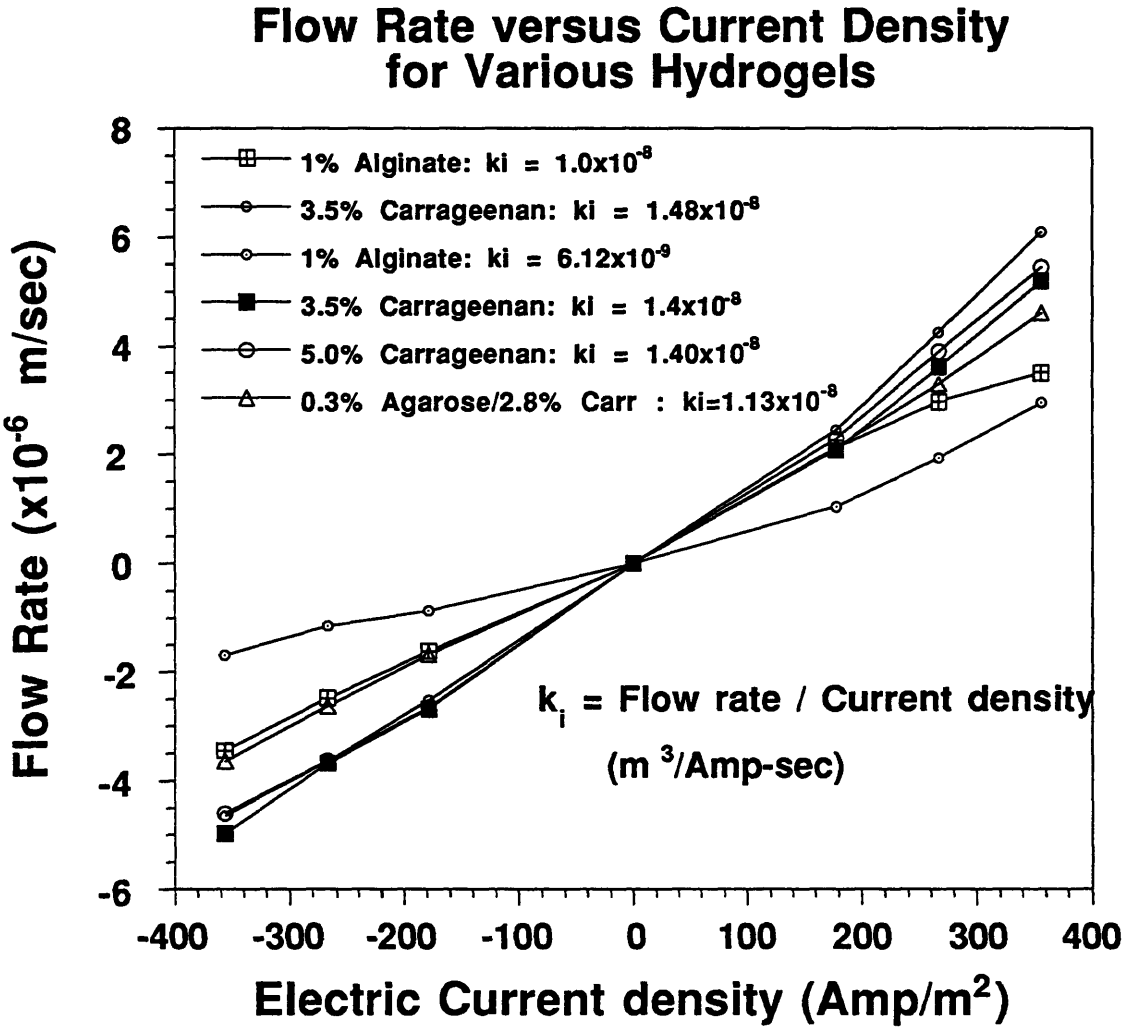

Figure-4.2: The flow rate versus electric current density for various hydrogels. The average ki was measured from the linear slope of the line for each hydrogel.

more porous than synthetic gels, higher k_i values for natural hydrogels are expected. For our hydrogel-entrapment cultures, it is desired to use a hydrogel which has a very high k_i. These studies of intra-membrane transport can also serve as a basis for understanding the effects of certain parameters, such as the fixed charge density and the crosslinking density of a hydrogel, on the k_i's of various hydrogels.

IV.1.1.1 PolyMethacrylic Acid (PMAA)

This hydrogel has been extensively studied by Grimshaw *et al.* (1989). PMAA has ionizable carbonate groups on its gel matrix and hence it is negatively charged. In our experiments, a membrane 500 μm thick was used. The crosslinker (diethylene glycol dimethacrylate) was used at concentrations ranging from 0.135% to 1.08% (mol crosslinker/mol monomer). Preliminary studies showed that the hydration, H (defined as the ratio of wet weight to dry weight of hydrogel), of PMAA varied from 4.0 to 16.4 for 0.135% crosslinking and from 2.1 to 9.7 for 0.54% crosslinking, respectively, when pH was changed from 3 to 7. These results show that the permeability (which is proportional to hydration) is very sensitive to the crosslinking density and the ionization of fixed charge groups due to pH changes.

For intra-membrane transport measurement, a pH 7, 100 mM KCl solution was used. A 320 A/m^2 current density was applied and the electric field polarity was changed once during the experiment. The average k_i value of the 0.135% crosslinked PMAA was found to be 3.2×10^{-9} $m^3/Amp\text{-}s$. As a result, PMAA hydrogel meets the requirement for inducible intra-membrane electroosmosis, but its biocompatibility with animal cells must be determined.

IV.1.1.2 PDMAEMA and PDMAEMA-MMA Copolymer

PDMAEMA (poly-dimethylaminoethyl methacrylate) has fixed amino groups on its gel matrix and hence is positively charged. A 1.08% (mol crosslinker/mol monomer) PDMAEMA hydrogel membrane with a thickness of 500 μm was used. The hydration of PDMAEMA varied from 4.7 to 30.1 when pH was changed from 8.2 to 5.0. Although the 1.08% crosslinking density of PDMAEMA is seven fold higher than the 0.135% crosslinking density of PMAA, the equilibrium hydration of PDMAEMA is 210% greater than that of PMAA. The greater hydration of PDMAEMA indicates that the permeability of PDMAEMA is greater than that of PMAA, and therefore PDMAEMA should possess a higher induced electroosmosis than PMAA.

For intra-membrane transport measurements, a pH 7, 100 mM KCl solution and an electric current density of 270 A/m^2 were used. The average k_i value was found to be 6.87×10^{-9} $m^3/Amp\text{-}s$. Although PDMAEMA crosslinking density is seven times greater than that of the 0.135% crosslinked PMAA, PDMAEMA's k_i value is still 1.2 times greater than that of PMAA. It is concluded that PDMAEMA could provide a higher induced transport augmentation than PMAA. A 0.27% (mol crosslinker/mol monomer) crosslinked PDMAEMA membrane with a thickness of 750 μm was prepared, and the DMEM solution (without serum) was used for our experiments. The average k_i value for this was obtained as 8.72×10^{-9} $m^3/Amp\text{-}s$.

Gharapetian *et al.*, (1986) successfully used non-crosslinked DMAEMA-MMA (methyl methacrylate) copolymers to encapsulate hybridoma cells. The same copolymer was therefore synthesized for our initial studies. A 65% DMAEMA-35% MMA (molar ratio) non-crosslinked copolymer with a thickness of 500 μm was prepared. The average k_i value

was found to be 1.48×10^{-8} m^3/Amp-s, which is 1.2 fold greater than that of the 1.08% crosslinked PDMAEMA membrane. Later a 65% DMAEMA-35% MMA copolymer with a crosslinked density of 0.135% (molar ratio) and a thickness of 500 μm in DMEM (without serum) was used for our studies. The average k_i value was found to be 6.90×10^{-9} m^3/Amp-s, which is half of that of the non-crosslinked copolymer. Since the DMAEMA/MMA copolymer had the greatest cell-biocompatibility and the highest k_i value, this copolymer was considered the best candidate among the different synthetic hydrogels available.

IV.1.1.3 Agarose and Agar

Agarose is widely used as the media for chromatography, electrophoresis and cell/enzyme immobilization. SeaKem HEEO® (FMC Co.) agarose, which is designed for electrophoretic uses and has the highest fixed charge density among the various types of agarose and therefore was selected for the initial investigations. A 2% (w/v) agarose was cast into a membrane with a thickness of 500 μm. The hydrogel membrane was laid between two filter papers for support and for reinforcement. An electric current density of 100 A/m^2 and DMEM solution (without serum) were used. A plot of accumulated liquid volume through the membrane as a function of time for agarose was shown earlier in Figure-4.1. As seen in this figure, no detectable intra-membrane electroosmotic solvent flux was observed. This confirms that highly purified agarose does not have significant fixed charges and is therefore not suitable for this research.

Agar has a small amount of fixed sulfuric groups in its structure and hence is slightly negatively charged. A 500 μm-thick, 5% (w/v) agar (Difco Co., Bacto-Agar) membrane was prepared, and an electric current

density of 320 A/m^2 and DMEM solution (without serum) were used in our study. The average k_i value was found to be 3.42x10^{-9} m^3/Amp-s, which is significantly lower than that for the crosslinked PDMAEMA. It was therefore concluded that the fixed charges on agar is not sufficient for inducing significant electroosmotic flux.

IV.1.1.4 Calcium-Alginate and Alginate-Agarose Blend

Alginate has fixed carbonate groups in its structure and hence is negatively charged. A 1% (w/v) calcium-alginate (CellPrep®, FMC) hydrogel membrane with a thickness of approximately 500 μm and DMEM (w/o serum) were used in our study. The hydrogel membrane was placed between two filter papers for support to ensure the gel had sufficient strength. The alginate gel shrinks during gel casting. This shrinkage generates numerous internal empty spaces (channels) in the gel matrix and makes the alginate membrane thinner than expected. Calcium-alginate hydrogel is considered the most compatible with animal cells, albeit having a weak and fragile structure. Moreover, calcium ions which crosslinked the linear alginate to form a matrix could be electrophoretically extracted by dc electric fields. These drawbacks render calcium-alginate membranes extremely unstable in dc electric fields, and the measurements of k_i became highly inconsistent with values ranging from 5.4x10^{-9} to 10.0x10^{-9} m^3/Amp-s. As a result, the dissolution of the calcium-alginate hydrogel in applied dc electric fields makes it unacceptable for this research.

In order to overcome the dissolution of calcium alginate, a 1.125% (w/v) alginate (CellPrep®, FMC) - 0.4% (w/v) agarose (SeaPlaque®, FMC) gel blend with a thickness of 500 μm was prepared. This blend has an improved structural strength and it also maintained structural integrity

in the presence of dc electric fields. The intra-membrane transport measurement was performed in DMEM (without serum) and a k_i of 1.2x10-8 m^3/Amp-s was obtained. Since this hydrogel blend possesses a high k_i value and is known to have good animal cell biocompatibility, it was selected for subsequent studies for hybridoma entrapment cultivation.

IV.1.1.5 Potassium-κ-Carrageenan

κ-carrageenan has fixed sulfate groups in its structure and hence is negatively charged. κ-carrageenan hydrogel has an improved structural strength and a higher density of negative fixed charges compared to calcium-alginate gels. Three and a half percent and five percent (w/v) potassium-κ-carrageenan gels 500 μm thick and DMEM (without serum) were used in our studies. The improved gel strength of κ-carrageenan allowed the measurements to be conducted without the use of filter papers for support. It was found that there is no discernible difference in the k_i values for the 3.5% and 5% (w/v) κ-carrageenans, and that the k_i measurements were highly consistent. The volumetric flow rate profiles of the 3.5% (w/v) κ-carrageenan was shown earlier in Figure-4.1. The average ki value was found to be 1.4x10-8 m^3/Amp-s, which is the highest among all synthetic and natural hydrogels.

κ-carrageenan has been widely used to entrap viable microbial cells, but has not been reported for the successful entrapment of animal cells. Since the crosslinking agent, potassium ions, can be electrophoretically extracted from the gel matrix in the presence of dc electric fields, it is necessary to add potassium ions into the culture medium in order to maintain structural integrity. The presence of extraneous potassium ions in the culture medium is acceptable for most microbial cells including *E. coli* cells.

In conclusion, potassium-κ-carrageenan possesses an greatest k_i value and a reasonable biocompatibility, and these qualities make it the best candidate for the hydrogel-entrapment microbial cultures. Its biocompatibility with hybridoma cells, however, remains to be determined. In the case of the alginate gels and the alginate/agarose blend, the later does not encounter the dissolution problem, and possesses a reasonable k_i value and biocompatibility with animal cells. The alginate/agarose blend will therefore be our first choice for hybridoma entrapment in case κ-carrageenan is later found to be not compatible for hybridoma cells. All synthetic hydrogels, on the other hand, possess only moderate k_i values and uncertain biocompatibility. Therefore synthetic hydrogels will not be used in our hydrogel-entrapment cultures. A summary of the k_i values of various hydrogels is shown in Figure-4.3.

IV.1.1.6 Detailed Study of Potassium-κ-Carrageenan

The three most important factors affecting the electroosmotic coupling coefficient, k_i, are the fixed charge density of the hydrogel matrix, the cell loading and the nature of the hydrogel additives. Since κ-carrageenan has been selected as the system for microbial cell entrapment, it is desired to further investigate the influences of these three factors on the k_i value of κ-carrageenan.

The first factor affecting electroosmosis is the fixed charge density which provides the electroosmotic flow in the hydrogel. As shown by eq. (3.7), k_i is proportional to the fixed charge density, C_m. In order to elucidate the effects of fixed charge density on k_i, hydrogel blends of agarose and κ-carrageenan were prepared. Since agarose is electrically neutral, the charge density on κ-carrageenan is reduced when blended with agarose. As shown in Figure-4.4, an increase in agarose

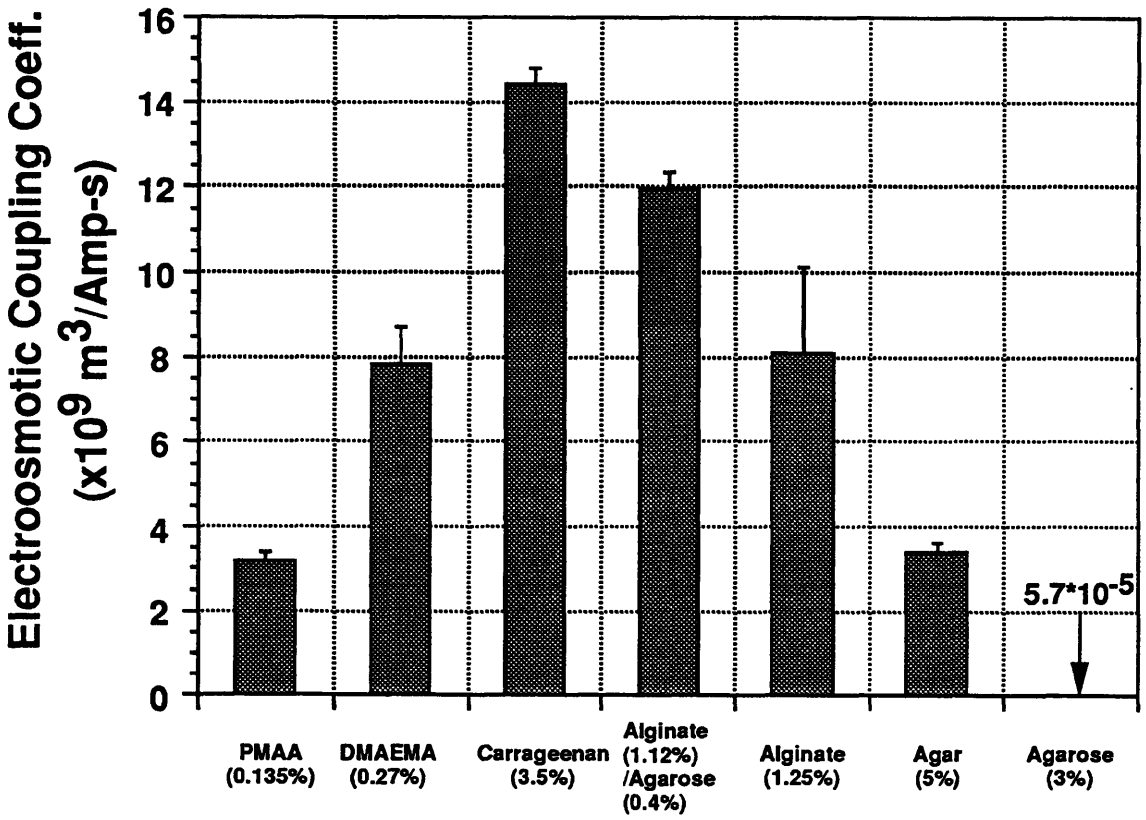

- k-Carrageenan - Good gel strength, high k_i, uncertain biocompatibility – *E. coli* cell entrapment
- Alginate/agarose gel blend - Reasonable gel strength and k_i, good biocompatibility – Hybridoma cell entrapment

Figure-4.3: Comparison of electroosmotic coupling coefficients (k_i) for various hydrogels

concentrations from 0 to 0.8% (w/v) accompanied with a decrease in κ-carrageenan concentrations from 3.5 to 0.7%(w/v) can reduce the charge density of the hydrogel blend by 53%. This resulted in a significant reduction in the k_i value by 80% (from $1.4x10^{-8}$ to $2.8x10^{-9}$ m^3/Amp-s). It was therefore concluded the fixed charge density strongly affects the electroosmotic property of the hydrogel.

The second factor affecting electroosmosis is the cell loading in the hydrogel. As shown by eq. (3.7), k_i is proportional to the hydraulic permeability, k', which will decrease with increasing cell concentrations in the hydrogel. It is expected that k_i will be inversely affected by cell loading. As shown in Figure-4.4, the k_i decreased by 10% (from $1.4x10^{-8}$ to $1.31x10^{-8}$ m^3/Amp-s) in κ-carrageenan hydrogel loaded with $1.2x10^7$ cells/ml-gel when compared to no cells were in the hydrogel. However when the cell loading was increased from $1.2x10^7$ to $7.2x10^7$ cell/ml-gel, the k_i value decreased only by 14% (from $1.4x10^{-8}$ to $1.24x10^{-8}$ m^3/Amp-s). These results show that the amount of cell loading does not have a significant effect on electroosmotic coupling coefficient. Since the natural hydrogel matrix is already extremely porous (e.g., average pore sizes ranging from 0.01 to 0.1 μm), the cell loading did not change the permeability significantly and, hence, k_i was not significantly affected.

The last factor affecting electroosmosis is the nature of the hydrogel additives for gel structure reinforcement and for the enhancement of cell immobilization efficiency. The most widely used additives for κ-carrageenan are polyethyleneimine (PEI), glutaraldehyde (GA) and GA/hexamethylenediamine (HMDA) (Takata *et al.*, 1982; Nishida *et al.*, 1979). These additives could interact with the fixed charge groups on the hydrogel matrix and with the matrix backbone to alter the fixed charge density and permeability of the hydrogel. As seen in Figure-4.4, the

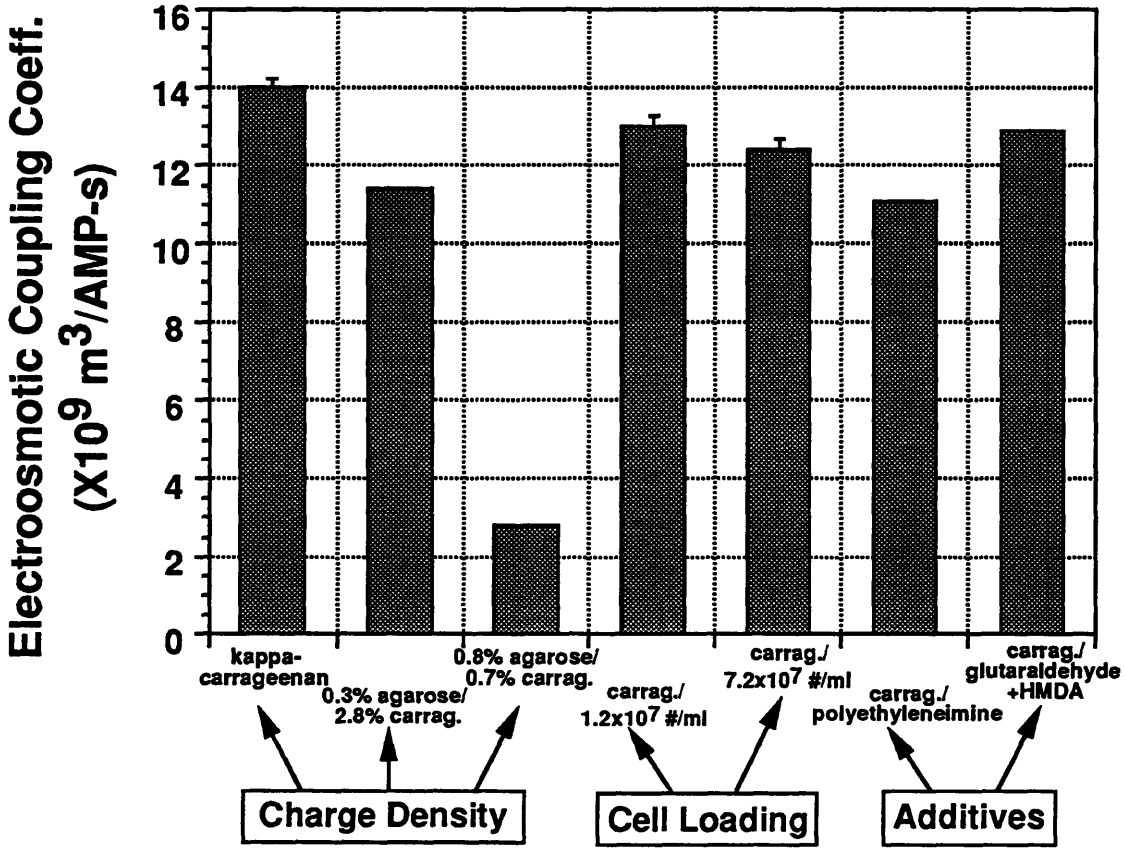

- Charge density strongly affects k_i
- Cell loading and Additives slightly affect k_i

Figure-4.4: The influence of various parameters on the k_i value of κ-carrageenan

addition of GA/HMDA reduced the k_i by 10% ($1.4x10^{-8}$ to $1.29x10^{-8}$ m^3/Amp-s), and PEI decreased the k_i by 23% (decreased to $1.11x10^{-8}$ m^3/Amp-s). The greater reduction of k_i when PEI was used could be attributed to the greater extent of charge neutralization in the hydrogel matrix. These effects are, however, only medial and it can be concluded that hydrogel additives did not markedly alter the electroosmotic properties of κ-carrageenan.

IV.1.2 Biocompatibility of Hydrogels

The biocompatibilities of natural hydrogels including agar, alginate, κ-carrageenan and alginate-agarose gel blend were investigated. Among these natural hydrogels, highly purified alginate and agarose are the most widely used for animal cell entrapment. Unfortunately, since agarose is electrically neutral and calcium-alginate tends to lose structural integrity in the presence of dc electrical fields, neither of them by itself fulfills our requirement for this research. The biocompatibilities of the other electrically-charged hydrogels such as agar and κ-carrageenan were first investigated. Later, alginate and agarose were blended so that agarose served as the backbone for maintaining the integrity of the gel while alginate provided the fixed electrical charges required for electroosmosis. Biocompatibility studies for synthetic gels were not conducted because of the presence of toxic monomer residues and the low k_i's.

Mattiasson (1983) has shown that many natural hydrogels are able to entrap and support the growth of microbial organisms such as bacteria and fungi. No significant differences were found in microbial cell growth and productivity between the hydrogel systems and freely-suspended cells. Hybridoma cells and plant cells, however, behave differently when entrapped in different hydrogels. All natural hydrogels have

polysaccharide backbones derived from different sugar monomers. The types of polysaccharide backbones and the concentrations of hydrogel determine the stiffness of the hydrogel matrix, which is a dominant factor regulating the presence of vacant channels in the matrix (see Section-II.2.3; a vacant channel is a closed vacant cavity inside the gel). It will be shown later that this availability of vacant channels in the hydrogel matrix is critical for hybridoma cell proliferation.

All experiments were performed in duplicate. The initial studies showed that the incubation of hybridoma cells, CRL-1606, at 45°C for 10 minutes did not affect cellular functionality, but at 50°C for 10 minutes completely suppressed cell growth. All melted hydrogels were, therefore, kept at 45°C in a water bath to prevent solidification before mixing with the viable cells. It is hoped that through the biocompatibility studies, the optimum hydrogel can be selected and used in subsequent hydrogel-entrapment hybridoma cultures.

IV.1.2.1 κ-Carrageenan and Agar

The biocompatibility of agar and κ-carrageenan with hybridomas CRL-1606 was first investigated. The 2% (w/v) agar (Kellco Co.) was cast into a gel slab with a thickness of 5 mm. The 3.5% (w/v) potassium-κ-carrageenan (CellPrep®, FMC Co.) liquid gel was cast into gel beads with diameters ranging from 1 to 3 mm. The viability of agar-entrapped hybridoma cells was determined by the MTT (3-(4,5-dimethylthiazol-2-yl)-2,5 diphenyl) assay. Agar-entrapped hybridoma cells remained viable after entrapment, but did not proliferate and gradually lost viability over a five-day cultivation period. This is probably due to the presence of impurities in the agar.

Hybridoma cells were inoculated into soluble κ-carrageenan, and

gelation of the hydrogel beads resulted in an initial concentration of 1.5-3x10^6 cells/ml-gel. Hybridoma cells remained viable for 30 days, but no discernible cell proliferation was observed (based on the MTT assay and lactate production). This may be due to the stiffness and an inadequate microenvironment inside the κ-carrageenan gel matrix (Nilsson *et al.*, 1986). As a result, potassium-κ-carrageenan can only be used for entrapping *E. coli* cells. As for entrapment of hybridoma cells, natural hydrogel blends were examined.

IV.1.2.2 Agarose, Alginate and Alginate-Agarose Gel Blend

The 1% and 4% (w/v) agarose (SeaPlaque®, FMC Co.) solutions were cast into 5 mm hydrogel slabs. Hybridoma cells CRL-1606 were suspended into the agarose solution and followed by gelation to become a slab with a cell concentration of 1.0x10^6 cells/ml-gel inside the gel. These cells entrapped in 1% (w/v) agarose gel proliferated for 10 to 13 days. We have observed the formation of cell clusters instead of the homogeneous distribution of cell population inside the agarose slab. On the other hand, hybridoma cells entrapped in 4% (w/v) agarose gel did not proliferate but remained viable for 10 days. This confirms the previous finding that the stiffness of the hydrogel matrix is a critical factor affecting proliferation of hybridoma cells (Nilsson *et al*,. 1986).

One and a quarter percent (w/v) calcium-alginate (Cellprep®, FMC Co.) was cast into gel beads with diameters ranging from 1 to 3 mm. Hybridoma cells, CRL-1606, were placed into the gel solution and followed by gelation to form beads at a cell concentration of 3.0x10^5 cells/ml-gel. Photomicrographs of the gel beads are shown in Figure-4.5. Hybridoma cells proliferated very well (based on the MTT assay and lactate production) for 18 days within the vacant channels of the calcium-alginate

Figure-4.5: Photomicrographs of hybridoma cell-entrapped gel beads. Cell proliferated well in the vacant channels of the gel beads.

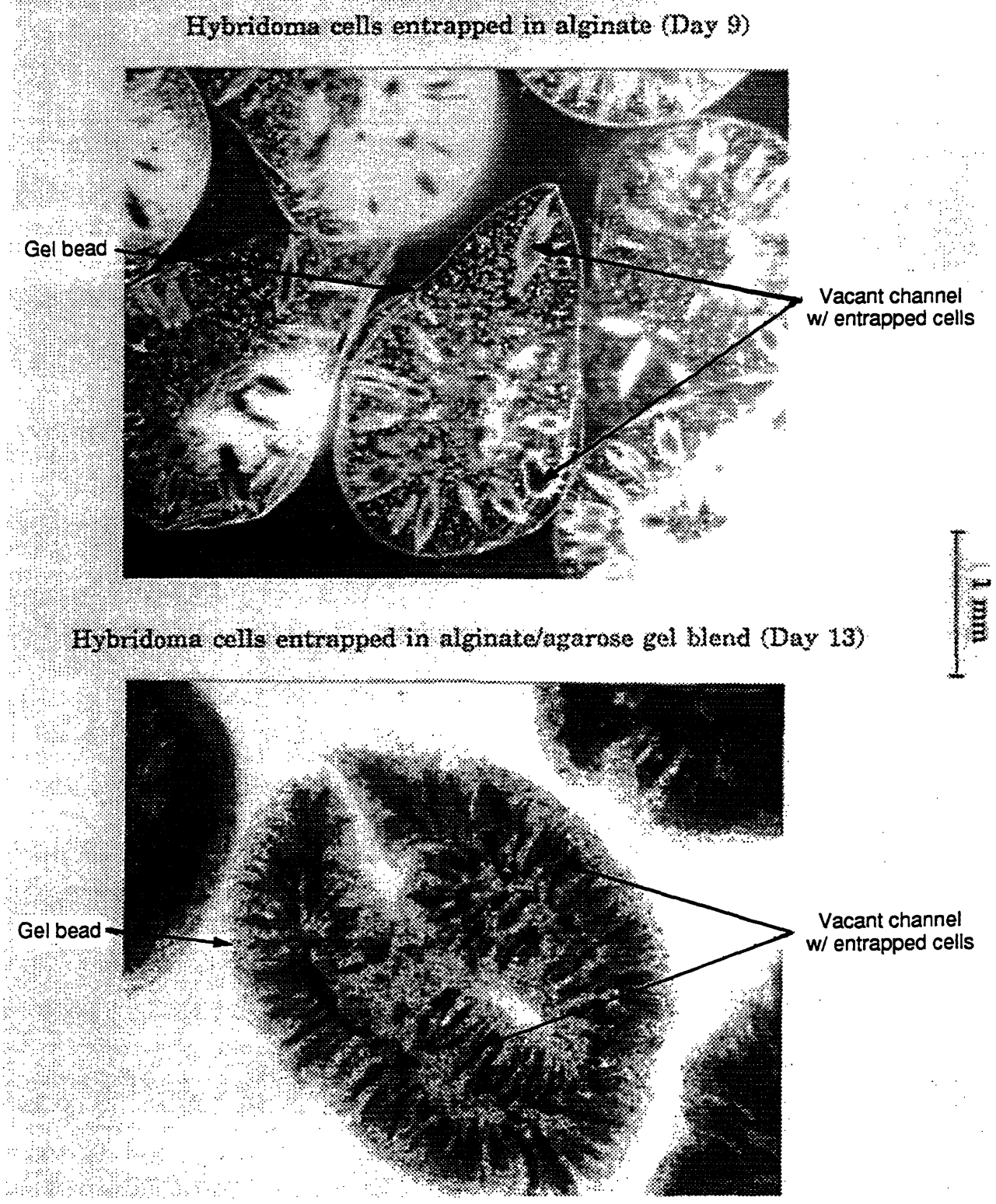

gel beads, but no discernible proliferation was observed inside the hydrogel beads but outside those vacant channels.

The biocompatibility of a calcium-alginate/agarose gel blend was investigated to use a 1% (w/v) agarose (SeaPlaque®, FMC Co.) gel and a 1.25% (w/v) sodium alginate (CellPrep®, FMC Co.). Various alginate-to-agarose ratios were tested and the gel blend was cast into gel beads. The screening of the optimal blending ratio was conducted as follows: the alginate concentration was maintained at 1.125% (w/v) and the agarose concentration was sequentially reduced until the optimal blending ratio (based on the biocompatibility and gel structure strength) was obtained. In the 1.125% alginate-1% agarose blend, it was found that the vacant channels in the hydrogel beads were absent and hybridomas CRL-1606 did not proliferate well in this blend. As the agarose concentration was reduced to 0.4% (w/v), vacant spaces in the hydrogel beads gradually appeared, and hybridoma cells were able to thrive well in these vacant spaces. As shown in Figure-4.6, cell density increased from 4.0×10^6 to 40.0×10^6 cells/ml-gel in 17 days. This finding is quantitatively similar to that observed by other researchers (Nilsson *et.al.*, 1896). From these results, the 1.125% (w/v) alginate-0.4% (w/v) agarose gel blend was chosen to entrap hybridoma cells CRL-1606.

In summary, it was found that the 3.5% (w/v) potassium-κ-carrageenan gel possessed the highest electroosmotic coupling coefficient, k_i, and the best gel strength among all the natural hydrogels. Unfortunately, its biocompatibility was shown to be unacceptable for hybridoma entrapment. κ-carrageenan was therefore used only for *E. coli* entrapment. On the other hand, the 1.125% (w/v) alginate/ 0.4% (w/v) agarose gel blend had a reasonable k_i and a good biocompatibility with hybridoma cells CRL-1606, and the gel blend was also able to maintain

Figure-4.6: Biocompatibility of alginate/agarose gel blend with hybridoma cells, CRL-1606.

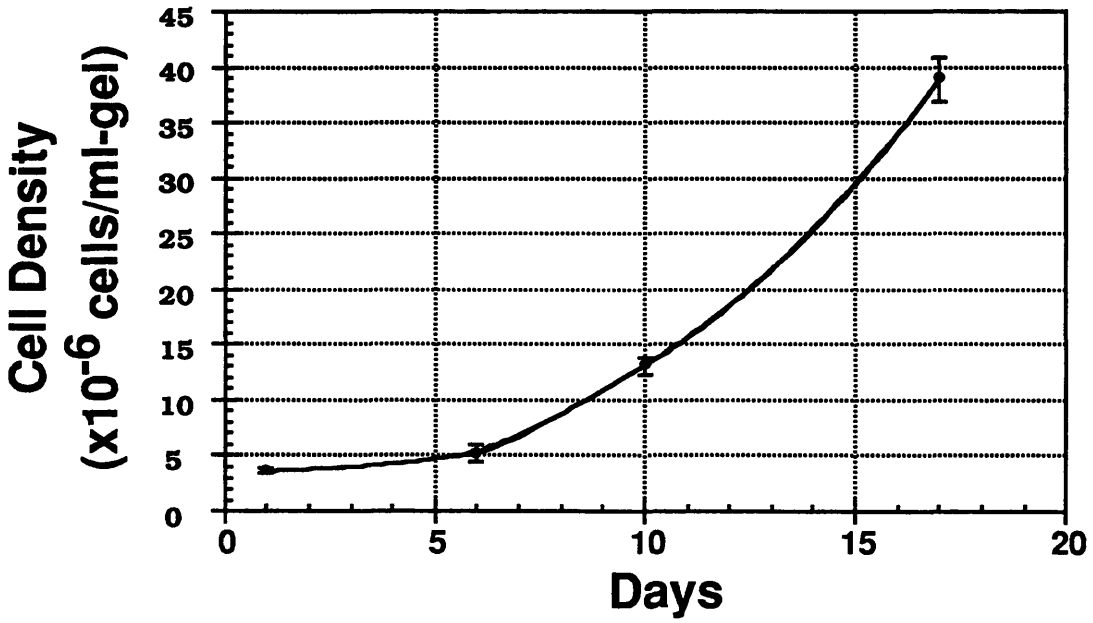

- 1.125%(W/V) alginate/0.4%(W/V) agarose gel blend
- Gel concentration (stiffness) affected cell proliferation
  - The importance of vacant spaces in hydrogel matrix
  - Low concentration of gel caused cell leakage
- Entrapped cells behaved totally different from suspended cells
  e.g. Doubling time increased from 16 hours to ~ 4 days
  - Data obtained from suspended hybridoma cells is not applicable to entrapped hybridoma cells

Conclusion

- **Hybridoma cells may not be a good system in illustrating this technique**

structural integrity in the presence of dc electric fields. Hence the alginate/agarose gel blend will be used to entrap hybridoma cells for cultivation.

IV.2 HYDROGEL-ENTRAPMENT CULTURES IN THE PRESENCE OF DC ELECTRIC FIELDS

IV.2.1 Hybridoma Cells Entrapped in Alginate/Agarose Gel Blend

A preliminary study showed that a current density of up to 120 A/m^2 did not affect the growth of suspension hybridoma cells, CRL-1606, during the early exponential growth phase (data not shown). Subsequently, an electric current density of 100 A/m^2 was applied in our hydrogel-entrapment hybridoma cultures.

The hybridoma cells, CRL-1606, were entrapped in a 1.125% (w/v) alginate-0.4% (w/v) agarose gel blend. The initial cell loading in the hydrogel slab was $4x10^6$ cells/ml-gel. The cultivation was terminated after 9 days. The cell density distributions within the hydrogel slab was measured and the data are shown in Figure-4.7. The upstream half of the hydrogel slab is the section of the slab facing the incoming convective solvent flux. This is also the side of the hydrogel slab which is in contact with the vigorously-agitated medium bath. As can be seen from the Figure-4.7, the hybridoma cells proliferated only within 1.0 mm from the surface of the upstream half of the hydrogel slab. Cells grew heterogeneously, i.e., cells formed clusters instead of a homogeneous distribution inside the hydrogel slab. Cell clusters mainly resided in the vacant channels of the hydrogel. Cells located in the interior of the hydrogel slab did not grow. There was no cell proliferation in the downstream half of the hydrogel slab. This is because the vigorous agitation occurred only in the upstream medium bath. Nutrient depletion (possibly oxygen) and/or waste product accumulation in the downstream medium bath might have limited cell growth in this half of the hydrogel slab.

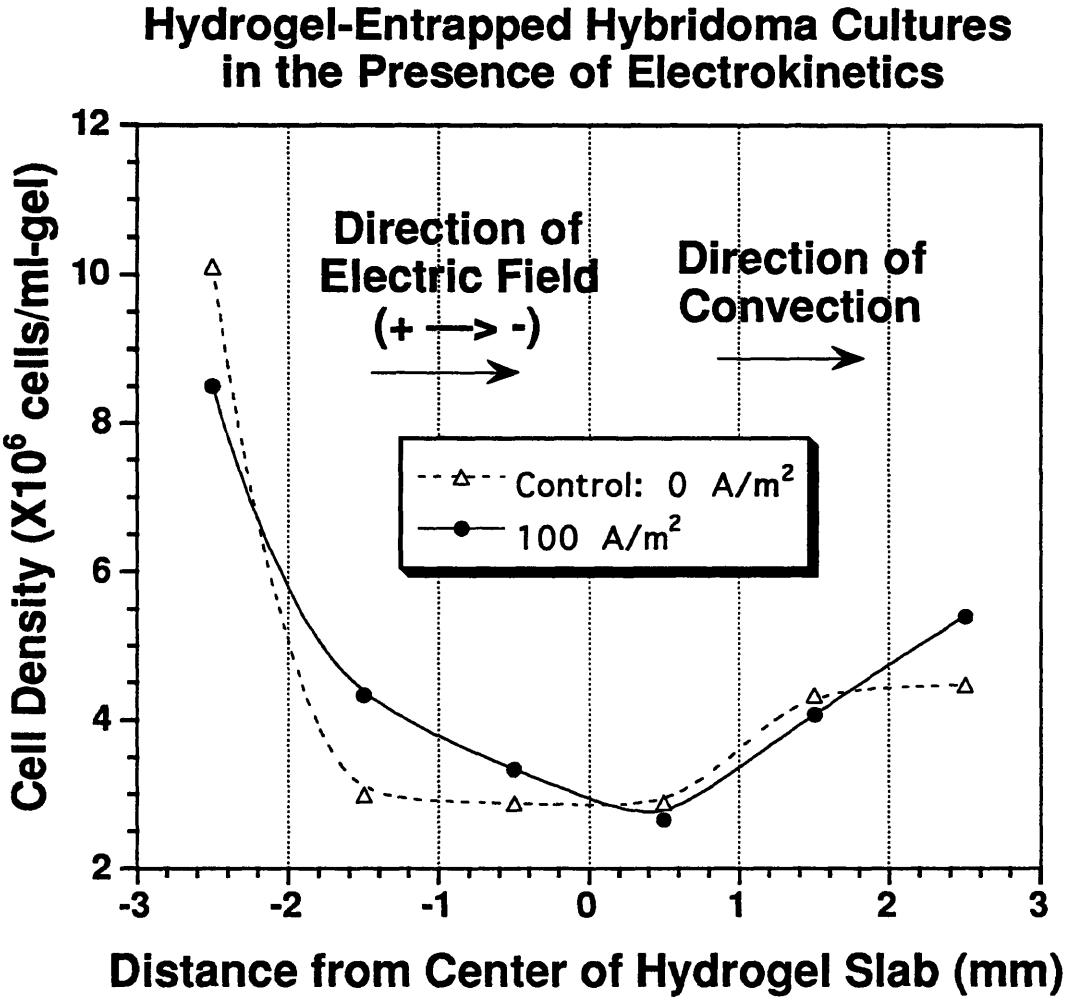

- Cell growth occurred in the 1.0 mm-thick surface layer facing incoming convection
- No enhancement of cell growth was observed in the electrokinetic culture
- Hydrogel matrix may be the limiting factor

Figure-4.7: The entrapped hybridoma culture in alginate/ agarose gel blend. 100 A/m^2 was applied.

A steady state mathematical model of entrapped hybridoma cell growth was shown by eq. (3.21). Where homogeneous cell distribution and no waste product inhibition were assumed. The growth kinetic data of hybridoma cells CRL-1606 from Glacken (1987) were used in this model. Based on the analysis, cells could grow up to 10^7 cells/ml-gel within a hydrogel slab with a thickness of 1 mm without encountering oxygen limitation. At a current density of 100 A/m^2, the cell growth inside the hydrogel in the presence of the electroosmotically-augmented transport of oxygen indicates an 50% increase in cell concentration compared to the electric-field-free cultivation. Experiments were thus conducted to compare the results from the mathematical simulation.

In our experiments, however, the hybridoma cells under an applied current density of 100 A/m^2 did not show enhanced growth compared to the control culture performed in the absence of an electric field. This indicates that other unknown factors in addition to oxygen limitation was hindering the growth of the entrapped hybridoma cells. As mentioned earlier (Section-IV.1.2.2) as well as published in the literature (Nilsson *et al.*, 1986), the stiffness of the agarose hydrogel matrix can strongly affect the proliferation of entrapped hybridomas. Furthermore, it has been reported that for BHK cells, growth occurred only in the vacant channels in the calcium-alginate gels (Shirai *et al.*, 1988; 1989). It was similarly observed in our earlier experiments that hybridoma cells CRL-1606 proliferated only in the vacant channels of the alginate-agarose gel blend. These imply that the hydrogel matrix physically affected the growth of entrapped cells. Due to this behavior, the hydrogel-entrapped hybridoma culture experiment was abandoned. As a result, *E. coli* cells, which are insensitive to the hydrogel matrix with respect to growth were used to illustrate the electrokinetic effects on transport augmentation and cell

growth.

IV.2.2 *E. coli* Cells Entrapped in Various Hydrogels

IV.2.2.1 Preliminary Suspension E. coli Cultures

Preliminary suspension *E. coli* cultures were conducted in order to ascertain the tolerance of these cells in suspension against dc electric fields. The growth of *E. coli* cells in suspension in the absence of the electric current density (the control culture), and in the presence of 120 and 270 A/m^2 are shown in Figure-4.8. Only pH and DO were monitored in these experiments. In less than two hours into cultivation, it was found that pH decreased to pH 5 and oxygen was depleted. Final cell densities reached only 3 DCW g/L for all cases. Comparing the cell growth of the electrokinetic cultures to the control culture, no apparent difference in either growth rate or final cell density was observed. This is probably due to the inhibition of cell growth by the decreased pH before the depletion of nutrients. The effects of electrokinetic removal of inhibitory end-products on suspension *E. coli* growth could not be observed.

IV.2.2.2 General Features of Entrapped *E. coli* Growth

Entrapped *E. coli* cells were cultivated in a rectangular culture chamber as described in Section-III.4.1. The pH and DO in the ambient medium bath did not change significantly until approximately 9 hours after cell inoculation. These changes in the medium were caused by the leaked *E. coli* cells from the hydrogel slab. As a result, all entrapped *E. coli* cultures were terminated after 10 hours of cultivation to prevent cell leakage.

In the presence of a dc electric field, electrophoretic movements of the charged solutes will always occur in a hydrogel which is electrically

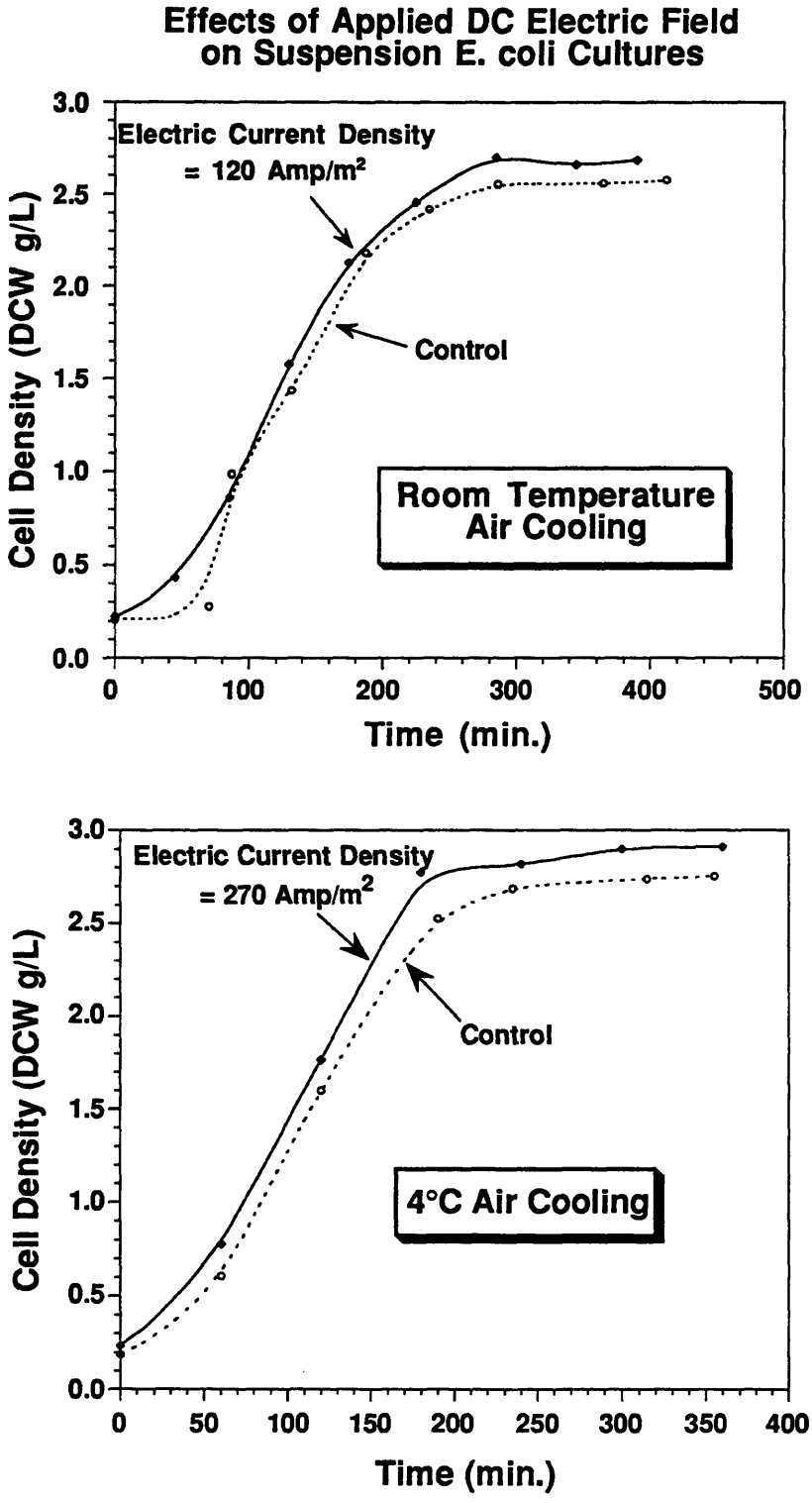

Figure-4.8: Suspension E. coli cultures in the presence of 120 and 270 Amp/m^2.

neutral or charged. But the existence of electroosmotic movements of solutes depends on the presence of the fixed charges in the gel structure. To distinguish the differences between the effects of electrophoresis and the effects of electroosmosis on mass transfer and cell growth, two kinds of natural hydrogels were used for cell entrapment. The first hydrogel is the negatively-charged κ-carrageenan, where electrophoresis of charged solutes and electroosmosis of both charged and neutral solutes exist. The second hydrogel is the electrically-neutral agarose, where only electrophoresis of charged solutes exists. Since the growth-limiting nutrient, either glucose or oxygen, is electrically neutral, the augmentation of nutrient transport across the hydrogel by a dc electric field only exists in the negatively-charged κ-carrageenan, and not in the electrically-neutral agarose. The enhanced removal of charged inhibitory end products by a dc electric field, on the other hand, exists in both κ-carrageenan and agarose. From these reasons, the effects of electrophoretic removal of inhibitory end products on entrapped cells could be identified using agarose-entrapped cell cultivations. The study using κ-carrageenan-entrapped cell cultures could then be used to identify the sole effect of electroosmotic augmentation of nutrient transport from the effects of the overall enhanced mass transfer on the growth of entrapped cells.

E. coli cells were entrapped in κ-carrageenan and in agarose through the procedures described in Section-III.3.2. The distributions of *E. coli* cell densities within various hydrogels are shown in Figure-4.9. This is the side-view of a hydrogel slab visualized along the direction of mass transfer traveling perpendicularly from medium bath through the hydrogel slab. The upstream half of the hydrogel slab is facing the incoming convective flux. Since κ-carrageenan possesses negatively charged groups on the hydrogel matrix, the direction of electroosmosis is

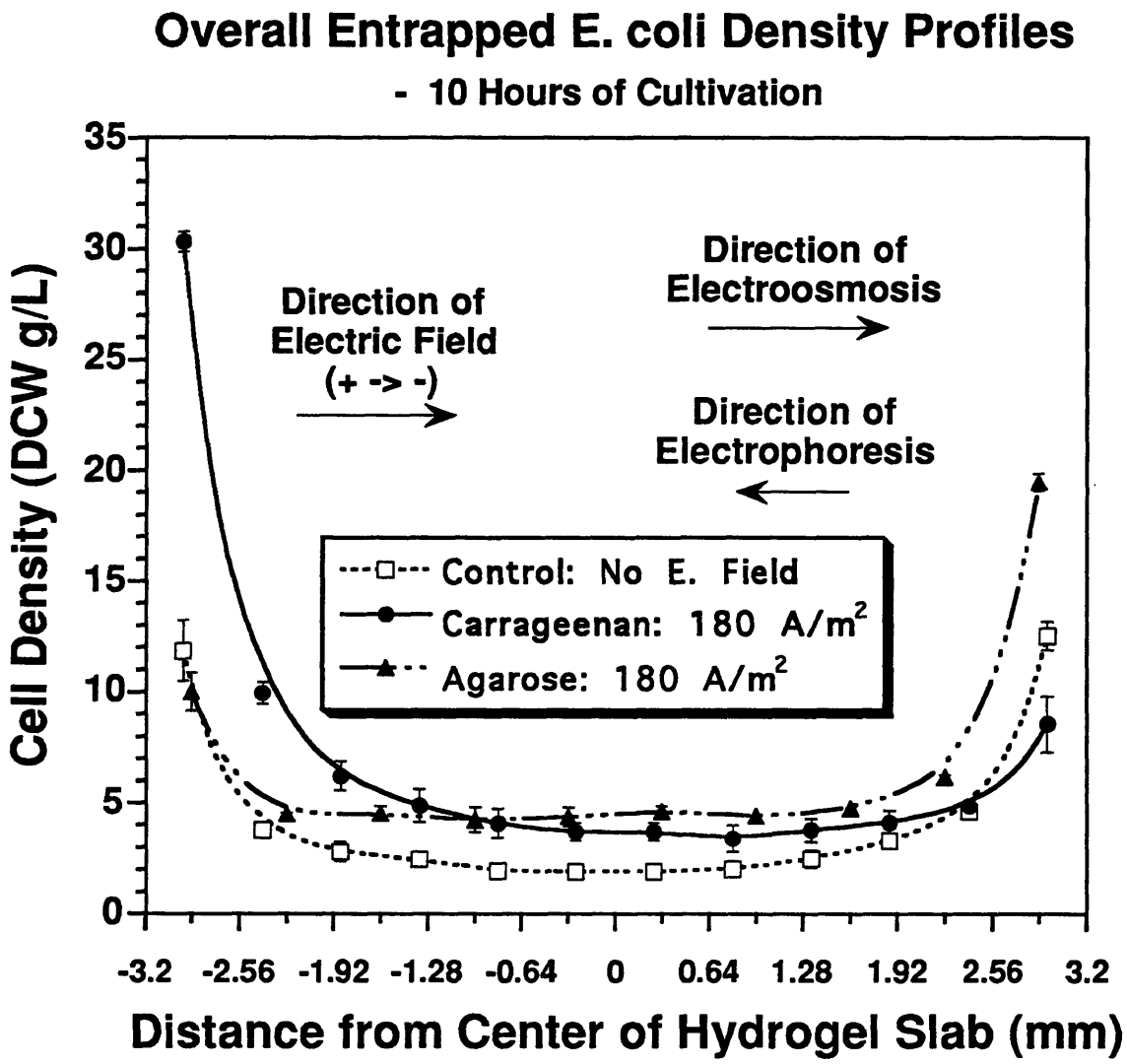

Figure-4.9: The overview of entrapped E. coli growth in agarose and in k-carrageenan. The control culture had no electric fields, and the electrokinetic culture had 180 A/m^2. Cultures were terminated 10 hours.

the same as that of the dc electric field directed from the anode to the cathode. The direction of electrophoresis is, however, opposite to the dc electric field for the negatively charged cellular end-products, such as organic acids as described by Karel and Robertson (1989). Since the electroosmotic flux is approximately 1.5 times greater than the electrophoretic flux for the negatively-charged solutes (with valence=1 and MW=60), the directions of overall convective flows in κ-carrageenan remain the same as that of electroosmosis for all kinds of solutes, be it electrically neutral or charged. Therefore the upstream half of the κ-carrageenan slab is on the left-hand side (facing the anode) in Figure-4.9. For the neutrally-charged agarose hydrogel, only charged solutes such as organic acids can possess convective flow (electrophoresis). Transport of neutral solutes, such as glucose and oxygen, is only through molecular diffusion and can not have convective flow in a dc electric field. Hence the upstream half of the agarose slab is shown on the right-hand side (facing the cathode side) in the figure. In addition, all solutes could diffuse from the medium baths into the hydrogel slab from both sides, and the inhibitory end products could also diffuse out of the slab through both sides into the medium baths. Therefore the convection and molecular diffusion occurs simultaneously and in the same direction in the upstream half of hydrogel slab but in the opposite direction in the downstream half. In order to compare the differences in cell density distributions in the presence and absence of a dc electric field without the complication of countercurrent molecular diffusion in the downstream half of hydrogel slab, only the upstream half of the hydrogel slab is analyzed and to be shown in later presentations.

The overall volume ratio of hydrogel slab versus medium bath is 1 to 83. During the nine-hour cultivation period, there was no detectable

variations in pH and DO, and no leaked cells were found in the medium bath. When cells began to leak out from the hydrogel slab after nine hours, the pH and DO in the medium bath decreased quickly to pH 5 and less than 10% of air-saturation, respectively within one hour. Therefore, all entrapped *E. coli* cultures were terminated after ten hours of cultivation. More interestingly, even when the upstream medium bath DO was higher than 40% air saturation over a long period of time (approximately 8 to 9 hours), the equilibrium *E. coli* cell densities after 10 hours of cultivation and the apparent growth rate (later estimated to be 0.48 hr^{-1}) were similar to the values observed in anaerobic cultivation of *E. coli* using complex medium (Wang *et al*, 1979). This possibility of switch from aerobic to anaerobic proliferation of entrapped *E. coli* cells will be discussed in Section-IV.2.3.3. Each experiment was performed in duplicate, and the average values are shown in the figures with the error bars.

The control cultures which did not have applied dc electric fields were conducted in both κ-carrageenan and agarose hydrogels. There was no discernible difference in entrapped cell growth in the two hydrogels. This suggests that *E. coli* cells are unaffected by hydrogel matrix, which has been observed by other researchers (Huang *et al.*, 1990). Cell density distributions show a symmetric profile along the hydrogel slab. Most of the cell growth occurred within a thin surface layer of the hydrogel slab with a thickness of approximately 600 μm. Cell growth was hindered beyond that depth, and low cell densities along that section of the hydrogel slab were observed.

E. coli cells entrapped in agarose under an applied current density of 180 A/m^2 showed an enhanced cell growth at the cathode side and a decreased cell growth at the anode side. This confirmed our earlier

hypothesis that growth-inhibitory product such as organic acids which should be negatively charged and could have had migrated electrophoretically towards the anodic side of the hydrogel.

E. coli cells entrapped in κ-carrageenan under an applied current density of 180 A/m^2 showed an opposite pattern of cell density distribution as compared to that in agarose. This was a markedly enhanced growth in the surface layer of hydrogel slab at the anodic side, but a slight decreased growth in the surface layer on the cathodic side when compared to the control culture. This is due to the cocurrent diffusive and convective flows of the rate limiting nutrient and inhibitory end products in the upstream half of the hydrogel slab, but countercurrent flows in the downstream half. The most significant cell growth had occurred within a 600 μm-thick surface layer of the hydrogel slab, although there was cell growth into the depths of 600 and 1200 μm from the surface. Beyond a depth of 1200 μm, there was little cell growth at very low cell densities. These low cell densities in the case of κ-carrageenan, however, are still approximately one-fold greater than those in the control culture.

IV.2.2.3 *E. coli* Entrapped in Potassium-κ-Carrageenan

Two electric current densities, 110 and 180 A/m^2, were applied to entrapped *E. coli* cells in 3% (w/v) potassium-κ-carrageenan (CellPrep®, FMC Co.) slabs. The control culture was conducted in the absence of an electric field. The cell density distributions in the upstream half of the hydrogel slab are shown in Figure-4.10. The cultures were terminated after ten hours of cultivation. The cell density in this figure represents the integrated value within a 530 μm-thick hydrogel slice. Each datum point in this figure was obtained from triplicate experiments. The standard deviations, as shown by the error bars, were between 5 and 10%

Figure-4.10: Cell Density distribution of entrapped E. coli in k-carrageenan. The upstream half of the hydrogel slab facing incoming convection is shown.

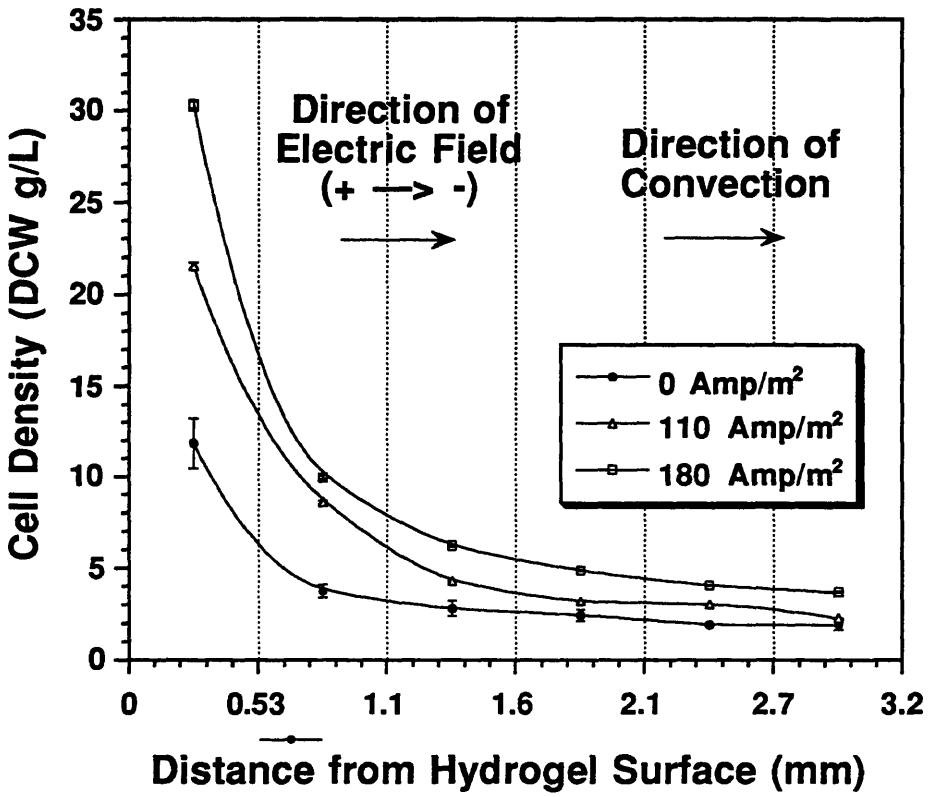

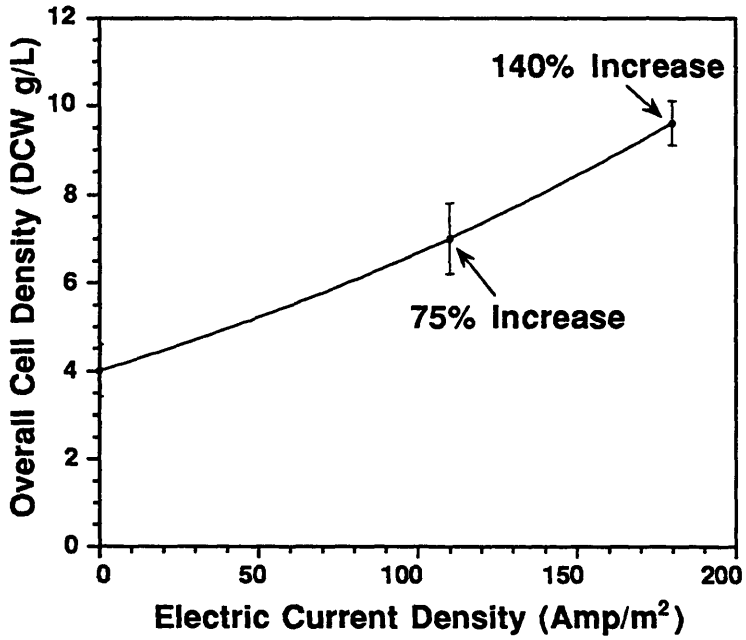

of the average values. The increases in the average overall total cell densities were 75% (from 3.9±0.6 to 7.0±0.8 DCW g/L) and 140% (from 3.9±0.6 to 9.6±0.5 DCW g/L) in the presence of 110 and 180 A/m^2, respectively. The greatest differences in cell densities were apparent in the 530 μm-thick surface layer of the hydrogel slab. The cell densities within this layer were 12, 21, and 30 DCW g/L at current densities of 0, 110 and 180 A/m^2, respectively. Cell densities decreased rapidly from the surface to the interior of the hydrogel slab. Beyond a depth of 1200 μm, there was no difference in the cell density. This indicates that cell growth was hindered either by nutrient limitation or end product inhibition in the interior of the hydrogel slab. This hypothesis will be examined in a later section through mathematical modeling.

IV.2.2.4 *E. coli* Entrapped in Agarose

An electric current density of 180 A/m^2 was applied to *E. coli* cells entrapped in a 2% (w/v) agarose (SeaKem® LE, FMC Co.) slab and compared to the control in the absence of an electric field. The cell density distributions in the upstream half of the agarose hydrogel slabs are shown in Figure-4.11. The upstream half of the hydrogel slab faces the cathode. At 180 A/m^2, the increase in the overall total cell density was 80% (from 4.5 to 8.0 DCW g/L) compared to that of the control culture. This increase is much lower than that in the κ-carrageenan slab under the same electric current density. Most of the cell growth occurred within the 530 μm-thick surface layer, where the cell densities were 12 and 20 DCW g/L at electric current densities of 0 and 180 A/m^2, respectively. As mentioned earlier, the electric field could only induce electrophoretic movements of charged inhibitory end products within the electrically-neutral agarose hydrogel. Therefore the increase in cell density using agarose hydrogel is the result

Figure-4.11: Cell Density distribution of entrapped E. coli in agarose. The upstream half of the hydrogel slab facing incoming convection is shown.

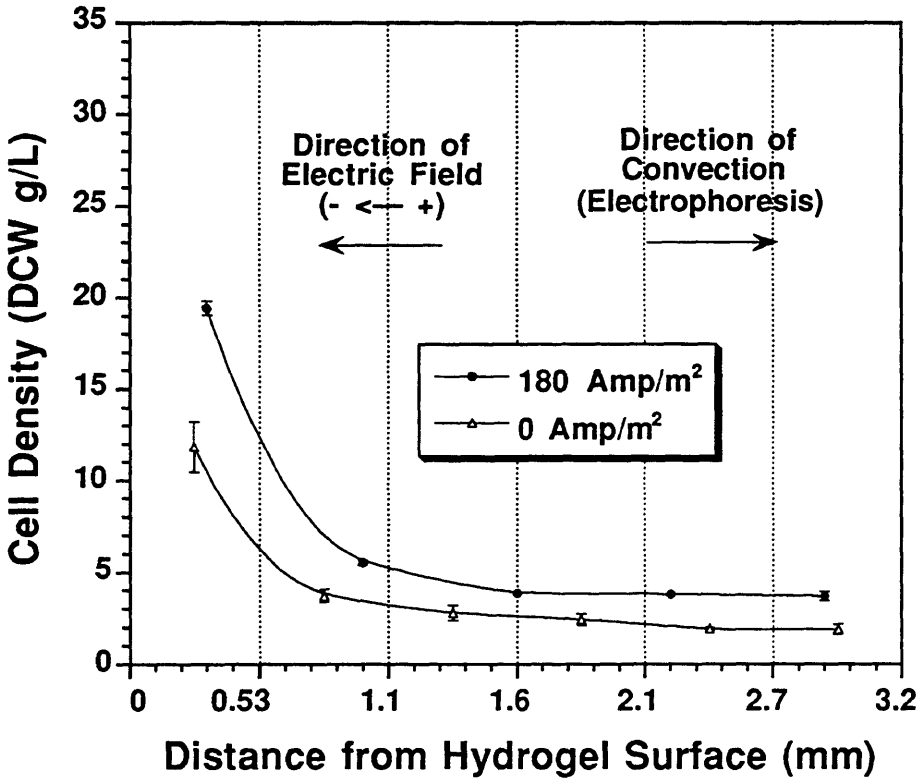

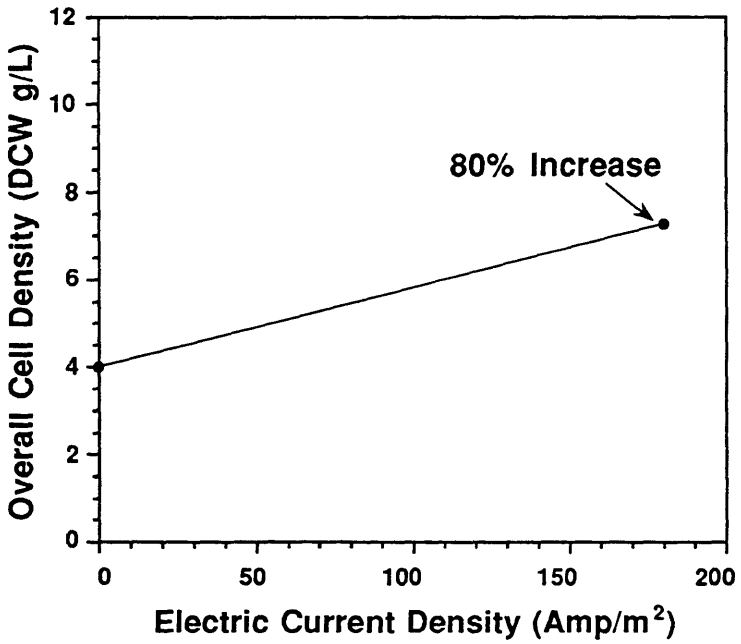

in the reduction of toxic end-products by the electric field.

The influences of augmented transport of glucose and inhibitory end-product on cell growth in κ-carrageenan can now be differentiated through an analysis of the data obtained from the agarose system. In κ-carrageenan, the overall increase in total cell density at 180 A/m^2 was 140%, i.e., from 3.9 to 9.6 DCW g/L, in comparison with that of the control culture. For the negatively charged inhibitory end products in κ-carrageenan, the electrophoretic flux is 40% of the electroosmotic flux, but in the opposite direction. Therefore the effective, overall convective flow of negatively charged inhibitory end-products is about 60% of the electroosmotic flows of neutral solutes in κ-carrageenan. If the same electric current density is applied, the effective convective flow of charged inhibitory end-products in κ-carrageenan will be 50% greater than that in agarose. Comparing the cell density increase from 3.9 to 7.0 DCW g/L for agarose gel at 180 A/m^2, it is estimated that the removal of inhibitory end products alone can result in an increase in cell density from 3.9 to 8.6 DCW g/L in κ-carrageenan. Therefore, the overall increase, i.e., from 3.9 to 9.6 DCW g/L, in κ-carrageenan was approximately 80% due to the removal of inhibitory end products and about 20% due to enhanced non-charged nutrient transport.

IV.2.3 Mathematical Modeling of Hydrogel-Entrapped *E. coli* Culture

Mathematical modelling and analyses were performed to assess the temperature changes due to electrical energy dissipation within the hydrogel, and to quantify and rationalize the growth kinetics of entrapped cells in the presence of electrically-induced, convective mass transfer. All analyses were conducted using a Cartesian coordinate system with one-

dimensional variation, i.e., a slab-like geometry.

An energy balance, which comprises a volumetric electrical energy dissipation and was described in Section-III.8.3, and the conductive and convective energy flows, was developed to describe the temperature profile within a hydrogel slab in the presence of a dc electric field. This was done to assess the temperature rise in the hydrogel slab and how this is affected by hydrogel thickness, electroosmotic coupling coefficient and electric current strength. Based on a steady state analysis, an analytical solution for the temperature profile can be obtained.

A model was developed to characterize the growth kinetics of entrapped *E. coli* cells in the presence or absence of electrically-induced mass transfer of nutrient and cellular end-products. The possibility of direct impact by dc electric fields on entrapped *E. coli* cells, such as the stimulation of cellular productivity, is not considered. At the same time, the hydrogel matrix is considered inert to *E. coli* cells, i.e., all parameters of cell growth kinetics obtained from the suspension cultures are the same as those in the hydrogel-entrapment cultures. Hydrogel matrix, however, creates a transport barrier which reduces the molecular diffusivity. Cell growth kinetics is coupled with the consumption of a rate-limiting nutrient and the production of an inhibitory end-product (this inhibition is not present in oxygen-limiting condition). These simultaneous, coupled, nonlinear parabolic partial differential equations were solved using the numerical package described in Appendix-I.

IV.2.3.1 Temperature Profile within Hydrogel Slab in Electric Field

Steady state condition was assumed for the energy balance, as shown by eq.(3.23). The following parameters, all assumed to be constant, were used for the analysis:

ρ = hydrogel density (1000 Kg/m^3)
$\overline{C_v}$ = specific heat capacity of hydrogel (4.1x10^{-3} joule/Kg-°C)
k_T = thermal conductivity of hydrogel (0.628 joule/m-s-°C)
σ = electrical conductivity of hydrogel and culture medium (1.5 mho/m)
J = applied current density (Amp/m^2)
J^2/σ = volumetric heat production rate (watt/m^3)
T_b = medium bath temperature (37°C)
L = hydrogel slab thickness (6.4 mm)
k_i = electroosmotic coupling coeff. of κ-carrageenan (1.4x10^{-8} m^3/Amp-s)

The k_i value of κ-carrageenan hydrogel was experimentally obtained. The temperature in the medium bath and at the medium-hydrogel interface was maintained at T_b. The analytical solution describing the temperature profile is shown by eq. (3.24).

The representative temperature profile within a hydrogel slab is shown in Figure-4.12. In the presence of electric fields, the temperature profile is symmetrical for the electrically-neutral hydrogel such as agarose, but becomes asymmetrical and shifts towards the downstream side with respect to the direction of convective flow for an electrically-charged hydrogel such as κ-carrageenan. This is due to the convective heat flux induced by electroosmosis.

Figure-4.12 also summarizes the highest temperature rise in the hydrogel slabs as functions of k_i values and gel thicknesses in the presence of 120 and 350 A/m^2. The highest temperature rise in κ-carrageenan hydrogel slab is less than 1.0°C at an electric current density of 350 A/m^2 as long as the hydrogel slab thickness is less than 8 mm. There is no significant difference in the highest temperature rise between agarose and κ-carrageenan under the same electric current density. Normally, the hydrogel beads used for cell entrapment in industry have the diameters

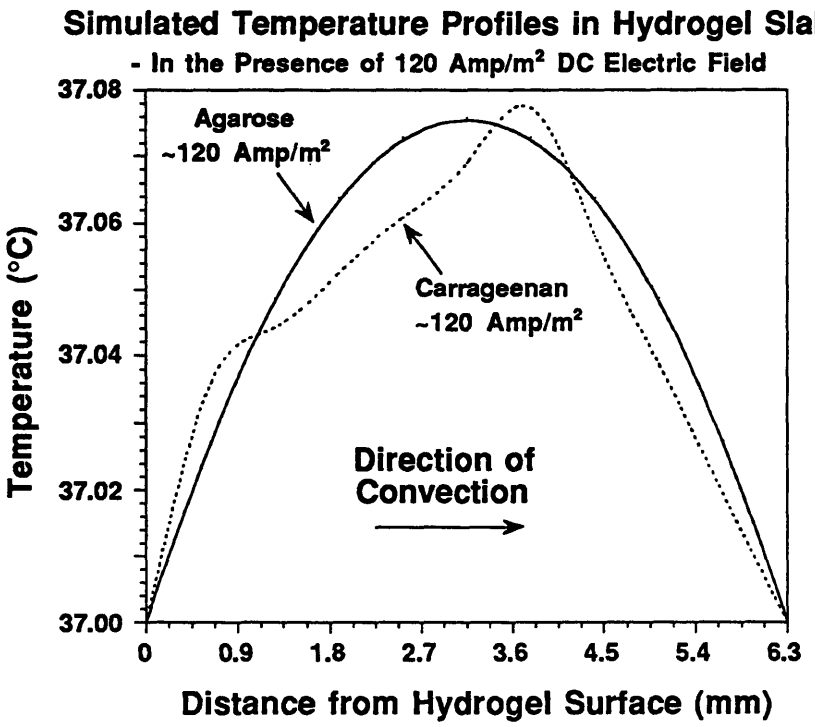

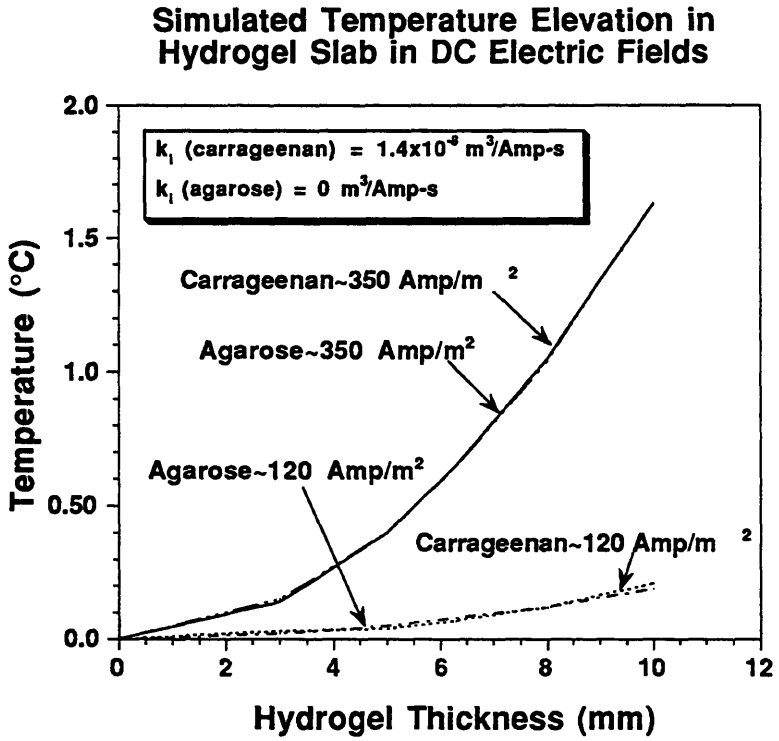

Figure-4.12: Temperature profiles and elevation in k-carrageenan and agarose in the presence of different electric current density and different hydrogel slab thickness.

less than 5.0 mm. The temperature elevation, hence, is less than 0.4°C in those hydrogel beads even in the presence of the high electric current density 350 A/m2.

In this research, the hydrogel slab thickness and the electric current densities used were 6.3 mm and less than 200 A/m2, respectively. Therefore the maximum temperature rise will be 0.27°C in both κ-carrageenan and agarose hydrogel slabs. The temperature rise was later confirmed by a direct temperature measurement through an immersed thermocouple in the hydrogel slab, and was found to be less than 0.3°C in a 6.3 mm thick hydrogel slab at an electric current density of 300 A/m2. This increase in temperature in the hydrogel slab will not pose a problem for either the hybridoma cells or the *E. coli* cells. In conclusion, the effects of temperature elevation caused by applied electric fields on entrapped cells in the hydrogel slab is negligible.

IV.2.3.2 Oxygen-Limiting Condition for Aerobic *E. coli* Culture

The purpose of the mathematical analysis is to assess, based on a more theoretical basis, the extent of aerobic growth of *E. coli* in the hydrogel with an oxygen-rich culture medium bath outside the gel. Oxygen was assumed to be the limiting nutrient for growth and *E. coli* was also assumed to be a strict aerobe. Strict aerobes use oxygen as the terminal electron acceptor and can completely dissimilate glucose to CO_2. In this case, no organic end-products should be produced in this type metabolism and thus there is no end-product inhibition. However, *E. coli* is a facultative microbe, which means it can grow either aerobically or anaerobically. Therefore while the theoretical *E. coli* aerobic growth is compared with the experimental data, this could provide an estimation on the extent of aerobic and anaerobic growth from our experiments. In

addition, it is desired to quantify enhanced growth of the entrapped strict aerobes in the presence of electroosmotic medium flux in order to elucidate how effectively the electrokinetic technique can improve the behaviors of strict aerobes under transport limited conditions.

As discussed in Section-II.6.2, Chang and Moo-Young (1988) calculated the oxygen penetration depths for cell-entrapped hydrogels, i.e., the distances beyond which oxygen concentrations are below the critical value (10% of the air-saturation). They assumed a zero-order kinetics and a homogeneous cell distribution, and found that the typical penetration depths of oxygen for immobilized microbial cells are in the range of 50 to 200 μm. There should be no growth of strict aerobes beyond that depth. As found in our experiments, however, the distribution of *E. coli* cells in the hydrogel was not homogeneous, and cell growth could be observed in a 1200 μm-thick surface layer of the hydrogel slab. Since the theoretical aerobic growth is calculated to occur within 20% of the 1200 mm depth from the surface, the difference between the observed and the calculated aerobic cell growth (Chang and Moo-Young, 1988) is concluded to arise from anaerobic growth.

A dynamic model, as shown by eq.(3.13), was used to describe the aerobic growth kinetics of entrapped *E. coli* cells. It was assumed that the growth of microbial cells is limited only by oxygen, and cells only proliferate aerobically. The inhibition of cell growth by cellular end-products is therefore neglected. A Monod-type cell growth kinetics was used. κ-carrageenan-entrapped microbial culture was chosen as our model system. The kinetic parameters used in this simulation are shown in Table-4.1, and a brief summary of all mathematical equations are listed in Table-4.2.

Table-4.1: Kinetic parameters for aerobic *E. coli* cultures

Kinetics Parameter	Value	Reference
Effective Diffusivity of O_2	4.0×10^{-6} m²/hr	Chang and Moo-Young (1988)
Specific growth rate (μ)	0.5 hr^{-1}	
Monod Constant (K_m)	$3.0 * 10^{-3}$ mol/m³	Chang and Moo-Young (1988)
Max. specific O_2 uptake rate	$1.13 * 10^{-2}$ (mol/hr-g-cell)	"
Saturated dissolved O_2	0.25 mol/m³ (O_2 conc. in medium bath)	

Table-4.2: Mathematical Equations for Describing Aerobic Growth of Entrapped *E. coli* Cells under Oxygen-Limiting Condition

- **Oxygen Balance**

$$\frac{\partial C_o}{\partial t} = \overline{D_o}\frac{\partial^2 C_o}{\partial x^2} - V_x\frac{\partial C_o}{\partial x} - Q_o N$$

Where C_o = Oxygen conc. in hydrogel

$\overline{D_o}$ = Effective diffusivity of oxygen in hydrogel

$V_x = k_i J$ (Electroosmotic flow rate)

$$Q_o = \frac{Q_{o,max} C_o}{K_m + C_o}$$

- **Cell Growth Kinetics**

$$\frac{\partial N}{\partial t} = \mu N$$

Where N = Cell density

$$\mu = \frac{\mu_{max} C_o}{K_m + C_o}$$

The results from computer simulation are shown in Figure-4.13 and -4.14. In the absence of an electric field, the transfer of oxygen into the hydrogel slab is through molecular diffusion alone. In this case, the dissolved oxygen concentration decreased to 17% of air-saturation after 10 hours of cultivation at a depth of 150 μm from the hydrogel surface. Approximately 90% cell growth was predicted to occur within a 500 μm thick surface layer. When an electric current density of 180 A/m^2 was applied, the DO concentration decreased to 22% of the air-saturation at a depth of 150 μm from the hydrogel surface, and the increase in overall cell density was 24%, from 2.5 to 3.1 DCW g/L, compared to that in the electric-field-free condition. When the current density was further increased to 350 A/m^2, the increase in the overall cell density was 51%, from 2.5 to 3.8 DCW g/L, and the level of DO was increased to 28% of the air-saturation at a depth of 150 μm from the hydrogel surface.

The experimental overall cell density was 9.7 DCW g/L, but the simulated total cell density was 3.1 DCW g/L under an aerobic condition in κ-carrageenan at 180 A/m^2. It is our conclusion that less than 30% of *E. coli* cells grew aerobically even though medium bath was maintained oxygen-rich outside of the gel during the 10 hours of cultivation. Therefore, the majority of entrapped *E. coli* cells grew anaerobically.

IV.2.3.3 Glucose-Limiting, Anaerobic Growth of *E. coli* in κ-Carrageenan

Entrapped *E. coli* Growth after 10 Hours of Cultivation

Based on the previous analysis of the growth of strict aerobes, we have concluded that the majority of entrapped *E. coli* cells in our experiments grew anaerobically. Therefore we conducted an analysis of entrapped *E. coli* growth in the κ-carrageenan hydrogel slab based on an

Figure 4.13: Simulated growth of k-carrageenan-entrapped aerobe in the presence of electrokinetics. Oxyen is considered the only limiting nutrient and no waste inhibition exists.

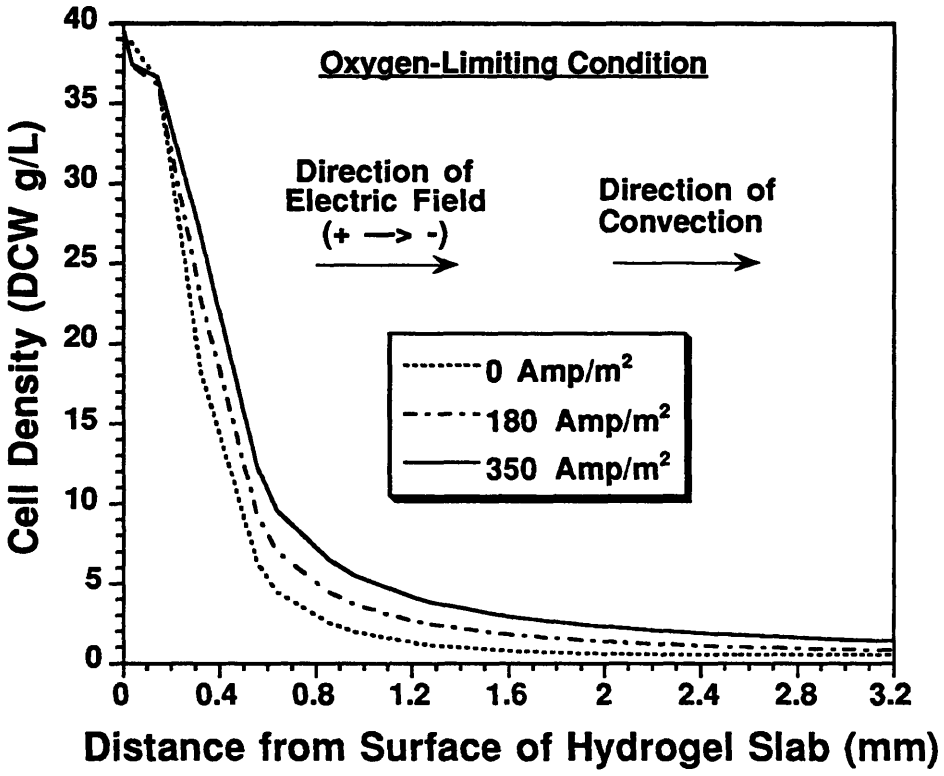

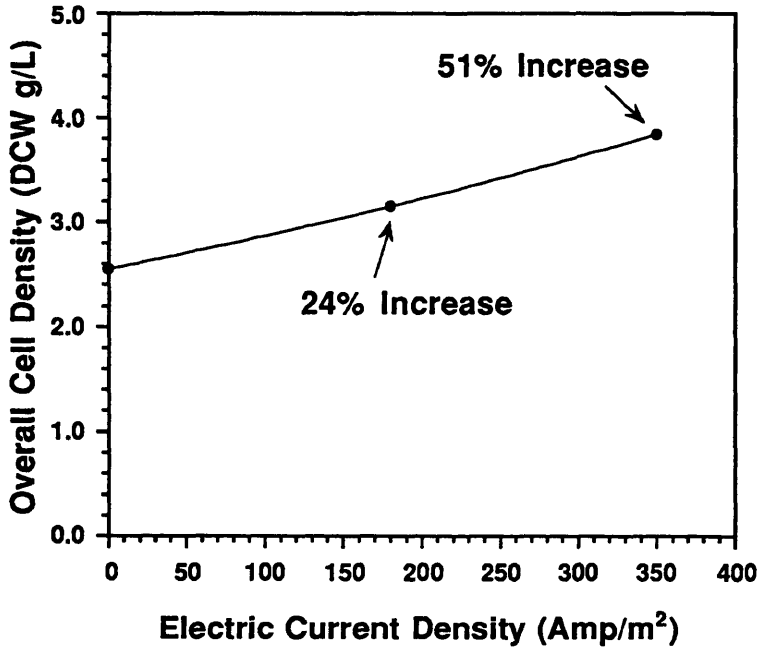

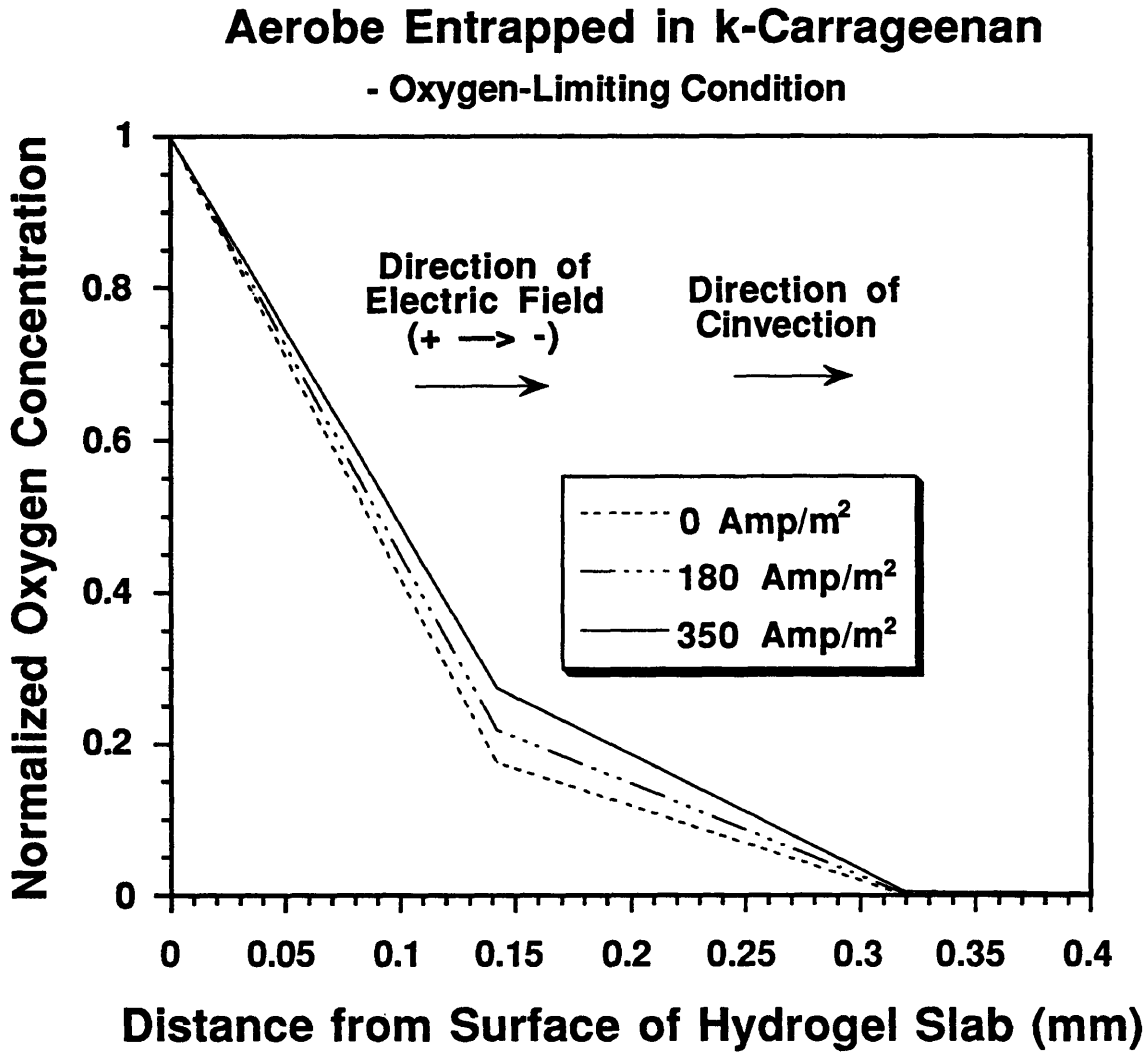

Figure-4.14: The simulated, dissolved oxygen concentration in a k-carrageenan hydrogel slab in the presence of electrokinetics and aerobes. Oxygen is the only limiting nutrient and no waste inhibition exists.

anaerobic condition. In this analysis, a Monod-type growth kinetics was used and shown by eq.(3.13). The growth is a function of the concentration of a rate-limiting nutrient, but also is inhibited by a toxic end-product. Mass balances of a rate-limiting nutrient, assumed to be glucose, and an inhibitory end product, an organic acid, can be expressed by eq.(3.15) and (3.14). Electric fields can induce electroosmosis as well as electrophoresis in the negatively-charged κ-carrageenan, but the direction of electroosmosis is opposite to that of electrophoresis for negatively charged solutes such as ionized organic acids. A brief summary of all mathematical equations are listed in Table-4.3.

The Monod constant, K_m, for glucose was assumed to be 4.0×10^{-3} g/L, which is typical for most microorganisms. The maximum specific growth rate, μ_{max}, was assumed to be 0.48 hr^{-1}. The yield of glucose to cell mass, $Y_{x/s}$, was taken from Wang *et al.* (1979) and assumed to be 0.14 g-DCW/g-glucose. The maximum glucose uptake rate, $Q_{s,max}$ was obtained by dividing μ_{max}, by $Y_{x/s}$. The non-growth-related specific glucose consumption (maintenance consumption) rate, m_s, used was 0.01 g-glucose/g-cell-hr (Wang *et al.*, 1979). The electroosmotic coupling coefficient, k_j, of κ-carrageenan was obtained experimentally. The effective diffusivities of glucose, $\overline{D}_s$, and organic acid, $\overline{D}_w$, in hydrogel were obtained from experimental values reported by Yabannavar (1988). It was assumed that the organic acid was produced in an ionized form and hence electrophoresis was involved in the electrically-induced convection. From Einstein's relationship, eq.(3.8), the electrical mobility of organic acid, $\overline{\mu_w}$, was calculated to be 40×10^{-5} m^2/V-hr. This could result in an electrophoretic movement of about 40% of the electroosmotic flow. Since electrophoresis and electroosmosis act in opposite directions, the resultant convective flow rate of the ionized organic acid is 60% of that of glucose,

Table-4.3: Mathematical Equations for Describing Anaerobic Growth of Entrapped *E. coli* Cells under Glucose-Limiting Condition

- **Glucose Balance**

$$\frac{\partial C_s}{\partial t} = \overline{D_s}\frac{\partial^2 C_s}{\partial x^2} - V_x\frac{\partial C_s}{\partial x} - Q_s N$$

Where C_s = Glucose conc. in hydrogel

$\overline{D_g}$ = Effective diffusivity of glucose in hydrogel

$V_x = k_i J$ (Electroosmotic flow rate)

$$Q_s = \frac{Q_{s,max} C_s}{K_m + C_s} + m_s$$

- **Organic Acid Balance**

$$\frac{\partial C_w}{\partial t} = \overline{D_w}\frac{\partial^2 C_w}{\partial x^2} - V_x'\frac{\partial C_w}{\partial x} + Q_w N$$

Where C_w = Organic acid conc. in hydrogel

$\overline{D_w}$ = Effective diffusivity of organic acid in hydrogel

$V_x' = k_i * J \pm \frac{\overline{\mu_w} J}{\sigma}$ (Electroosmosis ± Electrophoresis)

$Q_w = Y_{w/s} * Q_s$

- **Cell Growth Kinetics**

$$\frac{\partial N}{\partial t} = \mu N$$

Where N = Cell density in hydrogel

$$\mu = \frac{\mu_{max} C_s}{K_m + C_s} f_i(C_w)$$

$f_i(C_w) = (1 - C_w/C_{w1})\exp(-C_w/C_{w2})$

= Inhibitory function

which is affected only by electroosmosis.

Anaerobic metabolism of glucose by *E. coli* cells produces a mixture of organic acids. Karel and Robertson (1988) immobilized *E. coli* cells in macroporous hollow fiber membranes and found that cell growth occurred only in a thin surface layer at a rate similar to that of freely-suspended cells. They also studied the metabolism of glucose and observed that 58% of the glucose carbon was converted to organic acids (50-60% formate, 35-45% acetate and some other acids, see Table-2.1). Based on this composition of organic acid mixture, we calculated the average molecular weight of this organic acid mixture to be 51.8 dalton.

These organic acids produced in anaerobic cultures can inhibit entrapped *E. coli* growth differently, and the production pattern of organic acids is extremely complex and depends on the phases of cell growth. For simplicity, we lumped the different inhibitions by various organic acids into a single inhibition behavior for all of the organic acids. This single organic acid possesses the molecular weight represented by the average molecular weight calculated earlier for the organic acid mixture. The yield of glucose to organic acid, $Y_{w/s}$, was calculated based on the composition of organic acid mixture and was found to be 1.8 mol-organic acid/mole glucose (i.e., 0.5 g-organic-acid/g-glucose). The specific organic acid production rate, Q_w, was obtained by multiplying the specific glucose consumption rate, Q_s, and $Y_{w/s}$. The empirical inhibitory function, which was shown by eq.(3.14), is composed of a linear term and an exponential term which are used to account for the inhibitions by dissociated and undissociated organic acids, respectively, which was described by Yabannavar (1988). Two inhibition constants, C_{w1} and C_{w2}, used in eq.(3.14) were obtained by a trial-and-error fitting to the experimental cell growth data: the values of all kinetic parameters were first fixed. A set of

C_{w1} and C_{w2} was then selected to obtain a simulated entrapped *E. coli* density profile in κ-carrageenan under a certain electric current density. The initial selection of C_{w1} and C_{w2} (48.7 and 2.4 g/L, respectively) was based on the experimental data used to describe lactic acid inhibition on *lactobacillus* studied by Yabannavar (1988), in which the amount of undissociated acid was assumed to be 10% of that of the dissociated acid. This simulated result was then compared with our experimental results under the same conditions. When the discrepancy between the experimental and simulated total cell densities was greater than 10%, C_{w1} and C_{w2} were re-adjusted individually and used to obtain a second simulation. The entire procedure was iterated until a satisfactory fitting between the experimental and simulated results was obtained. The final set of C_{w1} and C_{w2}, together with all the kinetic parameters, were later used to simulate all of entrapped *E. coli* growth studies under different electric current densities and different cultivation time, as well as the different hydrogels used for the entrapment cultures. The kinetic parameters used are summarized in Table-4.4.

Since the total volume of the hydrogel slab (3 cm^3) is much smaller than that of the culture medium (250 cm^3), the concentrations of glucose, $C_{s,b}$, and inhibitory organic acid, $C_{w,b}$, in the medium bath were assumed constants at 20 g-glucose/L and no acid, respectively. These served as boundary conditions at the interface between the hydrogel and the medium bath as well as initial conditions at the beginning of the culture.

The simulated and experimental cell density profiles for the upstream half of the hydrogel slab are shown in Figure-4.15. The surface of the hydrogel slab contacting the culture medium is on the left side while the middle of the hydrogel slab is on the right side of the graph. The growth of *E. coli* cells in κ-carrageenan in the presence of four different

Table-4.4: Parameters for simulation of anaerobic *E. coli* growth

Kinetics Parameter	Value (unit)
Glucose conc. in medium ($C_{s,b}$)	20 g/L
Organic acid conc. in medium ($C_{w,b}$)	0 g/L
Max. specific growth rate (μ_{max})	0.48 hr^{-1}
Monod constant for glucose (K_m)	4 mg-glucose/L
Yield of glucose to cell mass ($Y_{x/s}$)	0.14 g-DCW/g-glucose
Sp.glucose consump. for maintenance (m_s)	0.01 g-glu./g-cell-hr
Molecular weight of organic acid	51.8 dalton
Yield of glucose to organic acid ($Y_{w/s}$)	0.5 g-organic-acid/g-glucose
Electroosmotic coupling coeff. (k_i)	5.04×10^{-5} m^3/Amp-hr
Effective glucose diffusivity ($\overline{D_s}$)	1.8×10^{-6} m^2/hr
Effective organic acid diffusivity ($\overline{D_w}$)	1.2×10^{-6} m^2/hr
Electrical mobility of organic acid ($\overline{\mu_w}$)	40×10^{-5} m^2/V-hr
Inhibition constant, C_{w1}	30.0 g-acid/L
Inhibition constant, C_{w2}	2.7 g-acid/L

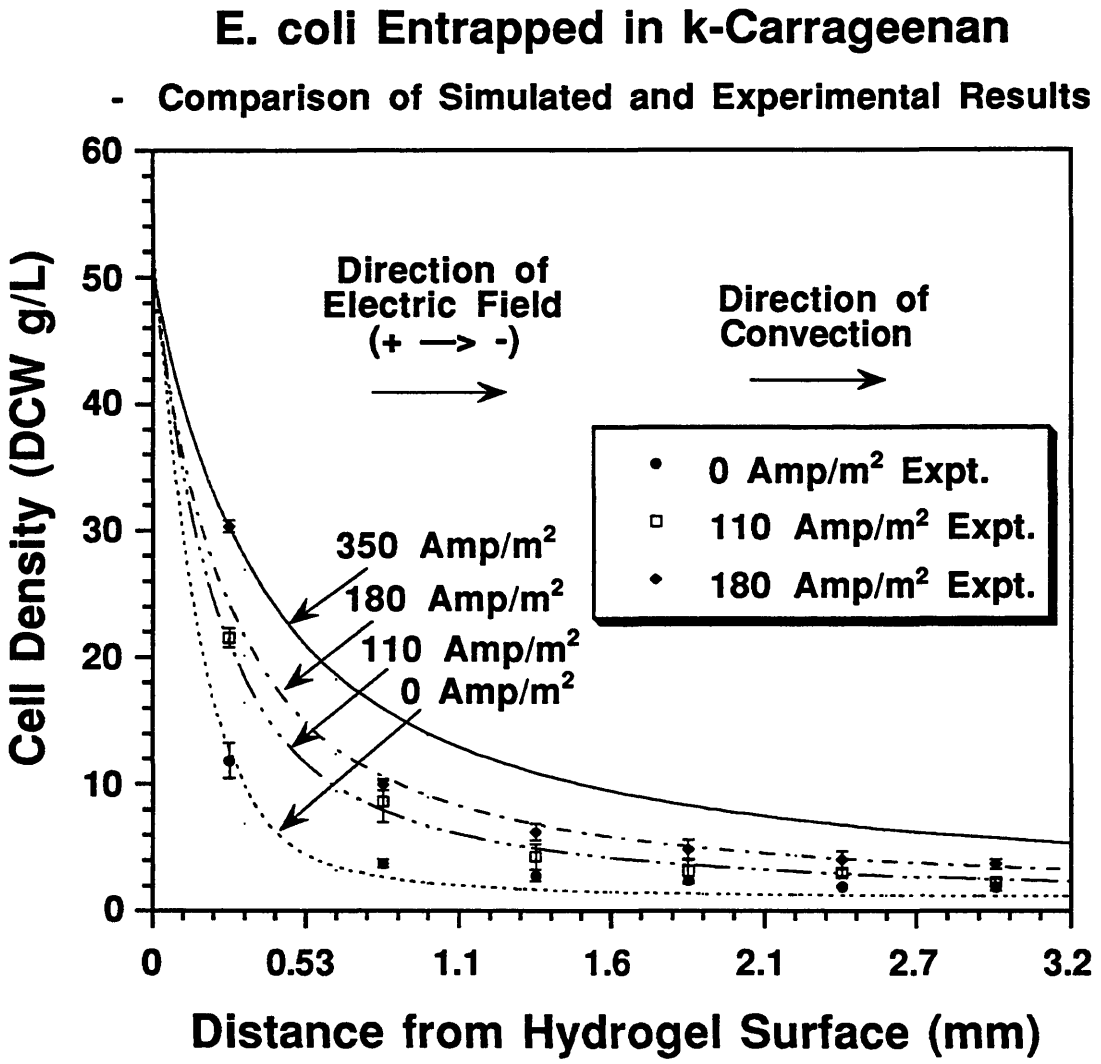

* Simulated cell density profiles are shown by lines.

Figure-4.15: The comparison of the simulated and experimental growth of k-carrageenan-entrapped E. coli in the presence of different current densities. The cell growth in the upstream half of hydrogel slab is shown.

electric current densities, 0 (the control culture), 110, 180 and 350 A/m^2, were first simulated. The experimental cell density profiles under 0, 110 and 180 A/m^2 are also presented for comparison. Each experimental point of cell density on the graph represents an average cell density in a 530 μm-thick gel slice, and is an average value from two or three repeated experiments. The simulated cell density was first obtained in a continuous profile, as shown by the line in Figure-4.15. This simulated continuous cell density profile was then evenly divided into six sections, each section representing a 530 μm-thick gel slice. The cell density in each gel slice was integrated and averaged to obtain a simulated, average cell density of each gel slice, as shown by the line in Figure-4.16. Finally, the simulated continuous cell density profile was integrated and averaged over the entire half of the hydrogel slab to obtain a simulated, total cell density under each electric current density, as shown by the line in Figure-4.16. It was found that the discrepancy between the simulated and experimental total cell densities was less than 10%, and the increase in total cell density was approximately proportional to the increase in electric current density. Based on this model, the increase in total cell density at an electric current density of 350 A/m^2 could be as high as 210% compared to that in the control culture.

In order to elucidate the cause for the increase in entrapped *E. coli* growth, the concentration profiles of glucose and inhibitory organic acid were simulated, and these results are shown in Figure-4.17. Since the glucose concentration in the medium bath equivalent to the gel surface was maintained at a high value of 20 g/L, the glucose concentration profile in diffusion-only condition, i.e., in the absence of an electric field, did not show any nutrient limitation even in the middle of the slab. This can be seen in the Figure-4.17 where the glucose concentration had decreased to

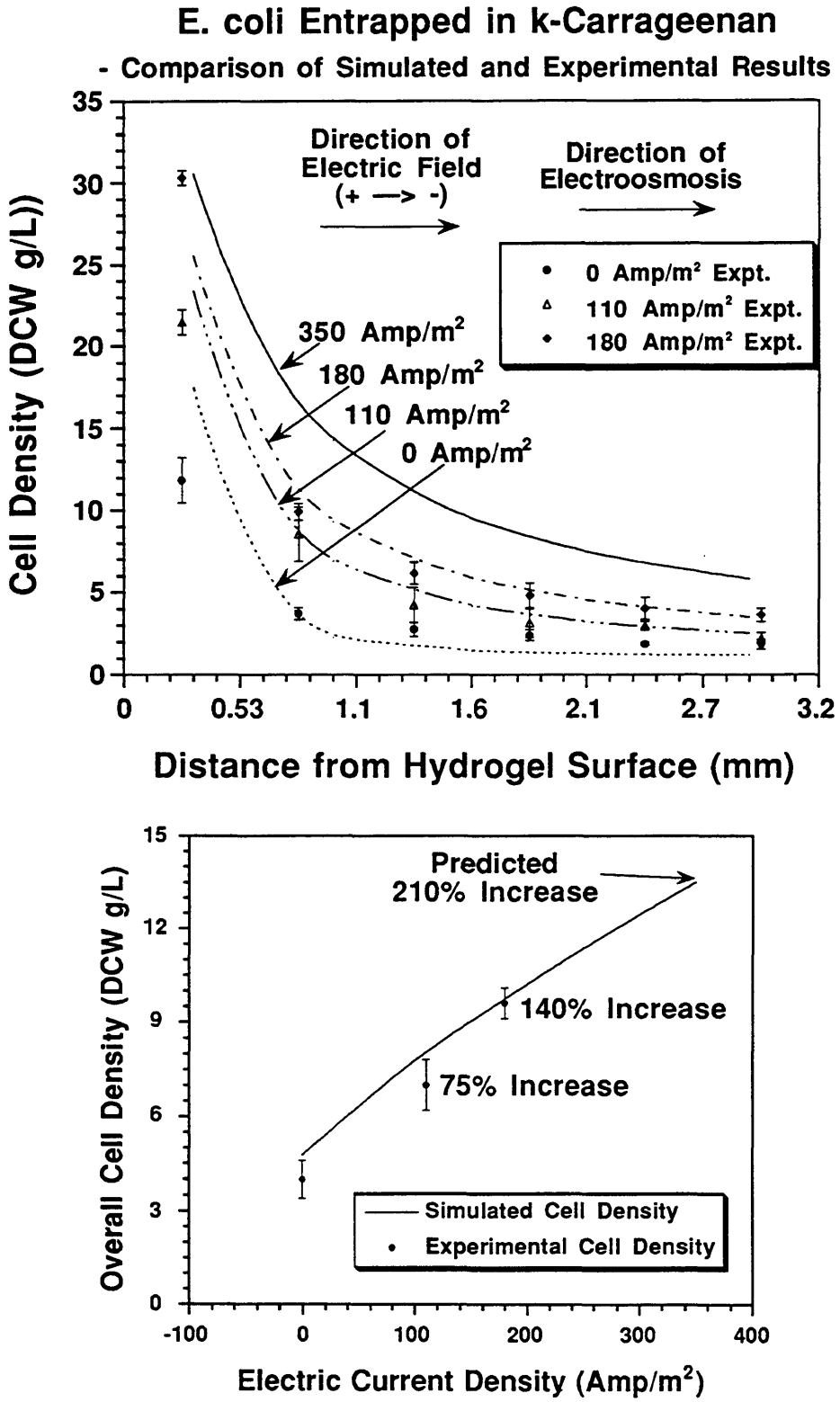

* Simulated cell density profile, which was integrated in each gel slice and in the entire half of hydrogel slab, respectively, is shown by line.

Figure-4.16: The comparison of the simulated and experimental growth of k-carrageenan-entrapped E. coli in the presence of different current densities. The cell growth in the upstream half of hydrogel slab is shown.

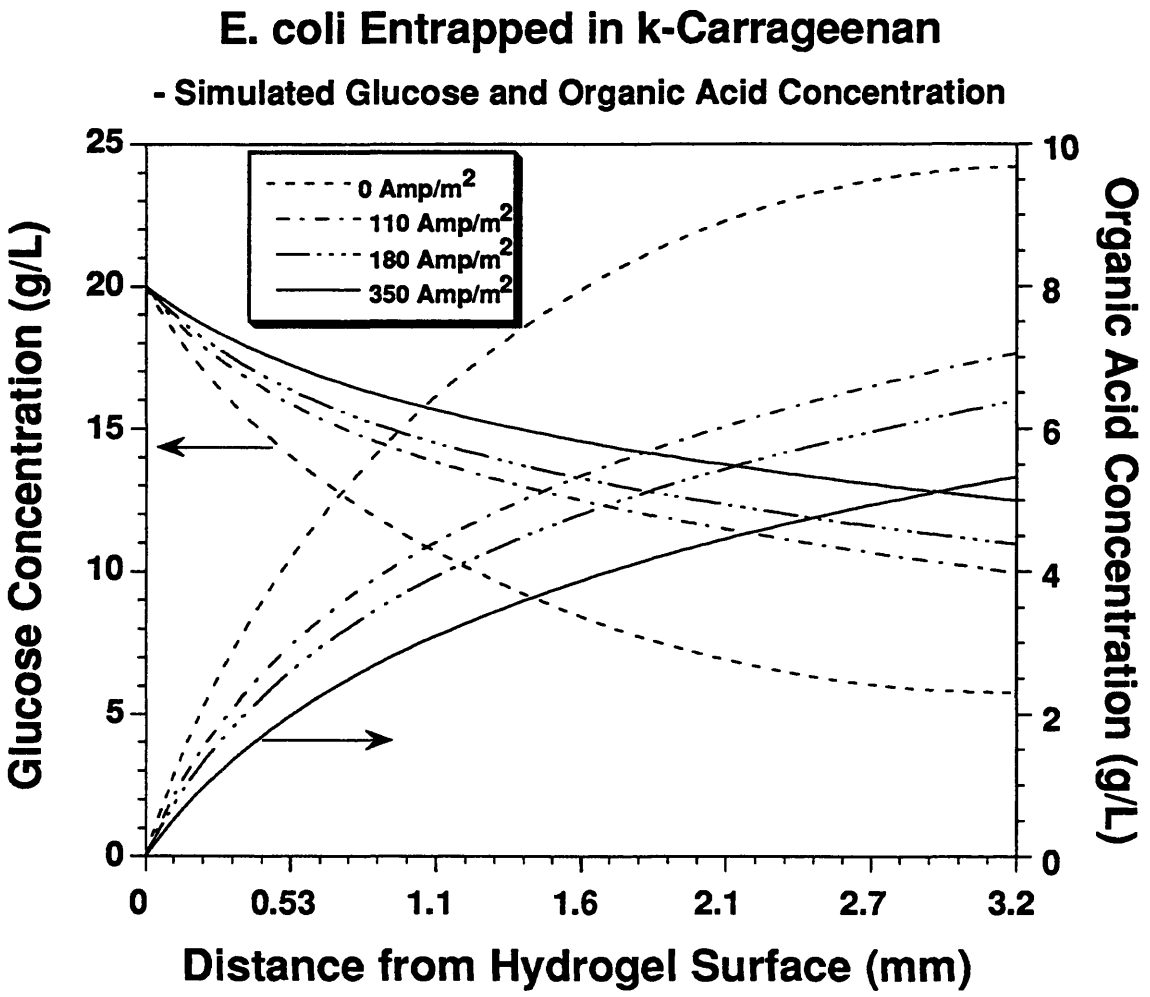

Figure-4.17: The simulated concentrations of glucose and organic acid in k-carrageenan hydrogel in the presence of different electric current densities. The concentration in the upstream half of hydrogel slab is shown.

5.0 g/L. The glucose concentration in the middle of the slab was increased by 100% and 150% at electric current densities of 110 and 350 A/m^2, respectively, compared to that of the electric-field-free condition. In the culture without an electric field, inhibitory organic acid accumulated throughout the hydrogel slab which severely inhibited the cell growth beyond a depth of 1.0 mm from the hydrogel surface. In the presence of electric fields, on the other hand, the concentration of organic acid in the middle of hydrogel slab was reduced by 25% and 50% at electric current densities of 110 and 350 A/m^2, respectively, compared to that of the electric-field-free condition. This reduction in organic acid accumulation would significantly decrease the inhibition by the organic acid throughout the slab. This is the reason cause for the increase in cell density throughout the entire half of the hydrogel slab in the presence of electric fields.

Time-Dependent Growth of Entrapped *E. coli* Cells

The experimental and simulated cell density profiles after 8 hours and 10 hours of cultivation can be seen in Figure-4.18. The simulated and experimental profiles of the cell density are presented by the line and by the symbols respectively in Figure-4.18. The cell growth of κ-carrageenan-entrapped *E. coli* cells after 8 hours of cultivation was successfully predicted by the mathematical model. This indicates that the kinetic parameters for cell growth, especially the specific cell growth rate, are quantitatively correct. The simulated results indicate that cell growth occurs only within the 530 μm-thick surface layer of the hydrogel slab during the last 2 hours before the cultivation was terminated. The decrease in the cell growth in the interior of the hydrogel slab was caused by the accumulated organic acids, as confirmed by the simulated organic

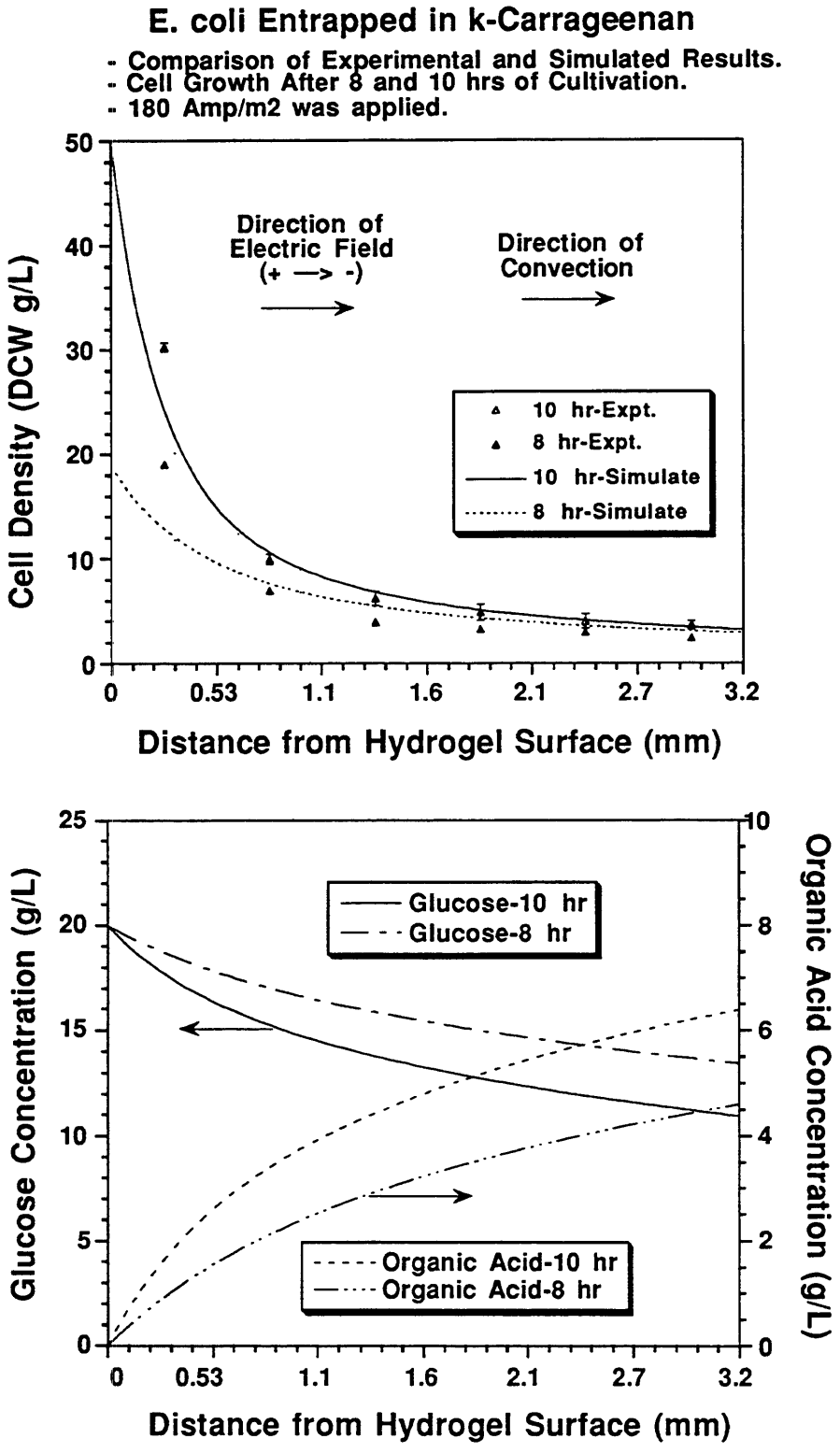

* Simulated results are shown by lines

Figure-4.18: The comparison of the simulated and experimental results of k-carrageenan-entrapped E. coli after different time of cultivation. The results in the upstream half of hydrogel slab are shown.

acid and glucose concentration profiles in Figure-4.18. According to the simulation, after 8 hours of cultivation, organic acid accumulated to more than 3.0 g/L in the hydrogel slab at a depth of 1000 μm from the hydrogel surface. This amount of organic acid can severely reduce the cell growth to less than 30% of that in an inhibition-free condition. The accumulation of organic acid became more serious after two more hours of cultivation, and resulted in an increase in the organic acid concentration by 40-50% throughout the whole hydrogel slab compared to the organic acid concentration obtained two hours ago. The glucose concentration showed no depletion even in the interior of the hydrogel slab.

The simulated cell density and organic acid concentration profiles after 2, 4 and 6 hours of cultivation are shown in Figure-4.19. During the six-hour period of cultivation, accumulation of organic acid was negligible and cell growth was not inhibited throughout the entire hydrogel slab. Therefore the cell densities at a certain point in time of the cultivation are approximately the same throughout the entire half of the hydrogel slab. The accumulation of organic acid in the interior of the hydrogel slab became serious after 8 hours of cultivation, when cell growth only occurred at the surface layer of the hydrogel slab. The simulated, continuous cell density profile at a certain time during the cultivation was integrated and averaged throughout the hydrogel slab to obtain the total cell density as shown in Figure-4.20. A good agreement between the simulated and the experimental results was found. The mathematical model, therefore, can successfully describe the time-dependent growth of κ-carrageenan-entrapped *E. coli* cells.

In conclusion, the mathematical model can predict the growth of entrapped *E. coli* in κ-carrageenan under different electric current densities and as well to follow the temporal changes within the gel. The

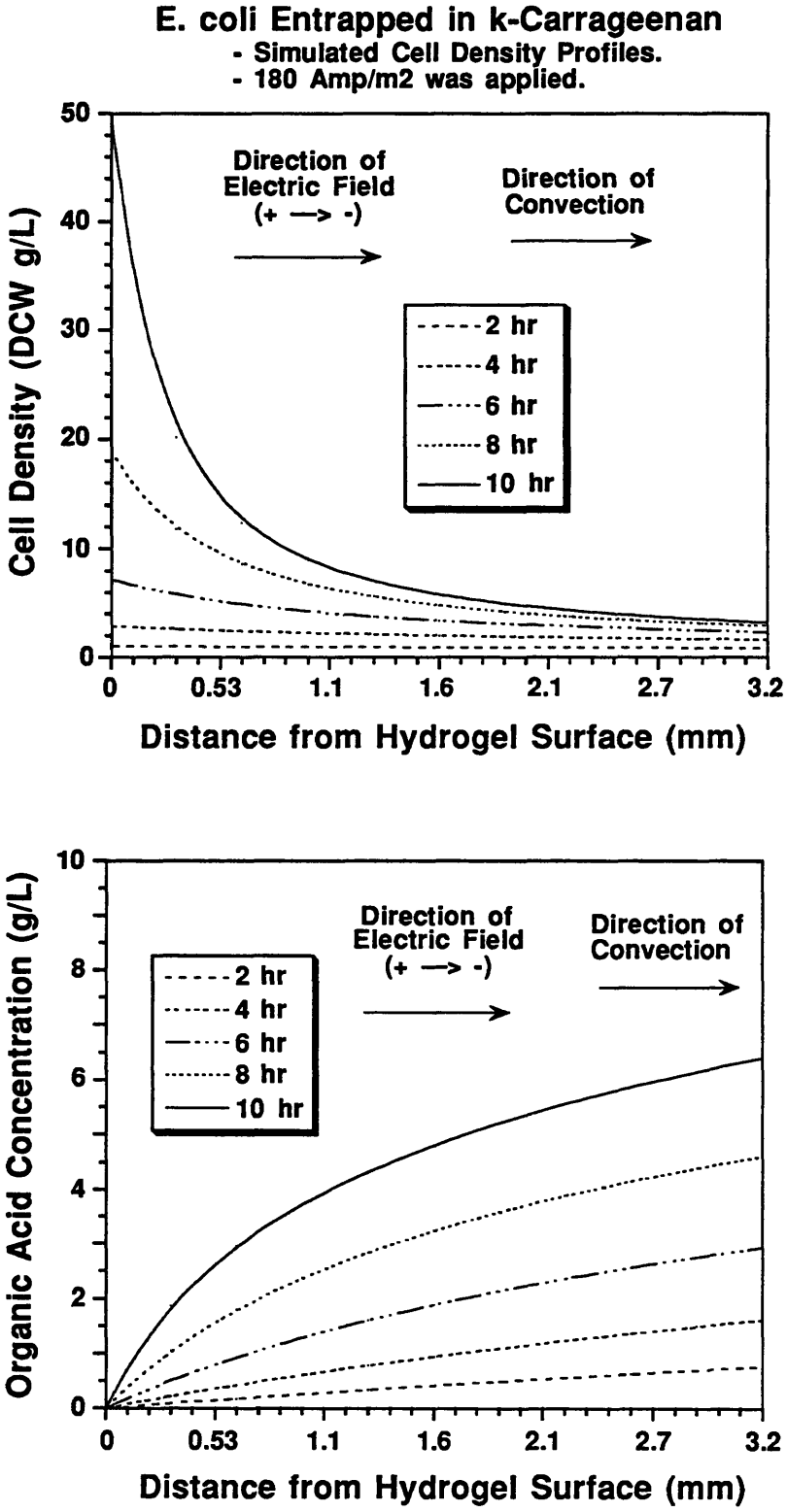

Figure-4.19: The simulated results of k-carrageenan-entrapped E. coli after different time of cultivation. The results in the upstream half of hydrogel slab are shown.

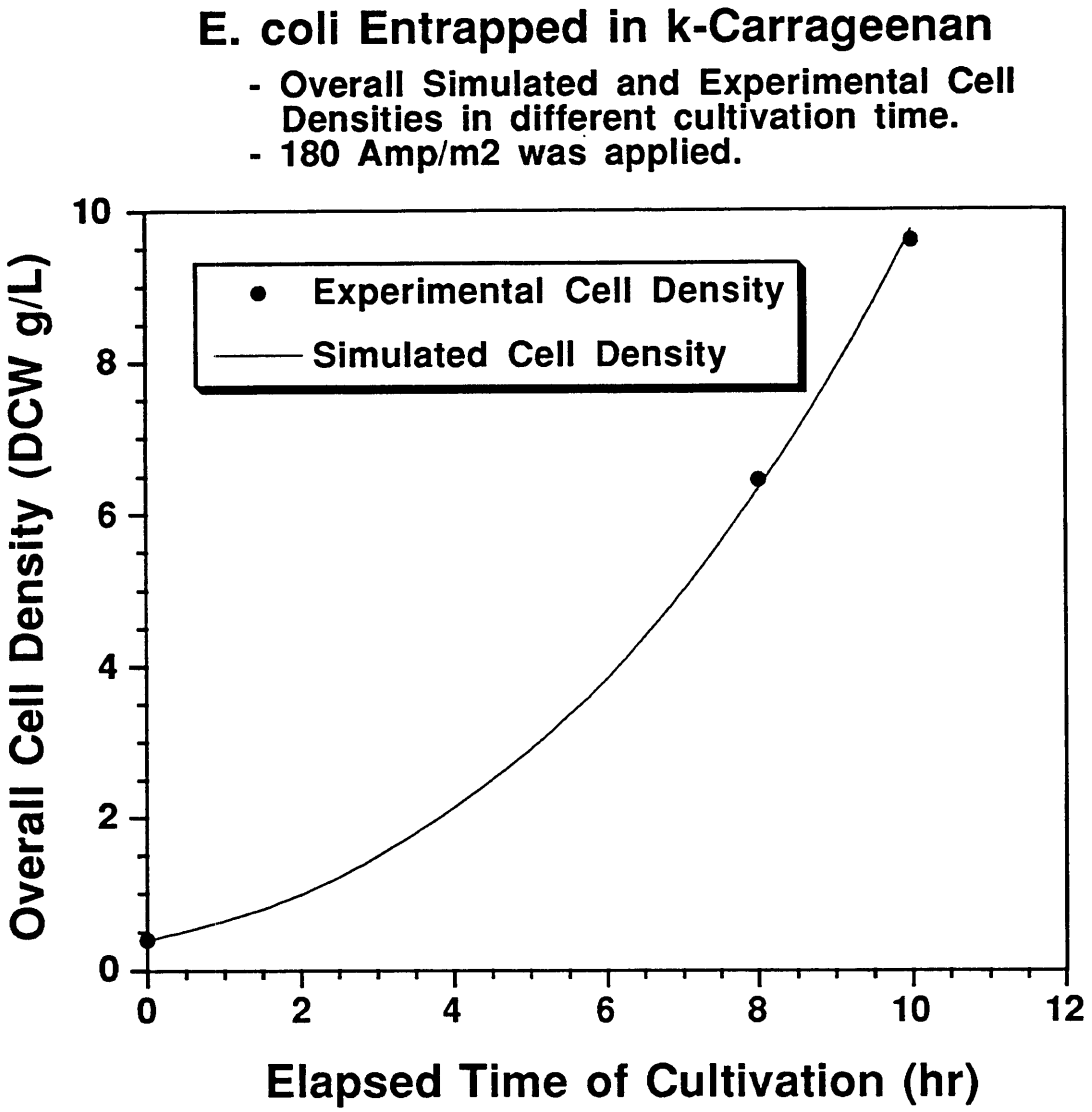

Figure-4.20: The comparison of the simulated and experimental overall E. coli cell densities in k-carrageenan after different time of cultivation. The results in the upstream half of hydrogel slab are shown.

simulated results also confirmed that the entrapped *E. coli* cells grew mainly anaerobically even though the gel surface (ambient medium bath) was maintained excess in substance. The good agreement between simulated and experimental results indicted that the generalized inhibition from the various organic acids on *E. coli* growth is quantitatively acceptable and the parameters of cell growth kinetics are accurate. The major reasons for the discrepancy between the experimental and simulated results can be attributed to the partial aerobic *E. coli* growth at the surface layer of the hydrogel slab.

IV.2.3.4 Glucose-Limiting, Anaerobic Growth of *E. coli* in Agarose

The analysis of glucose-limiting, anaerobic *E. coli* growth in agarose is similar to that of the κ-carrageenan-entrapped *E. coli* cultures under an anaerobic condition. The difference is mainly due to differences in mass transfer. The agarose hydrogel is electrically neutral, and hence only the transport of negatively-charged organic acid can be electrophoretically enhanced in dc electric fields. The transport of electrically-neutral glucose is not affected by dc electric fields. For the mass balance of glucose, eq.(3.15), the convective flow rate, V_x, is therefore zero. For the mass balance of inhibitory organic acid, the convective flow rate, V_x', is due only to electrophoresis and is directed towards the cathode. The same inhibitory function, eq.(3.18), can be used, and all kinetic parameters, boundary and initial conditions remain the same as listed in Table-4.3.

The anaerobic growth of agarose-entrapped *E. coli* cells in the presence of three different current densities, 0, 180 and 350 A/m^2, were simulated. The simulated cell density in the upstream half of the hydrogel slab was first presented as a continuous profile and shown in Figure-4.21. This is then presented as a discrete profile in which the cell density in

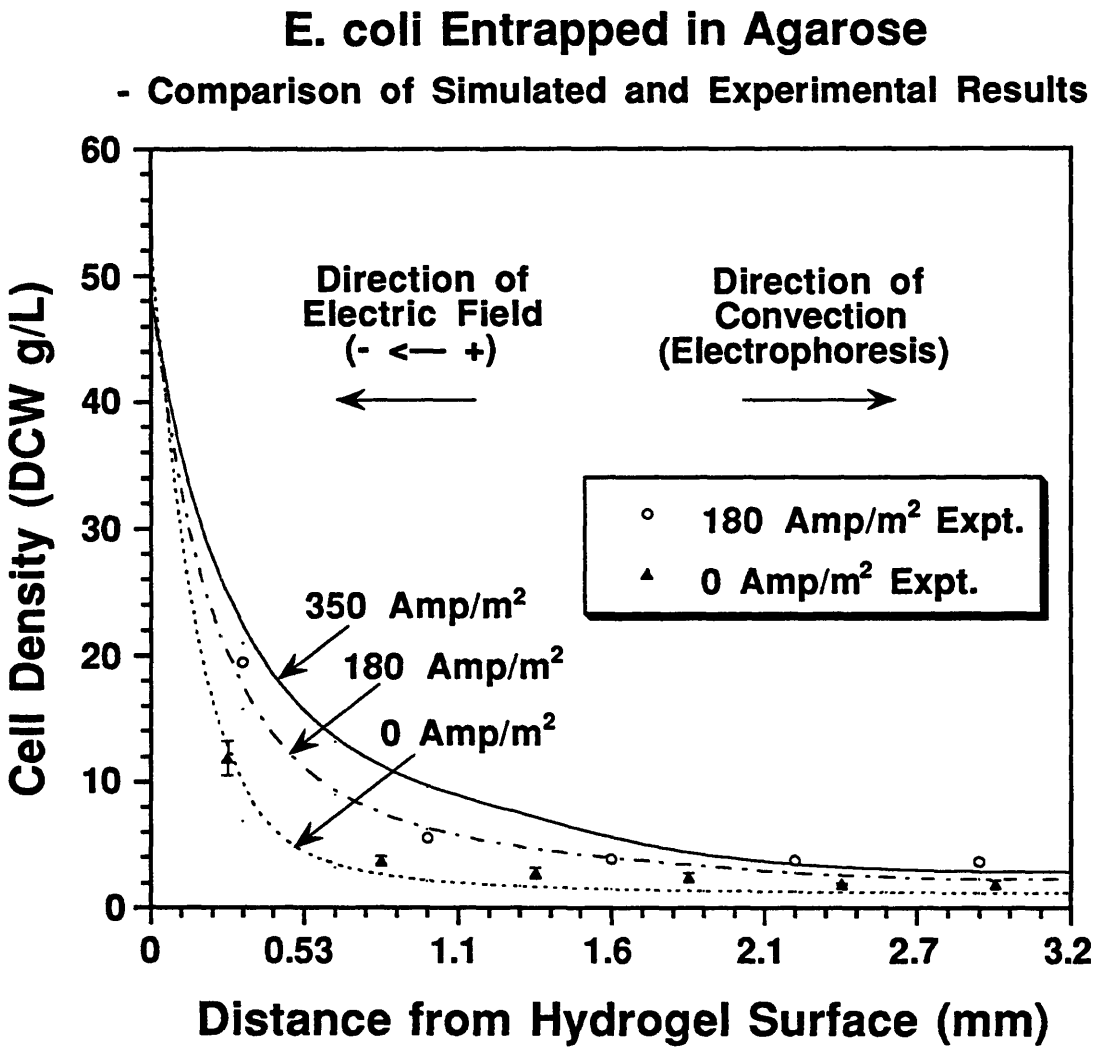

* Simulated cell density profiles are shown by lines.

Figure-4.21: The comparison of the simulated and experimental growth of agarose-entrapped E. coli in the presence of different current densities. The cell growth in the upstream half of hydrogel slab is shown.

each 530 μm-thick gel slice was averaged and shown in Figure-4.22. Finally, the overall total cell density in the entire half of the hydrogel slab at different electric current densities are shown in Figure-4.22. These simulated results were compared with the experimental results obtained at current densities of 0 and 180 A/m^2. As shown by the simulated results, cell growth was severely inhibited in the interior of the hydrogel slab even in the presence of 350 A/m^2 current density, very little difference in cell density was observed in the interior of the hydrogel slab in the presence or absence of an applied dc electric field. The predicted increase in total cell density at current densities of 180 and 350 A/m^2 compared to that at 0 A/m^2 were 80% and 140%, respectively. These values are much less than those κ-carrageenan-entrapped cells. The discrepancy between the simulated and experimental total cell densities was less than 10%. The major discrepancy occurred at the surface layer of the hydrogel slab, which was probably due to the partial aerobic proliferation at the surface. Nevertheless, the mathematical model could successfully predict the agarose-entrapped *E. coli* cell growth, and the acceptability of the empirically-obtained inhibitory function, eq.(3.14), is further confirmed.

The simulated concentration profiles of glucose and inhibitory organic acid are shown in Figure-4.23. When electric current densities of 180 and 350 A/m^2 was applied, the concentrations of organic acid in the middle of the hydrogel slab were decreased by 40% and 50%, respectively, compared to the case of no electric field. These decreases are similar to those observed in the κ-carrageenan system even though the induced convection of organic acid in agarose was only 67% of that in κ-carrageenan (since the electrophoretic rate was 40% of the electroosmotic rate, and they acted in opposite directions). This similarity can be attributed to the lower cell growth and hence less production of acid in the

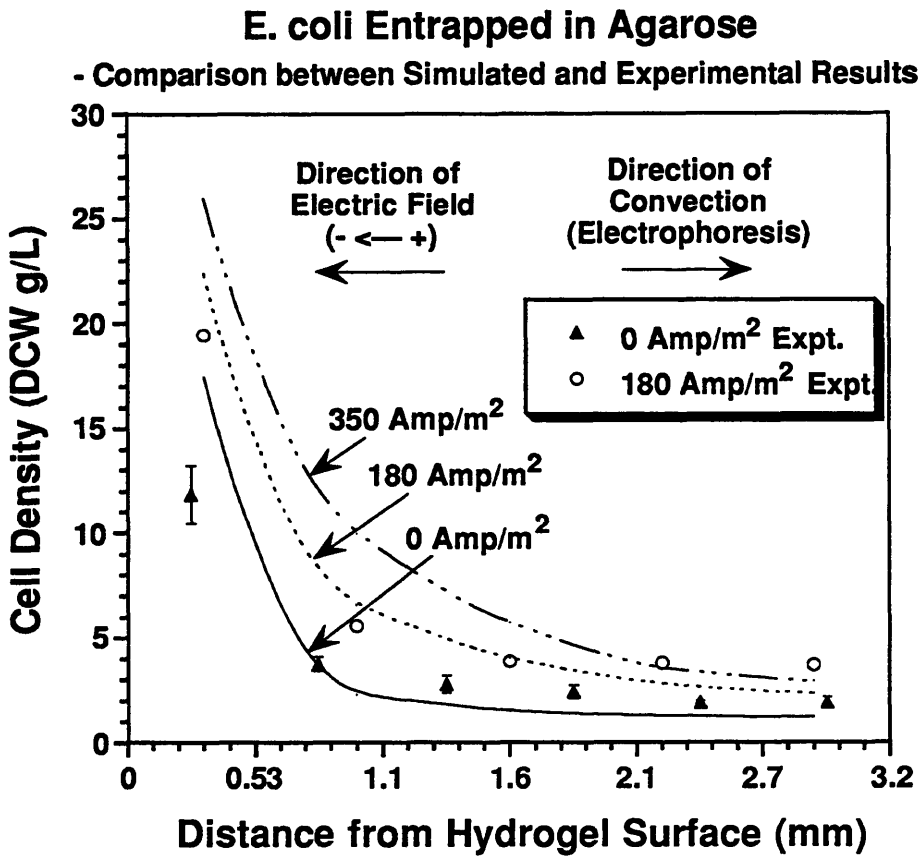

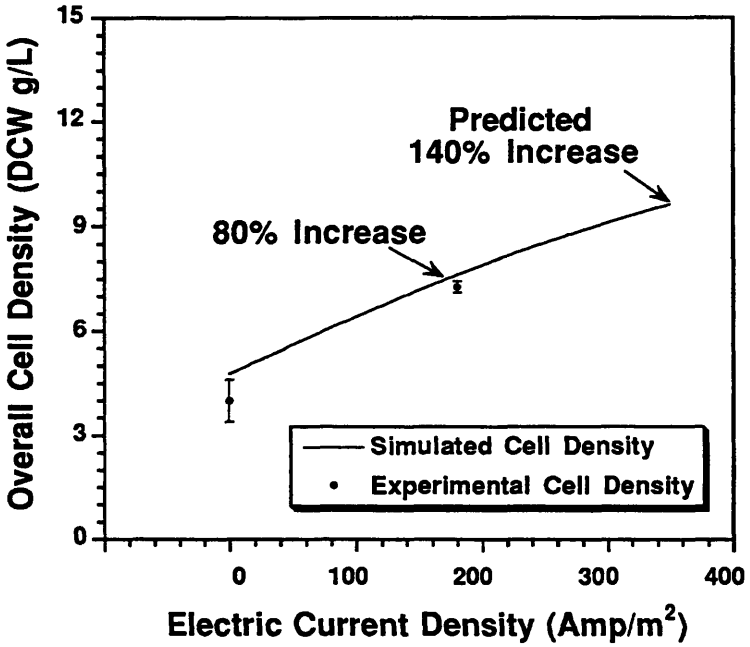

* Simulated cell density profile, which was integrated in each gel slice and in the entire half of hydrogel slab, respectively, is shown by line.

Figure-4.22: The comparison of the simulated and experimental growth of agarose-entrapped E. coli in the presence of different current densities. The cell growth in the upstream half of hydrogel slab is shown.

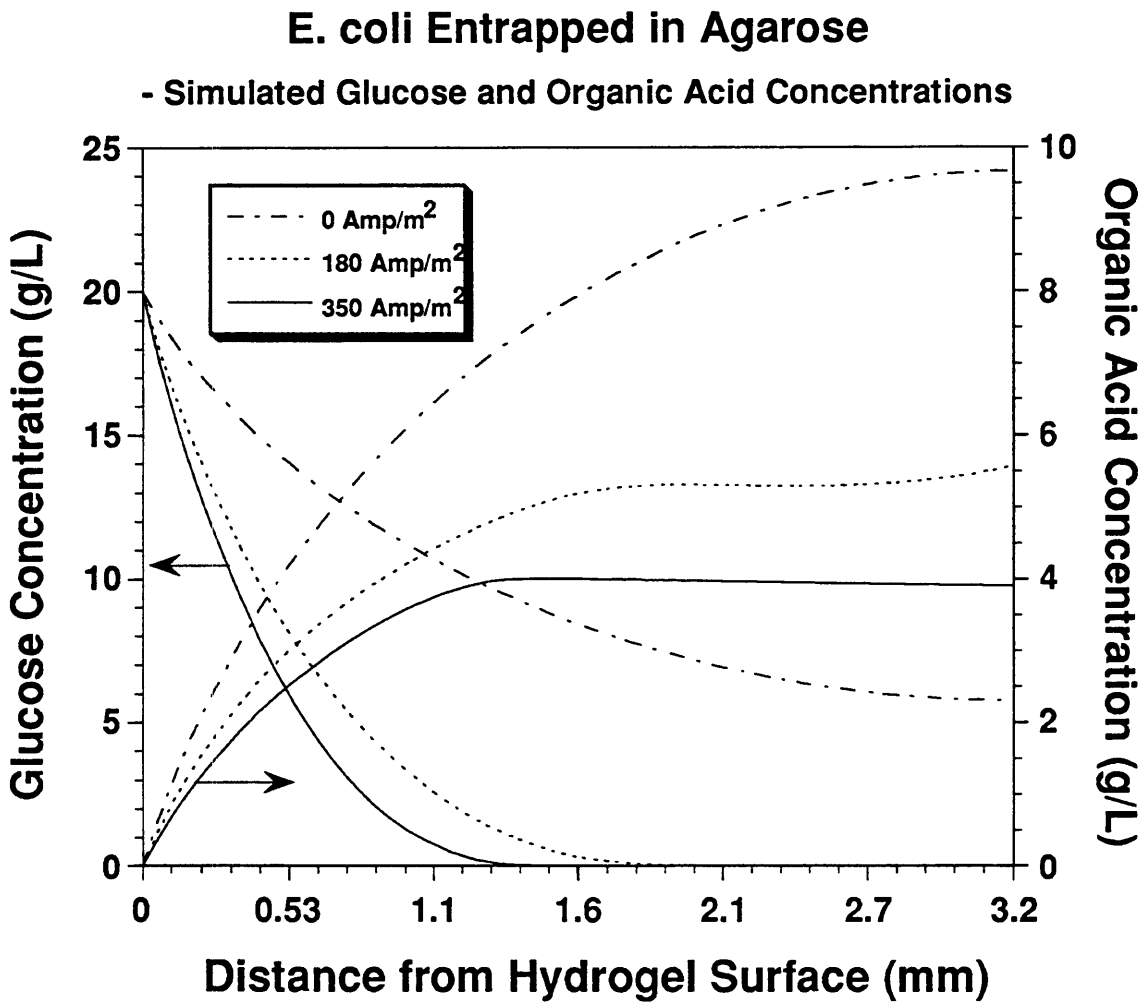

Figure-4.23: The simulated concentrations of glucose and organic acid in agarose hydrogel slab in the presence of different electric current densities. The concentration in the upstream half of hydrogel slab is shown.

case of agarose entrapment. The glucose in the interior of the agarose hydrogel slabs was depleted in the cultures with applied current densities of 180 and 350 A/m^2, in contrast to glucose-rich conditions in the entire κ-carrageenan hydrogel slab in the presence of electric fields. The depletion of glucose in the neutral agarose hydrogel can be attributed to the absence of electroosmosis of glucose, which can explain why lower increase in the total cell density was observed in agarose than in κ-carrageenan at the same electric current density.

In conclusion, the mathematical model has provided insights to the agarose-entrapped *E. coli* cultivations, and the simulated results show good agreement with the experimental data. The applicability of the same mathematical model to different hydrogels suggests that the growth of hydrogel-entrapped *E. coli* cells is not affected by the nature of the hydrogel matrices.

IV.2.3.5 Sensitivity Analysis of Mathematical Model

The kinetic parameters of *E. coli* cells used in the mathematical model, such as specific nutrient uptake rates, Monod constants for nutrients, maximum specific growth rate (μ_{max}), glucose to cell and to organic acid yields ($Y_{w/s}$), and the production of organic acid mixture through anaerobic metabolism, were mostly obtained from literature. Other kinetic parameters such as inhibition constants C_{w1} and C_{w2} were obtained through a trial-and-error approach. It is necessary to analyze the sensitivity of total cell density using these parameters which were not obtained experimentally.

The κ-carrageenan experiment conducted in the presence of 180 A/m^2 was chosen to perform this sensitivity analysis. The values of kinetics parameters, μ_{max}, $Y_{w/s}$, C_{w1} and C_{w2} were changed for the

sensitivity analysis, in which each of the parameters was first decreased by 50% of its normal value and then increased by 100% above the normal value while keeping all other parameters unchanged. The corresponding total cell density based on the varied parameter was simulated. The varied kinetic parameters and the corresponding total cell densities were normalized by the normal values used in the mathematical model and are shown in Figure-4.24. Among the four parameters under investigation, the maximum specific growth rate, μ_{max}, was the most sensitive parameter with regards to total cell density. For example, a 50% variation of μ_{max} could change the total cell density by 50-75%. The inhibition constant, C_{w1}, on the other hand, was the least sensitive parameter with regards to total cell density since there was only a 5% change in total cell density in response to a 100% change in the parameter. This is reasonable since C_{w1} represents the inhibition of dissociated acid on cells, and it has been found that dissociated acid only mildly inhibits cell growth (Yabannavar, 1988). The inhibition constant, C_{w2}, and the yield of glucose to organic acid, $Y_{w/s}$, markedly affect total cell density by approximately the same amount, i.e., 25-40% variations in total cell density were obtained while one-fold change was made in the parameters. An increase in C_{w2} reduces the inhibition by undissociated acid, and a decrease in $Y_{w/s}$ reduces the production of organic acid. C_{w2} and $Y_{w/s}$, hence, affect the total cell density in an opposing manner.

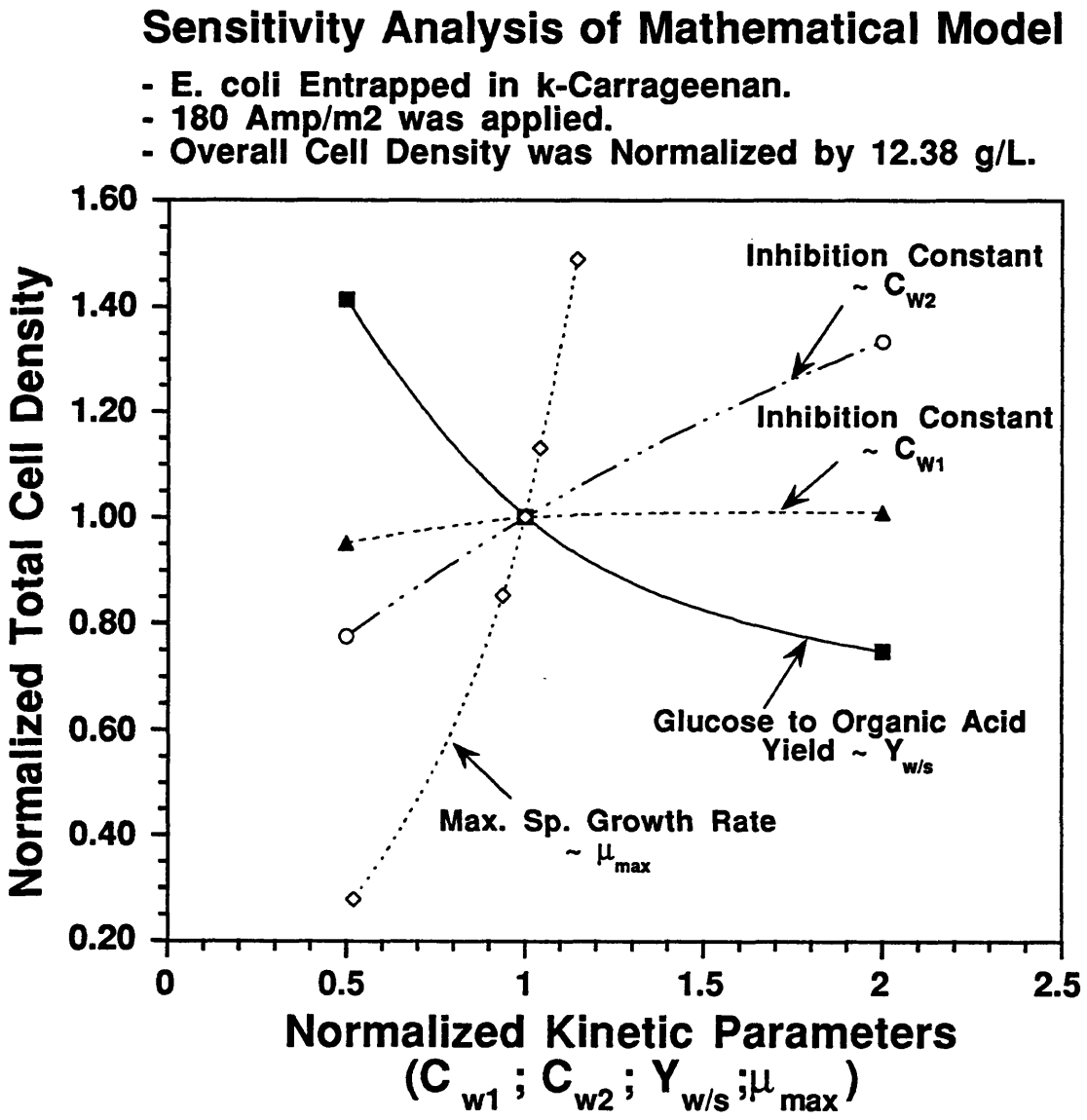

Figure-4.24: The sensitivity analysis of entrapped E. coli growth in k-carrageenan in the presence of 180 Amp/m2. The sensitivity of total cell density variation on different values of four kinetic parameters is shown.

IV.3 CHARACTERIZATION AND ELECTROKINETICS OF SUSPENSION HYBRIDOMA CULTURES

IV.3.1 Toxicity of Lactate and Ammonia on Hybridomas

The purpose of this study is to elucidate the toxic influences of lactate and ammonia on the cell growth and metabolic activities of hybridoma cells, CRL-1606. All experiments except for the control were conducted as duplicates in T-175 flasks using DMEM.

IV.3.1.1 Lactate Toxicity

Toxicity of lactate on hybridoma cells, CRL-1606, was examined first. Four hundred mM sodium lactate stock solution was added to the cultures to attain an initial sodium lactate concentrations of 40 and 80 mM. For comparison, four hundred mM sodium chloride (NaCl) stock solution was used to obtain the initial 40 and 80 mM sodium chloride concentrations in the different cultures. The respective control cultures were conducted by adding the same amount of phosphate buffer saline (PBS) instead of sodium lactate.

The viable cell density and viability profiles are shown in Figure-4.25 and -4.26. Cell growth was slightly affected, and the maximum viable cell density decreased 18% (from 2.6 to 2.1×10^6 cells/ml) by 40 mM sodium lactate, as compared to the control culture. Cell growth was not affected by 40 mM NaCl. On the other hand, when 80 mM sodium lactate or 80 mM NaCl was added, cell growth was severely inhibited. The maximum viable cell density decreased 52% (from 2.3 to 1.1×10^6 cells/ml) and 30% (from 2.3 to 1.6×10^6 cells/ml) in the presence of 80 mM sodium lactate and 80 mM NaCl, respectively, compared to that of the control culture. The monoclonal antibody (MAb) production was not markedly affected by 40 mM lactate or by 40 mM NaCl. The specific MAb production rate, q_p, was

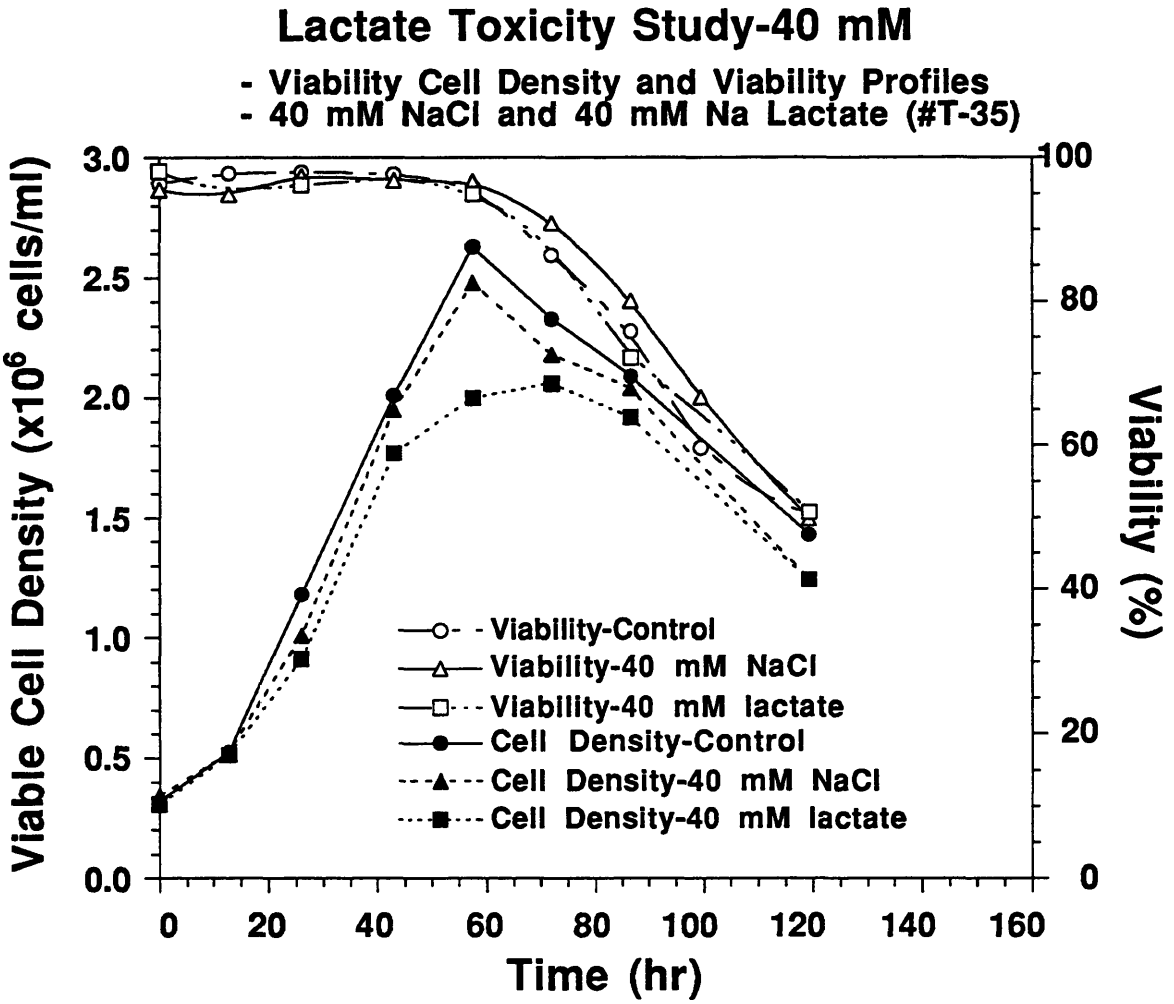

Experiments	MAb Titer (mg/L)	q_{MAb} (pg/cell-hr)
Control	90	0.43
40 mM NaCl	93	0.46
40 mM Na Lactate	89	0.48

Figure-4.25: The viable cell density and viability profiles of the cultures with 40 mM sodium chloride or sodium lactate.

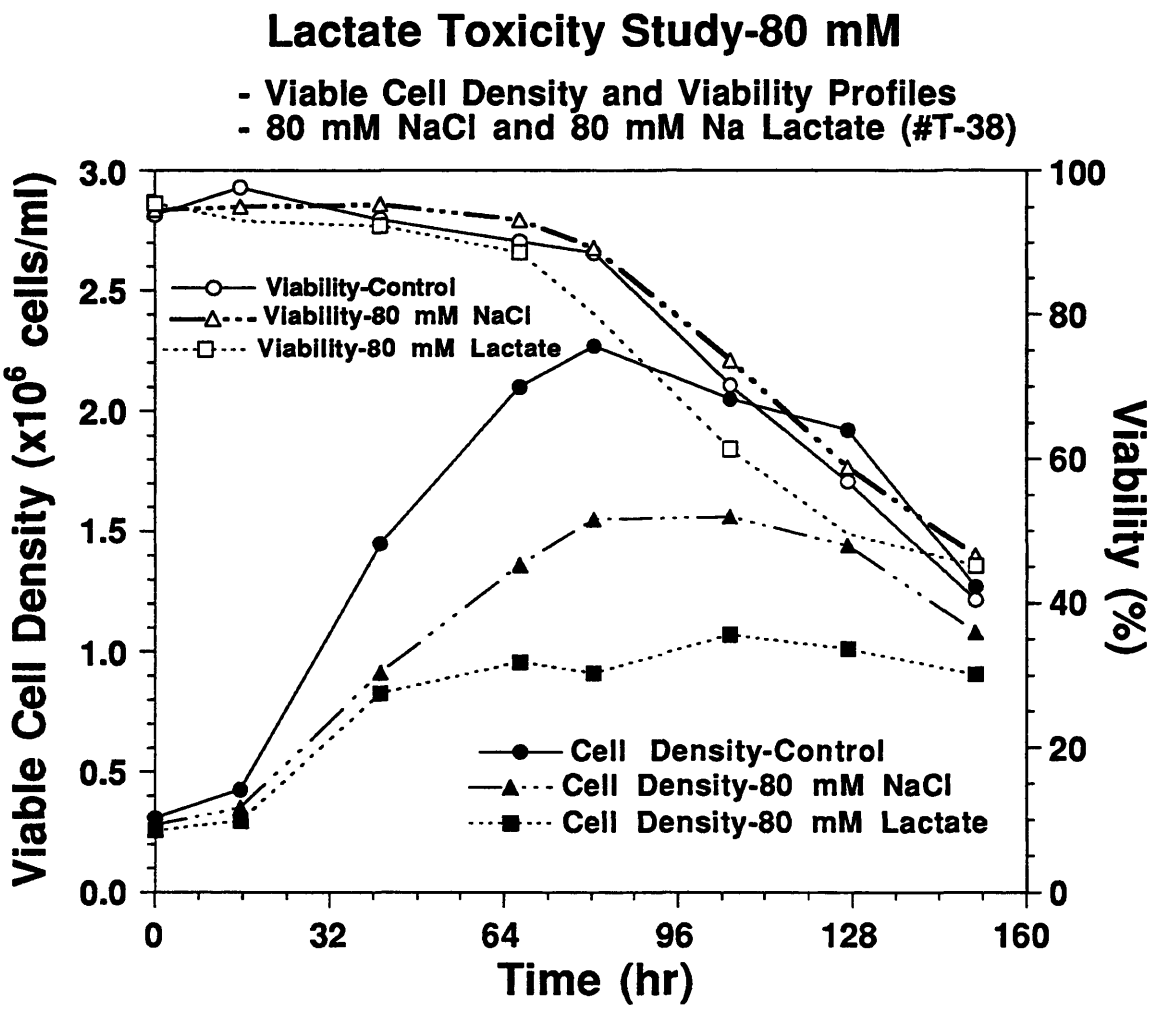

Experiments	MAb Titer (mg/L)	q_{MAb} (pg/cell-hr)
Control	108	0.45
80 mM NaCl	100	0.59
80 mM Na Lactate	96	0.77

Figure-4.26: The viable cell density and viability profiles of the cultures with 80 mM sodium chloride or sodium lactate.

calculated to range from 0.43 to 0.48 pg/cell-hr, and the final MAb titer was measured to be about 90 mg/L for all cases. The q_p's, however, markedly increased 70% (from 0.45 to 0.77 pg/cell-hr) and 30% (from 0.45 to 0.59 pg/cell-hr) in the presence of 80 mM sodium lactate and 80 mM NaCl, respectively. Regardless of the inhibition to cell growth by either 80 mM sodium lactate or NaCl, the final MAb titer was approximately the same for all cultures and was found to be about 100 mg/L. The significant enhancement in q_p in the presence of 80 mM sodium lactate or NaCl can be partially attributed to the initial higher osmolarity in these culture media. With the addition of 80 mM solute, the medium osmolarity increased by 80 mOsm/Kg above that of the normal DMEM (300 mOsm/Kg). The similar enhancement in q_p by the elevated osmolarity have been observed by other researchers (Oh et.al., 1993). Sodium chloride is usually found to be an inert material and its influence on cells is believed to arise mainly from the osmolarity elevation. Since the influences of sodium lactate were different from those of NaCl on cell growth and productivity at the same concentration, lactate might affect cells through different ways than osmolarity elevation. One possible explanation is the presence of extra-lactate might change the medium and intracellular redox states and thus affect cellular functions.

The lactate and ammonia concentration profiles are shown in Figure-4.27. The presence of 40 mM sodium lactate or 40 mM NaCl did not affect the production of lactate (~30 mM) and ammonia (~2.7 mM) compared to the control culture. Surprisingly, the presence of 80 mM sodium lactate only slightly decreased the production of ammonia (from 4.0 to 3.6 mM) and lactate (from 26 to 23 mM), as compared to those of the control culture; even though the maximum viable cell density was severely decreased by 50%. This phenomenon may be due to the overflow

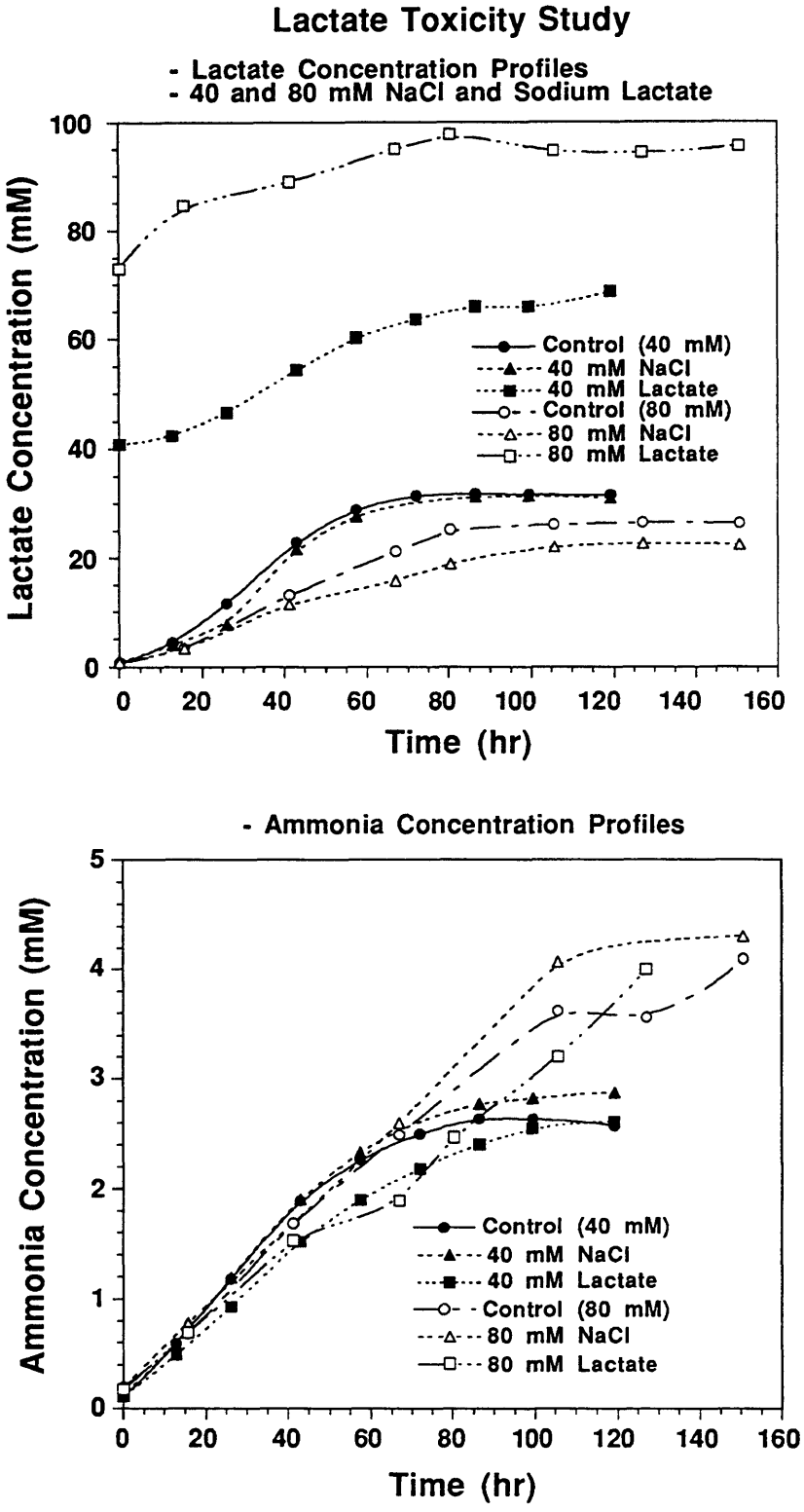

Figure-4.27: The lactate and ammonia concentration profiles of the cultures with 40 or 80 mM sodium chloride or sodium lactate added.

metabolism of glutamine and glucose in the cultures using DMEM, and due to the glutamine self-degradation. In conclusion, the presence of the externally-added 40 mM sodium lactate did not affect culture performance such as cell growth, MAb production, and nutrient metabolism. Forty mM lactate is thus considered the toxicity threshold for the hybridoma cells, CRL-1606.

IV.3.1.2 Ammonia Toxicity and Adaptation

Hybridoma cells, CRL-1606, start to show inhibited growth when the ammonia is accumulated to above 4.0 mM, and the growth is completely inhibited when the ammonia concentration reaches 8.0 mM (Glacken 1987). However, it is possible that hybridomas CRL-1606 can be adapted to a high concentration of ammonia and thus possess a greater tolerance against ammonia toxicity. Four hundred mM ammonium chloride stock solution was used to attain an initial ammonia concentration of 12.5 mM in order to test the possibility of the adaptation of hybridomas CRL-1606 to ammonia. The control culture was prepared by adding the same amount (in volume) of PBS.

The viable cell density profiles are shown in Figure-4.28. In comparison with the normal growth and productivity of cells in the control culture, cell growth and MAb production during the first 120 hours of cultivation in the presence of 12.5 mM ammonium chloride were completely retarded. After this period, cells gradually adapted to the ammonium chloride and were able to grow to approximately the same maximum viable cell density compared to that of the control culture. Cells quickly lost viability after 200 hours of cultivation in the ammonia-added culture. It was found later that the depletion of glutamine accounted for the abrupt decrease in viability. The q_p decreased 30% in the presence of

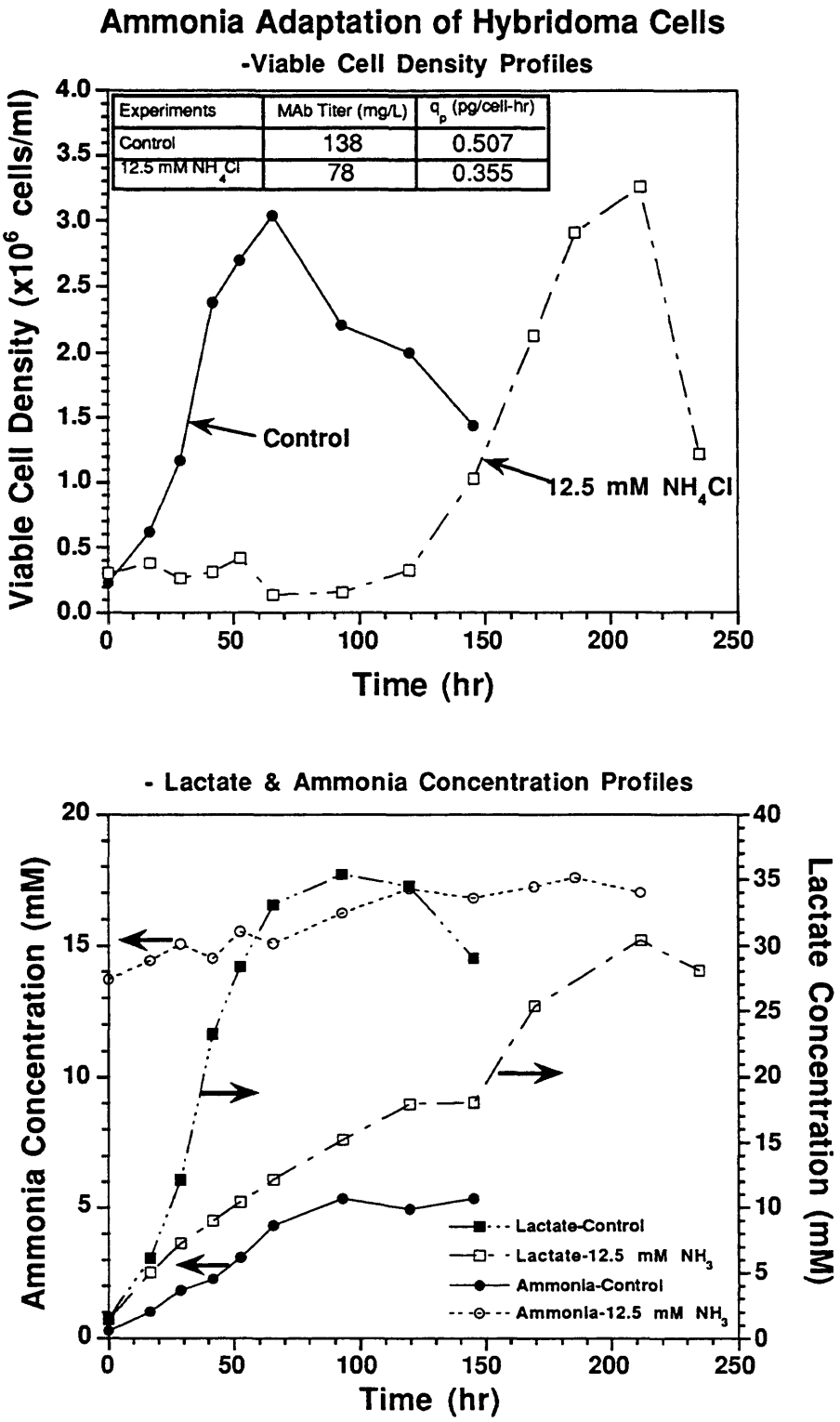

Figure-4.28: The adaptation of hybridoma cells, CRL-1606, to 12.5 mM ammonia.

12.5 mM ammonium chloride, and therefore the final MAb titer decreased by 60% (from 138 to 78 mg/L) compared to the control culture.

The lactate and ammonia concentration profiles are shown in Figure-4.28. The total lactate production was similar in these two cultures (30±5 mM). Even though there was no apparent cell growth during the early 120-hour cultivation of the ammonia-added culture, there was still 17 mM lactate produced during this period. This suggests that an overflow metabolism of glucose for cell maintenance occurred in the ammonia-added culture. The total ammonia production was 5.0 mM in the control culture and was less than 3.0 mM for the ammonia-added culture. It is noteworthy to note that less than 1.0 mM ammonia was produced in the ammonia-added culture during the period between 120 to 240 hours of cultivation in which cell growth truly occurred. This apparent decrease of ammonia production might be due to the less active metabolism at the late cell growth phase and due to a possible reverse reaction which incorporates ammonia into α-ketoglutarate or glutamate when ammonia concentration is high.

In conclusion, we have successfully adapted hybridoma cells CRL-1606 to a high concentration of ammonia (12.5 mM). Since ammonia-adapted hybridoma cells could tolerate a higher concentration of ammonia in the culture medium, the cells in general are able to grow to a higher density. The percentage of success for a direct cell adaptation to 12.5 mM ammonia was very low (less than 50%), hence the ammonia adaptation process should be conducted gradually, i.e., the cellular tolerance against ammonia should be increased step-by step by gradually increasing the amount of ammonia present in the culture medium.

IV.3.2 Effects of Sodium Butyrate on Hybridoma Cultures

Sodium butyrate is known to be a pharmacological agent that retards cell growth and concomitantly increases protein synthesis (Oh et.al., 1993). The optimal concentration of sodium butyrate and the time of feeding for the greatest enhancement of the specific MAb production rate, q_p, without severely inhibiting cell growth are cell-line specific and need to be determined experimentally. In a preliminary study, sodium butyrate concentrations higher than 1.5 mM were found to be toxic to hybridoma cells CRL-1606. Concentrations of sodium butyrate ranging from 0.5 to 1.0 mM were thus added during the different times in the growth phases in separate cultures for this screening study.

The results are summarized in Table-4.5. When 0.5 or 1.0 mM sodium butyrate was added at the beginning of the exponential growth phase of a culture (viable cell density was 0.75×10^6 cells/ml), it was found that 0.5 mM sodium butyrate slightly affected cell growth, but 1.0 mM sodium butyrate reduced the maximum viable cell density by 50% (1.3×10^6 cells/ml) compared to that of the control culture (2.6×10^6 cells/ml). The q_p was the highest (50% higher than the q_p of the control culture) in the presence of 0.5 mM sodium butyrate. When 0.7 mM sodium butyrate was added in the late exponential growth phase (viable cell density was 2.0×10^6 cells/ml), the maximum viable cell density was measured to be the same as that of the control culture. The q_p was calculated to be 50% greater than that of the control culture. When 0.5 or 1.0 mM sodium butyrate was added during the early stationary growth phase of the culture (cell density was 2.2×10^5 cells/ml), the presence of 0.5 mM sodium butyrate slightly affected cell growth and q_p compared to the control culture. However, 1.0 mM sodium butyrate appeared to be toxic to cells. The cells immediately lost viability after the addition of the sodium

Table-4.5: Summary of the effects of sodium butyrate on hybridoma cultures

Na Butyrate Supplement Timing / Butyrate Conc.	Early Exponential Phase		Late Exponential Phase		Early Stationary Phase	
	Max. Viable Cell Density	q_p (pg/cell-hr)	Max. Viable Cell Density	q_p (pg/cell-hr)	Max. Viable Cell Density	q_p (pg/cell-hr)
0.0 mM	$2.5x10^6$	0.51	$2.7x10^6$	0.51	$2.5x10^6$	0.55
0.5 mM	$2.4x10^6$	0.75	N/A	N/A	$2.3x10^6$	0.50
0.7 mM	N/A	N/A	$2.7x10^6$	0.77	N/A	N/A
1.0 mM	$1.3x10^6$	0.66	N/A	N/A	$2.2x10^6$	0.40

- **1.5 mM** or higher sodium butyrate is toxic for hybridoma cells CRL-1606
- In the early exponential growth phase , viable cell density and viability were $0.75x10^6$ cells/ml and 95%, respectively, when sodium butyrate was added
- In the late exponential growth phase , viable cell density and viability were $2.0x10^6$ cells/ml and 92%, respectively, when sodium butyrate was added
- In the early stationary growth phase , viable cell density and viability were $2.2x10^6$ cells/ml and 92%, respectively, when sodium butyrate was added

butyrate even though it did not markedly affect q_p.

In conclusion, the addition of 0.5 or 0.7 mM sodium butyrate during the exponential growth phase of the culture can greatly enhance antibody production in hybridomas, CRL-1606, without severely affecting cell growth. The addition of sodium butyrate during the stationary growth phase, however, did not have a significant impact on cell growth or MAb production. Sodium butyrate concentrations greater than 1.0 mM were shown to be toxic when added in all different growth phases of the culture. Therefore, for the purpose of the enhancement of the MAb production and the deceleration of the cellular metabolism, it was decided to feed 0.7 mM sodium butyrate during the exponential growth phase of the hybridoma culture.

IV.3.3 Effects of a dc Electric Field on Various Solutes in DMEM in a Cell Free Condition

In order to evaluate the effectiveness of removing lactate and ammonium by a dc electric field, a transport experiment was conducted with a cell-free condition. In this experiment, a large rectangular culture chamber, a set of electrode baths and a set of salt bridges, as described in Section-III.4, were used. Forty-five mM sodium lactate and ten mM ammonium chloride were added to the medium (200 ml DMEM supplemented with 5% serum) at the beginning and a dc electric current density of 50 A/m^2 (total electric current was 75 mAmp) was applied for 130 hours.

The concentration profiles of the externally-added ammonium and lactate and the concentration profiles of the glucose and glutamine are shown in Figure-4.29. Ammonium was nearly completely removed from DMEM within 60 hours. Lactate, on the other hand, was effectively, but

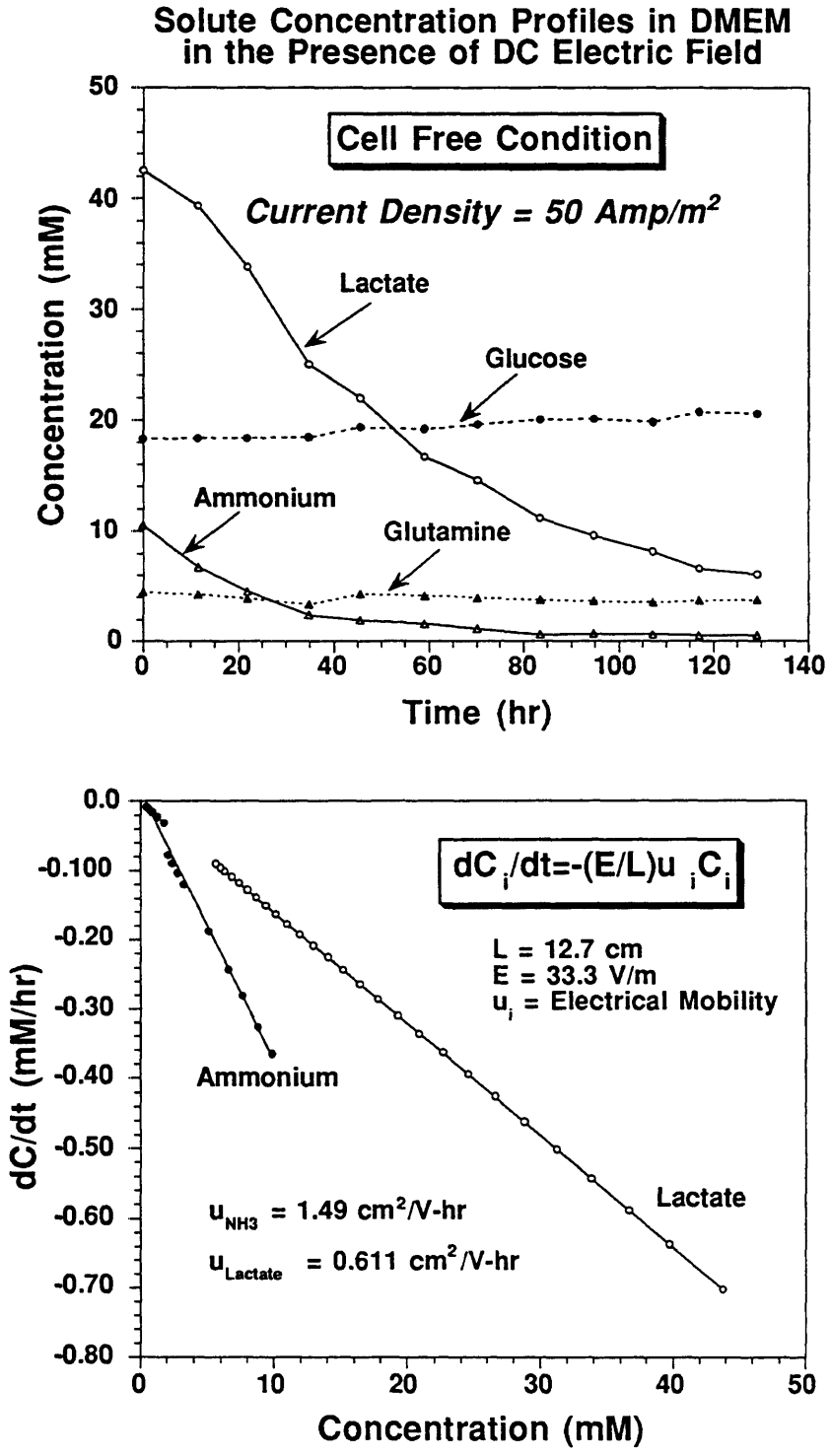

Figure-4.29: The solute concentration profiles in DMEM in the presence of 50 Amp/m2 (electrokinetics).

not completely, removed at a slower rate from DMEM. This difference between the removal of lactate and ammonia can be attributed to the lower electrical mobility and larger amount of lactate present in the medium. Since ammonia is the most toxic waste product for mammalian cells, the prompt and complete removal of ammonia by electrokinetics is critically valuable for mammalian cell culture. The concentrations of the DMEM constitutive components, whether they are electrically charged (such as glutamine) or neutral (such as glucose), remained undisturbed during the entire application of the current density of 50 A/m^2. In addition, the osmolarity remained constant during the experiment. The successful maintenance of the medium chemostatic condition can be attributed to the design of the inner sets of the salt bridges and electrode baths, which were made of DMEM-based gel and solution, respectively. Whenever one of the medium components was removed from one of the inner set of the salt bridges (electrode baths), it can be supplemented from another. In conclusion, this transport experiment proved that the experimental set-up shown in Figure-3.4 can effectively remove the externally-added ammonia and lactate, which are equivalent to these produced by the cells, and maintain the chemostatic condition of the medium in the presence of dc electric fields.

The electrical mobilities of ammonium and lactate in DMEM solution can be obtained from our experiment. The mass balance of the externally-added, charged solutes in the presence of a dc electric field is shown by equation (4.2),

$$\frac{\partial C_i}{\partial t} = -\frac{Z_i}{|Z_i|}\frac{E}{L} u_i C_i \qquad \text{----------(4.2)}$$

where C_i = concentration of charged solute i ($mole/cm^3$)
Z_i = valence of charged solute i

E = potential gradient (volt/cm)
L = length of the chamber (cm)
u_i = electrical mobility of charged solute (cm^2/volt-hr)

A plot of dC_i/dt versus C_i, as shown in Figure-4.29, gives a straight line with a slope directly proportional to the electrical mobility, u_i. The u_i of ammonium, 1.49 cm^2/volt-hr, was calculated to be 140% greater than that of lactate, 0.61 cm^2/volt-hr. These u_i values can be used to determine the strength of an applied dc electric field to a culture for complete removal of ammonia and lactate. For hybridoma cells, CRL-1606, the maximum specific production rate of lactate and ammonia were measured to be 0.2 and 0.02 pmol/cell-hr, respectively (Lindell, 1993). If one would like to maintain the ammonia and lactate concentrations below 1.0 and 30.0 mM, respectively in a culture containing 5 to $10x10^6$ viable-cells/ml, it requires a volumetric electric current density of 0.5-1.0 A/L. Our rectangular culture chamber has a working volume of 200 ml and a cross-sectional area of 15 cm^2 for the passage of electric current, we need to apply a total electric current of 100-200 mAmp, which is equivalent to an electric current density of 70 to 140 A/m^2. Since cells generally have a lower metabolic activity, which can be 50% lower, when reaching a high cell density, the above values can be considered as an extreme limit for hybridoma cultures.

IV.3.4. Release of Ammonia Inhibition by Electrokinetics

It is known that the growth of hybridoma cells, CRL-1606, begins to be inhibited when the ammonia concentration reaches 4.5 mM, and it is completely inhibited when ammonia accumulates to 8.0 mM (Glacken, 1987). In addition, we have demonstrated that the toxicity of lactate on hybridoma cells mainly arises from its high concentration, which thus

changes medium osmolarity. Since electrokinetics can only selectively exchanges one charged solute with another without altering the total amount of charged solutes, the elevated osmolarity due to the accumulation of the cell-produced lactate can not be reduced by electrokinetics. Therefore the study of the release of hybridoma cellular waste toxicity by electrokinetics concentrated only on ammonia.

There were four different experiments conducted to study the reversibility of ammonia toxicity. The first experiment is the control in which only electrokinetics was applied. The second is the 12.5 mM NH_3/START experiment in which 12.5 mM NH_4Cl was added and electrokinetics was applied at the beginning. The third is the 7.5 mM NH_3/START experiment in which 7.5 mM NH_4Cl was added and electrokinetics was applied at the beginning. The fourth is the 9.5 mM NH_3/DELAY experiment in which 9.5 mM NH_4Cl was added at the beginning but electrokinetics was not applied until 12 hours later. A round culture chamber with a working volume of 90 ml, as shown in Figure-3.5, was used in this study. A total electric current of 40 to 60 mAmp was applied.

The ammonia concentration profiles are shown in Figure-4.30. In the control experiment, the ammonia concentration was maintained below 1.0 mM during the entire culture. But in the 12.5 mM NH_3/START experiment, it took 12 hours to reduce the ammonia concentration from 12.5 to 5.5 mM, and another 12 hours to 1.5 mM. In the 7.5 mM NH_4Cl/START experiment, the ammonia concentration decreased from 7.5 to 2.5 mM in 12 hours. In the 9.5 mM NH_4Cl/DELAY experiment, the ammonia remained unchanged at 9.5 mM for 12 hours. When electrokinetics was applied, ammonia concentration decreased from 9.5 to 1.5 mM in 12 hours. The lactate concentration was maintained below 18

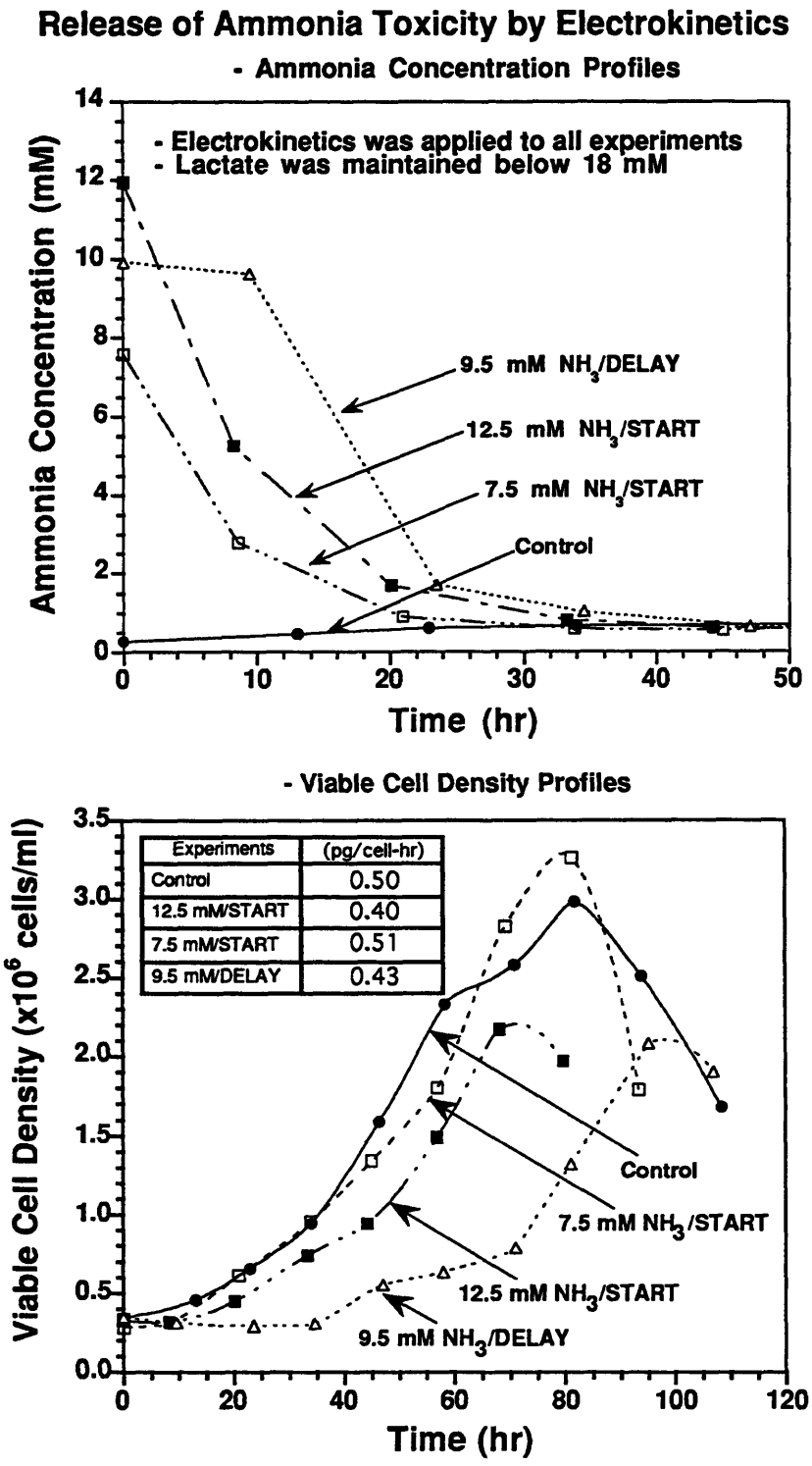

Figure-4.30: The Ammonia concentration and viable cell density profiles of the culture in the presence of externally-added ammonium chloride and electrokinetics.

mM by electrokinetics for all the experiments.

The viable cell density profiles are shown in Figure-4.30. Inhibition of cell growth early in the culture was present in all ammonia-added experiments as compared to the control. The inhibition was released by electrokinetics, and the restored cell growth was first observed in the 7.5 mM NH_3/START experiment, then in the 12.5 mM NH_3/START experiment, and finally in the 9.5 mM NH_3/DELAY experiment. The difference in the residence time of a toxic level of ammonia among different experiments showed a strong influence on the growth and productivity of the hybridoma cells. In both the control and the 7.5 mM NH_3/START experiments, the viable cell density reached 3.0×10^6 cells/ml. But in the 12.5 mM NH_3/START and the 9.5 mM NH_3/DELAY experiments, the viable cell density reached only to 2.0×10^6 cells/ml. Neither glucose or glutamine was depleted (1.0 mM of glutamine and 2.0 mM of glucose were left) when the viable cell density started to decline in all the experiments. Therefore the 12-hour incubation of cells with 8.0 mM or more ammonia appeared to permanently damage hybridoma cells. The influence of the externally-added ammonia on MAb production was similar to the influence on cell growth. The specific antibody production rate, q_p, decreased by about 20% in both the 12.5 mM NH_3/START and 9.5 mM NH_3/DELAY experiments, but q_p was about the same in the 7.5 mM NH_3/START experiment as compared to the q_p of the control. Therefore the final MAb titer was much lower in both the 12.5 mM NH_4Cl/START and the 9.5 mM NH_4Cl/DELAY experiments.

In conclusion, we have confirmed the effectiveness of electrokinetics on ammonia removal. The externally-added ammonium was promptly removed from the suspension hybridoma cultures under a total electric current of 60 mAmp. The inhibition on cell growth was removed as the

externally-added ammonia concentration was decreased below the inhibition threshold (~4.5 mM). The incubation of the hybridoma cells with 8.0 mM or more ammonia for 12 hours seemed to cause a permanent damage on both cell growth and MAb production.

IV.4 SUSPENSION HYBRIDOMA CULTURES IN THE PRESENCE OF DC ELECTRIC FIELDS

IV.4.1 Batch and Glutamine Fed-Batch Cultures Using XMEM

Our preliminary experiments have demonstrated the effective removal of charged species, lactate and ammonium, and the successful maintenance of the chemostatic condition of a culture medium in the presence of dc electric fields. The next goal is to apply this electrokinetic technique to hybridoma cultures. XMEM was initially used to cultivate suspended hybridoma cells, CRL-1606, in the presence of electrokinetic conditions. XMEM, described in Section-III.2.2, is the modification of the commercially-available DMEM by changing the basal concentration of $NaHCO_3$ concomitantly allowing the pH of XMEM to be buffered by atmospheric air. It should be noted that the pH during hybridoma cultivations using XMEM was monitored on-line but not controlled.

The data on cell densities and metabolite concentrations are average values from the three segregated compartments of the culture chamber. Cultures performed in the presence of applied dc electric fields are designated as electrokinetic cultures, while those conducted without applied electric fields are designated as control cultures. All electrokinetic cultures were repeated at least once and the results were highly reproducible. As a result, only one representative culture among the repeated experiments will be presented.

IV.4.1.1 Batch, Suspension Hybridoma Cultures

<u>Cell Growth and Monoclonal Antibody Production</u>

A 50 A/m^2 dc electric current density was applied to the batch hybridoma cultures. The viable cell density, percent viability and

monoclonal antibody (MAb) titer profiles are shown in Figure-4.31. In both the electrokinetic and the control cultures, pH decreased from 7.2 to 6.6 in a gradual manner during the total 120 hours of cultivation. During the early growth phases of the cultures (less than 45 hours of cultivation), hybridoma cells in both the electrokinetic and the control cultures showed similar rates of growth and MAb production. During the period between 45 to 90 hours, however, the hybridoma cells in the electrokinetic culture showed higher specific growth rate, μ, and specific MAb production rate, q_p, compared to the control culture. After 90 hours of cultivation, the hybridoma cells in the control culture completely ceased proliferating but remained viable for 30 hours. In the case of the electrokinetic culture, the cells continued to grow and reached a higher maximum viable cell density, 2.7×10^6 versus 2.0×10^6 viable-cells/ml (35% greater), albeit the cells in both the electrokinetic and the control cultures showed approximately the same q_p's during this period. After 120 hours of cultivation in both cases, the cell viability quickly dropped from 90 to 60% in less than 12 hours, and the cultures were terminated. The final MAb titer achieved in the electrokinetic culture was 115 mg/L, which is 37% higher than that (85 mg/L) in the control culture. The average q_p of the electrokinetic culture (0.67 pg/cell-hr) was slightly higher than that (0.57 pg/cell-hr) of the control culture. These relatively higher q_p's (compared to later hybridoma cultures) are due to the shorter total cultivation time of these batch cultures which include only the exponential and the stationary growth phases.

Nutrient Consumption and Cellular Waste Production

The ammonia and glutamine concentration profiles are shown in Figure-4.32. Ammonia produced in the electrokinetic culture was

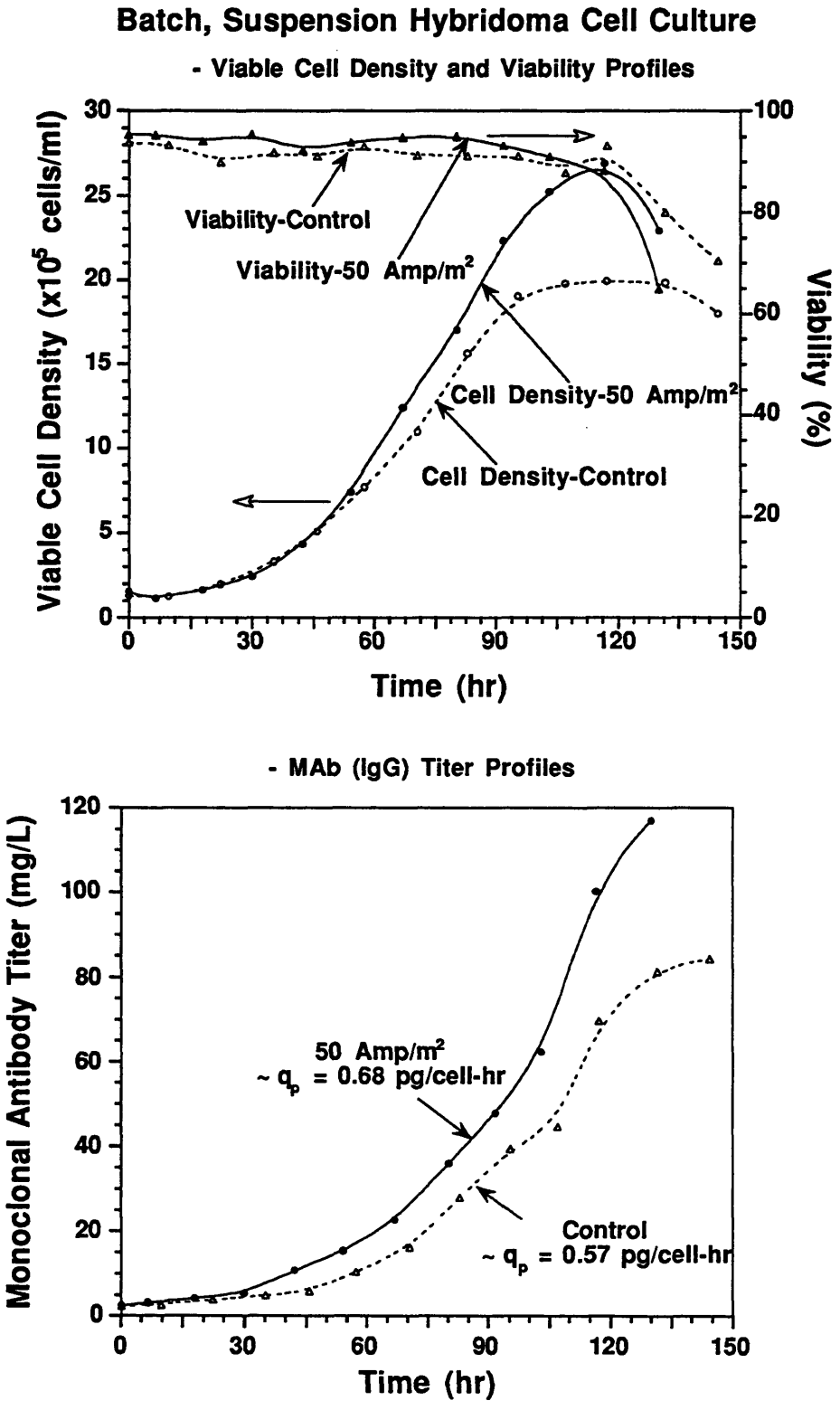

Figure-4.31: Viable cell density, viability and MAb titer profiles of batch, suspension hybridoma cultures using XMEM.

~ The control culture was conducted in the absence of DC electric fields and the electrokinetic culture was subjected to 50 Amp/m^2 of DC current density.

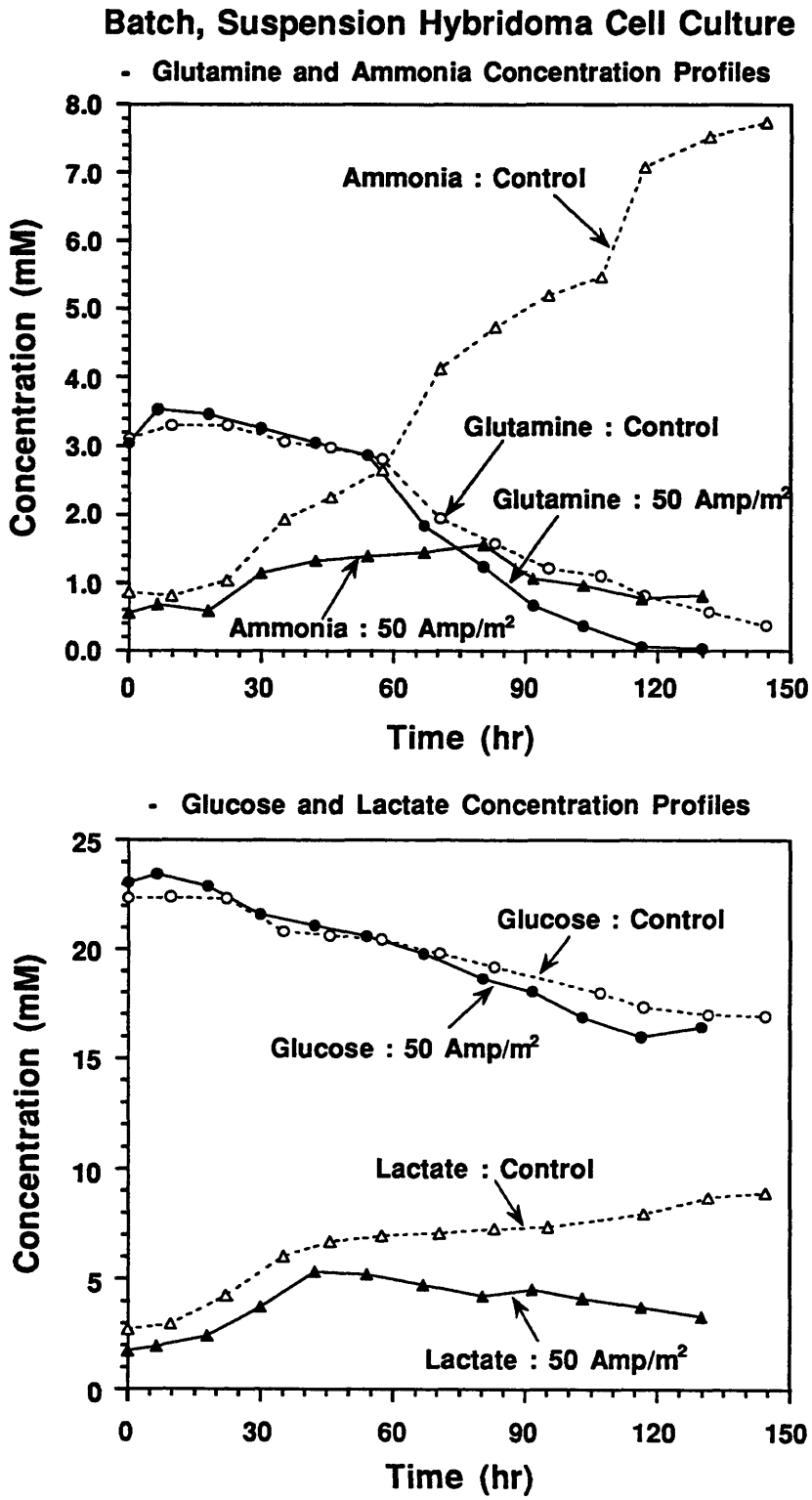

Figure-4.32: Glutamine, ammonia, glucose and lactate concentration profiles of batch, suspension hybridoma cultures using XMEM.

~ The control culture was conducted in the absence of DC electric fields and the electrokinetic culture was subjected to 50 Amp/m^2 of DC current density.

successfully removed and the concentration was maintained below 1.5 mM throughout the entire period. In contrast, the ammonia concentration in the control culture reached a level of 7.5 mM, which is much higher than the levels of 4 to 5 mM normally obtained in batch cultures using DMEM. The successful removal of ammonia was responsible for the increases in the final cell density and final MAb titer in the electrokinetic culture.

In the electrokinetic culture, glutamine was consumed at a greater rate as compared to the control culture during the late growth phase (after 60 hours of cultivation), and was completely consumed at the end of the cultivation period. This glutamine depletion was mainly due to the greater number of viable cells. Glutamine in the control culture, however, had a residual concentration of 1.5 mM even after 100 hours of cultivation. The availability of glutamine at that time explains why cells remained viable (although did not proliferate) during the subsequent 30 hours of cultivation in the control culture. Glutamine was finally exhausted after 130 hours of cultivation in the control culture. In both the electrokinetic and the control cultures, however, approximately the same specific glutamine consumption rates (~0.03 pmol/cell-hr) were observed despite a higher volumetric depletion rate of glutamine in the electrokinetic culture.

The glucose and lactate concentration profiles are shown in Figure-4.32. The lactate concentration reached 8.0 mM for the control culture, and it was maintained below 5.0 mM in the electrokinetic culture. The decrease in lactate concentration during the late growth phase in the electrokinetic culture is attributed to the effective removal by the applied electric fields. The accumulated lactate concentrations in both cultures are far below the toxicity threshold (~30 mM) for hybridomas CRL-1606 (Glacken, 1987). The specific lactate production rates in both cultures were approximately the same (~0.04 pmol/cell-hr).

The volumetric glucose consumption rate was greater in the electrokinetic culture during the late phase of cell growth compared to the control culture. This can be attributed to the enhanced cell growth in the electrokinetic culture. The total glucose consumption in each of the electrokinetic and the control culture was less than 10 mM, which is much less than the total glucose demand (ranging form 20 to 40 mM) normally found in cultures using DMEM. These reduced glucose consumption using XMEM are mainly due to the decreases in medium pH's during cultivation. Generally speaking, hybridoma cells preferentially use glutaminolytic pathway instead of the glycolytic pathway for energy production in acidic culture conditions. This shift from glucose metabolism to glutamine metabolism for energy production enhances glutamine consumption and ammonia production, and which concomitantly reduces the glucose consumption and lactate production (Miller *et al.*, 1988b; Medina and de Castro, 1990).

A brief summary of the results from the batch suspension cultures is shown in Table-4.6. In conclusion, it has been demonstrated that the electrokinetic technique can successfully improve the performance of batch suspension hybridoma cultures in both cell growth (44% higher maximum viable cell density) and MAb production (36% higher). Approximately the same q_p, and specific glucose and glutamine consumption rates were observed in both the electrokinetic and the control cultures. These observations suggest that neither the applied electric field of 50 A/m^2 or the accumulated ammonia level of 7.5 mM in the control culture affects cellular metabolic activities, as opposed to the severe hindrance of cell growth in the control culture by accumulated ammonia.

Table-4.6: Summary of batch hybridoma cultures using XMEM

Kinetic Parameters (Unit)	Control Culture	50 Amp/m^2 Cultures
Max. viable cell (cells/ml)	$2.0x10^6$	$2.7x10^6$
Final total cell (cells/ml)	$2.6x10^6$	$3.5x10^6$
Final MAb titer (mg/L)	85	115
Total glutamine consump. (mM)	2.8	3.0
Final ammonia conc. (mM)	7.5	<1.5
Total glucose consump. (mM)	5.5	7.5
Final lactate conc. (mM)	8	<5
Sp. growth Rate (hr^{-1})	+0.030	+0.029
Sp. MAb production rate (pg/cell-hr)	+0.67	+0.57
Sp. ammonia production rate (pmol/cell-hr)	+0.048	N/A
Sp. lactate production rate (pmol/cell-hr)	+0.042	N/A
Sp. glutamine consumption rate (pmol/cell-hr)	-0.029	-0.032
Sp. glucose consumption rate (pmol/cell-hr)	-0.043	-0.040

IV.4.1.2 Glutamine Fed-Batch, Suspension Hybridoma Cultures

In the previous batch culture experiments, hybridoma cells grew to a higher maximum cell density in the electrokinetic culture than in the control culture, but encountered glutamine exhaustion at the end of the cultivation period. In the batch, control culture, both ammonia accumulation (7.5 mM) and glutamine depletion have hindered cell growth. In the batch, electrokinetic culture, cell growth was mainly limited by glutamine utilization. As a result, glutamine fed-batch cultures were conducted to eliminate the limitation of cell growth due by glutamine depletion.

Cell Growth and Monoclonal Antibody Production

An electric current density of 50 A/m^2 was applied to the electrokinetic culture. XMEM with a basal concentration of glutamine of 4.0 mM was used, and an additional 4.0 mM glutamine (from a 200 mM glutamine stock solution) was fed once during the middle of the exponential growth phase (approximately 40 hours after inoculation) to both the electrokinetic and the control cultures. All data are the average values from the three compartments of the culture chamber. The viable cell density, MAb titer and percentage viability profiles are shown in Figure-4.33. Both the electrokinetic and the control cultures were inoculated with a cell density of 5.0×10^5 cells/ml, which is much higher than the inocula of 1.0×10^5 cells/ml in the previous batch cultures. As soon as cultivation was initiated, hybridoma cells in the electrokinetic culture immediately showed a higher growth rate compared to the control culture; in contrast to the previous batch cultures, where there was no discernible difference in cell growth between the electrokinetic and control culture until 60 hours after inoculation. This immediate faster cell

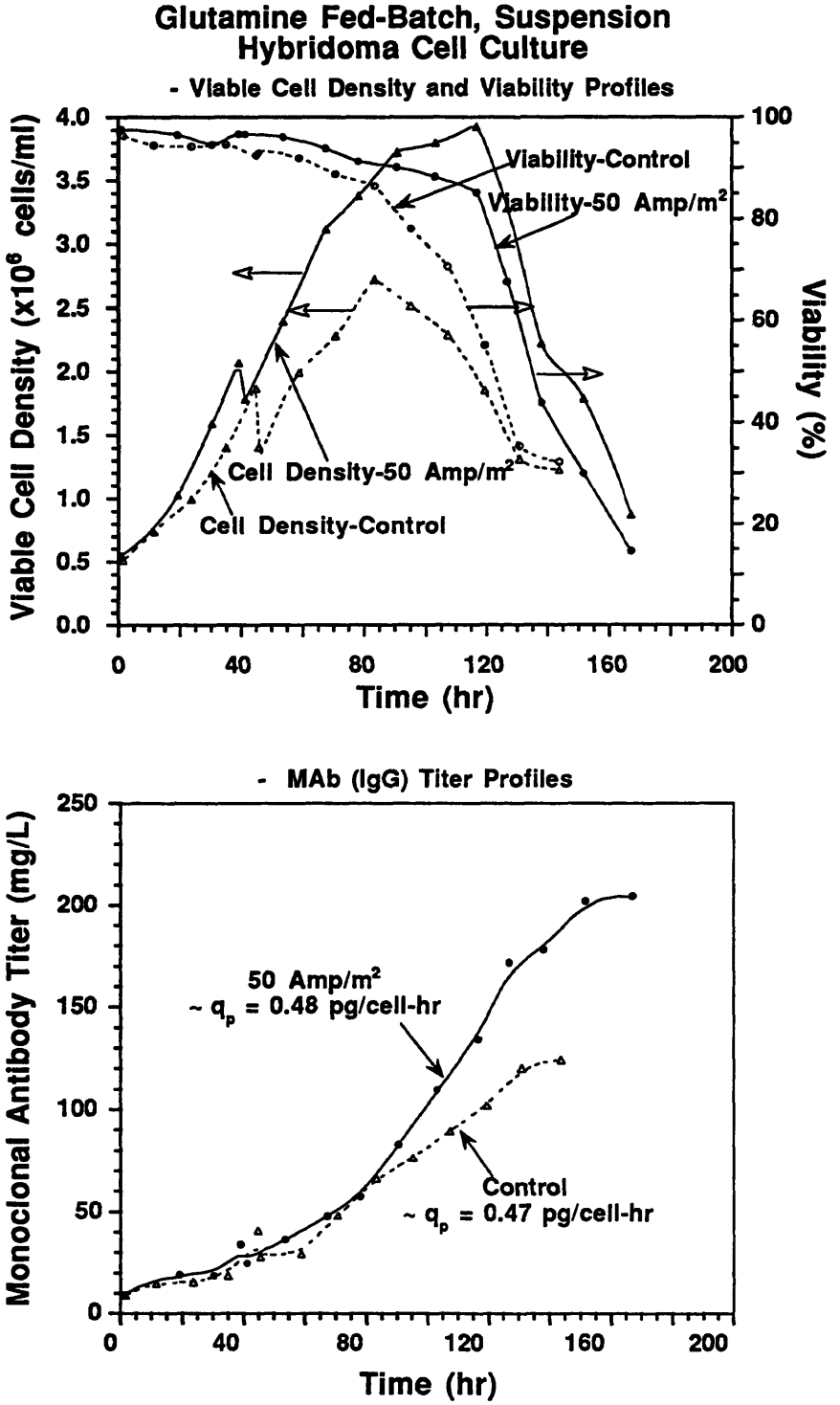

Figure-4.33: Viable cell density, viability and MAb titer profiles of glutamine fed-batch hybridoma cultures using XMEM.

~ The control culture was conducted in the absence of DC electric fields and the electrokinetic culture was subjected to 50 Amp/m^2 of DC current density.

growth in the glutamine fed-batch culture in the presence of electrokinetics is mainly attributed to the higher inoculated cell density. Cell densities were slightly diluted when 4.0 mM glutamine was fed at the 40th hour of cultivation. At the end of the cultivation period, hybridoma cells in the electrokinetic culture reached a 50% higher maximum viable cell density ($3.9x10^6$ versus $2.6x10^6$ cells/ml) and an 84% higher final total cell density ($7.0x10^6$ versus $3.8x10^6$ cells/ml). These cells also produced 55% more total MAb (205 versus 125 mg/L) compared to the control culture. Cell viabilities finally decreased to less than 30% in both the electrokinetic and the control cultures.

The time profiles of specific MAb production rates, q_p, and the specific cell growth rates, μ, are shown in Figure-4.34. These specific rates are similar for both the electrokinetic and the control cultures. It can be concluded that the dc electric field, at the strength of 50 A/m^2, does not affect cell growth and protein production, as was observed earlier in the previous batch cultures. The q_p decreased during the early exponential growth phase (from 0.7 to 0.3 pg/cell-hr), but increased during the late exponential phase, the stationary phase and the early declining phase (from 0.3 to 0.55 pg/cell-hr). The q_p rapidly decreased to zero in the late declining growth phase. The specific growth rate, on the other hand, monotonously decreased as the culture progressed except during the lag and the late declining phases. The increase in μ during the declining phase might be due to experimental errors. Since cells have extensively lysed and formed cell debris, these could result in significant errors in cell enumeration using the hemocytometer or the Coulter counter. If we examine the relationship between q_p and μ, as shown in Figure-4.35, the MAb production showed a non-growth associated pattern. Even though MAb production was not directly related to cell growth, the q_p was

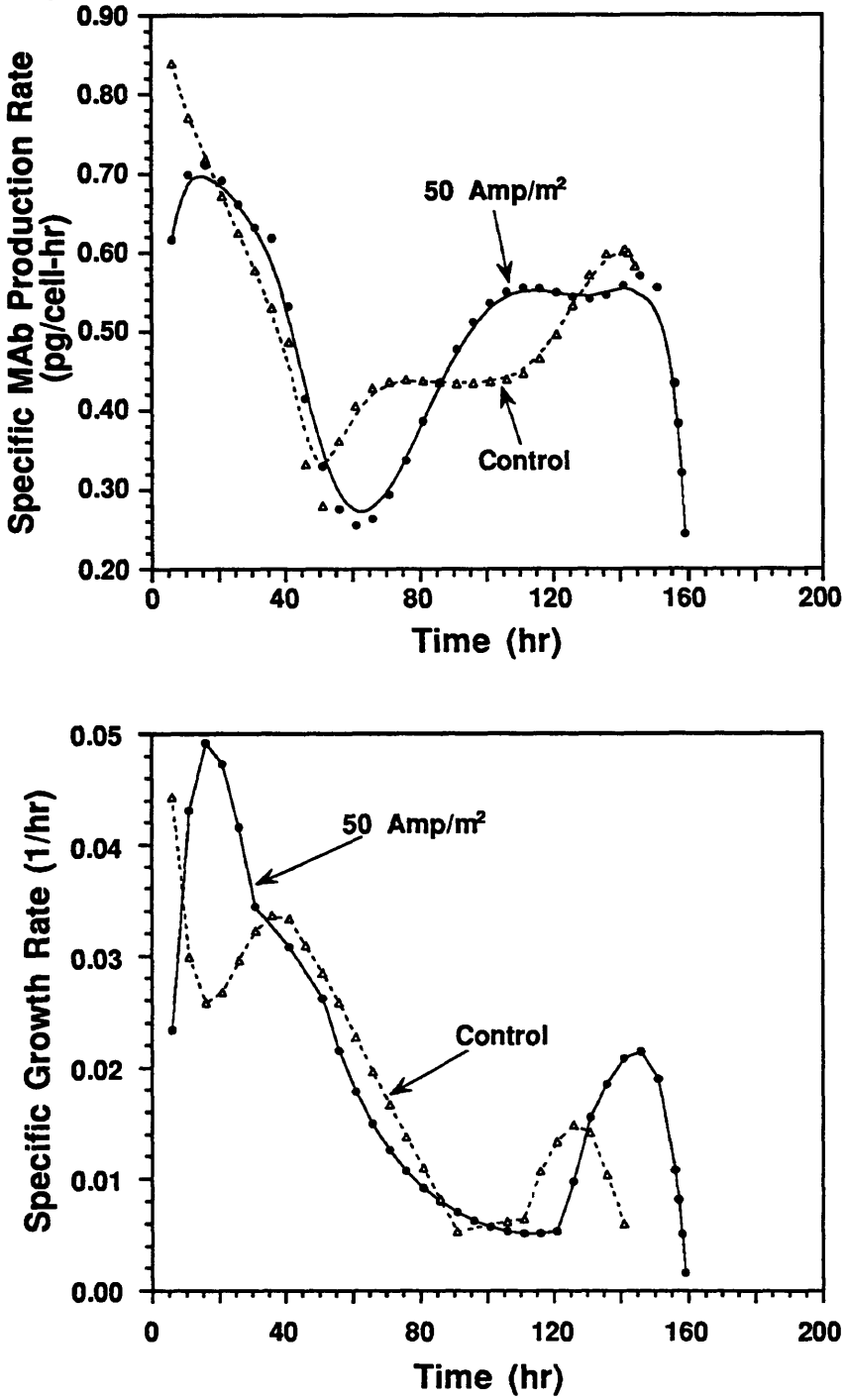

Figure-4.34: Profiles of specific MAb production rates and specific growth rates in glutamine fed-batch hybridoma cultures.

~ The control culture was conducted in the absence of DC electric fields and the electrokinetic culture was subjected to 50 Amp/m^2 of DC current density.

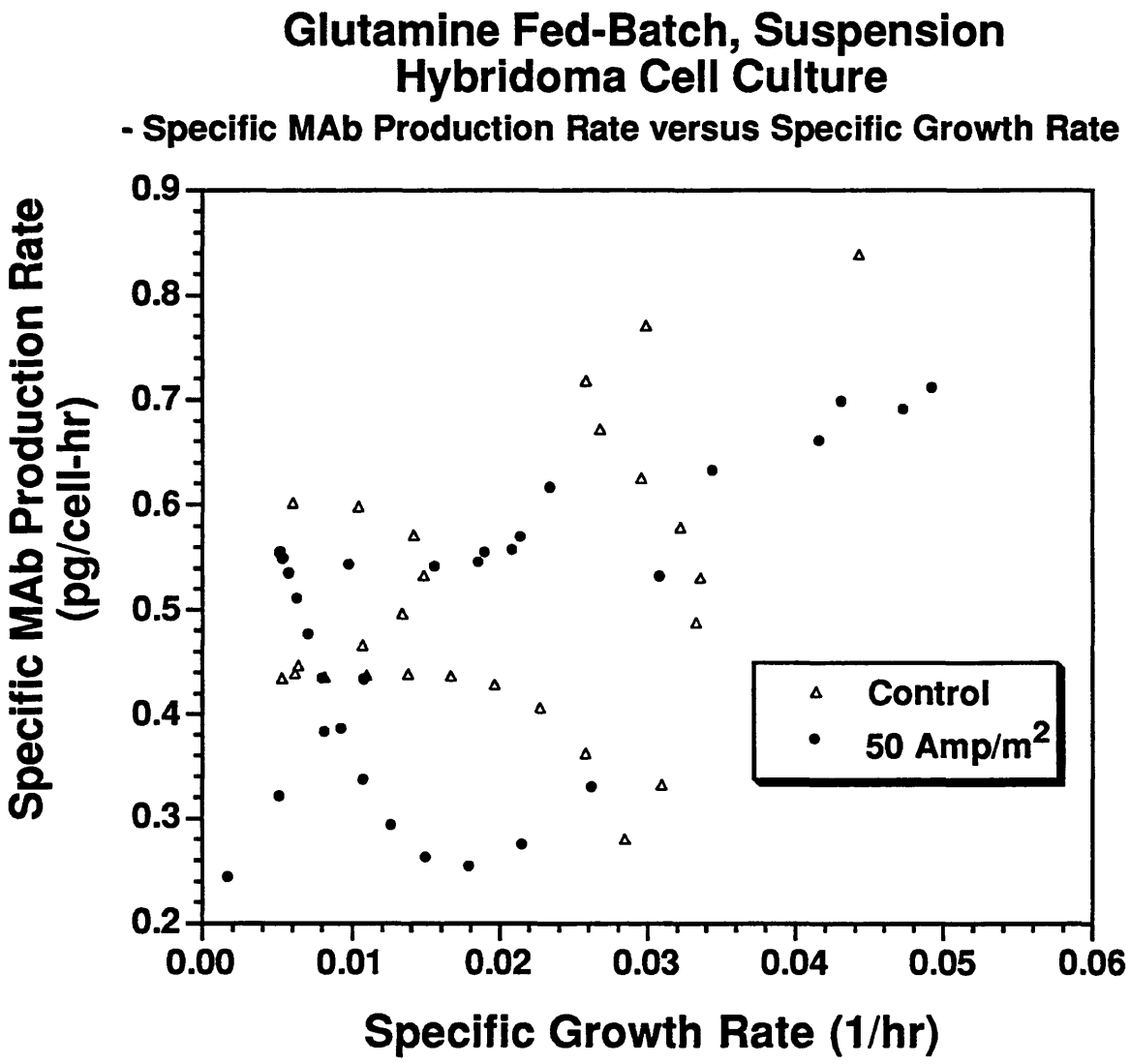

Figure-4.35: Specific MAb production rate versus specific growth rate for the glutamine fed-batch hybridoma cultures using XMEM. MAb production showed non-growth-associated pattern.

generally higher in the stationary growth phase and comparatively lower in the exponential growth phase. This observation suggests that, in order to maximize MAb production, we should maintain maximal viable cells in the stationary phase for as long as possible.

Nutrient Consumption and Cellular Waste Production

The glutamine and ammonia concentration profiles are shown in Figure-4.36. The glutamine concentration was increased from 2.0 to 6.5 mM after the additional feeding of 4.0 mM glutamine at the 40th hour of cultivation. After feeding, the glutamine consumption rate was greater in the electrokinetic culture than in the control culture. This observation directly supports that there was an enhanced cell growth in the electrokinetic culture after the glutamine feeding. Glutamine was completely consumed in the electrokinetic culture, as opposed to the 3.0 mM remained in the control culture at the end of the cultivation period. It can therefore be concluded that glutamine depletion was limitation to cell growth in the electrokinetic culture. Since there was no glutamine depletion in the case of the control culture, cell growth in the control culture must have been hindered by factors other than glutamine depletion.

Ammonia was close to be completely removed by the applied dc electric field and its concentration was maintained below 3.0 mM in the electrokinetic culture. In the control culture, however, ammonia accumulated to a potential toxic level of 7.2 mM. There was a slight accumulation of ammonia in the electrokinetic culture during the period between cultivation time of 90 to 120 hours, which corresponded to the period in which the maximum viable cell density was reached. In order to minimize the effect of this surge in ammonia accumulation, an electric

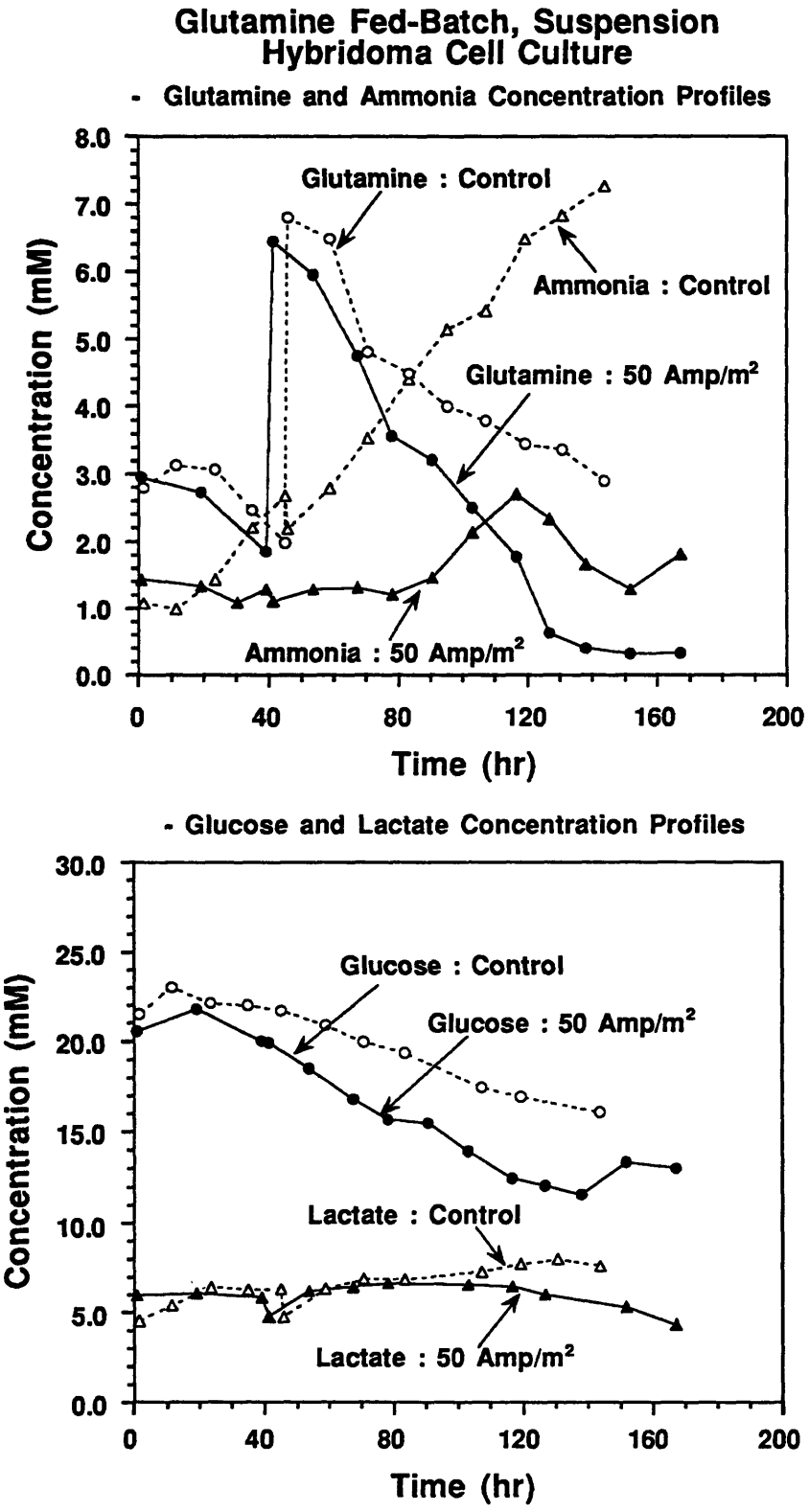

Figure-4.36: Glutamine, ammonia, glucose and lactate concentration profiles of glutamine fed-batch hybridoma cultures using XMEM.

~ The control culture was conducted in the absence of DC electric fields and the electrokinetic culture was subjected to 50 Amp/m^2 of DC current density.

current density greater than 50 A/m^2 should be used. In conclusion, ammonia accumulation in the control culture was found to be the cause for the decrease in the cell growth. The depletion of glutamine and the effective removal of ammonia in the case of the electrokinetic culture suggested that the potential of electrokinetic technique for improving cell culture performance and further exploration in nutrient replenishment and/or enrichment should be fruitful.

The glucose and lactate concentration profiles are shown in Figure-4.36. The glucose concentration profile in the electrokinetic culture, especially after the glutamine feeding, showed an enhanced consumption pattern compared to the control culture. The total glucose consumed was less than 10 mM in both the electrokinetic and the control cultures. The inefficient metabolism of glucose in these fed-batch cultures is attributed to the decrease in the medium pH values, as described in the previous section. The total lactate produced was less than 8.0 mM in both the electrokinetic and the control cultures. Lactate was effectively removed and hence we observed a decrease in lactate concentration after 80 hours of cultivation in the case of the electrokinetic culture.

The results of glutamine fed-batch cultures are summarized in Table-4.7. The effective removal of ammonia and the replenishment of glutamine have resulted in an improvement in both cell growth (50% higher maximum viable cell density) and MAb production (65% higher final MAb titer) compared to the enhancement achieved in the previous batch, electrokinetic culture. The cell metabolic rates were found to be similar in both the electrokinetic and the control cultures. This suggests that the applied dc electric field of 50 A/m^2 does not affect cellular metabolic activities. These values are, however, lower than these observed in the previous batch culture experiments. The reason for this difference

Table-4.7:Summary of glutamine fed-batch hybridoma cultures using XMEM*

Kinetic Parameters (Unit)	Control Culture	50 Amp/m^2 Cultures
Max. viable cell (cells/ml)	$2.7x10^6$	$3.9x10^6$
Final total cell (cells/ml)	$3.8x10^6$	$6.0x10^6$
Final MAb titer (mg/L)	124	204
Total glutamine consump. (mM)	4.7	7.3
Final ammonia conc. (mM)	7.3	<2.5
Total glucose consump. (mM)	5.5	7.5
Final lactate conc. (mM)	8	<6.5
Sp. growth Rate (hr^{-1})	+0.033	+0.035
Sp. MAb production rate (pg/cell-hr)	+0.48	+0.47
Sp. ammonia production rate (pmol/cell-hr)	+0.039	N/A
Sp. lactate production rate (pmol/cell-hr)	+0.045	N/A
Sp. glutamine consumption rate (pmol/cell-hr)	-0.033	-0.043
Sp. glucose consumption rate (pmol/cell-hr)	-0.032	-0.042

* Data were obtained during the exponential growth phase

is because in the previous batch cultures, cells had only progressed through the exponential and the stationary growth phases, when they generally possess higher metabolic activities. In contrast, for the glutamine fed-batch cultures, the cells were cultivated for a time period which lasted into the end of the declining growth phase, and therefore the overall average metabolic activities in these cells are lower in the glutamine fed-batch cultures than in the previous batch cultures.

IV.4.2 Fed-Batch Cultures with Enriched Culture Media

Cell culture experiments using XMEM (equivalent to DMEM) have demonstrated the effectiveness of the electrokinetic technique to improve cell growth and protein production. It was also found that the depletion of glutamine has limited cell growth in the case of the electrokinetic, glutamine fed-batch culture. Consequently, the full potential of the electrokinetic technique to improve cell culture performance can be further explored. In addition, it is believed that the electrokinetic culture using XMEM will encounter depletion of other nutrients apart from glutamine and glucose when only glutamine and glucose are repeatedly fed. Therefore, the obvious choice is to enrich all nutrients including all amino acids and vitamins in the culture medium used in the electrokinetic cultures. The procedures for preparing the enriched media were described in Section-III.2.2. It is hoped that the enriched media will fully support cell growth and protein production with the help of the electrokinetic technique.

Three hybridoma cultures were conducted using the enriched culture media, f5MEM and f10MEM. The first culture, designated as f5MEM/control culture, used f5MEM medium and did not have an applied electric field. The second culture, designated as f5MEM/electrokinetic

culture, used f5MEM medium with the applied electric current densities ranging from 70 to 90 A/m^2. The last culture, designated as f10MEM/electrokinetic culture, used f10MEM medium and also had applied electric current densities ranging from 70 to 90 A/m^2. The formulae for f5MEM and f10MEM were shown earlier in Table-4.7.

In the previous experiments, it was observed that the total electric current of 70 mAmp used in the glutamine fed-batch culture using XMEM (working volumes ranged from 150 to 200 ml) was not high enough to completely remove all of the cell-produced ammonia. Based on calculations using the electrical mobilities and volumetric production rates of lactate and ammonium obtained in our previous experiments, the total electric current should be increased by 30-40% in order to completely remove ammonia from the culture chamber.

In addition to enriching the culture medium, glucose and glutamine were periodically replenished in all the three cultures. A 200 mM glutamine and a 1.0 M glucose stock solutions were used to replenish the depleted glutamine and glucose in the culture medium respectively. The glutamine and glucose concentrations were increased by approximately 4.0 mM and 20 mM, respectively, after the replenishment. The feeding schedules of glutamine and glucose were determined based on the previously-measured specific glutamine and glucose consumption rates. A supplemental medium was also formulated, as described in Section-III.2.2, for the replenishment of amino acids and vitamins in the case of the f10MEM/electrokinetic culture only. The feeding schedule of supplemental medium was also determined based on the measured, average consumption rates of amino acids. In summary, in the cultures using f5MEM, only glucose and glutamine were replenished. In the cultures using f10MEM, however, supplemental medium in addition to glucose and

glutamine was periodically fed in order to replenish all depleted nutrients. Since the volume of each feeding was approximately equal to the volumes of the removed samples, there was no significant variation in volumes for the three cultures.

Both f5MEM and f10MEM contained 44 mM $NaHCO_3$, which is the same as DMEM. Therefore, the pH's of these cultures using f5MEM or f10MEM were adjusted by changing the CO_2 content (between 0% to 10% of total air volume) in the gas phase of the chamber or by the addition of 1.0 M NaOH. The pH's in these cultures were maintained at 7.0 and the variations were less than 0.1 pH unit. The dissolved oxygen concentrations in these cultures using f5MEM and f10MEM were first measured off-line by a microelectrode, and then adjusted to 30% of air-saturation by varying the oxygen content (between 21% and 50% of total air volume) in the gas phase. The dissolved oxygen concentrations in these cultures were maintained between 30% and 70% of air-saturation.

IV.4.2.1 Cell Growth and Monoclonal Antibody Production

The viable cell density, viability, total cell density and monoclonal antibody (MAb) titer profiles are shown in Figure-4.37, -4.38 and -4.39. In comparing the f5MEM/control culture with the previous glutamine fed-batch control culture using XMEM, it was found that only a slight improvement in the f5MEM/control culture on cell growth (from 3.8 to $5.5x10^6$ total cells/ml) and MAb production (from 125 to 170 mg/L). This is an indication that nutrient enrichment alone can not markedly improve cell culture performance unless there is a way to remove inhibitory cellular wastes.

In the f5MEM/electrokinetic culture, an electric current density of 70 A/m^2 was applied, and both glutamine and glucose were repeatedly

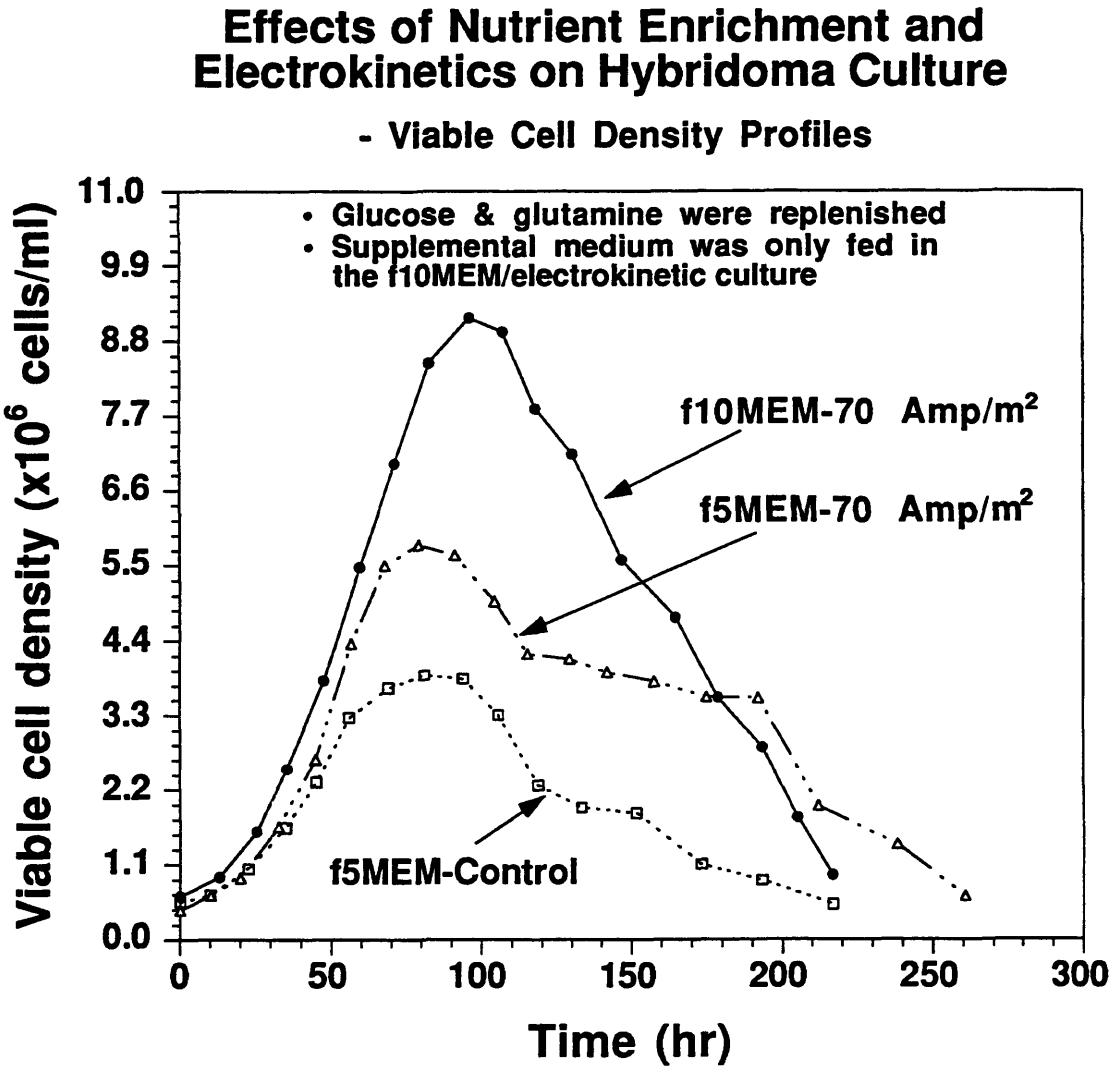

Figure-4.37: Viable cell density profiles of the cultures using enriched media: f5MEM and f10MEM.

~ The control culture was conducted in the absence of DC electric fields and the electrokinetic culture was subjected to 70 Amp/m^2 of DC current density.

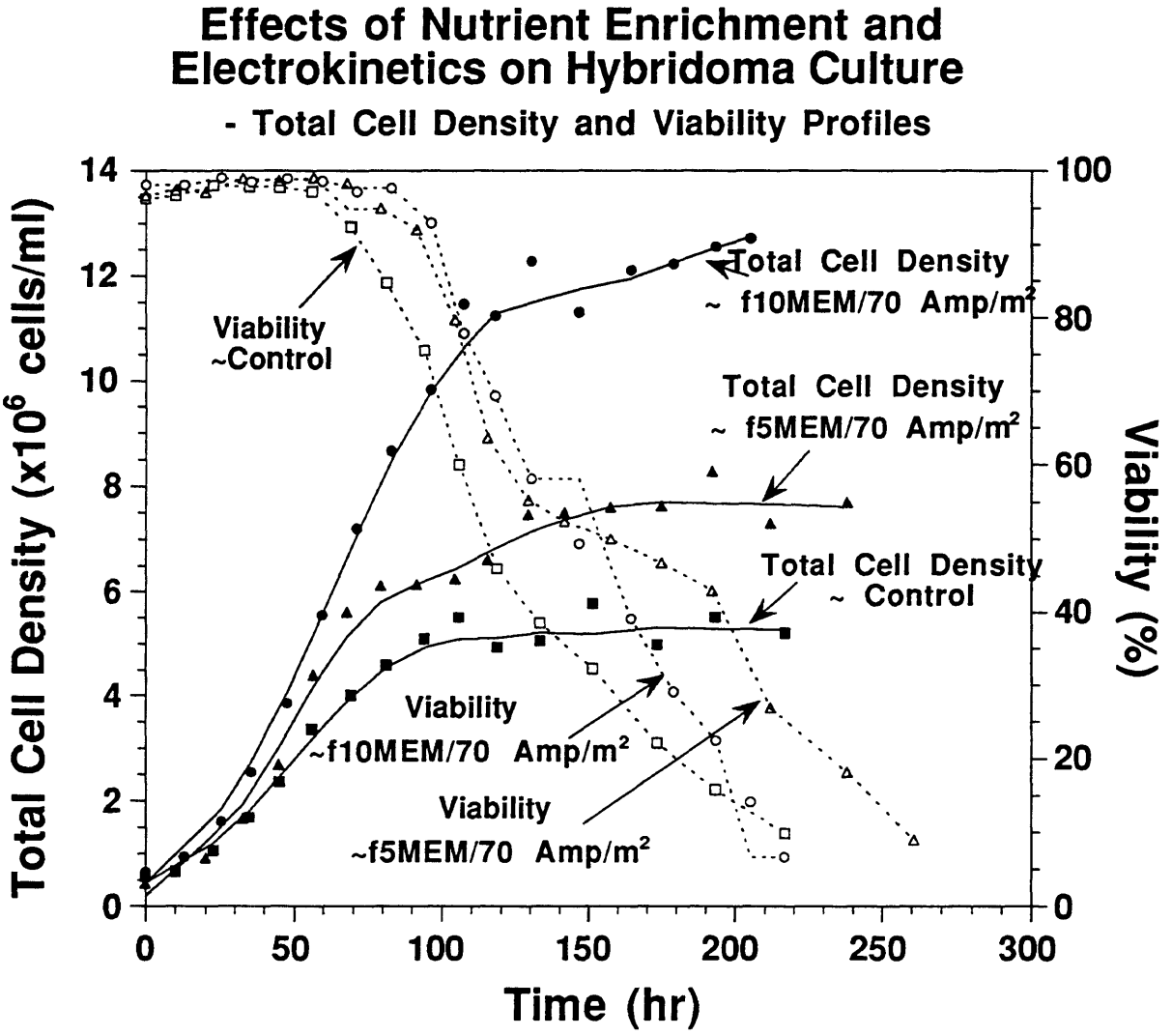

Figure-4.38: Total cell density and viability profiles of the fed-batc cultures using enriched media: f5MEM and f10MEM.

~ The control culture was conducted in the absence of DC electric fields and the electrokinetic culture was subjected to 70 Amp/m^2 of DC current density.

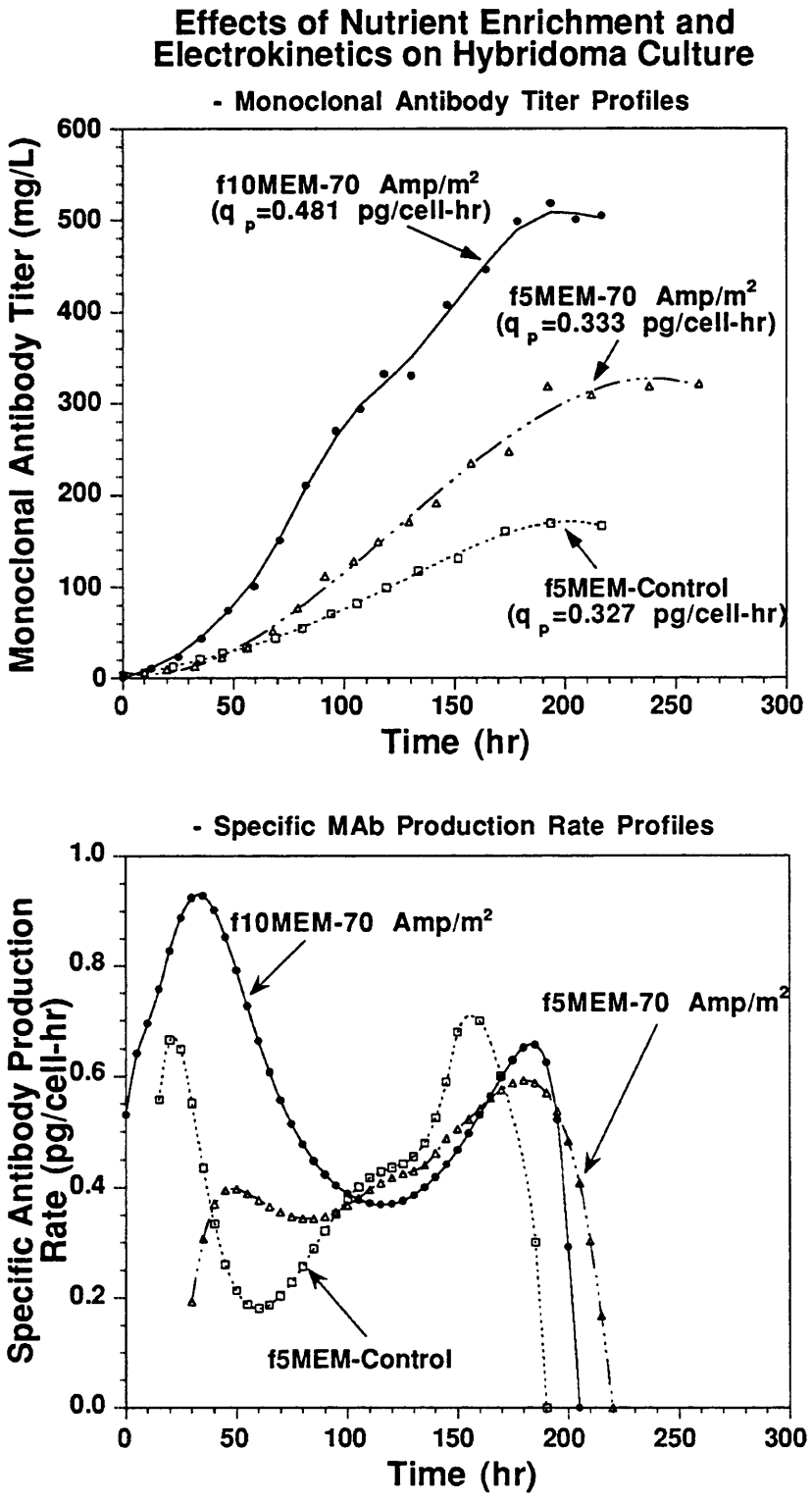

Figure-4.39: MAb titer and Specific MAb production rate profiles of fed-batch cultures using the enriched media: f5MEM and f10MEM.

~ The control culture was conducted in the absence of DC electric fields and the electrokinetic culture was subjected to 70 Amp/m^2 of DC current density.

replenished. The maximum viable cell density, final total cell density and final MAb titer were increased by 50% (from 3.9 to 5.8x10^6 viable cells/ml), 38% (from 5.5 to 7.6x10^6 total cells/ml) and 90% (from 170 to 320 mg/L) respectively, compared to those in the f5MEM/control culture. The greater increase in MAb production compared to the increase in maximum viable cell density is due to the longer cell longevity and the decreased death rate in the f5MEM/electrokinetic culture. The overall average specific MAb production rates were the same at approximately 0.33 pg/cell-hr in both the f5MEM/control and the f5MEM/electrokinetic cultures. This means that the applied electric field of 70 A/m^2 had not affect cellular functionalities.

An electric current density of 70 A/m^2 was applied to the f10MEM/electrokinetic culture in which all amino acids, vitamins, and glucose were periodically replenished by feeding the supplemental medium, glutamine and glucose stock solutions. The maximum viable cell density, final total cell density and final MAb titer achieved were 9.1x10^6 viable-cells/ml, 1.25x10^7 total-cells/ml and 505 mg/L respectively, and these values are about two-fold higher than those in the f5MEM/control culture. The cell longevity in the f10MEM/electrokinetic culture remained approximately the same as that in the f5MEM/control culture. In contrast, cell growth observed in fed-batch cultures where no removal of cellular wastes was employed, the cell longevity is generally prolonged but the maximum viable cell density remains the same despite of nutrient replenishment and/or enrichment. These toxic products prohibited the increase in maximum viable cell density in the fed-batch cultures and accumulated cellular wastes limited cell proliferation. The specific antibody production rate of the f10MEM/electrokinetic culture was 0.48 pg/cell-hr, which is 40% higher than that of the f5MEM cultures. This is

probably due to the higher concentrations of nutrients, especially amino acids (Duval *et al.*, 1991) in the f10MEM formula, and a higher osmolarity (300 mOsm/Kg) in the f10MEM formula than in the f5MEM formula (280 mOsm/Kg) (Oh *et al.*, 1993).

The numerical integration of viable cell densities versus time was performed to provide the "viable-cell-indices" which have the units of viable-cells-hr/ml. This viable-cell-index indicates the length of time and the quantity of the viable cells are present during cultivation which produce primary and secondary metabolites. This index is an indicator on the performance of the culture. The viable-cell-indices of the f5MEM/control, f5MEM/electrokinetic and f10MEM/electrokinetic cultures are calculated to be 4.4×10^8, 8.2×10^8 and 10.5×10^8 viable-cells-hr/ml respectively. While only a 33% increase in the viable-cell-indices, it was observed a 60% increase in total MAb production in the f10MEM/electrokinetic culture compared to those in the f5MEM/electrokinetic culture. This difference can be attributed to the enhanced specific MAb production rate in the f10MEM/electrokinetic culture.

The time profiles of the specific MAb production rates, q_p, of the three cultures are shown in Figure-4.39. The enhanced q_p of the f10MEM/electrokinetic culture occurred mainly in the exponential growth phase (i.e., during the first 100-hour cultivation period), and no discernible difference in q_p was observed in the late growth phases as opposed to that in the f5MEM cultures. This indistinguishable q_p in the late growth phase may be due to the occurrence of certain adverse changes in the late growth phase of these three cultures. These adverse changes had masked the possible contribution by the enriched nutrients and a higher osmolarity of f10MEM for enhancing q_p.

One interesting phenomenon worthy of note occurred in the declining growth phase of the f5MEM/electrokinetic culture. This is shown in the viable cell density and viability profiles of Figure-4.37 and -4.38. The cells in both the f5MEM/control and the f10MEM/electrokinetic cultures decreased in their viability during the declining growth phase at a fairly constant rate; hence the viability decreased to less than 10% viable after 220 hours of cultivation. The cells in f5MEM/electrokinetic culture, however, retained their viability at approximately 50% without a significant reduction for more than 45 hours in the early declining growth phase (during the period between 130 and 175 hours of cultivation). This point requires in-depth discussion and will be presented in a later section on the analysis of nutrient metabolism. This prolonged period of constant cell viability of the cells in the f5MEM/electrokinetic culture significantly increased the cell longevity and the viable-cell-index by 18% (from 220 to 260 hours) and by 86% (from 4.4 to 8.2×10^8 viable-cells-hr/ml) respectively, compared to those in the f5MEM/control culture.

IV.4.2.2 Nutrient Consumption and Cellular Waste Production

In order to rationalize the marked increases in both cell growth and MAb production in the electrokinetic cultures, an analysis on the consumption of various nutrients, including glucose, glutamine and amino acids as well as the production of cellular wastes, such as lactate and ammonia, was conducted.

Glutamine Consumption and Ammonia Production

The profiles for the accumulated glutamine consumption are shown in Figure-4.40. Glutamine concentration was maintained between 2 to 7 mM in all three cultures through the periodic feeding of a 200 mM

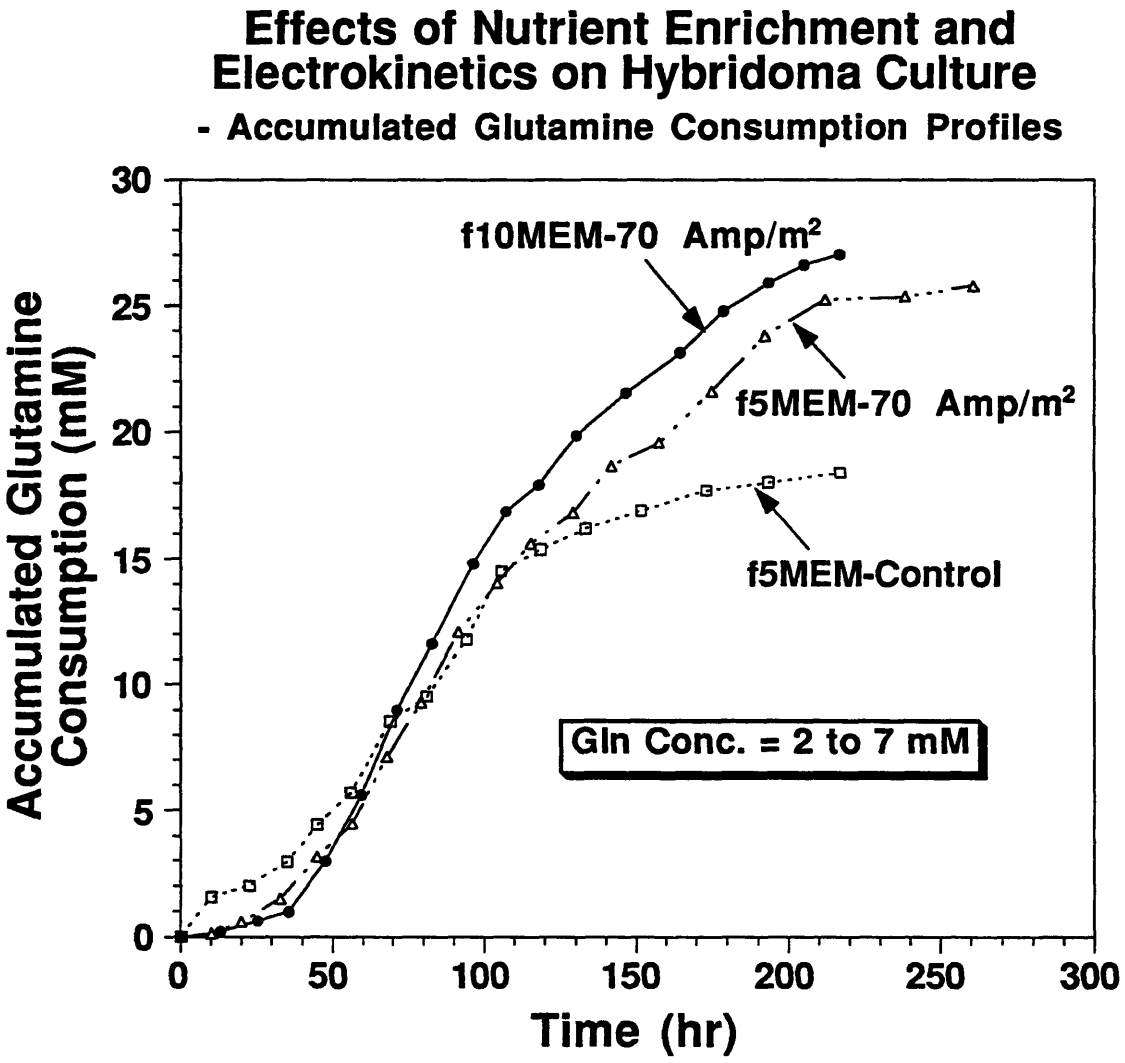

Figure-4.40: Accumulated glutamine consumption profiles of the fed-batch cultures using enriched media: f5MEM and f10MEM.

~ The control culture was conducted in the absence of DC electric fields and the electrokinetic culture was subjected to 70 Amp/m^2 of DC current density.

glutamine stock solution. The total consumption of glutamine in the f5MEM/electrokinetic culture was 25.8 mM compared to 18.4 mM in the f5MEM/control culture. There was no significant difference in total glutamine consumption between the electrokinetic cultures using f5MEM (25.8 mM) and f10MEM (27.1 mM) media. The large decrease in the volumetric glutamine consumption rate occurred during the declining growth phase of the f5MEM/control culture, but remained fairly high during the declining growth phase of the two electrokinetic cultures. This is due to presence of much fewer viable cells in the f5MEM/control culture. The overall average specific glutamine consumption rates, q_{gln}, were found to be 0.042, 0.031 and 0.026 pmol/cell-hr for the f5MEM/control, the f5MEM/electrokinetic and the f10MEM/electrokinetic cultures respectively. The causes of the variations in overall q_{gln} will be discussed later through the theoretical analysis. The q_{gln} decreased monotonously as culture progressed in each of these three cultures. This monotonous decrease in q_{gln} may be attributed to the less active metabolic functionalities of the cells at the later stages of cell growth.

A theoretical analysis, detailed in Appendix-II, was conducted in order to rationalize glutamine consumption in these three cultures. It was assumed that glutamine utilization was involved in the non-enzymatic self-degradation and the syntheses of cell mass (including intracellular proteins and nucleotides) and antibodies. Glutamine consumption through the glutaminolytic pathway was neglected. The non-enzymatic self-degradation of glutamine was calculated to account for 4.2 to 5.0 mM, and the glutamine demand for the syntheses of cell mass and antibodies was calculated to range from 1.5 to 3.4 mM in these three cultures. Hence, the total glutamine demand was calculated to range from 5.7 to 7.7 mM in these three cultures. In comparison with experimental glutamine

consumption (ranging from 18.4 to 27.1 mM), it was found that more than 70% of the total glutamine (ranging from 12.7 to 19.3 mM) was consumed through metabolism other than glutamine self-degradation and cell mass and antibody synthesis requirement. The most possible pathway is believed to be the glutaminolytic pathway.

Glutamine was present at high concentrations (2 to 7 mM) during cultivation, and this high concentration of glutamine can drive the glutamine conversion first to glutamate and then to α-ketoglutarate through the glutaminolytic pathway. α-ketoglutarate can directly enter the TCA cycle for either energy (ATP) production or formation of amino acid precursors which eventually leads to formation of pyruvate (Zupke, 1993). Evidences supporting the above arguments will be the reduced consumption, or even formation, of the non-essential amino acids such as glutamate, aspartate, asparagine and alanine. These were found to be true and will be discussed later in the later section on the analysis of amino acid consumption. Since the role of the glutaminolytic pathway for production of energy and amino acid precursors can mostly be replaced by the glycolytic pathway, it is therefore a non-obligatory metabolism. We can reduce the overflow of glutamine metabolism through the glutaminolytic pathway by manipulating the environment of the culture. For example, the glutaminolytic metabolism can be largely reduced if the fed-batch cultures were operated in a glutamine-limited condition. Although there was a difference in glutamine demand for cell mass and antibody syntheses between the two electrokinetic cultures, this difference was masked by the glutamine metabolism overflow and thus we did not observe a discernible difference in total glutamine consumption, i.e., 25.8 and 27.1 mM respectively, in the two electrokinetic cultures.

Glutamine concentration profiles were similar in the three cultures

(maintained between 2 to 7 mM), and the similarity of glutamine concentration profiles suggested the amounts of the non-enzymatic glutamine degradation were the same for the three cultures. Since q_{gln} through the glutaminolytic pathway was the lowest (0.018 pmol/cell-hr) in the f10MEM/electrokinetic culture and the highest (0.029 pmol/cell-hr) in the f5MEM/control culture, it seems that the non-obligatory glutamine metabolism overflow through the glutaminolytic pathway was primarily due to the presence of glutamine and other nutrients, while less relevant to the presence of the viable cells. These two outcomes resulted in a lower q_{gln} in the culture with the highest viable-cell-index. As a result, the f10MEM/electrokinetic culture, which has the highest viable-cell index, possesses the lowest overall q_{gln}.

The ammonia concentration profiles are shown in Figure-4.41. Since only the ammonia concentration in the f5MEM/control culture remained unchanged by electrokinetics, the following analysis was conducted based only on the results of the f5MEM/control culture. In the f5MEM/control culture, 11.8 mM of glutamine was consumed and 7.2 mM of ammonia was produced during the initial 100-hour cultivation period (including the exponential and the stationary growth phases). In the subsequent 120 hours of cultivation (the declining growth phase), less than 2.0 mM ammonia was produced even though 6.6 mM glutamine was further consumed. This monotonous decrease in the yield of ammonia from glutamine (from 0.61 to 0.24 mol-ammonia/mol-glutamine) as the culture progressed was probably due to the incorporation of ammonia into metabolic intermediates, such as α-ketoglutarate (the major one) and glutamate. The incorporation of ammonia into metabolic intermediates reduces ammonia concentrations in the culture medium and the apparent yield of glutamine to ammonia. The high accumulation of ammonia during

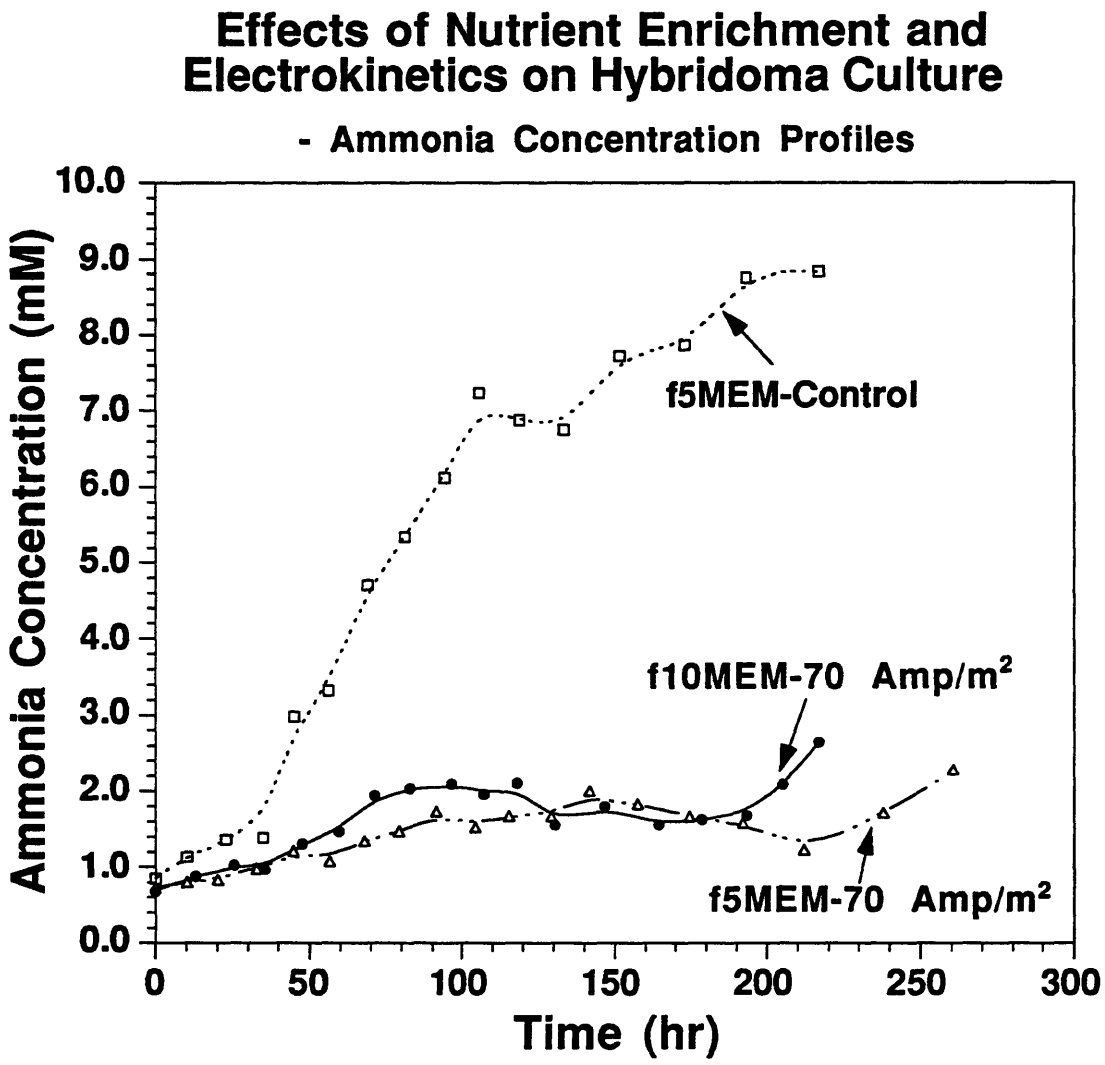

Figure-4.41: Ammonia concentration profiles of the fed-batch cultures using enriched media: f5MEM and f10MEM.

~ The control culture was conducted in the absence of DC electric fields and the electrokinetic culture was subjected to 70 Amp/m^2 of DC current density.

the early stage of cultivation could drive α-ketoglutarate to react with ammonia to produce glutamate. Glutamate can incorporate another ammonia molecule to produce glutamine. This hypothesis is supported by our previous ammonia-adaptation experiment described in Section-IV.3.1.2. In addition, the specific ammonia production rate, q_{NH3}, monotonously decreased as the culture progressed. This was probably due to the less active metabolism by the cells at the later stage of growth and consumption of ammonia through the ammonia-incorporating reactions. The overall q_{NH3}, was calculated to be 0.018 pmol/cell-hr in the f5MEM/control culture, which is similar to the q_{NH3} of 0.05 pmol/cell-hr in a glutamine/glucose fed-batch culture using DMEM (Lindell, 1992) and the q_{NH3} of 0.005 pmol/cell-hr in a fed-batch culture using a stoichiometrically-designed medium (Xie, 1993) and the same hybridoma cells, CRL-1606. The excess production of ammonia at the early stage of the f5MEM/control culture caused a severe accumulation of ammonia, which completely hindered cell growth and markedly reduced cell viability.

The ammonia produced in the electrokinetic cultures using f5MEM and f10MEM, on the other hand, was effectively removed and its concentration was remained below 2.0 mM. The successful removal of ammonia through electrokinetics was the key factor responsible for the marked improvement on cell growth and productivity in these electrokinetic cultures. A summary of the theoretical and experimental analyses of glutamine consumption and ammonia production can be found in Table-4.8.

Glucose Consumption and Lactate Production

The profiles of the accumulated glucose consumption are shown in

Table-4.8: Analysis of metabolism of glucose, lactate, glutamine and ammonia

Glucose (mM)

		f5MEM ~Control	f5MEM ~Electrokinetic	f10MEM ~Electrokinetic	f10MEM-Elec.K (Na Byturate)	Xie (1993)
Calculation	Energy Prod.	22.7	41.4	54.4	40.7	
	Cell Mass Synth.	8.0	11.0	18.1	13.1	
	Total Requirement	**30.6**	**52.4**	**72.6**	**53.7**	
Experiment	Total Requirement	**66.8**	**92.1**	**163.0**	**96.0**	**30~70**
	Over-consumption	36.2	39.7	90.5	42.3	
	Yield*	0.082	0.083	0.077	0.094	0.3~0.48

* The yield (x1E9 cells/mmole) represents the yield of glucose to cell mass

Glutamine (mM)

		f5MEM ~Control	f5MEM ~Electrokinetic	f10MEM ~Electrokinetic	f10MEM-Elec.K (Na Byturate)	Xie (1993)
Calculation	Self-degradation	4.2	5.0	4.2	4.4	
	Cell Mass+Protein	1.5	2.1	3.4	2.6	
	Total Requirement	**5.7**	**7.1**	**7.7**	**7.0**	
Experiment	Total Requirement	**18.4**	**25.8**	**27.0**	**23.0**	**14~18**
	Over-consumption	12.7	18.7	19.3	16.0	
	Yield*	0.30	0.29	0.46	0.39	

* The yield (x1E9 cells/mmole) represents the yield of glutamine to cell mass

Specific Consumption and Production Rates (Experiment)

		f5MEM ~Control	f5MEM ~Electrokinetic	f10MEM ~Electrokinetic	f10MEM-Elec.K (Na Byturate)	Xie (1993)
Viable Cell Inde	10^8 cells-hr/ml	4.40	8.20	10.60	8.18	
Glucose	pmole/cell-hr	0.15	0.11	0.16	0.12	
Lactate	pmole/cell-hr	0.20	N/A	N/A	N/A	0.048
Glutamine	pmole/cell-hr	0.042	0.031	0.026	0.028	
Ammonia	pmole/cell-hr	0.018	N/A	N/A	N/A	0.005

Figure-4.42. Glucose concentration was maintained between 10 to 30 mM in these three cultures through the periodic feeding of a 1.0 M glucose stock solution. The total glucose demands were calculated to be 67, 92 and 163 mM, respectively, in the f5MEM/control, the f5MEM/electrokinetic and the f10MEM/electrokinetic cultures. There were considerable increases in the total glucose demands of the electrokinetic cultures, especially in the f10MEM/electrokinetic culture compared to that in the control culture. If we assume that the specific glucose consumption rate, q_{glc}, is the same in the three cultures, the total glucose demands would then be proportional to the viable-cell indices, i.e., the total amounts of glucose consumption should have had a relative ratio of 1.0:1.9:2.5 among the three cultures. However, the experimental ratios of the total glucose demand among these three cultures were found to be 1.0:1.4:2.4. This behavior indicates that the cells in the f5MEM/control and the f10MEM/electrokinetic cultures metabolized glucose at a similar q_{glc} (about 0.15 pmol/cell-hr) while the cells in the f5MEM/electrokinetic culture metabolized glucose at a slower q_{glc} of 0.112 pmol/cell-hr. In each culture, q_{glc} decreased monotonously as culture progressed, which was probably due to the less active metabolism of the cells at the later stages of cell growth.

A theoretical analysis was conducted and detailed in Appendix-II in order to rationalize the glucose consumption. Glucose was assumed to be used only for cell mass synthesis and energy production. Based on this analysis, the respective calculated glucose demands for cell mass (including carbohydrates, lipid and nucleotides) synthesis and for energy production ranged from 8 to 18 mM and from 23 to 55 mM, respectively, in the three cultures. Hence, the total theoretical glucose demands were obtained by adding the above two demands and thus calculated to be 31, 52

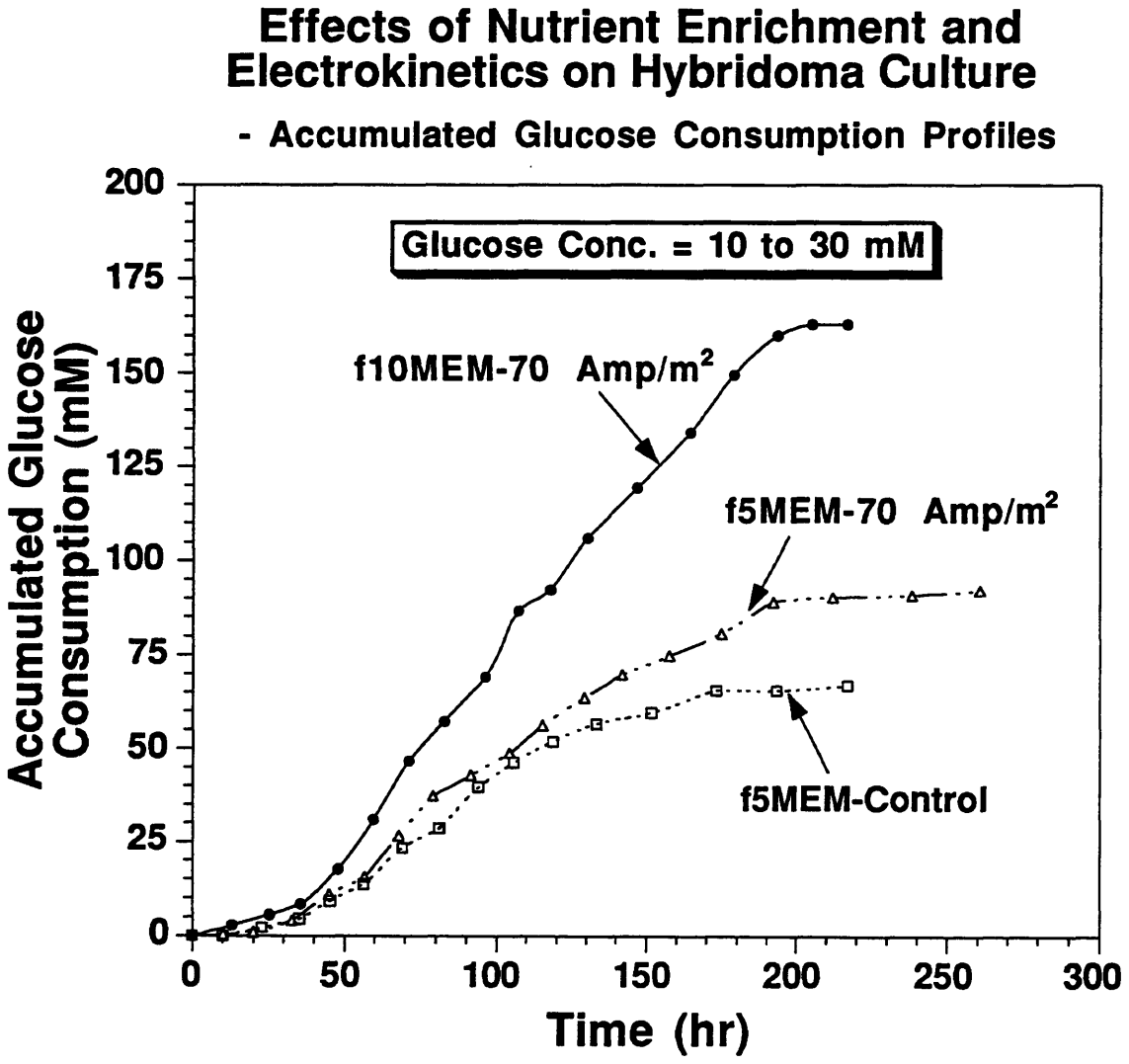

Figure-4.42: Accumulated glucose consumption profiles of the fed-batch cultures using enriched media: f5MEM and f10MEM.
~ The control culture was conducted in the absence of DC electric fields and the electrokinetic culture was subjected to 70 Amp/m^2 of DC current density.

and 73 mM, respectively, for the f5MEM/control, the f5MEM/electrokinetic and the f10MEM/electrokinetic cultures. These calculated values are more than one fold lower than the experimental values (ranging from 67 to 163 mM) listed in the table. These significant differences suggest that overflow metabolism of glucose had occurred in these three cultures. In addition, a hybridoma culture conducted by Xie (1993) showed that only 70 mM glucose was consumed to achieve a final total cell density of $1.4x10^7$ cells/ml, which is similar to the final total cell density of the f10MEM/electrokinetic culture. This experimental comparison further confirms the severe overflow metabolism of glucose in our three cultures.

The lactate concentration profiles are shown in Figure-4.43. Lactate was accumulated to 90 mM in the f5MEM/control culture, while only 30 to 50 mM in the electrokinetic cultures. As described by eq (4.2), the rate of the electrophoretic removal of an ionic solute is proportional to the concentration and to the electrical mobility of the ionic solute. Since lactate possesses an electrical mobility 60% lower than that of ammonium, and is produced at a rate much greater than ammonia, thus the removal of lactate from the culture medium under an electric current of 100 mAmp was incomplete in the electrokinetic cultures. If the yield of glucose to lactate is assumed to be the same in these three cultures, the total lactate produced should be 122 mM for the f5MEM/electrokinetic culture and 217 mM for the f10MEM/electrokinetic culture. When these calculated total lactate concentrations were compared with the concentrations of lactate in the media of the electrokinetic cultures, it was found that more than 75% of the lactate produced have been removed from the electrokinetic cultures. In conclusion, the removal of lactate was fairly effective but not complete in these electrokinetic cultures with the enriched media. The detailed analyses of glucose consumption and lactate production are

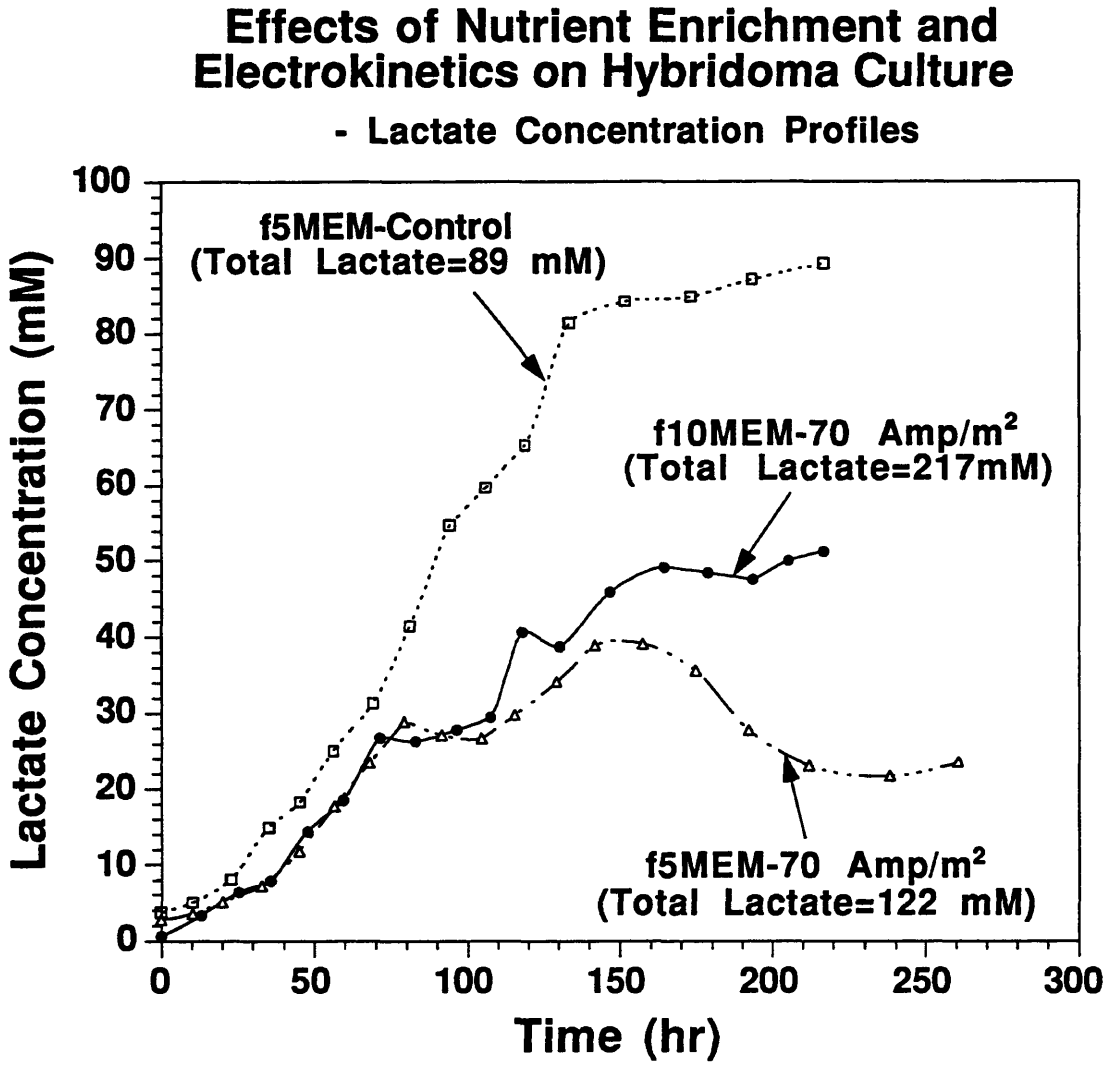

Figure-4.43: Lactate concentration profiles of the fed-batch cultures using enriched media: f5MEM and f10MEM.

~ The control culture was conducted in the absence of DC electric fields and the electrokinetic culture was subjected to 70 Amp/m^2 of DC current density.

summarized in Table-4.8.

Electrokinetics can only replace lactate ions with other ionic solutes but is unable to change the total concentration of ionic solutes. The changes in osmolarity due to excess production of lactate, therefore, could not be altered by electrokinetics. Osmolarity profiles of these three cultures are shown in Figure-4.44. In the f5MEM/control, the f5MEM/electrokinetic, and the electrokinetic/f10MEM cultures, osmolarity increased from 280 to 380, from 280 to 330 and from 300 to 390 mOsm/kg respectively. Even though 30 to 50 mM of lactate, based on the earlier study of the lactate toxicity in Section-IV.3.1.1, should not be severely toxic to cells, the marked changes in osmolarity induced by excess production of the lactate could severely damage cells and reduce culture longevity. It is believed that the marked increase in osmolarity is one of the major causes of cell death in our culture experiments. It is noteworthy that the osmolarity increase is much less in the f5MEM/electrokinetic culture than in the other two cultures. This will be discussed later in the section on amino acid analysis.

Lactate concentration remained unchanged only in the f5MEM/control culture, and we therefore analyzed the lactate production in this culture. The overall specific lactate production rate, q_{lac}, was calculated to be 0.20 pmol/cell-hr in the f5MEM/control culture. It was found that in the glutamine/glucose fed-batch cultures using DMEM (Lindell, 1992), the q_{lac} ranged from 0.076 to 0.14 pmol/cell-hr, and in a fed-batch culture using a stoichiometrically-designed medium (Xie, 1993), the q_{lac} was 0.048 pmol/cell-hr. In our experiment, it was found that f5MEM resulted in a much higher q_{lac} than the less rich DMEM and the stoichiometrically-designed medium. In the f5MEM/control culture, the q_{lac} monotonously decreased as the culture progressed. This was probably

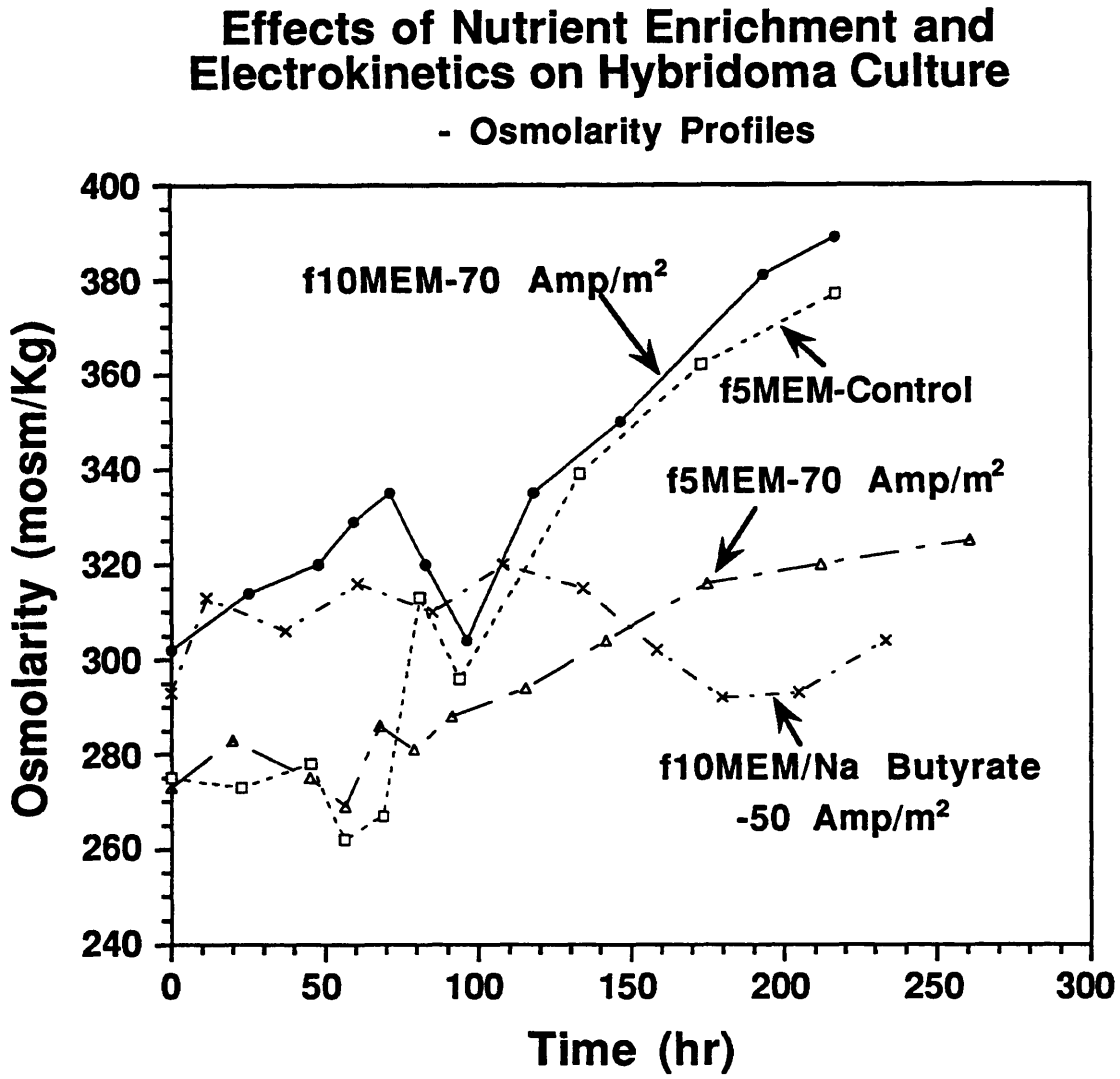

Figure-4.44: Osmolarity profiles of the fed-batch cultures using enriched media: f5MEM and f10MEM.

~ The control culture was conducted in the absence of DC electric fields and the electrokinetic culture was subjected to 70 Amp/m^2 of DC current density.

due to less active metabolism of the cells at the later stages of cell growth. The overall yield of glucose to lactate was calculated to be 1.33 mol-lactate/mol-glucose in the f5MEM/control culture, which is a typical value in most of the cultures using medium such as DMEM.

Consumption of Various Amino Acids

The consumption of various amino acids was analyzed. Proline, cysteine and histidine could not be determined by the amino acid HPLC protocol which we currently used and hence are not analyzed. The peaks of arginine and threonine can not be resolved on the HPLC histogram, and neither could the peaks of valine and tryptophan. The combined concentrations of these two sets of overlapped amino acids were therefore presented collectively. Both glucose and glutamine were replenished in all three cultures, but supplemental medium was only fed in the f10MEM/electrokinetic culture.

The concentration profiles and total consumption of various amino acids are shown in Figure-4.45 and Table-4.9, respectively. In the f5MEM/control culture, none of the amino acids was completely consumed, while in the f5MEM/electrokinetic culture, methionine was exhausted after 120 hours of cultivation, and aspartate was completely consumed during the period between 25 and 120 hours of cultivation. The other amino acids were not consumed totally. These depletion can be attributed to the enhanced cell growth and the absence of supplemental medium feeding in the f5MEM/electrokinetic culture. Since methionine is an essential amino acid, its depletion was critical and could limit cell growth. In the f10MEM/electrokinetic culture, the amino acid concentrations at any time during the cultivation were one fold higher than those in the two f5MEM cultures, and therefore no amino acid was limiting in this culture.

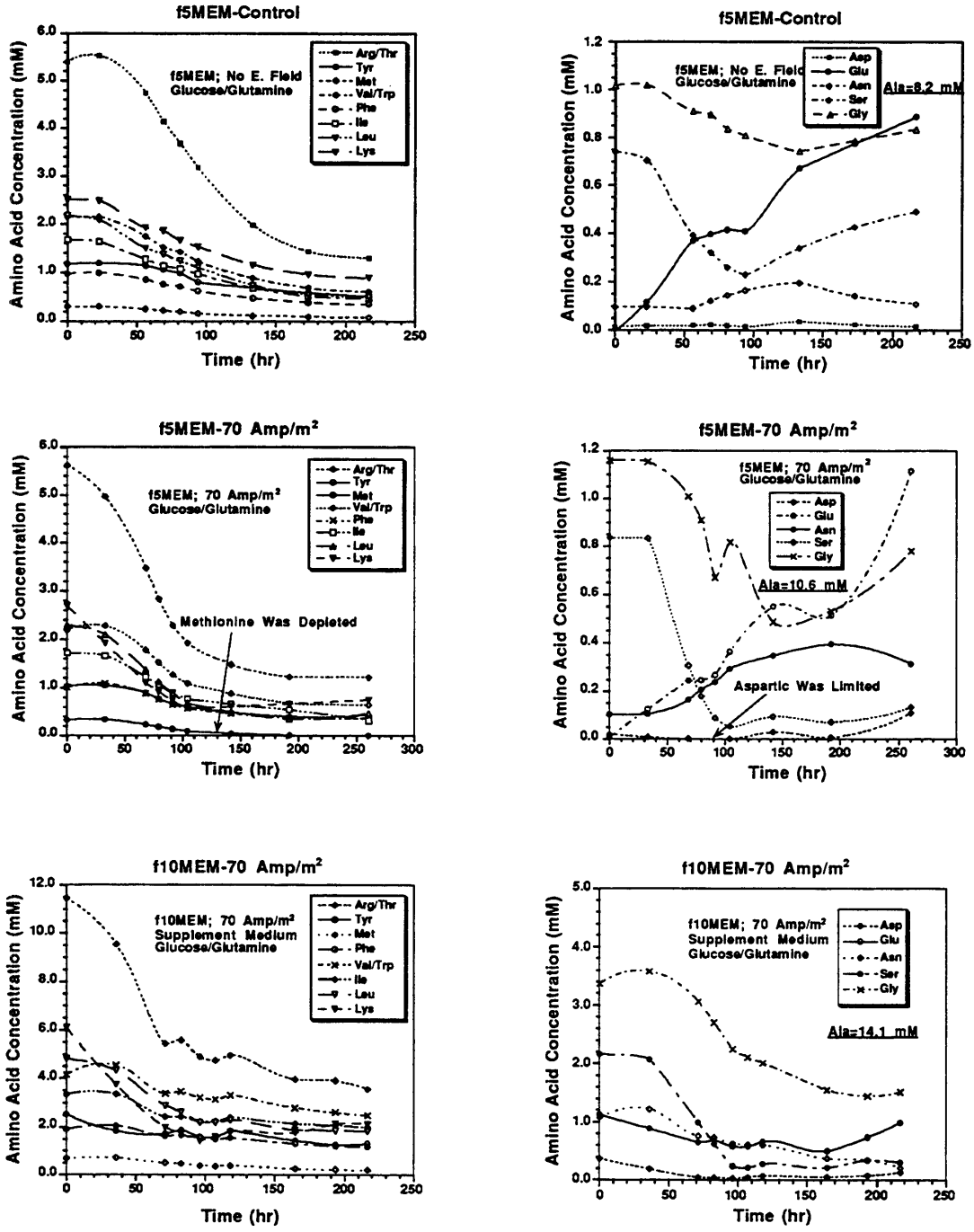

Figure-4.45: The concentration profiles of amino acids for the cultures using enriched media and electrokinetics.

Table-4.9: Summary of the experimental total demands of various amino acids

	f5MEM ~Control	f5MEM ~Electrokinetics	f10MEM ~Electrokinetics	f10MEM Elec.K.(Na Buty.)	Xie (1993)*
Essential Amino Acids			(mM)		
Arg/Thr	4.56	4.99	12.27	9.66	4.17
Ile	1.40	1.65	3.10	2.86	1.84
Leu	1.86	2.06	4.76	3.89	3.10
lys	1.80	2.19	5.76	6.26	2.93
Met	0.28	0.38	0.92	0.72	0.82
Phe	0.71	0.76	1.61	1.49	1.17
Val/Trp	1.77	1.83	3.66	3.09	2.80
Tyr	0.76	0.73	2.10	1.58	1.06
Non-Ess. Aminoi Acids			(mM)		
Ala	-7.72	-10.10	-12.25	-12.60	-5.72
Asn	0.0019	-0.20	1.35	1.23	1.09
Asp	-0.001	0.013	0.41	0.31	3.64
Glu	-0.88	-1.1	0.57	0.03	-0.76
Gly	0.28	0.5	5.82	4.33	1.95
Ser	0.34	0.82	5.82	5.24	1.48

"Negative Sign" stands for production

* The final total cell density was 1.4x10^7 cells/ml in Xie's experiment (1993)

† This calculation did not include the A.A. requirement for the synthesis of secreted proteins other than of antibody

This was due to the higher initial amino acid concentrations in the f10MEM formula and the feeding of the supplemental medium. The presence of higher concentrations of the amino acids and a higher initial medium osmolarity (7% higher) in the f10MEM formula than in the f5MEM formula explain the higher specific MAb production rate in the f10MEM/electrokinetic culture.

The apparent yields of various amino acids to cell mass are summarized in Table-4.10. We also calculated the theoretical yields based on the approach developed by Xie (1993) as described in Appendix-II. The experimental results from Xie (1993) are also listed in this table for comparison. We examined first the yields of essential amino acids to cell mass. The yields of essential amino acids to cell mass were the highest in the f5MEM/electrokinetic culture and the lowest in the f10MEM/electrokinetic culture, although the yield of each essential amino acid to cell mass differed by less than 20% among these three cultures. When we compared our experimental yields with those by Xie (1993), it was found that our experimental yields are 50 to 100% lower than Xie's amino acid yields. When we further compared our experimental yields with the calculated values in each culture, the experimental yields are more than one to two fold lower than those calculated values. The differences between the experimental and the theoretical yields are partially caused by under-estimation in the calculated values. This under-estimation can be attributed to the specificity of our cell line (since the theoretical analyses are conducted based on an average composition of the cell mass and protein for mammalian cells), and to neglecting the essential amino acid consumption for the non-obligatory energy production and the synthesis of the non-essential amino acids. The relative differences among the experimental yields were similar to the

Table-4.10: Analysis of the experimental and theoretical yield of the essential amino acid to cell mass and to antibody

Apparent Yield of Amino Acid to Cell Mass

Essential Amino Acid	f5MEM-Control		f5MEM-Elec.K.		f10MEM-Elect.K.		f10MEM-Elec.K.(Na Buty.)		Xie(1993)*
	Expt.	Theo.*	Expt.	Theo.*	Expt.	Theo.*	Expt.	Theo.*	Expt.
	Yield (x10^9 cells/mmole)								
Arg/Thr	1.2	6.2	1.5	5.8	1.0	5.8	0.9	5.0	3.4
Ile	3.9	14.5	4.6	13.6	4.0	13.7	3.1	11.8	7.6
Leu	3.0	8.8	3.7	8.3	2.6	8.4	2.3	7.2	4.5
lys	3.1	9.5	3.5	8.9	2.2	9.0	1.4	7.7	4.8
Met	20.0	38.8	19.8	36.4	13.6	36.7	12.5	31.6	17.1
Phe	7.7	18.9	10.0	17.7	7.8	17.9	6.0	15.4	12.0
Val/Trp	3.1	8.2	4.2	7.7	3.4	7.8	2.9	6.7	5.0
Tyr	7.2	18.9	10.5	17.7	6.0	17.9	5.7	15.4	13.2

Apparent Yield of Amino Acid to Antibody

Essential Amino Acid	f5MEM-Control		f5MEM-Elec.K.		f10MEM-Elect.K.		f10MEM-Elec.K.(Na Buty.)		Xie(1993)*
	Expt.	Theo.*	Expt.	Theo.*	Expt.	Theo.*	Expt.	Theo.*	Expt.
	Yield (x10^2 g/mol)								
Arg/Thr	0.4	1.9	0.6	2.4	0.4	2.4	0.6	3.5	1.3
Ile	1.2	4.5	1.9	5.7	1.6	5.5	2.2	8.1	3.0
Leu	0.9	2.7	1.6	3.5	1.1	3.4	1.6	5.0	1.8
lys	0.9	2.9	1.5	3.7	0.9	3.6	1.0	5.3	1.9
Met	6.2	12.0	8.4	15.3	5.5	14.8	8.6	21.8	6.8
Phe	2.4	5.9	4.2	7.5	3.1	7.2	4.2	10.6	4.8
Val/Trp	1.0	2.5	1.7	3.2	1.4	3.1	2.0	4.6	2.0
Tyr	2.2	5.9	4.4	7.5	2.4	7.2	3.9	10.6	5.3

* This calculation did not include the A.A. requirement for the synthesis of secreted proteins other than antibody

relative differences among those calculated values. For instance, the experimental yields of Leu and Lys to cell mass were both 3.0×10^9 cells/mmol, and the calculated values were both 9.0×10^9 cells/mmol. This qualitative similarity between the experimental and theoretical yields suggested that the methodology adopted in the theoretical analysis is qualitatively accurate for our fed-batch cultures using the enriched media. In conclusion, the comparison suggested that the essential amino acids were metabolized extremely inefficiently in these three cultures. A significant overflow of the amino acid metabolism for syntheses of the cell mass and antibodies occurred in the cultures using the enriched media. Similar results, as shown in Table-4.10, were also observed in the yields of essential amino acids to antibody.

Our experimental yields of non-essential amino acids to cell mass are markedly different from the that calculated theoretically and the experimental values observed by Xie (1993). Some of these non-essential amino acids were actually produced instead of consumed in these three cultures. These significant differences can be attributed to the marked overflow of glutamine metabolism through the glutaminolytic pathway, which resulted in a large production of these non-essential amino acids.

In the previous sections, we have observed lower specific rates of glucose consumption, amino acid consumption and lactate production in the f5MEM/electrokinetic culture. These resulted in a smaller elevation in the medium osmolarity (only increased 14% in the f5MEM/electrokinetic culture as compared to an increase of 36% in the other two cultures) and a slower cell death rate in the declining growth phase of the f5MEM/electrokinetic culture compared to the other two cultures. Since the only difference in nutrient metabolism between the f5MEM/electrokinetic culture and the other two cultures is the depletion

of methionine, we believe that the amino acid depletion in the f5MEM/electrokinetic culture had reduced the overflow of various nutrient metabolism, especially the glucose metabolism, and inhibited cell growth. A similar decrease in glutamine metabolism by limiting glutamine concentration during the culture was also observed by Ljunggren and Haggstrom (1992). These observations suggest that, by limiting the concentration of one of the essential nutrients, such as glucose or glutamine, to a low level without depletion during the culture, the overflow of the nutrient metabolism can be controlled and the production rates of lactate and ammonia in the fed-batch cultures using the enriched media can be reduced. The overproduction of lactate in the cultures using the enriched media causes a significant increase in the medium osmolarity, and this is believed to be the major cause of reduced cell growth or even cell death. The glucose-limited and/or glutamine-limited fed-batch operations in combination with the electrokinetic technique should be able to further enhance cell growth and productivity in the cultures using the enriched culture media. The above results for these fed-batch cultures using the enriched culture media, f5MEM and f10MEM, are summarized in Table-4.11.

IV.4.3 Effects of Sodium Butyrate on Hybridoma Cultures

Sodium butyrate is known as a pharmacological agent that retards cell growth and concomitantly increases protein production (Oh *et al.*, 1993). In the previous fed-batch cultures using the enriched culture media, such as f5MEM and f10MEM, we have observed an overflow metabolism of the nutrients. An excess production of lactate and a large increase in osmolarity also occurred. These adverse changes can be a the major limitation on cell growth and protein production. We therefore

Table-4.11: Summary of effects of nutrient enrichment and electrokinetics on fed-batch, suspension hybridoma cultures

- Glucose and glutamine were replenished in all three cultures
- 70 Amp/m^2 was applied to the electrokinetic culture
- Supplemental medium was fed only in the f10MEM/electrokinetic culture

Kinetic parameters	f5MEM/control culture	f5MEM/electrokinetic culture	f10MEM/electrokinetic culture
Max. viable cell density (cells/ml)	3.9x10^6	5.8x10^6	9.1x10^6
Final total cell density (cells/ml)	5.5x10^6	7.6x10^6	12.5x10^6
Final antibody titer (mg/L)	170	320	505
Specific antibody production rate (pg/cell-hr)	0.33	0.33	0.48
Total glucose consumption (mM)	66.8	92.1	163.0
Final lactate concentration (mM)	89.2	~30.0	~50.0
Total glutamine consumption (mM)	18.4	25.8	27.0
Final ammonia concentration (mM)	8.7	~2.0	~2.0
Possible causes of cell death	• Change of Osmolarity • Ammonia & Lactate accumulation	• Change of Osmolarity • Lactate accumulated • A.A. depletion	• Change of Osmolarity • Lactate accumulation

attempted to use sodium butyrate to decelerate cell growth as well as the metabolic rate of nutrient (especially glucose) and consequently to increase protein production. Through decelerating the glucose metabolism, we could reduce lactate production and osmolarity variation, and hopefully prolong cell longevity.

According to the previous screening studies, a sodium butyrate concentration of 0.7 mM was found to be able to stimulate antibody production of hybridomas, CRL-1606, by the greatest amount without severely affecting cell growth. Hence 0.7 mM sodium butyrate was fed during the middle of the exponential growth phase of the culture (approximately 40 hours after inoculation). After the feeding of sodium butyrate, all inner sets of salt bridges and electrode baths were supplemented with 0.7 mM sodium butyrate as well. f10MEM was used as the culture medium. Supplemental medium, 1.0 M glucose and 200 mM glutamine were periodically fed for nutrient replenishment. An electric current density of 50 A/m^2 was applied in this culture. The previous f10MEM/electrokinetic culture was used as a comparison in order to evaluate the improvement of cell culture performance in the presence of sodium butyrate.

IV.4.3.1 Cell Growth and Monoclonal Antibody Production

The viable and total cell density profiles are shown in Figure-4.46, and the monoclonal antibody (MAb) titer profiles and the specific MAb production rate (q_p) profiles are shown in Figure-4.47. When 0.7 mM sodium butyrate was added, cell growth was immediately retarded and specific growth rate decreased from 0.045 to 0.026 hr^{-1}. When comparing the results obtained in the two f10MEM/electrokinetic cultures, the maximum viable cell density and the final total cell density decreased 25%

Effects of Sodium Butyrate on Hybridoma Cells

- Viable and Total Cell Density Profiles

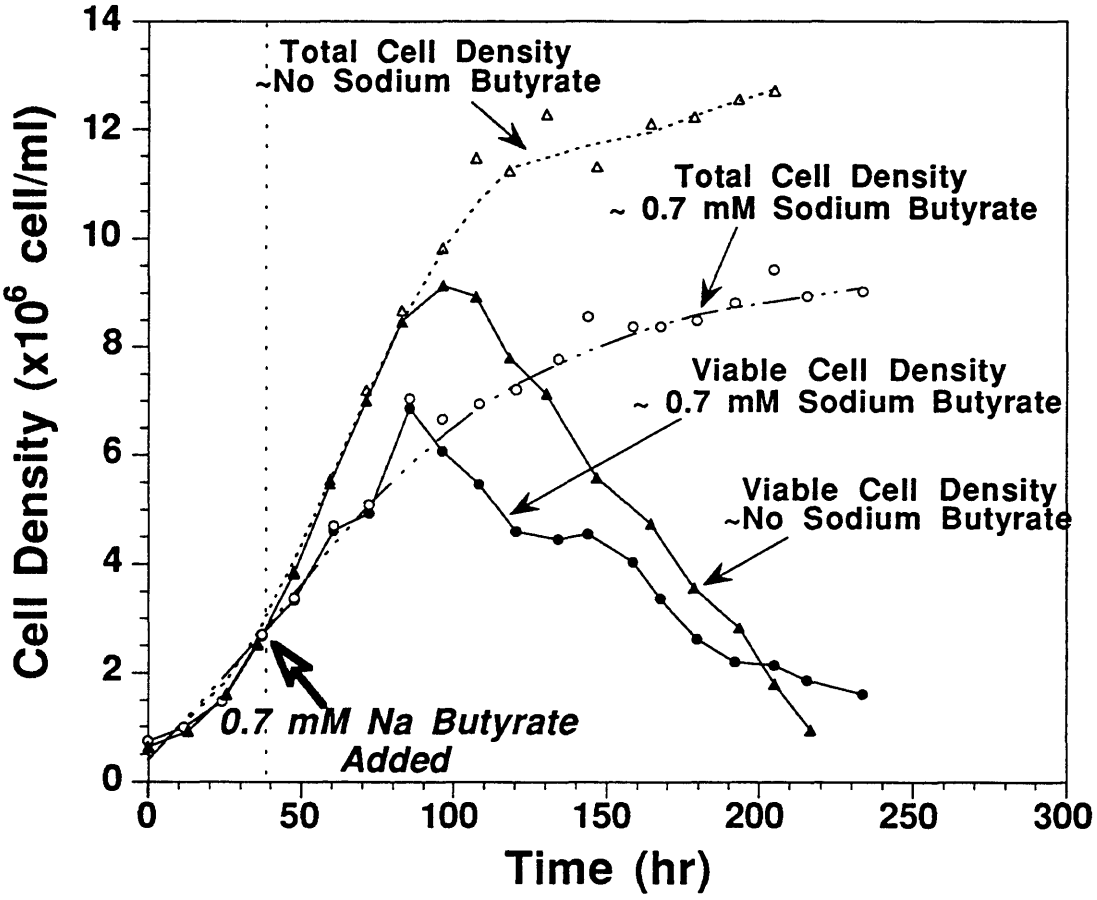

* 50 Amp/m^2 was applied to the sodium-butyrate-added culture, and 70 Amp/m^2 was applied to the sodium-butyrate-free culture.

Figure-4.46: Viable and total cell density profiles of the fed-batch cultures using f10MEM. 0.7 mM sodium butyrate was added during the middle of the exponential growth phase.

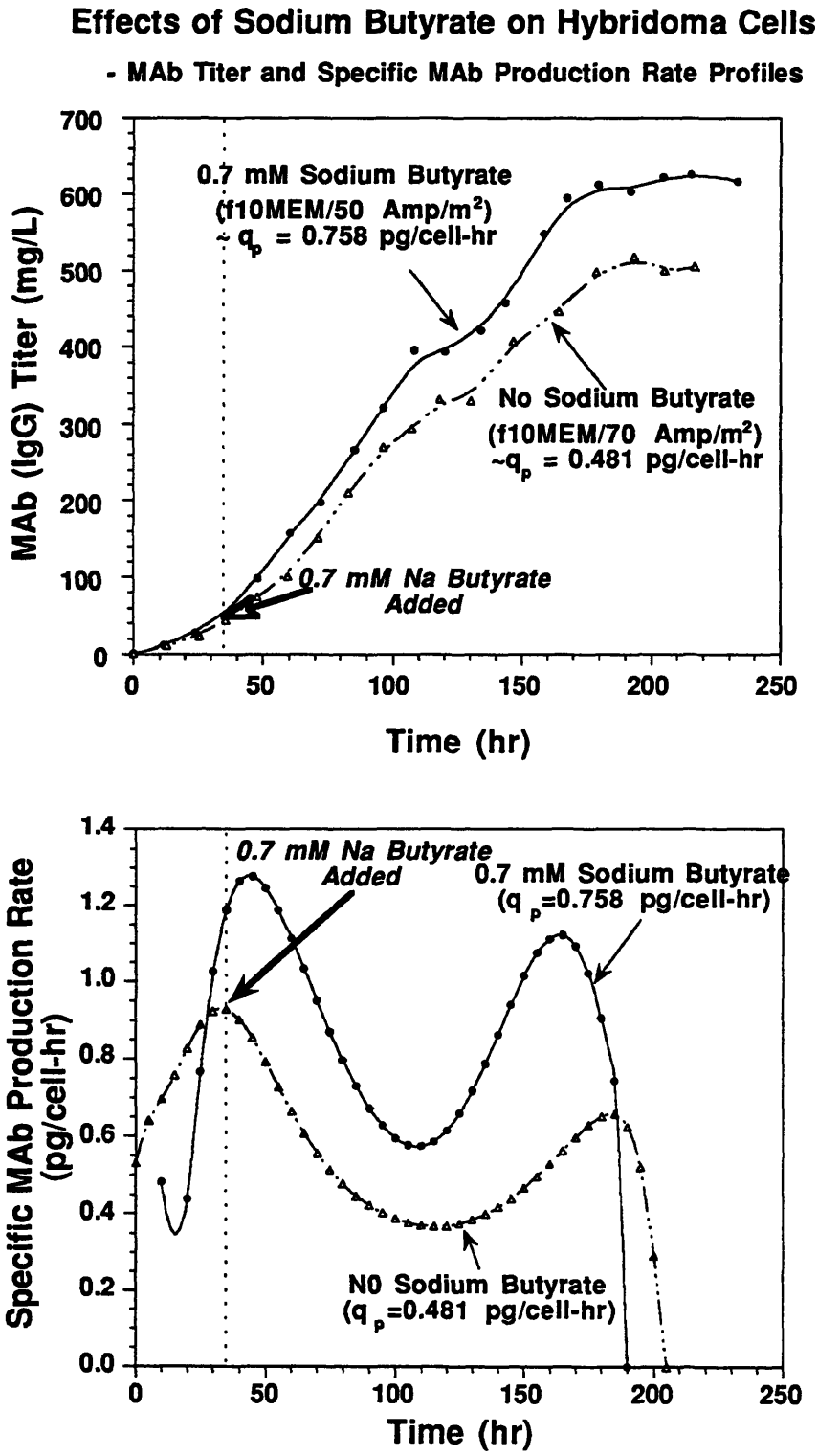

Figure-4.47: MAb titer and specific MAb production rate profiles of the fed-batch cultures using f10MEM. 0.7 mM sodium butyrate was added during the middle of the exponential growth phase.

(from $9.1x10^6$ to $6.9x10^6$ cells/ml) and 29% (from $12.7x10^6$ to $9.0x10^6$ total-cells/ml), respectively, in the presence of sodium butyrate. In both the sodium-butyrate-added and sodium-butyrate-free cultures, however, cells were not able to grow after 120 hours of cultivation. Therefore the culture longevity was approximately the same (220 to 240 hrs) in the two cultures although the viable-cell-index was found to decrease from $10.5x10^8$ to $8.18x10^8$ viable-cells-hr/ml in the presence of sodium butyrate. Overall q_p increased from 0.48 to 0.76 pg/cell-hr in the presence of sodium butyrate, and the increase in q_p occurred throughout the entire culture in the presence of sodium butyrate. Even though the viable-cell-index was decreased by 22%, the increase in q_p (58%) resulted in an increase of the final MAb titer to 620 mg/L in the presence of sodium butyrate.

IV.4.3.2 Nutrient Consumption and Cellular Waste Production

Accumulated glutamine consumption and ammonia concentration profiles are shown in Figure-4.48. Glutamine concentration was maintained between 1.5 and 5.0 mM in the sodium-butyrate-added culture through periodic replenishment. In comparing the two f10MEM/electrokinetic cultures with and without sodium butyrate, it was found that total glutamine demand decreased from 27.1 to 23.2 mM, consumption of glutamine through glutaminolytic pathway decreased from 19.3 to 16.0 mM, and specific glutamine consumption rate, q_{gln}, increased from 0.026 to 0.028 pmol/cell-hr in the presence of sodium butyrate. Hence, sodium butyrate was not able to decelerate the overflow metabolism of glutamine through the glutaminolytic pathway.

Ammonia was effectively removed and its concentration was maintained below 2.0 mM throughout the entire sodium-butyrate-added culture. This effective removal of ammonia accounted for the enhanced

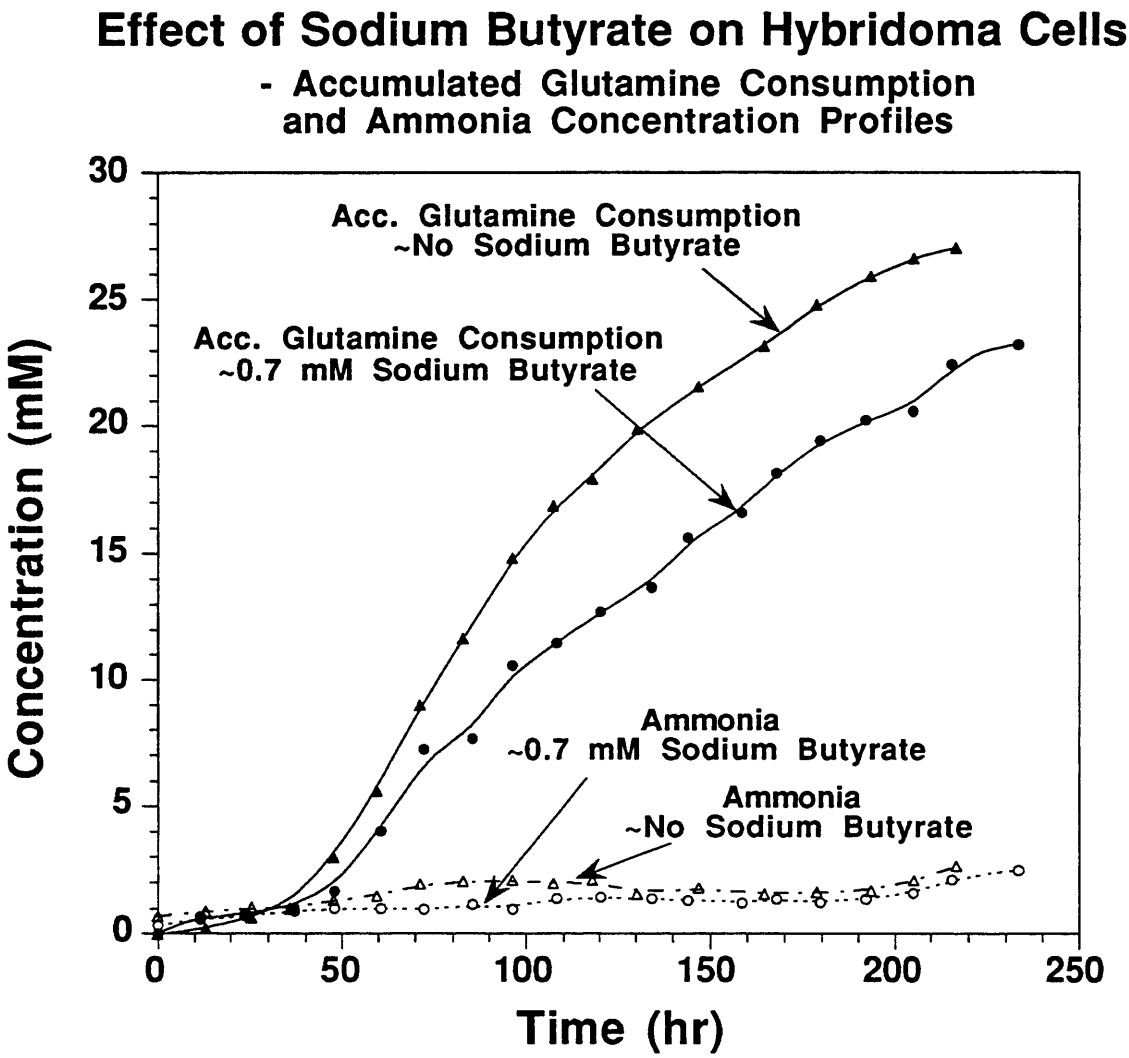

Figure-4.48: Accumulated glutamine consumption and ammonia concentration profiles of the cultures using f10MEM. 0.7 mM sodium butyrate was added during the middle of the exponential growth phase.

cell growth in the sodium-butyrate-added f10MEM/electrokinetic culture, even though the enhancement is not as great as that in the sodium-butyrate-free f10MEM/electrokinetic culture as both were compared with that of the previous f5MEM/control culture.

The total amino acid consumption and the yields of various essential amino acid to cell mass ($Y_{X/E.A.A.}$) and antibody ($Y_{P/E.A.A.}$) were listed earlier in Table-4.9 and -4.10. None of the amino acids was totally consumed. The total demands of various amino acids and the $Y_{X/E.A.A.}$'s are slightly lower, but the $Y_{P/E.A.A.}$'s are higher in the sodium-butyrate-added f10MEM/electrokinetic culture as compared to those in the sodium-butyrate-free f10MEM/electrokinetic culture. This implies that cells apparently used more amino acids for antibody synthesis than for cell mass synthesis in the presence of sodium butyrate. Nevertheless, sodium butyrate did not significantly affect the overflow metabolism of various essential amino acids.

The accumulated glucose consumption and the lactate concentration profiles are shown in Figure-4.49. Glucose concentration was maintained between 5.0 and 25.0 mM in the sodium-butyrate-added culture through periodic replenishment. In comparing the two f10MEM/electrokinetic cultures with and without sodium butyrate, it was found that the total glucose demand decreased from 163 to 96 mM and the specific glucose consumption rate, q_{glc}, decreased from 0.16 to 0.12 pmol/cell-hr in the presence of sodium butyrate. The q_{glc} of 0.12 pmol/cell-hr is similar to the q_{glc} of 0.11 pmol/cell-hr of the previous f5MEM/electrokinetic culture. It can be concluded that 0.7 mM sodium butyrate is able to decelerate glucose metabolism by 25% in the f10MEM/electrokinetic culture, and the influence of sodium butyrate on glucose metabolism is as potent as that of the essential-nutrient-limited

Effect of Sodium Butyrate on Hybridoma Cells

- Accumulated Glucose Consumption and Lactate Concentration Profiles

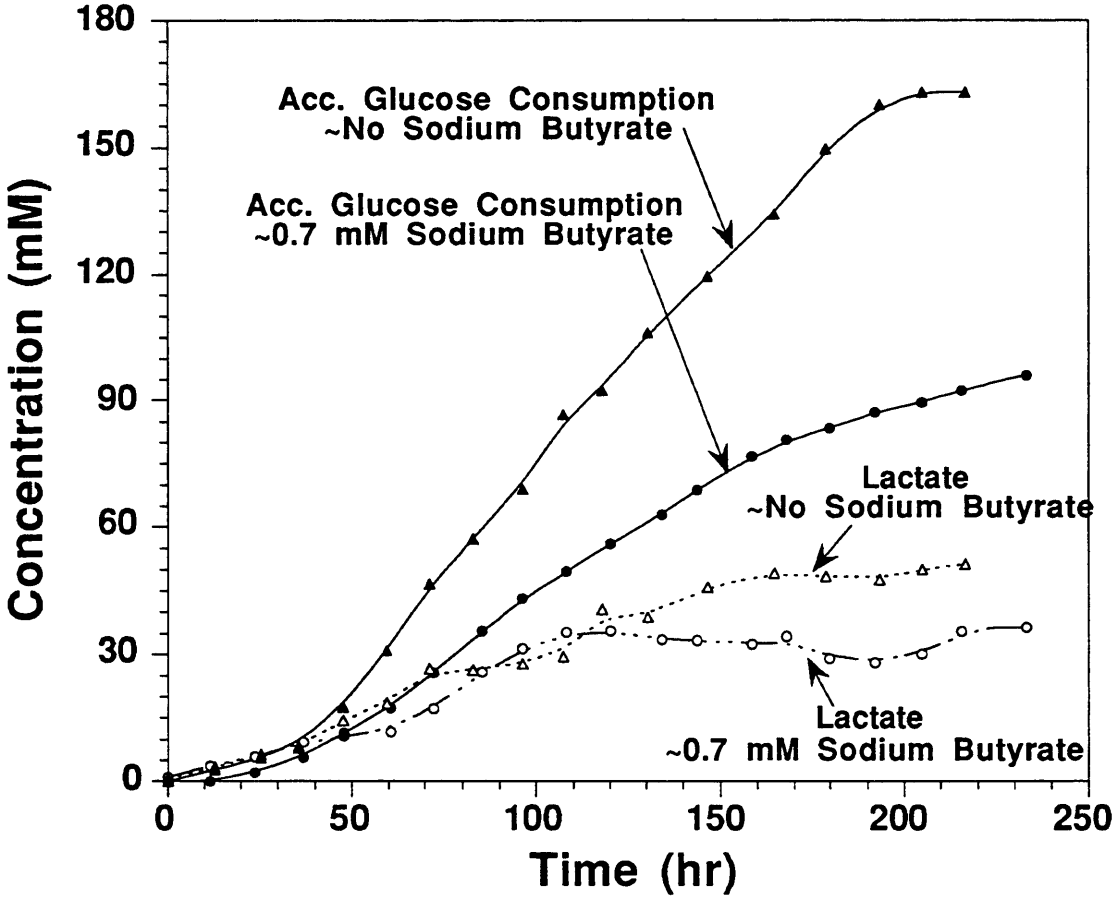

* 50 Amp/m^2 was applied to the sodium-butyrate-added culture, and 70 Amp/m^2 was applied to the sodium-butyrate-free culture.

Figure-4.49: Accumulated glucose consumption and lactate concentration profiles of the cultures using f10MEM. 0.7 mM sodium butyrate was added during the middle of the exponential growth phase.

fed-batch operation observed in the f5MEM/electrokinetic culture.

The lactate concentration profiles are shown in Figure-4.49. If the yield of glucose to lactate is assumed to be the same (1.33 mol-lactate/mol-glucose) in these cultures using the enriched media, the total lactate produced in the sodium-butyrate-added f10MEM/electrokinetic culture was calculated to be 128 mM. Since the final concentration of the residual lactate was 35 mM, it was estimated that 73% of the total lactate has been effectively removed by the 50 A/m^2 electric current density. Although we had expected that osmolarity should increase significantly in the sodium-butyrate-added f10MEM /electrokinetic culture, it was found that the osmolarity did not change markedly (less than 10%) throughout the entire culture. This is evident in Figure-4.44. The presence of sodium butyrate had altered metabolic activities in an unknown way which had reduced osmolarity variation as well as hindered cell growth. Therefore, osmolarity elevation was not the major cause of cell growth hindrance, and variation of some other environmental parameters, including the presence of sodium butyrate, might have hindered cell growth in the sodium-butyrate-added f10MEM/electrokinetic culture.

The results are summarized in Table-4.12. In conclusion, sodium butyrate had reduced cell growth and concomitantly enhanced MAb production in the culture using f10MEM and electrokinetics. The increase in final MAb titer was limited (about 20%) and the final MAb titer was found to be 620 mg/L in the presence of sodium butyrate. The presence of 0.7 mM sodium butyrate did not change the overflow metabolism of the essential amino acids and glutamine, but decelerated glucose metabolism by 25%. Sodium butyrate reduced the elevation of osmolarity to less than 10%, and hence variation of some unknown environmental factors other than osmolarity had hindered cell growth.

Table-4.12: Summary of the effects of sodium butyrate on hybridoma cultures using enriched media and electrokinetics

- Use f10MEM; Supplemental Medium; Glucose/Glutamine
- 70 or 50 Amp/m^2 was applied

	W/O Na Butyrate	With 0.7 mM Na Butyrate
Max. Viable Cell Density (cells/ml)	9.1×10^6	6.9×10^6
Glucose Consumption (mM)	163	96
Specific Glucose Consump. Rate (pmol/cell-hr)	0.16	0.12
Final Lactate Concentration (mM)	50	35
Glutamine Consumption (mM)	27	23
Final Ammonia Concentration (mM)	< 2.0	< 2.0
Specific MAb Production Rate (pg/cell-hr)	0.48	0.76
Final MAb Titer (mg/L)	505	620

V. CONCLUSIONS

This research was conducted to explore the possibility of using the enriched culture media and electrokinetic phenomena (electroosmosis and electrophoresis) to overcome the nutritional limitations and inhibitory product accumulation in various cell culture systems. We have successfully employed electrokinetics in hydrogel-entrapped *E. coli* cultures and suspension hybridoma cultures. The results showed significant enhancement of cell growth and protein product formation, and also revealed the detailed metabolic biochemistry of the cultured cells using the enriched culture media. The conclusions from this research are summarized below:

V.1 Hydrogel-Entrapped Cell Cultures

1. Various kinds of synthetic and natural hydrogels have been screened for the maximum intra-membrane electroosmotic flux and the optimal hybridoma biocompatibility. κ-carrageenan was found to have the structural strength and the highest electroosmotic coupling coefficient, k_i, but it was not biocompatible with hybridoma cells. It was found that κ-carrageenan is quite useful to entrap *E. coli* cells for cultivation. Agarose is an electrically-neutral hydrogel and thus will not support electroosmosis. Agarose was therefore used to entrap *E. coli* cells in order to distinguish the contributions of electroosmosis from electrophoresis in the growth enhancement of hydrogel-entrapped *E. coli*. An alginate/agarose gel blend possessed a high electroosmotic coupling coefficient, k_i, and a good biocompatibility with hybridoma cells, this was therefore used to entrap hybridoma cells to study the influence of electrokinetic behaviors in enhancing cell growth and product formation.

2. Hybridoma cells, CRL-1606, were entrapped in an alginate/agarose gel blend in the presence of 100 A/m^2, and cell growth was not enhanced by electrokinetics. It appeared that the physical structure of hydrogel matrix prevented cell proliferation and thus masked the enhancement of hybridoma growth by the application of the electric field.

3. *E. coli* cell growth within agarose and κ-carrageenan hydrogel slabs was markedly increased by 80% and 140%, respectively, in the presence of 180 A/m^2 compared to the cell growth in the absence of an electric field. Cell growth mainly occurred within a thickness of 1.0 mm at the surface of the hydrogel slab. Eighty percent of the total enhancement of the *E. coli* growth in κ-carrageenan under 180 A/m^2 was attributed to augmented transport of inhibitory end-product and twenty percent of the enhanced growth was attributed to augmented glucose transport.

4. A mathematical model was developed to investigate the overall phenomena in the cell-entrapped hydrogels. *E. coli* growth kinetics and metabolism, and the coupling of intra-membrane transport with various biological phenomena were considered in this model. Time-dependent *E. coli* growth in κ-carrageenan and in agarose was successfully simulated by this model. Based on this model, it is predicted that *E. coli* growth can be enhanced by 210% in κ-carrageenan in the presence of 350 A/m^2. This analysis also revealed that more than 70% of the *E. coli* cells grew anaerobically in κ-carrageenan in the presence of 180 A/m^2 even though dissolved oxygen was available in the ambient medium during the cultivation.

V.2 Suspension Hybridoma Cultures

1. The experimental design for applying the electric fields on suspension hybridoma cultures was able to effectively remove the externally added or cell produced ammonium and lactate and to maintain the chemostatic condition of the medium. It was calculated that volumetric electric current densities ranging from 0.5 to 1.0 A/Liter are required to completely remove the cell produced ammonia and lactate in the suspension hybridoma, CRL-1606, cultures with the viable cell densities ranging from 5 to $10x10^6$ cells/ml.

2. Externally added 40 mM sodium lactate did not affect hybridoma cell growth and antibody production. This lactate concentration (40 mM) was considered as the toxicity threshold for hybridoma cells, CRL-1606. The excess amount of externally-added lactate (e.g 80 mM) increased the medium osmolarity and thus resulted in a significant enhancement of specific monoclonal antibody (MAb) productivity.

3. Hybridoma cell growth was inhibited by the externally added ammonia at concentrations greater than 8.0 mM. This inhibition can be released by externally induced electric field, but the hybridoma cells were irreversibly damaged when incubated with 8.0 mM of ammonia for 12 hours. However, the hybridoma cells, CRL-1606, can be adapted to externally added 12.5 mM ammonia, and therefore they were able to grow in the presence of this high concentration of ammonia.

4. An electric field of 50 A/m^2 was applied to batch and glutamine fed-batch hybridoma cultures using commercial medium, DMEM. Cell-produced ammonia was completely removed, and thus resulted in a 30% to

50% increases in the maximum viable cell density and final antibody titer.

5. An electric field of 70 A/m^2 was also applied to the hybridoma cultures using enriched culture media, designated as f5MEM/control, f5MEM/electrokinetic and f10MEM/electrokinetic cultures. All of the amino acid and vitamin concentrations in f5MEM and f10MEM were 2.5 and 5 times concentrated, respectively, than those in DMEM. The maximum viable cell densities were $3.9x10^6$, $5.8x10^6$ and $9.1x10^6$ cells/ml, and the final MAb titers were 170, 320 and 505 mg/L respectively, in the f5MEM/control, the f5MEM/ electrokinetic and the f10MEM/electrokinetic cultures. A higher specific MAb productivity was observed in the cultures using f10MEM than in those using f5MEM. An electric current density of 70 A/m^2 did not affect cellular functionalities of the hybridoma cells, CRL-1606.

6. When the f5MEM/control culture was compared with the DMEM/control culture, it was found that the maximum viable cell density and final antibody titer increased by 45% and 50%, respectively. It was concluded that the improvement of the cell culture performance by nutrient enrichment was limited in the absence of the electrokinetic behaviors. In contrast, while the f10MEM/electrokinetic culture was compared with the DMEM/control culture, the maximum viable cell density and final antibody titer were found to increase by 230% and 300% respectively. These greater increases in the cell growth and protein production illustrated the importance of the electrokinetic behaviors for cell cultures.

7. The metabolism of these three cultures using the enriched media were

analyzed and compared to other researchers. It was concluded that the significant metabolism overflow of various nutrients, including all of the amino acids and glucose, occurred and thus resulted in the overproduction of lactate and ammonia. The excess production of lactate (100 to 220 mM) markedly raised the medium osmolarity.

8. The addition of 0.7 mM sodium butyrate during the mid-exponential growth phase of the hybridoma culture was able to enhance the specific MAb production rate by 60% (increased from 0.48 to 0.76 pg/cell-hr) without severely inhibiting cell growth using f10MEM in the presence of electrokinetics (50 A/m^2). The presence of 0.7 mM sodium butyrate decelerated the specific glucose metabolic rate (25% decrease), but it did not significantly affect other nutrient metabolism. The resultant osmolarity rise was therefore maintained within 10% of its initial value.

VI. RECOMMENDATIONS FOR FUTURE RESEARCH

In addition to illustrating the significant influences of enriched media and electrokinetics on cell culture, this thesis has also proposed several questions for future research. In this section, these questions will be addressed and recommendations for future research are outlined.

1. Removal of ammonium and lactate from the culture

The difficulty of scaling up electrokinetic technique suggests alternatives for *in-situ* removal of cellular wastes. Extraction of ammonia from the medium across a hydrophobic membrane into a gas stream has been successfully achieved by Hecht *et al.* (1990), and lactate from the lactate fermentation was successfully removed by using anion exchange resins (Srivastava *et al.*, 1992). Although the *in-situ* removal of ammonia and lactate from microbial processes has been successfully accomplished, little success has been shown in these techniques to mammalian cell cultures. The only successful technique for *in-situ* removal of mammalian cell wastes is dialysis (Kasehagen *et al.*, 1991; Linardos *et al.*, 1992). The challenges to apply these techniques to mammalian cell cultures to overcome the problems such as biocompatibility, product removal and scale-up are recommended.

2. Reduction of specific production rates of lactate and ammonia

Glutamine-limited fed-batch operations were shown to decrease ammonia production (Glacken, 1987; Ljunggren and Haggstrom, 1992). Our results further indicated the limitation of an essential amino acid could have decelerated glucose metabolism and lactate production (Section-IV.4.2.2). Therefore the fed-batch operations limiting the essential nutrient concentrations have a great potential in reducing

cellular waste production and is recommended for further studies.

Stoichiometrically-designed media were successfully used for microbial cultivation (Wang *et al.*, 1979), and the application in mammalian cell cultures was recently achieved by Xie (1993). While using a stoichiometrically-designed medium, mammalian cells are obliged to metabolize nutrients more efficiently and thus produce much less cellular wastes. This approach in conjunction with limiting the essential amino acid (see above) could further improve mammalian cell cultivation.

A biological approach in which mammalian cells were transfected with glutamine synthetase to prevent ammonia formation was reported by Bebbington *et al.* (1992). The successful transfectants can proliferate in a glutamine-free medium and completely avoid ammonia production. The overproduction of lactate through glycolysis is mainly controlled by the activity of lactate dehydrogenase (LDH). Deactivation of LDH should be able to reduce the production of lactate by mammalian cells. These biological-based methods for toxic end-product elimination appear to be fruitful for future research.

3. Death of cultured cell

Our results suggested that accumulation of lactate and ammonia and possibly osmolarity rise were the major causes of cell death in our hybridoma cultures. These changes however were unable to completely explain the cell death in our fed-batch cultures using the enriched media. In order to further enhance cell growth and protein production, other factors causing cell death need to be identified. The general features and morphological aspects of cell death were reviewed by Malorni and Donelli (1992) and should be studied in more detail.

The importance of programmed cell death (apoptosis) was recently

reported (Lockshin and Zakeri, 1992). Apoptosis is a directed form of cell death and is characterized by a clear sequence of signals (endocrine) that provoke a series of highly reproducible changes in the affected cells. Apoptosis is characterized by cell and chromatin condensation followed by nuclear DNA fragmentation. If programmed cell death is involved in hybridoma cell cultures, it is necessary to distinguish the programmed cell death from the other phenomena leading to cell death.

4. Application of electrical fields in cell culture

The responses of cultured cells to electric fields were reviewed by Bobinson (1985) to include nerve, muscle, fibroblast, and hybridoma cells. The common responses from the cells include induced mobility, morphological changes, directed cell proliferation, cell membrane permeabilization and enhanced protein production. Among these responses, cell membrane permeabilization and enhanced protein production could be attractive for further investigation. In addition, the exocytosis induced by applied electric fields potentially can be used to control the secretion of the intracellularly-stored proteins and is recommended for future study.

5. Metabolism and protein production of cultured mammalian cells

The glutaminolysis and glycolysis of cultured mammalian cells obtained a lot of attention in the past (Medina and Castro, 1990). Cultured mammalian cells maintain high rates of glutaminolysis and glycolysis even under aerobic condition. Neither energy nor biosynthetic requirements can totally explain these high rates. In addition, the interactions between glutaminolysis and glycolysis are cell-line specific

and culture-condition dependent. How one senses the activity of the other and how the regulation takes place between glutaminolysis and glycolysis remain mostly mysteries. All these questions need to be resolved before the attempt to minimize cellular waste production in the culture.

The rate of protein product formation in mammalian cell culture depends on culture conditions. We have observed that osmolarity rise and addition of sodium butyrate significantly enhanced specific antibody production rate, and the cells remaining in the stationary growth phase (i.e., the cells were arrested in the G1 phase of cell cycle) produced a greater amount of antibody. How these factors enhanced protein production and whether the enhancement occurred at the transcription or translation level are not clear and need to be answered.

One important question we have not tackled in this research is the dependence of protein product microheterogeneity, especially glycosylation, on culture conditions. Dutton (1994) reported that the cells grown at high density produced human IgG-type antibody (HMAb) with a noticeably lower level of glycosylation than did HMAb produced from the same cells grown at low density. In the past, researchers have put tremendous efforts into increasing antibody production by maximizing the viable cell density and the culture longevity. If insufficient glycosylation of antibodies occurred in these high cell density cultures, all the efforts for maximizing antibody titer would have been wasted. Consequently, we need to understand the dependence of glycosylation on culture conditions, thus we can optimize the antibody glycosylation as well as maximize the antibody titer.

NOMENCLATURE

$\overline{C}_i$	intra-membrane concentration of solute i (mol/m^3)
$\overline{C}_m$	concentration of ionized charge group in membrane (mol/m^3)
C_{w1}; C_{w2}	inhibition constants (mol/m^3)
$\overline{C}_v$	specific heat capacity of hydrogel (joule/Kg-°C)
$\overline{D}_i$	effective intra-membrane diffusivity of solute i (m^2/hr)
E	local electric field gradient (Volt/m)
F	Faraday constant (96490 Coul/mol)
J	applied current density (Amp/m^2)
K_m	equivalent Michaelis-Menton constant (mol/m^3)
k'	hydraulic (Darcy) permeability of membrane (m^4/Nt-hr)
k_i	electroosmotic coupling coefficient (m^3/Amp-hr)
k_T	thermal conductivity (joule/m-s-°C)
L	half thickness of hydrogel slab (m)
m_s	specific non-growth-associated (maintenance) nutrient uptake rate (mol/g-cell-hr)
N	cell density in hydrogel matrix (g-cell/m^3-gel)
Q; q	specific uptake (production) rate (mol/g-cell-hr)
Q_{max}	maximum specific uptake (production) rate (mol/g-cell-hr)
T	temperature (°C)
U	area-average fluid velocity relative to the solid matrix (m/hr)
u_i	electrical mobility of charged solute (cm^2/Volt-hr)
V_x	electroosmotic flow rate (m/hr)
W_i	hindrance factor for convective transport of solute i (nearly unity for ions and small solutes)
$Y_{w/s}$	yield of nutrient to waste (g-acid/g-glucose)
$Y_{P/E.A.A.}$	yield of essential amino acid to antibody (g-IgG/mM)
$Y_{X/E.A.A.}$	yield of essential amino acid to cell mass (cells/mM)
Z_i	electric valence of solute i
Z_m	electric valence of ionized charge group in membrane
δ_0	membrane thickness (m)

Φ	membrane porosity
Γ_i	i-th solute flux (mole/m^2-hr)
μ	specific cell growth rate (hr^{-1})
μ_{max}	maximum specific growth rate (hr^{-1})
$\overline{\mu}_i$	effective electrical mobility of solute i (m^2/Volt-hr)
ρ	hydrogel density (Kg/m^3)
σ	electrical conductivity (mho/m)

Subscript

b	condition in bulk medium
glc	glucose
gln	glutamine
lac	lactate
o	oxygen
p	antibody
s	rate-limiting nutrient
w	inhibitory waste product

REFERENCES

Adema, E. (1989). "Ammonium toxicity in mammalian cell culture." M.I.T. Ph.D. Thesis.

Aharonowitz, Y. and G. Cohen (1981). "The microbiological production of pharmaceuticals." in Industrial Microbiology and the Advent of Genetic Engineering. San Francisco, Freeman. 57-68.

Aiba, S., A. E. Humphrey and N. F. Millis (1973). Biochemical Engineering. New York, Academic Press, 18-55.

Applegate, M. (1991). "Development and characterization of mocroporous ceramic matrix bioreactors for mammalian cell culture." M.I.T. Ph.D. Thesis.

Arnaud, J. P., C. Lacroix and L. Choplin (1989). "Effect of lactic fermentation on the rheological properties of κ-carrageenan/locust bean gum mixed gels inoculated with *S. thermophilus*." Biotech Bioeng 34: 1403-1408.

Ataai, M. M. and M. L. Shuler (1985). "Simulation of the growth pattern of a single cell of *E. coli* under anaerobic conditions." Biotech Bioeng 27: 1027-1035.

Atkinson, B. and F. Mavituna (1983). Biochemical engineering and biotechnology handbook. New York, The Nature Press. 727-801.

Aunins, J. G. and D. I. C. Wang (1989). "Induced flocculation of animal cells in suspension culture." Biotech Bioeng 34: 629-638.

Avgerinos, G. C. (1982). Direct conversion of cellulosic biomass to ethanol by mixed culture fermentation of *Clostridium thermocellum* and *Clostridium saccharolyticum*. M.I.T. Ph.D. Thesis.

Backer, M. P., L. S. Metzger, P. L. Slaber, K. L. Nevitt and G. B. Boder (1988). "Large-scale production of monoclonal antibodies in suspension culture." Biotech Bioeng 32: 993-1000.

Baily, J. E. and D. F. Ollis (1986). Biochemical engineering fundamentals. New York, McGraw-Hill. 2nd Ed. 457-532.

Barbotin, J. N., J. E. N. Saucedo and B. Thomasset (1990). "Morphological observations on immobilized cells." in Physiology of Immobilized Cells. Netherlands, Elsevier Science Publishers, 487-498.

Bassi, A. S., S. Rohani and D. G. MacDonald (1987). "Measurement of effective diffusivities of lactose and lactic acid in 3% agarose gel membrane." Biotech Bioeng 30: 794.

Batt, B. C. and D. S. Kompala (1989). "A structured kinetics modeling framework for the dynamics of hybridoma growth and monoclonal antibody production in continuous suspension cultures." Biotech Bioeng 34: 515-531.

Bebbington, C. R., G. Renner, S. Thomson, D. King, D. Abrams and G. T. Yarranton (1992). "High-level expression of a recombinant antibody from myeloma cells using a glutamine synthetase gene as an amplifiable selectable marker." Bio/Technology 10: 169-175.

Bender, G. R. and R. E. Marquis (1987). "Membrane ATPase and acid tolerance of *Actinomyces viscosus* and *Lactobacillus casei*." Appl & Environ Microbiol 53(9): 2124.

Bhaskar, R. K., R. V. Sparer and K. J. Himmelstein (1985). "Effect of an applied electric field on liquid crystalline membranes : Control of permeability." J Membrane Science 24: 83-96.

Bibila, T. and M. C. Flickinger (1991). "A structured model for monoclonal antibody synthesis in exponentially growing and stationary phase hybridoma cells." Biotech Bioeng 37: 210-226.

Birch, J. R., P. W. Thompson and R. Boraston (1985). "Production of monoclonal antibodies in large-scale cell culture." Biochem Soc Trans 13: 10-12.

Bloemkolk, J.W., M. R. Gray, F. Merchant and T. R. Mosmann (1992). "Effect of temperature on hybridoma cell cycle and MAb production." Biotech Bioeng 40: 427-431.

Boffa, L. C., R. J. Gruss and V. G. Allfrey (1981). "Manifold effects of sodium butyrate on nuclear function." J Biol Chem 256 (18): 9612-9621.

Bree, M. A., P. Dhurjati, R. F. Geoghegan and B. Bobnett (1988). "Kinetic modelling of hybridoma cell growth and immunoglobulin production in a large-scale suspension culture." Biotech Bioeng 32: 1067-1072.

Brink, L. E. S. and J. Tramper (1985). "Modelling the effects of mass transfer on kinetics of propene epoxidation of immobilized *Mycobacterium* cells: 1. Pseudo-one-substrate conditions and negligible product inhibition. 2. Product inhibition." Enzyme Microb Technol 8: 281; 334.

Bucke, C. (1897). "Cell immobilization in calcium alginate." in Methods in Enzymology. New York, Academic Press 135; 175-189.

Burgmayer, P. and R. W. Murray (1982). "An ion gate membrane: Electrochemical control of ion permeability through a membrane with an embedded electrode." J Am Chem Soc 104: 6139-6140.

Butler, M. and R. E. Spier (1984). "The effects of glutamine utilization and ammonia production on the growth of BHK cells in microcarrier cultures." J Biotechnol 1: 187.

Chang, H. N. and M. Moo-Young (1988). "Estimation of oxygen penetration depth in immobilized cells." Appl Microb Biotech 29: 107-112.

Chibata, I., T. Tosa, T. Sato and I. Takata (1987). "Immobilization of cells in carrageenan." Meth Enz 135: 189-198.

Chiou, T. W. (1992). "A modified airlift fiber-bed bioreactor for animal cell culture." M.I.T. Ph.D. Thesis.

Cobley, J. G. and J. C. Cox (1983). "Energy conservation in acidophilic bacteria." Microbiol Review 47(4): 579.

Cohen, S. N. (1975). "The manipulation of genes." Sci Am 233: 25-33.

Comer, M. J., M. J. Kearns, J. Wahl, M. Munster, T. Lorenz, et al. (1990). "Industrial production of monoclonal antibodies and therapeutic proteins by dialysis fermentation." Cytotech 3: 295-299.

Constantinides, A. (1980). "Steroid transformation at high substrate concentrations using immobilized *Corynebacterium simplex* cells." Biotech Bioeng 22: 119-136.

Cooney, C. L. (1981). "Growth of microorganisms." in Biotechnology, volume 1: Microbial Fundamentals. Verlag Chemie, Weinheim. 75-111.

Cooney, C. L. (1985). "Growth of microorganisms." in Comprehensive Biotechnology. Oxford, Pergamon Press. 73-112.

Cooney, C. L. (1985). "Introduction." in Comprehensive Biotechnology. Oxford, Pergamon Press. 233-235.

Cooper, M. S. and M. Schliwa (1985). "Electrical and ionic controls of tissue cell locomotion in DC electric fields." J Neuroscience research 13: 223-244.

Croughan, M. S. (1988). "Hydrodynamic effects of animal cells in microcarrier bioreactor." M.I.T. Ph.D. Thesis.

Croughan, M. S. and D. I. C. Wang (1989). "Growth and death in over-agitated microcarrier cell cultures." Biotech Bioeng 33: 862-872.

Croughan, M. S. and D. I. C. Wang (1991). "Hydrodynamic effects on animal cells in microcarrier bioreactor." in Animal Cell Bioreactors. Boston, Butterworth-Heinemann. 213-252.

Cumming, D. A. (1991). "Glycosylation of recombinant protein therapeutics: control and functional implications." Glycobiol 1: 115-130.

Cysewski, G. R. and C. R. Wilke (1977). Biotech Bioeng 19: 1125.

Dean, R. C., S. B. Karkare, P. G. Phillips, N. G. Ray and P. W. Runstadler (1987). "Continuous cell culture with fluidized sponge beads." in Large Scale Cell Culture Technology. New York, Hanser Publishers.

Demain, A. L. and N. A. Solomon (1981). "Industrial Microbiology." in Industrial Microbiology and the Advent of Genetic Engineering. San Francisco, Freeman. 3-16.

Doyle, C. and M. Butler (1990). "The effect of pH on the toxicity of ammonia to a murine hybridoma." J Biotech 15: 91-100.

Domurado, M., F. Deramoudt and D. Thomas (1988). "Immobilization of murine lymphocytes by gel entrapment." Biotech, Tech 2(3): 211-216.

Drew, S. W. (1985). "Introduction." in Comprehensive Biotechnology. Oxford, Pergamon Press. 3-6.

Dutton, G. (1994). "Human monoclonal antibody manufacturers advance in overcoming production issues." Genetic Engineering News 14(6): 1.

Duval, D., C. Demangel, K. Munier-Jolain, S. Miossec and I. Geahel (1991). "Factors controlling cell proliferation and antibody production in mouse hybridoma cells : I. Influence of the amino acid supply." Biotech Bioeng 38: 561-570.

Eagle, H. (1956). Arch Biochem Biophys 61: 356-366.

Eagle, H. (1959). "Amino acid metabolism in mammalian cell cultures." Science 130: 432-437.

Eigenbrodt, E., P. Fister and M. Reinacher (1985). "New perspectives on carbohydrate metabolism in tumor cells." in Regulation of Carbohydrate Metabolism. Boca Raton, CRC Press. 141-179.

Eisenberg, S. R. and A. J. Grodzinsky (1984). "Electrically modulated membrane permeability." J Membrane Science 19: 173-194.

Esclade, L. R. J., S. Carrel and P. Peringer (1991). "Influence of the screen material on the fouling of spin filters." Biotech Bioeng 38: 159-168.

Eveleigh, D. E. (1981). "The microbiological production of industrial chemicals." in Industrial Microbiology and the Advent of Genetic Engineering. San Francisco, Freeman. 71-79.

Fieschko, J. C., K. M. Egan, T. Ritch, R. A. Koski, M. Jones and G. A. Bitter (1987). "Controlled expression and purification of human immune interferon from high- cell-density fermentations of *Saccharomyces*

cerevisiae." Biotech Bioeng 29: 1113-1121.

Finaz, C., A. Lefevre and J. Teissie (1984). "A new, highly efficient technique for generating somatic cell hybrids." Expt Cell Res 150: 477-482.

Freeman, A. and Y. Aharonowitz (1981). "Immobilization of microbial cells in crosslinked, prepolymerized, linear polyacrylamide gels: Antibiotic production by immobilized *Streptomyces clavuligerus* cells." Biotech Bioeng 23: 2747-2759.

Freshney, R. I. (1987). Culture of Animal Cells-A Manual of Basic Technique. 2nd Ed. New York, Wiley-Liss; 57-84.

Friedenberg, Z. B., M. C. Harlow and C. T. Brighton (1971). "Healing of nonunion of the medical malleolus by means of direct current, a case report." J Trauma 11: 883-885.

Friedman, M. R. and E. L. Gaden (1970). Biotech Bioeng 12: 961.

Gharapetian, H., M. Maleki, N. A. Davies and A. M. Sun (1986). "Polyacrylate membranes for encapsulation of viable cells." : 114-118.

Ghose, T. K., P. K. Roychoudhury and P. Ghose (1984). Biotech Bioeng 26: 377.

Ghose, T. K. and R. D. Tyagi (1979). "Rapid ethanol fermentation of cellulose hydrolysates II. Production and substrate inhibition and optimization of reactor design." Biotech Bioeng 21: 1401.

Glacken, M. W., R. J. Fleischaker and A. J. Sinskey (1986). "Reduction of waste product extraction via nutrient control: Possible strategies for maximizing product and cell yields on serum in cultures of mammalian cells." Biotech Bioeng 28: 1376-1389.

Glacken, M. (1987). "Development of mathematical description of mammalian cell culture kinetics for the optimization of fed-batch bioreactors." M.I.T. Ph.D. Thesis.

Glacken, M. W., C. Huang and A. J. Sinskey (1989). "Mathematical descriptions of hybridoma culture kinetics: III. Simulation of fed-batch bioreactors." J Biotechnol 10: 39-66.

Grimshaw, P. (1989). "Electrical control of solute transport across polyelectrolyte membranes." M.I.T. Ph.D. Thesis.

Grimshaw, P., A. J. Grodzinsky, M. L. Yarmush and D. M. Yarmush (1989). "Dynamic membranes for protein transport: Chemical and electrical control." Chem Eng Science 44(4): 827-840.

Grodzinsky, A. J. and A. M. Weiss (1985). "Electric field control of

membrane transport and separation." Separation and purification methods 14(1): 1-40.

Graff, S. H., O. Moser, A. M. Kastner and M. Tannenbaum (1965). "The significance of Glycolysis." J. Nat. Cancer Inst. 34: 511-519.

Griffiths, B. (1991). "Products from animal cells." in Mammalian Cell Biotechnology. New York, Oxford Univ. Press. 207-235.

Haggstrom, L. and N. Molin (1980). "Calcium alginate immobilized cells of *Clostridium acetobutylicum* for solvent production." Biotech Letters 2(5): 241-246.

Hannoun, B. J. K. and G. Stephanopoulos (1986). "Diffusion coefficients of glucose and ethanol in cell-free and cell-occupied calcium alginate membranes." Biotech, Bioeng 28: 829.

Hecht, V., L. Bischoff and K. Gerth (1990). "Hollow fiber supported gas membrane for *in-situ* removal of ammonium during an antibiotic fermentation." Biotech Bioeng 35: 1042-1050.

Herrero, A. A. (1983). "End-product inhibition in anaerobic fermentations." Trends in Biotech 1(2): 49.

Ho, C. S., L. K. Ju and R. Baddour (1990). "Enhancing penicillin fermentations by increased oxygen solubility through the addition of n-hexadecane." Biotech Bioeng 36: 1110-1118.

Hongo, M., Y. Nomura and M. Iwahara (1986). "Novel method of lactic acid production by electrodialysis fermentation." Appl & Environ Microbiol 52(2): 314-319.

Hooijmans, C. M., C. A. Briasco, J. Huang, B. G. M. Geraats, J.N. Barbotin, et al. (1990). "Measurement of oxygen concentration gradients in gel-immobilized recombinant *E. coli*." Appl Microbiol Biotechnol 33: 611-618.

Hopwood, D. A. (1981). "The genetic programming of industrial microorganisms." in Industrial Microbiology and the Advent of Genetic Engineering. San Francisco, Freeman. 31-42.

Hu, W. S., T. C. Dodge, K. K. Frame and V. B. Himes (1987). "Effect of glucose on the cultivation of mammalian cells." in Develop. Biol. Standard. 66: 279-290.

Hu, W. S. and M. V. Peshwa (1991). "Animal cell bioreactors-recent advances and challenges to scale-up." Can J Chem Eng 69: 409-420.

Hu, W. S. and D. I. C. Wang (1987). "Selection of microcarrier diameter for the cultivation of mammalian cells on microcarriers." Biotech Bioeng 30:

548-557.

Huang, J., C. M. Hooijmans, C. A. Briasco, S. G. M. Geraats, K. A. M. Luyben, et al. (1990). "Effect of free-cell growth parameters on oxygen concentration profiles in gel-immobilized recombinant *E. coli*." Appl Microb Biotech 33: 619-623.

Ishizaki, A., Y. Nomura and M. Iwahara (1990). "Built-in electrodialysis batch culture, a new approach to release of end product inhibition." J Ferment Bioeng 70(2): 108-113.

Jo, E. C., H. J. Park, J. M. Park and K. H. Kim (1990). "Balanced nutrient fortification enables high-density hybridoma cell culture in batch culture." Biotech Bioeng 36: 717-722.

Jo, E. C., H. J. Park, D. I. Kim and H. M. Moon (1993a). "Repeated fed-batch culture of hybridoma cells in nutrient-fortified high-density medium." Biotech Bioeng 42: 1229-1237.

Jo, E.c., D.i. Kim and H. M. Moon (1993b). "Step-fortifications of nutrients in mammalian cell culture." Biotech Bioeng 42: 1218-1228.

Ju, L.k. and C. S. Ho (1989). "Oxygen diffusion coefficient and solubility in n-hexadecane." Biotech Bioeng 34: 1221-1224.

Junker, B. H., T. A. Hatton and D. I. C. Wang (1990). "Oxygen transfer enhancement in aqueous/perfluorocarbon fermentation systems: I. Experimental observation & II. Theoretical analysis." Biotech Bioeng 35: 578-597.

Karel, S. F., S. B. Libicki and C. R. Robestson (1985). "The immobilization of whole cells: Engineering principles." Chem Eng Sci 40: 1321-1354.

Karel, S. F. and C. R. Robertson (1989). "Cell mass synthesis and degradation by immobilized E. coli." Biotech Bioeng 34: 337-356.

Kasehagen, C., F. Linz, G. Kretzmer and T. Scheper (1991). "Metabolism of hybridoma cells and antibody secretion at high cell densities in dialysis tubing." Enzyme Microb Technol 13: 873-881.

Katinger, H. W., W. Scheirer and E. Kromer (1979). "Bubble column reactor for mass propagation of animal cells in suspension." Ger Chem Eng 2: 31-38.

Kell, D. B. and H. V. Westerhoff (1986). FEMS Microbiol Rev 39: 305-320.

Kelley, W. N. (1972). "Purine and pyrimidine metabolism of cells in culture." in Growth, Nutrition, and Metabolism of Cells in Culture. New York, Academic Press. 211-256.

Kennedy, J. F. and J. M. Cabral (1983). "Immobilized living cells and their applications." in Applied Biochemistry & Bioengineering. New York, Academic Press. 4; 189-280.

Khosrovi, B. and P. P. Gray (1985). "Products from recombinant DNA." in Comprehensive Biotechnology. Oxford, Pergamon Press. 319-330.

Kierstan, M. and C. Bucke (1977). "The immobilization of microbial cells, subcellular organelle, and enzymes in calcium alginate gels." Biotech Bioeng 19: 387-397.

King, G. A., A. J. Daugulis, P. Faulkner and M. F. A. Goosen (1987). "Alginate-polylysine microcapsules of controlled membrane molecular weight cutoff for mammalian cell culture engineering." Biotech Progress 3(4): 231-240.

Kitano, K. (1991). "Serum-free medium." in Animal Cell Bioreactors. Boston, Butterworth-Heinemann. 73-106.

Klein, J. and K. D. Vorlop (1983). in Foundations of Biochemical Engineering. ACS Symp. Series. American Chemical Society, Washington. 377-392.

Kojima, T., K. Hashimoto, S. Ito, Y. Hori, T. Tomizuka and N. Oguri (1990). "Protection of rabbit embryos against fracture damage from freezing and thawing by encapsulation in calcium alginate gel." J Expt Zoology 254: 186-191.

Kojima, J., H. Shinohara, Y. Ikariyama, M. Aizawa, K. Nagaike and S. Morioka (1992). "Electrically promoted protein production by mammalian cells cultured on the electrode surface." Biotech Bioeng 39: 27-32.

Kooistra, T., J. V. D. Berg, A. Tons, G. Platenburg, D. C. Rijken and E. V. D. Berg (1987). "Butyrate stimulates tissue-type plasminogen-activator synthesis in cultured human endothelial cells." Biochem J 247: 605-612.

Kruh, J. (1982). "Effects of sodium butyrate, a new pharmacological agent, on cells in culture." Mol Cell Biochem 42: 65-82.

Kunas, K. T. and E. T. Papoutsakis (1990). "Damage mechanisms of suspended animal cells in agitated bioreactors with and without bubble entrainment." Biotech Bioeng 36: 476-483.

Kurosawa, H., M. Matsumura and H. Tanaka (1989). "Oxygen diffusivity in gel beads containing viable cells." Biotech Bioeng 34: 926-932.

Lambert, K. and S. J. Pirt (1975). "The quantitative requirements of human diploid cells (strain MRC-5) for amino acids, vitamins and serum." J Cell Sci 17: 397-411.

Lavine, L. S., I. Lustrin, M. H. Shamos, R. A. Rinaldi and A. R. Liboff (1972). "Electric enhancement of bone healing." Science 175: 1118-1121.

Lazo, P. A. (1981). "Amino acids and glucose utilization by different metabolic pathways." Eur J Biochem 117: 19-25.

Lee, G. M., A. S. Chunk and B. O. Palsson (1993). "Cell culture conditions determine the enhancement of specific monoclonal antibody productivity of calcium alginate-entrapped S3H5/r2bA2 hybridoma cells." Biotech Bioeng 41: 330-340.

Lee, G. M. and B. O. Palsson (1990). "Immobilization can improve the stability of hybridoma antibody productivity in serum-free media." Biotech Bioeng 36: 1049-1055.

Linardos, T. I., N. Kalogerakis and L. A. Behie (1992). "Monoclonal antibody production in dialyzed continuous suspension culture." Biotech Bioeng 39: 504-510.

Ljunggren, J. and L. Haggstrom (1992). "Glutamine limited fed-batch culture reduces the overflow metabolism of amino acid in myeloma cells." Cytotech 8: 45-56.

Lockshin, R. A. and Z. F. Zakeri (1992). "Physiology and protein synthesis in programmed cell death." Annals of the New York Academy of Sciences 663: 234-249.

Looby, D. and J. B. Griffiths (1988). "Fixed bed porous glass sphere." Cytotech. 1: 339-346.

Luong, J. H. T. (1985). "Cell immobilization in k-carrageenan for ethanol production." Biotech Bioeng 27: 1652.

Luther, P. W. and H. B. Peng (1983). "Changes in cell shape and actin distribution induced by constant electric fields." Nature 305(5): 61-64.

Lydersen, B. K., G. G. Pugh, M. S. Paris, B. P. Sharma and L. A. Noll (1985). "Ceramic matrix for large scale animal cell culture." Bio/Technology 3(1): 63-67.

Lyte, M., J. E. Gannon and G. D. O. Jr (1991). "Effects of in vitro electrical stimulation on enhancement and suppression of malignant lymphoma cell proliferation." J Natl Cancer Inst 83: 116-119.

MacGinitie, L. A., A. J. Grodzinsky, E. H. Frank and Y. A. Gluzband (1987). "Frequency and amplitude dependence of electric field interactions: electrokinetics and biosynthesis." in Mechanistic approaches to interactions of electric and electromagnetic fields with living systems : 133-149.

Maiorella, B., G. Dorin, A. Carion and D. Harano (1991). "Crossflow microfiltration of animal cells." Biotech Bioeng 37: 121-126.

Malorni, W. and G. Donelli (1992). "Cell death: General features and morphological aspects." Annuals of the New York Academy of Sciences 663: 218-233.

Maniatis, T., E. F. Fritsch and J. Sambrook (1982). Molecular Cloning: A Laboratory Manual. Cold Spring Harbor Laboratory. 440.

Margaritis, A., F. J. A. Merchant, A. Vardanis and J. B. Wallace (1986). "Diffusivity measurements in immobilized cell matrices using radioactive tracer techniques." Bioichemical Engineering 5:

Matsumura, M. and H. Markl (1984). "Application of solvent extraction to ethanol fermentation." Appl Microbiol Biotechnol 20: 371.

Mattiasson, B. (1983). "Immobilization methods." in Immobilized Cells and Organelles. CRC Press. 3-25.

McGarrity, G.J. (1979) "Sources of stable cell lines." in Cell Culture, Eds, W. B. Jakoby and I. H. Pastan, p. 439-444, Academic Press: New York.

McKeehan, W. L. (1986). "Glutaminolysis in animal cells." in Carbohydrate Metabolism in Cultured Cells. New York, Plenum Press. 111-150.

Mcleod, K. J., R. C. Lee and H. P. Ehrlich (1987). "Frequency dependence of electric field modulation of fibroblast protein synthesis." Science 236(6): 1465-1469.

McMillan, J. D. (1990). "Mechanisms of oxygen transfer enhancement during submerged cultivation in perfluorochemical-in-water dispersions." M.I.T. Ph.D. Thesis.

McQueen, A. and J. E. Bailey (1991). "Growth inhibition of hybridoma cells by ammonia ion: Correlation with effects on intracellular pH." Bioproc Eng 6: 49.

Medina, M. and I. N. de Castro (1990). "Glutaminolysis and glycolysis in proliferant cells." Int J Biochem 22: 681-683.

Meilhoc, E., K. D. Wittrup and J. E. Bailey (1990). "Influence of dissolved oxygen concentration on growth, mitochondrial function and antibody production by hybridoma cells in batch culture." Bioproc Eng 5: 263-274.

Melick, M. R., M. N. Karim, L. C. Linden, B. E. Dale and P. Mihaltz (1987). "Mathematical modelling of ethanol production by immobilized *Zymomonas mobilis* in a packed bed fermentor." Biotech Bioeng 29: 370.

Miller, G. J., H. Burchardt, W. F. Enneking and C. M. Tylkowski (1984). "Electromagnetic stimulation of canine bone grafts." J Bone and Joint Surg 66-A: 693-698.

Miller, W. M., C. R. Wilke and H. W. Blanch (1988a). "Transient responses of hybridoma cells to lactate and ammonia pulse and step change in continuous culture." Bioproc Eng 3: 113.

Miller, W. M., H. W. Blanch and C. R. Wilke (1988b). "A kinetic analysis of hybridoma growth and metabolism in batch and continuous suspension culture: Effect of nutrient concentration, dilution rate and pH." Biotech Bioeng 32: 947-965.

Miller, W. M., C. R. Wilke and H. W. Blanch (1989). "The transient response of hybridoma cells to nutrient additions in continuous cultures: II. Glutamine pulse and step change." Biotech Bioeng 33: 487-499.

Miller, W. M. and H. W. Blanch (1991). "Regulation of animal cell metabolism in bioreactor." in Animal Cell Bioreators. Boston, Butterworth-Heinemann. 119-164.

Millis, N. F. (1985). "The organisms of biotechnology." in Comprehensive Biotechnology. Oxford, Pergamon. 7-19.

Morris, J. G. (1985). "Anaerobic metabolism of glucose." in Comprehensive Biotechnology. Vol. 1, New York, Pergamon Press. 357-378.

Nathan, D. F., S. R. Burkhart and M. Morin (1990). "Increased cell surface EGF receptor expression during the butyrate-induced differentiation of human HCT-116 colon tumor cell clones." Expt Cell Research 190: 76-84.

Nguyen, A. L. and J. H. T. Luong (1986). "Diffusion in k-carrageenan gel beads." Biotech Bioeng 28: 1261.

Nilsson, K., P. Brodelius and K. Mosbach (1987). "Entrapment of microbial and plant cells in beaded polymers." in Methods in Enzymology. New York, Academic Press. 222-230.

Nilsson, K., W. Scheirer, H. W. D. Katinger and K. Mosbach (1986). Production of monoclonal antibodies by agarose-entrapped hybridoma cells. Methods in Enzymology. New York, Academic Press. 352-360.

Nishida, Y., T. Sato, T. Tosa and I. Chibata (1979). "Immobilization of *E. coli* cells having aspartase activity with carrageenan and locust bean gum." Enzyme Microb Tech 1(4): 95-99.

Nomura, Y., M. Iwahara and M. Hongo (1987). "Lactic acid production by electrodialysis fermentation using immobilized brewing cells." Biotech Bioeng 30: 788-793.

Nomura, Y., M. Iwahara and M. Hongo (1988). "Acetic acid production by an electrodialysis fermentation method with a computerized control system." Appl & Environ Microbiol 1: 137-142.

Oh, S. K. W., P. Vig, F. Chua, W. K. Teo and M. G. S. Yap (1993). "Substantial overproduction of antibodies by applying osmotic pressure and sodium butyrate." Biotech Bioeng 42: 601-610.

Onuma, E. K. and S. Hui (1986). "The effects of calcium on electric field-induced cell shape changes and preferential orientation." Ionic Currents in Development : 319-327.

Overbeek, J. T. J. and B. H. Bijsterbosch (1979). "The electrical double layer and the theory of electrophoresis." in Electrokinetic Separation Methods. Elsevier, 1-32.

Overgaard, S., J. D. Scharer, M. Moo-Young and N. C. Bols (1991). "Immobilization of hybridoma cells in chitosan alginate beads." Can J Chem Eng 69: 439-443.

Ozturk, S. S. and B. O. Palsson (1991). "Effect of medium osmolarity on hybridoma growth, metabolism, and antibody production." Biotech Bioeng 37: 989-993.

Ozturk, S. S., M. R. Riley and B. O. Palsson (1992). "Effects of ammonia and lactate on hybridoma growth, metabolism, and antibody production." Biotech Bioeng 39: 418-431.

Palermo, D. P., M. E. DeGraaf, K. R. Marotti, E. Rehberg and L. E. Post (1991). "Production of analytical quantities of recombinant proteins in Chinese hamster ovary cells using sodium butyrate to elevate gene expression." J Biotech 19: 35-48.

Park, S. and G. Stephanopoulos (1993). "Packed bed bioreactor with porous ceramic beads for animal cell culture." Biotech Bioeng 41: 25-34.

Parker, M. I., J. B. d. Haan and W. Gevers (1986). "DNA hypermethylation in sodium butyrate-treated WI-38 fibroblasts." J Biol Chem 261(6): 2786-2790.

Pasechnik, V. A. and R. S. Alimardanov (1979). "Effect of direct current on the permeability of ultrafiltration membranes." Kolloidnyl Zhurnal 41(3): 586-590.

Payton, M. A. and B. A. Haddock (1985). "Aerobic metabolism of glucose." in Comprehensive Biotechnology. Vol. 1, New York, Pergamon Press. 337-356.

Phaff, H. J. (1981). "Industrial microorganisms." in Industrial Microbiology and the Advent of Genetic Engineering. San Francisco, Freeman. 15-30.

Piskin, E. and T. M. S. Chang (1981). "Urea and ammonia removal from dialysate in an oxygenator : Effects of dialysate and air flow rates." J Membrane Sci 9: 343-350.

Posillico, E. G. (1986). "Microencapsulation technology for large-scale antibody production." Bio/Technology 4: 114-117.

Radovich, J. M. (1985). "Mass transfer effects in fermentations using immobilized whole cells." Enzyme Microb Tech 7(1): 2-10.

Radovich, J. M., R. E. Spark (1980). "Electrophoretic techniques for controlling concentration polarization in ultrafiltration." Ultrafiltration membranes and applications, Polymer Sci and Tech 13:

Reitzer, L. J., B. M. Wice and D. Kennell (1980). "The pentose cycle: Control and essential function in HeLa cell nucleic acid synthesis." J Biological Chemistry 255: 5616-5626.

Righelato, R. C. (1975). "Growth kinetics of mycelial fungi." in The Filamentous Fungi. Eds. J. E. Smith, D. R. Berry London, Edward Arnold. 1: 79.

Robinson, K. R. (1985). "The response of cells to electrical fields: A review." J Cell Biol 101: 2023-2027.

Salter, G. J. and D. B. Kell (1991). "New materials and technology for cell immobilization." Biochem Eng 2: 385-389.

Satterfield, C. N. (1970). Mass Transfer in Heterogeneous Catalysis. Cambridge, MIT Press.

Savinell, J. M., G. M. Lee and B. Palsson (1989). Bioprocess Eng 4: 231-234.

Schimazaki, K., N. Nishimura and H. Shibai (1986). "New separation system for mammalian cells with large-scale centrifugation." Ann NY Acad Sci 469: 63-72.

Schoen, R. C., K. L. Bentley and R. J. Klebe (1982). "Monoclonal antibody against human fibronectin which inhibits cell attachment." Hybridoma 1: 99-108.

Schuster, R. (1984). "Automatic on-column derivatization of free amino acids with OPA on Microbore column." Hewlett Packard Application Note : 12-5954-0805.

Scott, C. D. (1987). "Immobilized cells: a review of recent literature." Enzyme Microb Technol 9: 66-73.

Sefton, M. V., R. L. Broughton, M. E. Sugamori and C. L. Mallabone (1987).

"Hydrophilic polyacrylates for the microencapsulation of fibroblasts or pancreatic islets." J Controlled Releases 6: 177-187.

Sefton, M. V., R. G. Dawson, R. L. Broughton, J. Blysniuk and M. E. Sugamori (1986). "Microencapsulation of mammalian cells in a water-insoluble polyacrylate by coextrusion and interfacial precipitation." Biotech Bioeng 29(6): 1135-1143.

Shirai, Y., K. Hashimoto and S. Irie (1989). "Formation of effective channels in alginate gel for immobilization of anchorage-dependent animal cells." Appl Microbiol Biotech 31: 342-345.

Shirai, Y., R. Sasaki, K. Hashimoto and H. Chiba (1988). "Continuous production of erythropoietin with immobilized animal cells." Appl Microb Biotech 29: 544-549.

Spier, R. E. (1991). "Historical development of animal cell bioreactors." in Animal cell bioreactors. Stoneham, Butterworth-Heinemann. 3-20.

Srivastava, A., P. K. Rouchoudhury and V. Sahai (1992). "Extractive lactic acid fermentation using ion-exchange resin." Biotech Bioeng 39: 607-613.

Stephanopoulos, G. and K. Tsiveriotis (1989). "The effects of intraparticle convection on nutrient transport in porous biological pellets." Chem Eng Science 44(9): 2031-2039.

Sureshkumar, G. K. and R. Mutharasan (1991). "The influence of temperature on a mouse-mouse hybridoma growth and monoclonal antibody production." Biotech Bioeng 37: 292-295.

Suzuki, E., G. D. Sayles and D. F. Ollis (Nov. 29 1988). AIChE Annual Meeting, Washington, DC,

Suzuki, M., E. Tamiya, H. Matsuoka, M. Sugi and I. Karube (1986). "Electrical stimulation of hybridoma cells producing monoclonal antibody to cAMP." Biochim Biophys Acta 889: 149-155.

Takata, I., K. Kayashima, T. Tosa and I. Chibata (1982). "Improvement of stability of fumarase activity of *brevibacterium flavum* by immobilization with κ-carrageenan and polyethyleneimine." J Ferment Tech 60(5): 431-437.

Takazawa, Y., M. Tokashiki, K. Hamamoto and H. Murakami (1988). "High cell density perfusion culture of hybridoma cells recycling high molecular weight components." Cytotech 1: 171-178.

Tangu, S. K. and T. K. Ghose (1981). Process Biochem 8: 24-27.

Toda, K. and M. Skoda (1975). "Sucrose inversion by immobilized yeast cells in a complete mixing reactor." Biotech Bioeng 17: 481-497.

Toneguzzo, F., A. C. Hayday and A. Keating (1986). "Electric field-mediated DNA transfer: Transient and stable gene expression in human and mouse lymphoid cells." Mol Cell Biol 6(2): 703-706.

Varecka, R. and W. Scheirer (1987). "Use of a rotating wire-cage for the retention of animal cells in a perfusion fermentor." Dev Biol Stand 66: 269-272.

Velez, D., L. Miller and J. D. Macmillan (1989). "Use of tangential flow filtration in perfusion propagation of hybridoma cells for production of monoclonal antibodies." Biotech Bioeng 33: 938-940.

Vorlop, K. D. and J. Klein (1987). "Entrapment of microbial cells in chitosan." in Methods in Enzymology. New York, Academic Press. 259-268.

Wada, M., J. Kato and I. Chibata (1980). "Electron microscopic observation on immobilized growing yeast cells." J Ferment Technol 58(4): 327-331.

Wang, D. I. C., C. L. Cooney, A. L. Demain, P. Dunnill, A. E. Humphery and M. D. Lilly (1979). Fermentation and Enzyme Technology. New York, John Wiley & Sons, 157-193.

Wang, H. Y., F. M. Robinson and S. S. Lee (1981). Biotech Bioeng Symp 11: 55.

Wang, G. and D. I. C. Wang (1984). "Elucidation of inhibition of growth and acetic acid production of *Clostridium thermoaceticum*." Appl & Environ Microbiol 47(2): 294.

Weiss, A. M., A. J. Grodzinsky and M. L. Yarmush (1986). "Chemically and electrically controlled membranes : Size specific transport of fluorescent solutes through PMAA membranes." AIChE Symposium series 82(250): 85-98.

Wittler, R., H. Baumgartl, D. W. Lubbers and K. Schugerl (1986). "Investigations of oxygen transfer into *Penicillium chrysogenum* pellets by microprobe measurements." Biotech Bioeng 28: 1024-1036.

Wohlpart, D., J. Gainer and D. Kirwan (1991). "Oxygen uptake by entrapped hybridoma cells." Biotech Bioeng 37: 1050-1053.

Wollheim, C. B., S. Ullrich, P. Meda and L. Vallar (1987). "Regulation of exocytosis in electrically permeabilized insulin-secreating cells. Evidence for Ca^{2+} dependence and independent secretion." Bioscience Reports 7(5): 443-454.

Yabannavar, V. M. (1988). Extractive fermentation process for organic acid production. M.I.T. Ph.D. Thesis.

Zielke, H. R., C. L. Ziekle and P. T. Ozand (1984). "Glutamine: A major energy source for cultured mammalian cells." Federation Preceding 43: 121-125.

Zupke, C. A. (1993). "Metabolic flux analysis in mammalian cell culture." M.I.T. Ph.D. Thesis.

Appendix-I: Computer Program for Simulating Intramembrane Transport and κ-Carrageenan-Entrapped *E. coli* Growth Kinetics*

```
C     DO3PBF PROGRAM TEXT
C     E.COLI GROWTH AND METABOLISM UNDER ANAEROBIC CONDITION
C     in k-carrageenan
      IMPLICIT REAL*8(A-H,O-Z)
      PARAMETER        (NPDE=2,NPTMAX=200,NX=21,
     *                  IWK=NPDE*(3*NPDE*NPTMAX+12*NPTMAX+7)+40)
      DIMENSION U(NPDE,NPTMAX), UOUT(NPDE,NX), WORK(IWK),
     *          X(NPTMAX), XOUT(NX), CD(41), CDOUT(NX)
      EXTERNAL         BNDY1, D03PBF, INTERX, PDEF1
      INTRINSIC        DBLE,COS
      COMMON /COMN1/ DT,CBO,NPTS,A,B,NOUT,CD
      COMMON /COMN2/ UMAX,ZKM,ZKI,QSMAX,AJ,DS,YHG,DH,CWO,ZM
C     SPECIFY OUTPUT (NOUT) AND INPUT (NINP) MECHANISMS, AND MAXIMUM
C      SIZE OF WORK SPACE (NPTS)
      DATA NOUT/9/,NPTS/41/,NINP/11/
C     DEFINE FILE, cn.r, FOR PRINTOUT
      OPEN (NOUT,File='cn.r')
      REWIND (NOUT)
      OPEN (NINP,FILE='para3.d')
      REWIND (NINP)
C     SPECIFIC VARIOUS PARAMETERS
      READ (NINP,*) DT,CBO,CNO
      READ (NINP,*) UMAX,ZKM,ZKI,QSMAX,AJ,DS,YHG,DH,CWO,ZM
      WRITE (NOUT,FMT=999)DT
      WRITE (NOUT,FMT=998)CBO
      WRITE (NOUT,FMT=997)CNO
      WRITE(NOUT,FMT=993)UMAX,ZKM,ZKI,QSMAX,AJ,DS,YHG,DH,CWO,ZM
      M = 0
C     SPECIFY THE BORDERS OF THE HYDROGEL SLAB
      A = -1.0D0
      B = 1.0D0
C     AN ACCURACY OF 0.00005H IS USED IN THE TIME DIRECTION
      ACC = 0.5D-4
      WRITE (NOUT,FMT=99998) ACC
C     SPECIFY POINTS FOR PRINTOUT
      DO 10 I=1,NX
         XOUT(I)=DBLE(I-1)*(B-A)/(NX-1)+A
 10   CONTINUE
      IMESH = 1
      WRITE (NOUT,FMT=99997) NPTS, IMESH
C     U(1)=GLUCOSE; U(2)=ORGANIC ACID; CD=CELL DENSITY
      DO 20 I = 1, NPTS
            U(1,I) = CBO/CBO
            U(2,I) = 0.0D0
            CD(I)=CNO*1.0D3
 20   CONTINUE
      WRITE (*, FMT=9997)
      READ (*,*) ITIME
      N =INT(ITIME/2)+1
      TS = 0.0D0
      IND = 0
      DO 60 IT = 1, N
            TOUT = DBLE(IT-1)*2.0D0
            IF (IT .EQ. 1) TOUT=0.5D0
            WRITE (NOUT,FMT=996)TOUT
            IFAIL = 1
            DO 30 J=1,NPDE
            DO 25 K=1,NPTS
```

```
               IF (U(J,K) .LT. 0.0D0) U(J,K)=0.0D0
 25          CONTINUE
 30          CONTINUE
C       CALL DO3PBF TO COMPUTE AT TIME TOUT
            CALL D03PBF(NPDE,M,PDEF1,BNDY1,A,B,TS,TOUT,U,NPTS,IMESH,X,
     *                  ACC,WORK,IWK,IND,IFAIL)
            IF (IFAIL.EQ.0) THEN
               DO 40 I=1,NX
C       CALL INTERX TO INTERPOLATE THE RESULTS
                  CALL INTERX(XOUT(I),UOUT(1,I),CDOUT(I),NPDE,X,NPTS,U
     *                        ,CD,NPDE)
 40            CONTINUE
               WRITE (NOUT,FMT=995)
               DO 50 J=1,NX
               WRITE (NOUT,FMT=994) XOUT(J),UOUT(1,J),UOUT(2,J)/1.0D3,
     *                CDOUT(J)/1.0D3
 50            CONTINUE
            ELSE
               WRITE (NOUT,FMT=99993) IFAIL
               IF (IFAIL.LE.5) WRITE (NOUT,FMT=99992) TOUT
            END IF
 60       CONTINUE
C
 999   FORMAT('THE THICKNESS OF HALF OF THE GEL IS',2X,E12.4,' m')
 998   FORMAT('THE INITIAL (BULK) NUTRIENT CONCENTRATION IS',2X,
     *       E12.4,'   g/m3')
 997   FORMAT('THE INITIAL CELL DENSITY IS',2X,F8.3,' g/L')
 996   FORMAT('THE TIME FOR CELL TO GROW IS',2X,F9.4,' hr')
 995   FORMAT(8X,'L/DT',11X,'S/SBO',11X,'H (g/L)',11X,'N (g/L)')
 994   FORMAT(5X,F9.4,5X,F11.5,5X,F11.5,5X,F11.5)
 993   FORMAT('THE Umax OF CELL GROWTH IS',F10.4,' (1/hr)',/,
     *       'THE Km OF NUTRIENT IS',G13.5,' (g/m3)',/,
     *       'THE Ki OF HYDROGEL IS',G13.5,' (m3/A-hr)',/,
     *       'THE Qsmax is',G13.5,' (g-glu./hr-g-cell)',/,
     *       'THE J IS',G10.2,' (A/m2)',/,
     *       'THE DS IS',G13.5,' (m2/hr)',/,
     *       'THE YHG IS',G13.5,'(g-acid/g-glucose)',/,
     *       'THE DH IS',G13.5,' (m2/hr)',/,
     *       'THE CWO IS',G13.5,' (g-acid/m3)',/,
     *       'THE ZM IS',G13.5,'(g-glu./hr-g-cell)',/)
 9997 FORMAT (' THE TOTAL TIME FOR CELL TO GROW IS (hr)')
99998 FORMAT ('ACCURACY IN THE TIME INTEGRATION IS',D10.1)
99997 FORMAT ('NUMERICAL SOLUTION USING',I5,' MESH POINTS WITH MESH S',
     *  'PACING',I3,/)
99993 FORMAT (' D03PBF FAILS WITH IFAIL =',I3)
99992 FORMAT (' AT T = ',F8.3)
      END
C
C*******************************************************************
C
C     SUBROUTINE THAT DEFINE P.D.E.
      SUBROUTINE PDEF1(NPDE,X,T,UX,DUX,F,G,C)
      IMPLICIT REAL*8 (A-H,O-Z)
      DIMENSION C(NPDE), DUX(NPDE), F(NPDE), G(NPDE), UX(NPDE),
     *          CD(41),CDP(41)
      COMMON /COMN1/ DT,CBO,NPTS,A,B,NOUT,CD
      COMMON /COMN2/ UMAX,ZKM,ZKI,QSMAX,AJ,DS,YHG,DH,CWO,ZM
      RNODE=(X-A)*(NPTS-1)/(B-A)+1.1
      NODE=INT(RNODE)
      IF (T.NE. 0.0D0) GOTO 100
      TO=0.0D0
      CDP(NODE)=CD(NODE)
 100  IF (NODE.EQ.1) TP=T-TO
C     COMPUTE SPECIFIC GROWTH RATE
      SGR=UMAX*UX(1)/(ZKM/CBO+UX(1))*(1-UX(2)/CWO)
```

```
      IF (SGR .LT. 0.0D0) SGR=0.0D0
C     COMPUTE AND UPDATE CELL DENSITY
      CD(NODE)=CDP(NODE)*EXP(SGR*TP)
      CDP(NODE)=CD(NODE)
      TO=T
      C(1) = 1.0D0
      G(1) = DS/DT**2.0D0
C     COMPUTE SPECIFIC GLUCOSE UPTAKE RATE
      QS = QSMAX*UX(1)/(ZKM/CBO+UX(1))+ZM
C     COMPUTE CONVECTIVE FLOW RATE OF GLUCOSE
      VX = ZKI*AJ
      F(1) = -VX*DUX(1)/DT-CD(NODE)/CBO*QS
      C(2) = 1.0D0
      G(2) = DH/DT**2.0D0
C     COMPUTE SPECIFIC ORGANIC ACID PRODUCTION RATE
      QH = QS*YHG
C     CONVECTIVE FLOW RATE OF ORGANIC ACID IS 60% OF THAT OF GLUCOSE
      F(2) = -0.60*VX*DUX(2)/DT+CD(NODE)*QH
      RETURN
      END
C
C*********************************************************************
C
C     SUBROUTINE THAT DEFINE BOUNDARY CONDITIONS
      SUBROUTINE BNDY1(NPDE,T,UX,IBND,P,Q,R)
      IMPLICIT REAL*8(A-H,O-Z)
      DIMENSION P(NPDE), Q(NPDE), R(NPDE), UX(NPDE)
      IF (IBND.EQ.0) THEN
C        SET UP LEFT HAND BOUNDARY CONDITION
         P(1) = 1.0D0
         Q(1) = 0.0D0
         R(1) = 1.0D0
         P(2) = 1.0D0
         Q(2) = 0.0D0
         R(2) = 0.0D0
      ELSE
C        SET UP RIGHT HAND BOUNDARY CONDITION
         P(1) = 1.0D0
         Q(1) = 0.0D0
         R(1) = 1.0D0
         P(2) = 1.0D0
         Q(2) = 0.0D0
         R(2) = 0.0D0
      END IF
      RETURN
      END
C
C*********************************************************************
C
C     UBROUTINE THAT INTERPOLATES THE RESULTS
      SUBROUTINE INTERX(XP,UP,CDUP,NPDE,X,NPTS,U,CD,IU)
      IMPLICIT REAL*8 (A-H,O-Z)
      DIMENSION  U(IU,NPTS), UP(NPDE), X(NPTS),CDUP,CD(NPTS)
      DO 20 I = 2, NPTS
         IF (XP.LE.X(I)) GO TO 40
   20 CONTINUE
      I = NPTS
   40 XI1 = X(I-1)
      XI = X(I)
      DO 60 J = 1, NPDE
         UI1 = U(J,I-1)
         UI = U(J,I)
         UP(J) = UI1 + (XP-XI1)*(UI-UI1)/(XI-XI1)
   60 CONTINUE
      CDI1=CD(I-1)
```

```
CDI=CD(I)
CDUP=CDI1+(XP-XI1)*(CDI-CDI1)/(XI-XI1)
RETURN
END
```

* The program for simulating the agarose-entrapped *E. coli* growth is different from the κ-carrageenan-entrapped *E. coli* growth in the the matrix parameter F(1)= -CD(NODE)/CBO*QS, and F(2)= 0.4*VX*DUX(2)/DT+CD(NODE)*QH.

Appendix -II: Theoretical Analysis of Nutrient Metabolism

This theoretical analysis of nutrient consumption was developed by Xie (1993) and is detailed in the following. The average cell composition is summarized in Table-A.1.

Table-A.1 : Cell Composition

Wet Cell Weight	180 mg/10^8 cells	
Dry Cell Weight	36 mg/10^8 cells	Dry Wt. %
Protein	13.5 mg/10^8 cells	37.5%
DNA	0.9 mg/10^8 cells	2.5%
RNA	2.5 mg/10^8 cells	6.9%
Lipid $(CH_2)_n$	7.2 mg/10^8 cells	20.0%
Carbohydrate (CH_2O)	9.0 mg/10^8 cells	25.0%

The average of amino acid occupancies in protein is summarized in Table-A.2. Based on this composition, the average molecular weight of protein was found to be 110 g/mole.

Table-A.2 : Average Occupancies ($Y_{i,p}$) of Amino Acids in Protein

Essential Amino Acids	Non-Essential Amino Acids
Arg : 4.7%	Ala : 9.0%
Cys : 2.8%	Asn : 4.4%
His : 2.1%	Asp : 5.5%
Ile : 4.6%	Glu : 6.2%
Leu : 7.5%	Gln : 3.9%
Lys : 7.0%	Gly : 7.5%
Met : 1.7%	Ser : 7.1%
Phe : 3.5%	Pro : 4.6%
Thr : 6.0%	Total = 48.2%
Trp : 1.1%	
Tyr : 3.5%	
Val : 6.9%	
Total = 51.4%	

The average occupancies of amino acids in cell mass were calculated based on the following methodology,

• All amino acids are incorporated into cellular proteins with the same occupancies as shown in Table-A.2.

• Only Gln, gly, and Asp are used in nucleotide synthesis, Glu is produced during the nucleotide synthesis. The reactions are summarized as follows,

3 Gln+Gly+Asp -> Guanine+3 Glu

2 Gln+Gly+2 Asp -> Adenine+2 Glu

2 Gln+Asp -> Cytosine+2 Glu

Gln+Asp -> Thymine+Glu

Gln+Asp -> Uracil+Glu

• Average molecular weight of DNA is 307.7 g/mole, average molecular weight of RNA is 319.25 g/mole (since 40% of nucleotide s are G & C and 60% are A & T). The average occupancies of amino acids in cell mass are summarized in Table-A.3.

Table-A.3 : Average Occupancies ($Y_{i,c}$) of Amino Acids in Cell Mass

(mmole/10^9 cells)

Essential Amino Acids	Non-Essential Amino Acids
Arg : 0.058	Ala : 0.111
Cys : 0.0344	Asn : 0.054
His : 0.026	Asp : 0.203
Ile : 0.056	Glu : 0
Leu : 0.092	Gln : 0.260
Lys : 0.086	Gly : 0.143
Met : 0.021	Ser : 0.087
Phe : 0.043	Pro : 0.056
Thr : 0.074	
Trp : 0.014	
Tyr : 0.043	
Val : 0.085	

Glucose is used for the synthesis of cell mass, which includes lipids, carbohydrates and nucleotides. The glucose efficiency in cell mass synthesis was therefore calculated to be 1.45 mmole/10^9-cells. Glucose is also used for

energy production, and the consumption rate was found to be ($9.2\times10^{-10}\times\mu+4.1\times10^{-11}$) mmole/viable-cell-hr, where μ is the specific growth rate (hr^{-1}), and the yield of glucose to lactate was assumed to be 1.3. Glutamine is consumed by self-degradation and by the requirements for the syntheses of cell mass and protein.

The procedures for calculating various nutrient consumption are summarized as following,

- Glucose consumption in energy production (mM) = ($9.2\times10^{-10}\times\mu+4.1\times10^{-11}$)x(total viable cells density-time), where μ is in hr^{-1} and cell density is in cells/L.
- Glucose consumption for cell mass synthesis (mM) = (1.45 mmole/10^9-cells)xN_t, where N_t is the final total cell density (cells/L).
- Glutamine consumption = ((0.0048/hr)x(4 mM)x(time)) + ($Y_{gln,c}$ mmole/10^9-cells)xNt + ($Y_{gln,p}$ %)x(final antibody titer, mg/L)/(110 mg/mmole).
- Total consumption of each amino acid *i* = (final cell density x $Y_{i,c}$) + (final antibody titer x $Y_{i,p}$).
- To obtain the yield of each nutrient to cell mass or to antibody, the final total cell density or the final antibody titer is divided with the total amount of each nutrient consumed.